



VOL. 585 NO. 1 OCTOBER 25, 1991

JOURNAL OF

CHROMATOGRAPHY

INCLUDING ELECTROPHORESIS AND OTHER SEPARATION METHODS



EDITORS

R. W. Giese (Boston, MA)
J. K. Haken (Kensington, N.S.W.)
K. Macek (Prague)
L. R. Snyder (Orinda, CA)

EDITORS, SYMPOSIUM VOLUMES,
E. Heftmann (Orinda, CA), Z. Deyl (Prague)

EDITORIAL BOARD

D. W. Armstrong (Rolla, MO)
W. A. Aue (Halifax)
P. Boček (Brno)
A. A. Boulton (Saskatoon)
P. W. Carr (Minneapolis, MN)
N. H. C. Cooke (San Ramon, CA)
V. A. Davankov (Moscow)
Z. Deyl (Prague)
S. Dilli (Kensington, N.S.W.)
F. Erni (Basle)
M. B. Evans (Hatfield)
J. L. Glajch (N. Billerica, MA)
G. A. Guiochon (Knoxville, TN)
P. R. Haddad (Kensington, N.S.W.)
I. M. Hais (Hradec Králové)
W. S. Hancock (San Francisco, CA)
S. Hjertén (Uppsala)
Cs. Horváth (New Haven, CT)
J. F. K. Huber (Vienna)
K.-P. Hupe (Waldbronn)
T. W. Hutchens (Houston, TX)
J. Janák (Brno)
P. Jandera (Pardubice)
B. L. Karger (Boston, MA)
E. sz. Kováts (Lausanne)
A. J. P. Martin (Cambridge)
L. W. McLaughlin (Chestnut Hill, MA)
E. D. Morgan (Keele)
J. D. Pearson (Kalamazoo, MI)
H. Poppe (Amsterdam)
F. E. Regnier (West Lafayette, IN)
P. G. Righetti (Milan)
P. Schoenmakers (Eindhoven)
R. Schwarzenbach (Dübendorf)
R. E. Shoup (West Lafayette, IN)
A. M. Siouffi (Marseille)
D. J. Strydom (Boston, MA)
N. Tanaka (Kyoto)
S. Terabe (Hyogo)
K. K. Unger (Mainz)
R. Verpoorte (Lüden)
Gy. Vigh (College Station, TX)
J. T. Watson (East Lansing, MI)
B. D. Westerlund (Uppsala)

EDITORS, BIBLIOGRAPHY SECTION

Z. Deyl (Prague), J. Janák (Brno), V. Schwarz (Prague), K. Macek (Prague)

ELSEVIER

JOURNAL OF CHROMATOGRAPHY

INCLUDING ELECTROPHORESIS AND OTHER SEPARATION METHODS

Scope. The *Journal of Chromatography* publishes papers on all aspects of chromatography, electrophoresis and related methods. Contributions consist mainly of research papers dealing with chromatographic theory, instrumental development and their applications. The section *Biomedical Applications*, which is under separate editorship, deals with the following aspects: developments in and applications of chromatographic and electrophoretic techniques related to clinical diagnosis or alterations during medical treatment; screening and profiling of body fluids or tissues with special reference to metabolic disorders; results from basic medical research with direct consequences in clinical practice; drug level monitoring and pharmacokinetic studies; clinical toxicology; analytical studies in occupational medicine.

Submission of Papers. Manuscripts (in English; four copies are required) should be submitted to: Editorial Office of *Journal of Chromatography*, P.O. Box 681, 1000 AR Amsterdam, Netherlands, Telefax (+31-20) 5862 304, or to: The Editor of *Journal of Chromatography, Biomedical Applications*, P.O. Box 681, 1000 AR Amsterdam, Netherlands. Review articles are invited or proposed by letter to the Editors. An outline of the proposed review should first be forwarded to the Editors for preliminary discussion prior to preparation. Submission of an article is understood to imply that the article is original and unpublished and is not being considered for publication elsewhere. For copyright regulations, see below.

Publication. The *Journal of Chromatography* (incl. *Biomedical Applications*) has 39 volumes in 1992. The subscription prices for 1992 are:

J. Chromatogr. (incl. *Cum. Indexes, Vols. 551-600*) + *Biomed. Appl.* (Vols. 573-611):
Dfl. 7722.00 plus Dfl. 1209.00 (p.p.h.) (total ca. US\$ 4421.25)

J. Chromatogr. (incl. *Cum. Indexes, Vols. 551-600*) only (Vols. 585-611):
Dfl. 6210.00 plus Dfl. 837.00 (p.p.h.) (total ca. US\$ 3488.50)

Biomed. Appl. only (Vols. 573-584):
Dfl. 2760.00 plus Dfl. 372.00 (p.p.h.) (total ca. US\$ 1550.50).

Subscription Orders. The Dutch guildler price is definitive. The US\$ price is subject to exchange-rate fluctuations and is given as a guide. Subscriptions are accepted on a prepaid basis only, unless different terms have been previously agreed upon. Subscriptions orders can be entered only by calendar year (Jan.-Dec.) and should be sent to Elsevier Science Publishers, Journal Department, P.O. Box 211, 1000 AE Amsterdam, Netherlands, Tel. (+31-20) 5803 642, Telefax (+31-20) 5803 598, or to your usual subscription agent. Postage and handling charges include surface delivery except to the following countries where air delivery via SAL (Surface Air Lift) mail is ensured: Argentina, Australia, Brazil, Canada, Hong Kong, India, Israel, Japan*, Malaysia, Mexico, New Zealand, Pakistan, PR CHINA, Singapore, South Africa, South Korea, Taiwan, Thailand, USA. *For Japan air delivery (SAL) requires 25% additional charge of the normal postage and handling charge. For all other countries airmail rates are available upon request. Claims for missing issues must be made within three months of our publication (mailing) date, otherwise such claims cannot be honoured free of charge. Back volumes of the *Journal of Chromatography* (Vols. 1-572) are available at Dfl. 208.00 (plus postage). Customers in the USA and Canada wishing information on this and other Elsevier journals, please contact Journal Information Center, Elsevier Science Publishing Co. Inc., 655 Avenue of the Americas, New York, NY 10010, USA, Tel. (+1-212) 633 3750, Telefax (+1-212) 633 3990.

Abstracts/Contents Lists published in Analytical Abstracts, Biochemical Abstracts, Biological Abstracts, Chemical Abstracts, Chemical Titles, Chromatography Abstracts, Clinical Chemistry Lookout, Current Contents/Life Sciences, Current Contents/Physical, Chemical & Earth Sciences, Deep-Sea Research/Part B: Oceanographic Literature Review, Excerpta Medica, Index Medicus, Mass Spectrometry Bulletin, PASCAL-CNRS, Pharmaceutical Abstracts, Referativnyi Zhurnal, Research Alert, Science Citation Index and Trends in Biotechnology.

See inside back cover for Publication Schedule, Information for Authors and information on Advertisements.

© ELSEVIER SCIENCE PUBLISHERS B.V. — 1991

0021-9673/91/503.50

All rights reserved. No part of this publication may be reproduced, stored in a retrieval system or transmitted in any form or by any means, electronic, mechanical, photocopying, recording or otherwise, without the prior written permission of the publisher, Elsevier Science Publishers B.V., Permissions Department, P.O. Box 521, 1000 AN Amsterdam, Netherlands.

Upon acceptance of an article by the journal, the author(s) will be asked to transfer copyright of the article to the publisher. The transfer will ensure the widest possible dissemination of information.

Submission of an article for publication entails the authors' irrevocable and exclusive authorization of the publisher to collect any sums or considerations for copying or reproduction payable by third parties (as mentioned in article 17 paragraph 2 of the Dutch Copyright Act of 1912 and the Royal Decree of June 20, 1974 (S. 351) pursuant to article 16 b of the Dutch Copyright Act of 1912) and/or to act in or out of Court in connection therewith.

Special regulations for readers in the USA. This journal has been registered with the Copyright Clearance Center, Inc. Consent is given for copying of articles for personal or internal use, or for the personal use of specific clients. This consent is given on the condition that the copier pays through the Center the per-copy fee stated in the code on the first page of each article for copying beyond that permitted by Sections 107 or 108 of the US Copyright Law. The appropriate fee should be forwarded with a copy of the first page of the article to the Copyright Clearance Center, Inc., 27 Congress Street, Salem, MA 01970, USA. If no code appears in an article, the author has not given broad consent to copy and permission to copy must be obtained directly from the author. All articles published prior to 1980 may be copied for a per-copy fee of US\$ 2.25, also payable through the Center. This consent does not extend to other kinds of copying such as for general distribution, resale, advertising and promotion purposes, or for creating new collective works. Special written permission must be obtained from the publisher for such copying.

No responsibility is assumed by the Publisher for any injury and/or damage to persons or property as a matter of products liability, negligence or otherwise, or from any use or operation of any methods, products, instructions or ideas contained in the materials herein. Because of rapid advances in the medical sciences, the Publisher recommends that independent verification of diagnoses and drug dosages should be made.

Although all advertising material is expected to conform to ethical (medical) standards, inclusion in this publication does not constitute a guarantee or endorsement of the quality or value of such product or of the claims made of it by its manufacturer.

This issue is printed on acid-free paper.

Printed in the Netherlands

CONTENTS

(Abstracts/Contents Lists published in Analytical Abstracts, Biochemical Abstracts, Biological Abstracts, Chemical Abstracts, Chemical Titles, Chromatography Abstracts, Current Contents/Life Sciences, Current Contents/Physical, Chemical & Earth Sciences, Deep-Sea Research/Part B: Oceanographic Literature Review, Excerpta Medica, Index Medicus, Mass Spectrometry Bulletin, PASCAL-CRNS, Referativnyi Zhurnal, Research Alert and Science Citation Index)

Publisher's note	1
REGULAR PAPERS	
<i>Column Liquid Chromatography</i>	
Hydrophobicity of β -lactam antibiotics. Explanation and prediction of their behaviour in various partitioning solvent systems and reversed-phase chromatography by A. A. Petrauskas and V. K. Švedas (Moscow, USSR) (Received May 8th, 1991)	3
(2 <i>R</i> ,3 <i>R</i>)-Dicyclohexyl tartrate as a chiral mobile phase additive by E. Heldin, N. H. Huynh and C. Pettersson (Uppsala, Sweden) (Received May 27th, 1991)	35
Adsorption and elution of bovine γ -globulin using an affinity membrane containing hydrophobic amino acids as ligands by M. Kim, K. Saito, S. Furusaki, T. Sato (Tokyo, Japan), T. Sugo and I. Ishigaki (Gunma, Japan) (Received March 20th, 1991)	45
Determination of picomole amounts of lipoxins C ₄ , D ₄ and E ₄ by high-performance liquid chromatography with electrochemical detection by F.-P. Gaede, M. Kirchner, D. Steinhilber and H. J. Roth (Tübingen, Germany) (Received May 8th, 1991)	53
Chromatographic fractionation of nucleic acids using microcapsules made from plant cells by A. Jäschke, D. Cech and R. Ehwald (Berlin, Germany) (Received March 27th, 1991)	57
Determination of chlorotriazines in aqueous environmental samples at the ng/l level using preconcentration with a cation exchanger and on-line high-performance liquid chromatography by V. Coquart and M.-C. Hennion (Paris, France) (Received May 28th, 1991)	67
Quality control of cured epoxy resins. Determination of residual free monomers (<i>m</i> -xylylenediamine and bisphenol A diglycidyl ether) in the finished product by P. Paseiro Losada, (Santiago de Compostela, Spain), S. Paz Albuín (Lago-Valdoviño, Spain), L. Vázquez Odériz, J. Simal Lozano and J. Simal Gándara (Santiago de Compostela, Spain) (Received May 28th, 1991)	75
<i>Gas Chromatography</i>	
Prediction of retention in gas-liquid chromatography using the UNIFAC group contribution method. II. Polymer stationary phases by G. J. Price (Bath, UK) and M. R. Dent (London, UK) (Received February 13th, 1991)	83
Determination of sulphur and nitrogen gases by gas chromatography on polystyrene porous polymer columns by G. Castello and G. D'Amato (Genova, Italy) (Received May 16th, 1991)	93
Synthesis of novel selenium-containing choline and acetylcholine analogues and their quantitation using a pyrolysis-gas chromatography-mass spectrometry assay by A. V. Terry, Jr., L. A. Silks III, R. B. Dunlap, J. D. Odom and J. W. Kosh (Columbia, SC, USA) (Received May 22nd, 1991)	101
Gas chromatographic-mass spectrometric determination of ethyl carbamate as the xanthylamide derivative in Italian aqua vitae (grappa) samples by C. Giachetti, A. Assandri and G. Zanolo (Ivrea, Italy) (Received Received June 3rd, 1991)	111
<i>Supercritical Fluid Chromatography</i>	
Separation of secondary alcohol enantiomers using supercritical fluid chromatography by K. Sakaki and H. Hirata (Ibaraki, Japan) (Received May 27th, 1991)	117

(Continued overleaf)

Electrophoresis

Determination of some drugs by micellar electrokinetic capillary chromatography. The pseudo-effective mobility as parameter for screening
by M. T. Ackermans, F. M. Everaerts and J. L. Beckers (Eindhoven, Netherlands) (Received May 24th, 1991) 123

Separation of antibiotics by high-performance capillary electrophoresis with photodiode-array detection
by S. K. Yeo, H. K. Lee and S. F. Y. Li (Singapore, Singapore) (Received May 21st, 1991) 133

Micellar electrokinetic capillary chromatography of vitamin B₆ with electrochemical detection
by Y. F. Yik, H. K. Lee, S. F. Y. Li and S. B. Khoo (Singapore, Singapore) (Received May 14th, 1991) 139

Purification of ovalbumin and lysozyme from a commercial product by recycling isotachopheresis
by J. Caslavská, P. Gebauer and W. Thormann (Berne, Switzerland) (Received June 4th, 1991) 145

Preparative high-yield electroelution of proteins after separation by sodium dodecyl sulphate-polyacrylamide gel electrophoresis and its application to analysis of amino acid sequences and to raise antibodies
by T. Ohhashi, C. Moritani, H. Andoh, S. Satoh and S. Ohmori (Okayama, Japan), F. Lottspeich (Martinsried, Germany) and M. Ikeda (Okayama, Japan) (Received May 24th, 1991) 153

SHORT COMMUNICATIONS

Column Liquid Chromatography

Data compression in computerized signal processing for isocratic chromatography
by J. C. Reijnga (Eindhoven, Netherlands) (Received June 17th, 1991) 160

High-performance liquid chromatographic determination of dinitroaniline herbicides in soil and water
by P. Cabras, M. Melis, L. Spanedda and C. Tuberoso (Cagliari, Italy) (Received June 11th, 1991) 164

Determination of carotenoid pigments in several tree leaves by reversed-phase high-performance liquid chromatography
by J. De Las Rivas, J. C. G. Milicua and R. Gomez (Bilbao, Spain) (Received June 11th, 1991) 168

Determination of calcium ions tightly bound to proteins
by K. Nitta and A. Watanabe (Hokkaido, Japan) (Received May 27th, 1991) 173

Gas Chromatography

Enhanced resolution of organic compounds from sediments by isotopic gas chromatography-combustion-mass spectrometry
by E. Lichtfouse, K. H. Freeman, J. W. Collister and D. A. Merritt (Bloomington, IN, USA) (Received June 20th, 1991) 177

Planar Chromatography

Simultaneous effect of geometrical isomerism and chelate ring size of tris(aminocarboxylato)cobalt(III) complexes on their behaviour in thin-layer chromatography on silica gel and alumina
by G. Vučković, N. Juranić, D. Miljević and M. B. Čelap (Beograd, Yugoslavia) (Received June 11th, 1991) 181

Announcement of Special Issue on Applications of Chromatography and Electrophoresis in Food Science 186

* In articles with more than one author, the name of the author to whom correspondence should be addressed is indicated *
* in the article heading by a 6-pointed asterisk (*) *
* *****

JOURNAL OF CHROMATOGRAPHY

VOL. 585 (1991)

JOURNAL of CHROMATOGRAPHY

INCLUDING ELECTROPHORESIS AND OTHER SEPARATION METHODS

EDITORS

R. W. GIESE (Boston, MA), J. K. HAKEN (Kensington, N.S.W.), K. MACEK (Prague), L. R. SNYDER (Orinda, CA)

EDITORS, SYMPOSIUM VOLUMES

E. HEFTMANN (Orinda, CA), Z. DEYL (Prague)

EDITORIAL BOARD

D. W. Armstrong (Rolla, MO), W. A. Aue (Halifax), P. Boček (Brno), A. A. Boulton (Saskatoon), P. W. Carr (Minneapolis, MN), N. H. C. Cooke (San Ramon, CA), V. A. Davankov (Moscow), Z. Deyl (Prague), S. Dilli (Kensington, N.S.W.), F. Erni (Basle), M. B. Evans (Hatfield), J. L. Glajch (N. Billerica, MA), G. A. Guiochon (Knoxville, TN), P. R. Haddad (Kensington, N.S.W.), I. M. Hais (Hradec Králové), W. S. Hancock (San Francisco, CA), S. Hjertén (Uppsala), Cs. Horváth (New Haven, CT), J. F. K. Huber (Vienna), K.-P. Hupe (Waldbronn), T. W. Hutchens (Houston, TX), J. Janák (Brno), P. Jandera (Pardubice), B. L. Karger (Boston, MA), E. sz. Kováts (Lausanne), A. J. P. Martin (Cambridge), L. W. McLaughlin (Chestnut Hill, MA), E. D. Morgan (Keele), J. D. Pearson (Kalamazoo, MI), H. Poppe (Amsterdam), F. E. Regnier (West Lafayette, IN), P. G. Righetti (Milan), P. Schoenmakers (Eindhoven), R. Schwarzenbach (Dübendorf), R. E. Shoup (West Lafayette, IN), A. M. Siouffi (Marseille), D. J. Strydom (Boston, MA), N. Tanaka (Kyoto), S. Terabe (Hyogo), K. K. Unger (Mainz), R. Verpoorte (Leiden), Gy. Vigh (College Station, TX), J. T. Watson (East Lansing, MI), B. D. Westerlund (Uppsala)

EDITORS, BIBLIOGRAPHY SECTION

Z. Deyl (Prague), J. Janák (Brno), V. Schwarz (Prague), K. Macek (Prague)



ELSEVIER
AMSTERDAM — LONDON — NEW YORK — TOKYO

J. Chromatogr., Vol. 585 (1991)

All rights reserved. No part of this publication may be reproduced, stored in a retrieval system or transmitted in any form or by any means, electronic, mechanical, photocopying, recording or otherwise, without the prior written permission of the publisher, Elsevier Science Publishers B.V., Permissions Department, P.O. Box 521, 1000 AN Amsterdam, Netherlands.

Upon acceptance of an article by the journal, the author(s) will be asked to transfer copyright of the article to the publisher. The transfer will ensure the widest possible dissemination of information.

Submission of an article for publication entails the authors' irrevocable and exclusive authorization of the publisher to collect any sums or considerations for copying or reproduction payable by third parties (as mentioned in article 17 paragraph 2 of the Dutch Copyright Act of 1912 and the Royal Decree of June 20, 1974 (S. 351) pursuant to article 16 b of the Dutch Copyright Act of 1912) and/or to act in or out of Court in connection therewith.

Special regulations for readers in the USA. This journal has been registered with the Copyright Clearance Center, Inc. Consent is given for copying of articles for personal or internal use, or for the personal use of specific clients. This consent is given on the condition that the copier pays through the Center the per-copy fee stated in the code on the first page of each article for copying beyond that permitted by Sections 107 or 108 of the US Copyright Law. The appropriate fee should be forwarded with a copy of the first page of the article to the Copyright Clearance Center, Inc., 27 Congress Street, Salem, MA 01970, USA. If no code appears in an article, the author has not given broad consent to copy and permission to copy must be obtained directly from the author. All articles published prior to 1980 may be copied for a per-copy fee of US\$ 2.25, also payable through the Center. This consent does not extend to other kinds of copying, such as for general distribution, resale, advertising and promotion purposes, or for creating new collective works. Special written permission must be obtained from the publisher for such copying.

No responsibility is assumed by the Publisher for any injury and/or damage to persons or property as a matter of products liability, negligence or otherwise, or from any use or operation of any methods, products, instructions or ideas contained in the materials herein. Because of rapid advances in the medical sciences, the Publisher recommends that independent verification of diagnoses and drug dosages should be made.

Although all advertising material is expected to conform to ethical (medical) standards, inclusion in this publication does not constitute a guarantee or endorsement of the quality or value of such product or of the claims made of it by its manufacturer.

This issue is printed on acid-free paper.

Publisher's note

The most obvious new feature introduced with this issue is the larger page size. The journal also moves to a two-column format and some typographic style changes have been made to the bibliographic information at the beginning of each article.

The new format will enhance readability and allow a more efficient use of space because of the increased flexibility in the positioning of figures and tables. There is also a trend towards a limited num-

ber of standardized journal sizes, which has obvious advantages for the optimization of shelf space use in libraries.

The amount of information per volume will not be affected by the changes, and as these can be made on a cost-neutral basis, they will not have an effect on the subscription price.

We trust that our readers and librarians will welcome our attempts to improve the readability of the journal.

Hydrophobicity of β -lactam antibiotics

Explanation and prediction of their behaviour in various partitioning solvent systems and reversed-phase chromatography

Alanas A. Petrauskas* and Vytas K. Švedas

A.N. Belozersky Laboratory of Molecular Biology and Bioorganic Chemistry, Moscow State University, Moscow 119899 (USSR)

(First received November 27th, 1990; revised manuscript received May 8th, 1991)

ABSTRACT

β -Lactam antibiotics tend to undergo self-association in hydrophilic organic solvents, which leads to a strong dependence of their experimentally observable $\log P$ values on the partitioning conditions. As a result, most of the earlier obtained $\log P$ values for β -lactam antibiotics cannot be applied as a common hydrophobicity measure, but they proved to be linearly related to each other and to a large body of reversed-phase chromatographic data. The retention of cephalosporins on reversed-phase liquid chromatographic columns is complicated by silanophilic interactions. However, under elution conditions that eliminate these silanophilic interactions, good correlations with $\log P$ data are observed, and a unified hydrophobicity scale for 90 penicillin and cephalosporin compounds could be evaluated. The Hansch and Leo additive scheme was shown to be valid for the calculation of hydrophobicities for penicillin and cephalosporin C-6(7) substituents, but it failed when applied to the prediction of cephalosporin C-3-substituent hydrophobicities. The hydrophobic increments for the sixteen most common cephalosporin C-3-substituents were empirically evaluated from literature data, and a simple equation was derived for an overall β -lactam antibiotic hydrophobicity calculation. The proposed scale is valid for predicting the partitioning of most β -lactam antibiotics in both hydrophilic and lipophilic organic–water systems, although it should be used with caution when applied to antibiotics containing additionally charged side-chains.

INTRODUCTION

It is essential to identify relationships between the physico-chemical properties of β -lactam antibiotics and their biological activity when searching for new pharmaceuticals of this class. As far back as 1963 Hansch and Fujita [1,2] established the need to proceed from the hydrophobicities of investigated substances when tackling the problem of any structure–activity relationships. In fact, the biological activity of β -lactam antibiotics and their hydrophobicities have been shown to be interrelated in numerous studies [3–21]. Meanwhile, the problem of determining the hydrophobic properties of penicillins and cephalosporins is still far from being solved completely.

First, in spite of a number of studies devoted to this problem [5–8,17–29], many of them considered the partitioning of antibiotics under different conditions, which makes their joint analysis complicated. As a result, at present only limited and often contradictory data sets are available in the literature on the partitioning for a maximum of about twenty antibiotics in each set. However, many publications devoted to the chromatographic separation and determination of β -lactams have appeared but have not yet been analysed in order to characterize the hydrophobicity of antibiotics.

Second, so far the generally accepted rules of hydrophobicity calculations suitable for other classes of compounds have been thought to be inapplicable to penicillins and cephalosporins [23,30,31].

A rough estimate of $\log P$ reported [8] for a series of cephalosporins is obviously unsatisfactory and, as we show in this paper, contradicts the experimental results obtained in other work. Therefore, the aim of this study was to survey the available data on the hydrophobic properties of β -lactam antibiotics, and to demonstrate the possibility of their theoretical estimation according to the conventional rules of Hansch and Leo [32].

THEORETICAL

To establish a common hydrophobicity scale characterizing the partitioning of solutes in various organic-water systems, the free energies of partition should be linearly related:

$$\Delta G_i = \alpha \Delta G_j + \beta \quad (1)$$

where $\Delta G_{i(j)}$ is the free energy of the solute transition from water to the $i(j)$ organic phase. Depending on the system studied, $\Delta G_{i(j)}$ is proportional to the logarithm of partition coefficient, $\log P$, the capacity factor, $\log k$, or the value of $R_M = \log(1/R_F - 1)$.

In 1951, Collander [33] found that the eqn. 1 was valid for substances of various classes partitioned between water and different alcohols. Later, Leo showed [34] that in a more general case the linear dependence in eqn. 1 is observed only separately for hydrophilic (e.g., alcohols and ketones) and lipophilic (e.g., alkanes, benzene and chloroform) organic solvents. Seiler [35], however, asserted that the partition coefficients in lipophilic and hydrophilic organic systems were likewise related:

$$\log P_{\text{octanol}} = \log P_{\text{alkane}} + \sum I_H + \beta \quad (2)$$

where I_H denotes the additive increment to hydrogen bonding by a solute molecular segment in hydrophilic organic solvent.

Eqn. 2 is obviously transformed into the single-parameter dependence in eqn. 1 only for certain classes of substances with $\sum I_H = \text{constant}$. Indeed, Leo [34] showed $\log P$ for octanol-water partition to be linearly dependent on $\log P$ for partition in lipophilic solvents only for proton-acceptor (H-acceptor) or proton-donor (H-donor) solutes separately.

It is convenient to consider the β -lactam antibiotics as properly substituted nuclei (Table I). It is reasonable to assume that for β -lactam antibiotics

with substituents similar in their H-donor or -acceptor ability, the linear dependence in eqn. 1 between their partition in hydrophilic and lipophilic systems will be observed as the nucleus hydrogen-bonding increment is always the same or very similar. Indeed, our own experience confirms that this is so for the majority of solutes listed in Table I.

An analysis of literature data shows that in the absence of side-group ionization in β -lactam antibiotics, eqn. 1 is valid irrespective of the temperature change. Thus, the $\log k$ values for six penicillins (2, 4, 5, 13, 23 and 29 in Table I) at five different temperatures have been reported [36]. Using these data in the form of the Van't Hoff equation, we were able to calculate values proportional to the enthalpy and entropy of sorption for each solute:

$$\ln k = -\frac{\Delta H}{RT} + \frac{\Delta S}{R} + \phi \quad (3)$$

where ΔH , ΔS and T represent the enthalpy, entropy and temperature of sorption on the bonded reversed-phase, respectively, ϕ is the volume ratio of the stationary and mobile phases and R is the universal gas constant. The slope is equal to $\Delta H/R$ and the intercept to $\Delta S/R + \phi$. The latter effective values proved to be linearly interrelated:

$$\text{slope} = -387 \times \text{intercept} - 638; n^a = 5, r = 0.9776, s = 201$$

where n , r and s represent the number of correlated points, correlation coefficient and standard deviation, respectively. Having analogously processed the data from ref. 37 where $\log k$ values are reported for four cephalosporins (51, 56, 64 and 76 in Table I), we obtained:

$$\text{slope} = -248 \times \text{intercept} + 1283; n^a = 3, r = 0.9999, s = 12.2$$

A theoretical analysis performed by Melander *et al.* [38] showed that the above-mentioned compensation relationships between ΔH and ΔS account for the linear dependence in eqn. 1 irrespective of temperature.

^a $\log k$ values of amoxicillin from ref. 36 and deacetylcephapirin from ref. 37 have been excluded from the common sets as they largely depended on determination of the column void volume.

TABLE I
PENICILLIN AND CEPHALOSPORIN STRUCTURES

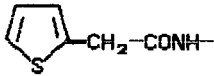
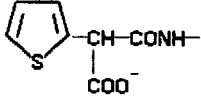
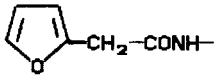
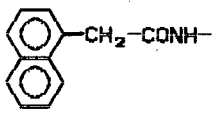
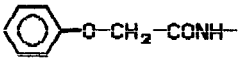
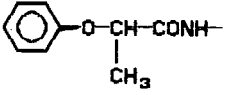
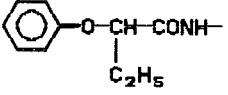
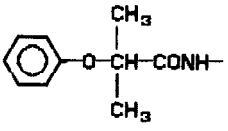
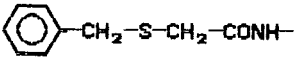
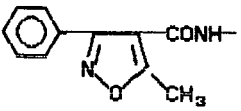
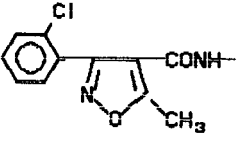
No.	Generic name or code	R ₁	R ₂	R ₃ ^a	
		<p>Penicillins</p>			
1	6-Aminopenicillanic acid (6-APA)	NH ₂	H	H	
2	Benzylpenicillin (penicillin G)		H	H	
3	<i>p</i> -Oxybenzylpenicillin (penicillin X)		H	H	
4	Ampicillin		H	H	
5	Amoxicillin		H	H	
6	Methylenampicillin (metampicillin)		H	H	
7	α -Oxybenzylpenicillin		H	H	
8	Carbenicillin (anion)		H	H	
9	Carbenicillin phenyl (carfecillin)		H	H	
10	Carbenicillin indanyl		H	H	

(Continued on p. 6)

TABLE I (continued)

No.	Generic name or code	R ₁	R ₂	R ₃ ^a
11	Sulbenicillin (anion)		H	H
12	Azidocillin		H	H
13	Piperacillin		H	H
14	<i>p</i> -Oxypiperacillin		H	H
15	Desoxyaspoixillin		H	H
16	Aspoixillin		H	H
17	Apalcillin		H	H
18	Clometocillin		H	H

TABLE I (continued)

No.	Generic name or code	R ₁	R ₂	R ₃ ^a
19	2-Thienylmethylpenicillin		H	H
20	Ticarcillin (anion)		H	H
21	2-Furylmethylpenicillin		H	H
22	1-Naphthylmethylpenicillin		H	H
23	Phenoxymethylpenicillin (penicillin V)		H	H
24	Pheneticillin (phenoxyethyl- penicillin)		H	H
25	Propicillin (phenoxypropyl- penicillin)		H	H
26	Phenoxyisopropylpenicillin		H	H
27	Benzylthiomethylpenicillin		H	H
28	Oxacillin		H	H
29	Cloxacillin		H	H

(Continued on p. 8)

TABLE I (continued)

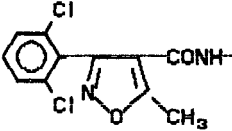
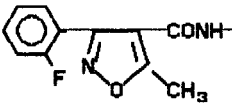
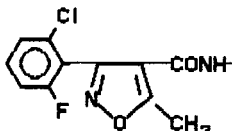
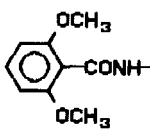
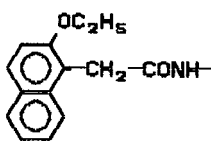
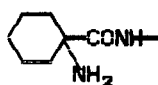
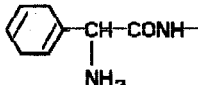
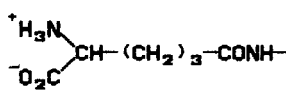
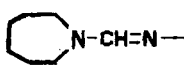
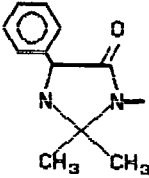
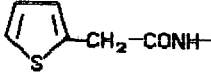
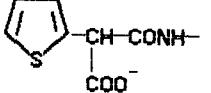
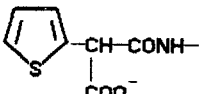
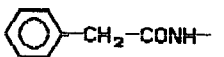
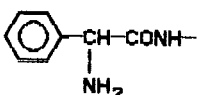
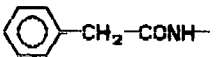
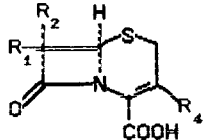
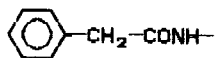
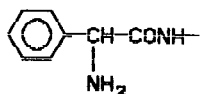
No.	Generic name or code	R ₁	R ₂	R ₃ '
30	Dicloxacillin		H	H
31	Fluoxacillin (floxacillin)		H	H
32	Flucloxacillin		H	H
33	Methicillin		H	H
34	Nafcillin		H	H
35	Cyclacillin		H	H
36	Epicillin		H	H
37	<i>n</i> -Heptylpenicillin (penicillin K)	CH ₃ -(CH ₂) ₆ -CONH-	H	H
38	D-α-(δ-Aminoadipyl)penicillin (penicillin N)		H	H
39	Chlormethylpenicillin	Cl-CH ₂ -CONH-	H	H
40	Mecillinam (amdinocillin)		H	H

TABLE I (continued)

No.	Generic name or code	R ₁	R ₂	R ₃ ^a
41	Hetacillin		H	H
42	BRL 20 153		OCH ₃	H
43	Temocillin (anion)		OCH ₃	H
44	BRL 26 277 (anion)		SCH ₃	H
45	Penamecillin		H	CH ₂ OAc
46	Pivampicillin		H	CH ₂ OCC(CH ₃) ₃
47	Penethacillin		H	C ₂ H ₄ NEt ₂
 <p>Cephalosporins</p>				
No.	Generic name or code	R ₁	R ₂	R ₄
48	7-Aminocephalosporanic acid (7-ACA)	NH ₂	H	CH ₂ OAc
49	Cephalexin		H	CH ₂ OAc
50	Cephaloglycin		H	CH ₂ OAc

(Continued on p. 10)

TABLE I (continued)

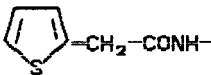
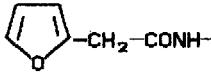
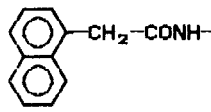
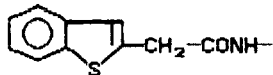
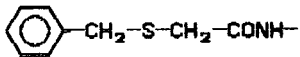
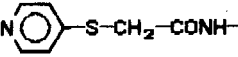
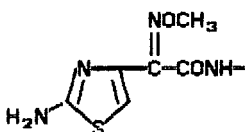
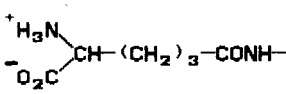
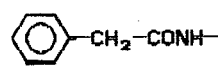
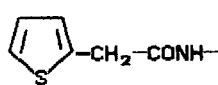
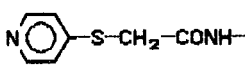
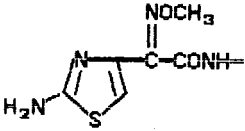
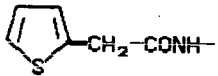
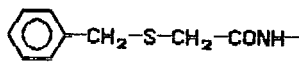
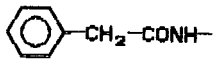
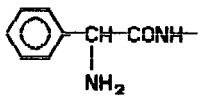
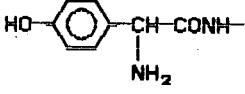
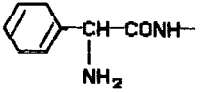
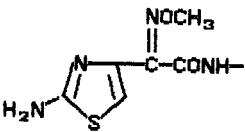
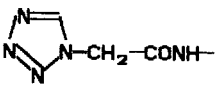
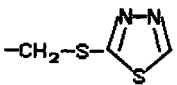
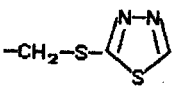
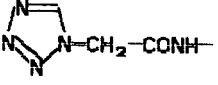
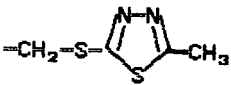
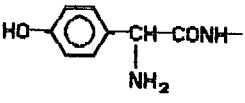
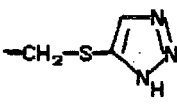
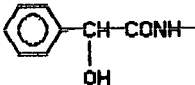
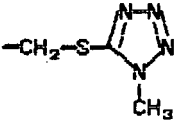
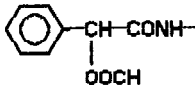
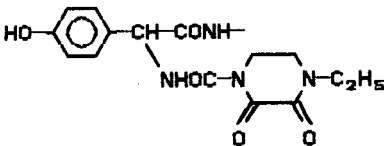
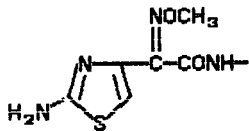
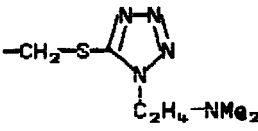
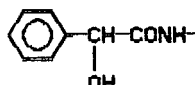
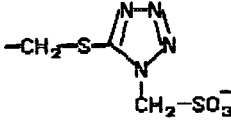
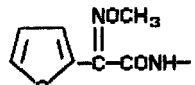
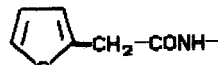
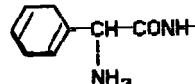
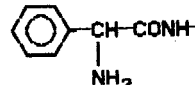
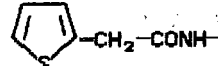
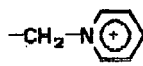
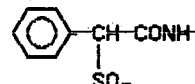
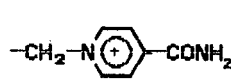
No.	Generic name or code	R ₁	R ₂	R ₄
51	Cephalothin		H	CH ₂ OAc
52	2-Furylacetamidocephalosporin		H	CH ₂ OAc
53	1-Naphthylacetamidocephalosporin		H	CH ₂ OAc
54	Benzothienylacetamidocephalosporin		H	CH ₂ OAc
55	Benzylthioacetamidocephalosporin		H	CH ₂ OAc
56	Cephapirin		H	CH ₂ OAc
57	Cefotaxime		H	CH ₂ OAc
58	Caprylacetamidocephalosporin	CH ₃ -(CH ₂) ₆ -CONH-	H	CH ₂ OAc
59	Cephalosporin C		H	CH ₂ OAc
60	Cephacetrile	NC-CH ₂ -CONH-	H	CH ₂ OAc
61	Chloracetamidocephalosporin	Cl-CH ₂ -CONH-	H	CH ₂ OAc
62	Deacetylcephaloram		H	CH ₂ OH
63	Deacetylcephalothin		H	CH ₂ OH
64	Deacetylcephapirin		H	CH ₂ OH

TABLE I (continued)

No.	Generic name or code	R ₁	R ₂	R ₄
65	Deacetylcefotaxime		H	CH ₂ OH
66	Deacetoxy-3'-azidocephalothin		H	CH ₂ N ₃
67	7-(Benzylthioacetyl)aminodeacetoxy-3'-azidocephalosporanic acid		H	CH ₂ N ₃
68	7-Aminodeacetoxycephalosporanic acid (7-ADCA)	NH ₂	H	CH ₃
69	Deacetoxycephaloram		H	CH ₃
70	Cephalexin		H	CH ₃
71	Cefadroxil		H	CH ₃
72	Cefradine		H	CH ₃
73	Ceftizoxime		H	H
74	Ceftezole		H	
75	C 49 753 (Ciba Geigy)	NC-CH ₂ -CONH-	H	
76	Cefazolin		H	
77	Cefatrizine		H	

(Continued on p. 12)

TABLE I (continued)

No.	Generic name or code	R ₁	R ₂	R ₄
78	Cefamandole		H	
79	Cefamandole nafate		H	As No. 78
80	Cefoperazone		H	As No. 78
81	C 49 288 (Ciba Geigy)	NC-CH ₂ -CONH-	H	As No. 78
82	7-H-Cefmetazole	NC-CH ₂ -S-CH ₂ -CONH-	H	As No. 78
83	Cefotiam		H	
84	Cefonicid		H	
85	Cefuroxime		H	CH ₂ OCONH ₂
86	Cefoxitin		OCH ₃	CH ₂ OCONH ₂
87	Cefrodaxin		H	OCH ₃
88	Cefaclor		H	Cl
89	Cephaloridine (cation)		H	
90	Cefsulodin (zwitterion)		H	

^a The relative hydrophobicity values for penicillins do not depend on the cation near the C-3 carboxyl anion (except in the case of protonation), therefore the R₃ radical conventionally is denoted as H. Ac = Acetyl; Me = methyl; Et = ethyl.

As far as the aqueous phase properties are concerned, the situation seems to be much more complicated. It follows from the results of many studies that varying the mobile phase composition in reversed-phase liquid chromatography (RP-LC) does not necessarily lead to a linear change in $\log k$. It may be assumed, however, that such unpredictable behaviour during chromatography is due to eluate interactions with free silanol groups on the column [39]. Indeed, the data from ref. 40 indicate that under conditions eliminating silanophilic interactions, the variation of the organic solvent content or pH of the eluent leads to linear $\log k$ changes (eqn. 1) for cephalosporins without C-7 and C-3 ionogenic groups. Analogously, the mobile phase variation in refs. 20–22 led merely to linear changes in R_M for cephalosporins and penicillins in RP thin-layer chromatography (TLC).

The evidence cited above testifies that by the linear transformations in eqn. 1 the literature partition data of at least the majority of β -lactam antibiotics can be brought into a single hydrophobicity scale.

RESULTS AND DISCUSSION

A unified penicillin hydrophobicity scale

It is most convenient to choose partitioning between water and octanol as standard conditions when reducing a large body of literature data to a common scale, as in this instance the hydrophobicity of individual antibiotics might be calculated according to well known rules [32,41]. However, the $\log P$ values of β -lactam antibiotics for octanol–water partitioning are not convenient owing to their self-association in hydrophilic media (see the last section). We believe that ignoring this fact was the main reason why earlier attempts to predict the partitioning of penicillins [30,89] were unsuccessful, and only poor correlations between calculated and experimental $\log P$ values were achieved ($r < 0.94$). In fact, at present no octanol–water partition data on β -lactam antibiotics free from the self-association contribution are available. Therefore, we tried to find an “ideal” hydrophobicity scale that would satisfy the following requirements: it should describe the partitioning of β -lactam antibiotics adequately, and it should be free from contributions of various secondary equilib-

rium processes, so that the hydrophobicity for the simplest structures could be easily calculated.

$\log P$ values for octanol–water partitioning of penicillin R_1 -substituent amides proved to meet these requirements. The calculated $\log P$ values for single amides correlated well with experimental data for the proper penicillins from refs. 19–22, with a correlation coefficient always exceeding 0.99. A detailed calculation of these $\log P$ values is given in the Appendix. Tables II and III list the standardized penicillin hydrophobicity values, f_{Common} , obtained by linear transformations of the literature data to the $\log P$ scale of the R_1 -substituent amides. The correlation parameters of these transformations are listed in Table IV for each case.

Methicillin appeared to contain an R_1 substituent with a large H-acceptor ability in comparison with other penicillins. Therefore, the two individual f_{C6} values were necessary for it in hydrophilic and lipophilic organic phases.

As the antibiotics 43–47 in Table I contain modified penicillin nuclei, their f_{Common} values should be regarded as a sum of hydrophobicity increments, f_{C6} for the C-6 substituent (or f_{C7} in the case of cephalosporins) and f_{Nuclei} for the modified nucleus:

$$f_{\text{Common}} = f_{C6(C7)} + f_{\text{Nuclei}} \quad (4)$$

Such an additive hydrophobicity representation is permissible, as the distance between the various substituents in the solute molecules is large enough, and their intramolecular interactions, according to ref. 32, can be neglected. The corresponding values of f_{Common} and f_{Nuclei} are given in Table III.

The problem of the correct determination of the column void volume often arises when reversed-phase high-performance liquid chromatographic (RP-HPLC) data have to be correlated. For instance, the eluent retention time obtained in refs. 54 and 66 exceeds that of the first antibiotics. As the accuracy of t_0 determination greatly affects the $\log k$ value for the most hydrophilic antibiotics, in some instances it has been estimated by us proceeding from the correlation standard error minimization. The chromatographic data in refs. 43 and 47 cannot be described by the f_{Common} scale, indicating large non-hydrophobic interactions between the eluted penicillins and the stationary phases. Amino-containing compounds are known to be especially disposed to enhanced silanophilic interactions [39].

TABLE II

STANDARD PENICILLIN HYDROPHOBICITY VALUES NORMALIZED TO COMMON OCTANOL-WATER PARTITION LOG *P* SCALE OF THEIR 6-SUBSTITUENT AMIDES

No. ^a	Standard hydrophobicity value, f_{C6}^b	References which confirm the f_{C6} value ^c
1	-0.800 ^d (H, L) ^e	21, 26, 45, 56
2	0.451 (H, L)	9, 17-19, 21-25, 28, 36, 43-45, 48, 51-57, 59, 60, 63, 64, calc. ^f
3	-0.220 (H, L)	48, 53, calc.
4	-0.098 (H, L)	9, 17, 20-22, 25, 26, 36, 42-45, 47, 49, 52, 55-57, 59, 60, 64, calc.
5	-0.743 (H, L)	9, 17, 25, 26, 36, 42, 44-46, 49, 57, 59, 60, calc.
6	-0.573 (L)	20, 21, 64
7	-0.060 (H)	19, calc.
8	-0.820 (L)	9, 20-22, 44, 45, 47, 54, 57, 58
9	2.250 (H, L)	24, 25, 44, 63
10	3.230 (H)	24
11	-1.125 (L)	9, 25
12	1.230 (H, L)	18, 44, 45, 57
13	0.450 (H, L)	36, 42, 46, 47, 54, calc.
14	-0.220 (L)	42
15	0.070 ^g (L)	42
16	-0.510 ^g (L)	42
17	-0.110 ^g (L)	46
18	2.142 (L)	44
19	0.289 (H, L)	21, calc.
20	-1.013 (L)	9, 44, 46, 47, 54, 58, 61
21	-0.042 (H, L)	21, calc.
22	1.557 (H, L)	21, calc.
23	0.890 (H, L)	17-28, 36, 43-45, 48, 52, 53, 55-57, 59, 60, 63, calc.
24	1.101 (H, L)	17-25, 28, 44, 45, 55, 56, 63, calc.
25	1.683 (H, L)	17, 19, 23-25, 28, 43-45, calc.
26	1.580 (H)	19, calc.
27	1.226 (H, L)	21, calc.
28	1.189 (H, L)	9, 17, 18, 20-28, 43-45, 49-51, 59, 60, 62, 64
29	1.467 (H, L)	9, 17, 18, 20-27, 36, 44, 45, 49-51, 60, 62-65
30	1.950 (H, L)	9, 17, 21-25, 27, 44, 45, 49-51, 60, 62, 65
31	1.588 (H, L)	17, 24, 25, 43
32	1.640 (L)	20, 27, 44, 45, 49, 63-65
33	0.385 (L)	9, 21, 22, 27, 44, 45, 53, 60, 62
	-0.250 (H)	18, 19, 23, 24
34	1.545 (L)	21, 22, 45, 46, 58-60
35	0.613 (H, L)	17, 25, 45, 57
36	-0.010 (H, L)	17, 44, 57
37	1.943 (H, L)	21, calc.
38	-1.242 (L)	21
39	-0.690 (H, L)	21, calc.
40	0.552 ^{d,g} (L)	57
41	0.060 ^d (L)	45, 49

^a The numbers correspond to those in Table I.^b For penicillins $f_{C6} = f_{Common}$ (see text).^c References in which predicted hydrophobicity differed from the standard f_{Common} value by less than 0.1 are included here.^d These antibiotics possess a non-traditional penicillin structure, therefore the hydrophobic values cannot be experimentally measured as log *P* for the proper amides.^e The letters in parentheses indicate the type of organic-water system for which the given value was shown to be valid: H = hydrophilic; L = lipophilic.^f Calculated in Appendix.^g These are uncertain values.

TABLE III
STANDARD HYDROPHOBICITY VALUES FOR THE
PENICILLINS WITH MODIFIED NUCLEI (f_{Common})

No. ^a	f_{Common}	f_{C_6} ^b	f_{Nuclei}	References which confirm the f_{Common} value ^c
42	0.176 (L) ^d	0.289	-0.113	61
43	-1.126 (L)	-1.013	-0.113	44, 61
44	-1.040 (L)	-1.013	-0.027	61
45	2.300 (L)	0.450	1.850	45
46	2.370 (L)	-0.098	2.468	45
47	1.820 (L)	0.450	1.370	45

^{a,c,d} See footnotes *a*, *c* and *e*, respectively, in Table II.

^b The f_{C_6} values have been taken from Table II.

This appears to be the reason why the f_{C_6} values of penicillins 4, 5, 6, 35 and 36 most often deviate from the relationships established in Table IV.

In refs. 38–40, the conditions for virtually complete elimination of silanophilic interactions between the eluate and RP stationary phases were enumerated: an enhanced ionic strength and pH, a moderate concentration of organic cosolvent and the presence of a hydrophobic alkylamine in the eluent. In fact, the chromatographic parameters from refs. 20–22, 25 and 49, where these requirements for elution were satisfied, correlate perfectly with the hydrophobic parameters in Table II.

Retention of cephalosporins in reversed-phase chromatography

In contrast to penicillins, no data are available on relations between the chromatographic behaviour of cephalosporins and their partition in water-organic solvent systems. Moreover, studying retention of fifteen cephalosporins on different RP-HPLC columns, Wouters and co-workers [66,67] came to the conclusion that no relationships among the structure of antibiotics, their elution time and different properties of RP-HPLC columns could be established. However, if reassessed, these data indicate that such relationships do in fact exist.

Table V presents a matrix of correlation coefficients between $\log k$ of all the cephalosporins reported in refs. 66 and 67 (top right part of the table) and between $\log k$ of selected cephalosporins with the same C-3 substituent (bottom left part of

the table) on different RP-HPLC columns. Considering the relationships between $\log k$ values of the cephalosporins with different C-3 radicals, it will be easy to see that all the columns listed in this table can be divided into two groups: columns 1–8 and columns 10–13; column 9 occupies an intermediate position. The retention of cephalosporins on the columns inside each group can be interrelated by the eqn. 1, with the slope being close to 1. $\log k$ values for cephalosporins on columns from different groups are poorly correlated. Of all the columns, Zorbax C₈ is distinguished as the $\log k$ values in this instance cannot be linearly related to those on other columns.

According to the theory of Horváth and co-workers [38,39,68], a least two types of forces contribute to solute-stationary phase interactions, hydrophobic and silanophilic. Therefore, in order to describe the interrelation of the $\log k$ values of cephalosporins on different columns, eqn. 1 should be supplemented by taking account of the additional type of interaction:

$$\begin{aligned} \Delta G_i &= a_i \Delta G_{\text{Hydroph}} + b_i \Delta G_{\text{Non-hydroph}} + c_i \\ \Delta G_j &= a_j \Delta G_{\text{Hydroph}} + b_j \Delta G_{\text{Non-hydroph}} + c_j \end{aligned} \quad (5)$$

where $\Delta G_{\text{Hydroph}}$ and $\Delta G_{\text{Non-hydroph}}$ are, respectively, the free energies of hydrophobic and silanophilic interactions between the eluate and the stationary phase. $\Delta G_{i(j)}$ is the total free energy of eluate sorption on the column, so it is directly proportional to $\log k$; $b_{i(j)}$ is a certain characteristic of the column which depends on the number of free silanol groups. $\Delta G_{\text{Hydroph}}$ and $\Delta G_{\text{Non-hydroph}}$ values depend only on the eluate properties, and $a_{i(j)}$, $b_{i(j)}$ characterize only the stationary and mobile phases. The equation system 5 is reduced to the single-parameter eqn. 1 in the following cases:

(a) For all the eluates either $\Delta G_{\text{Hydroph}} = \text{constant}$ or $\Delta G_{\text{Non-hydroph}} = \text{constant}$. Since this would mean the existence of the linear relationships in eqn. 1 between the $\log k$ values of cephalosporins on any of the two columns, irrespective of their division into separate groups, this case is not observed here.

(b) For columns from the same group the following condition is satisfied:

$$\frac{a_i}{a_j} = \frac{b_i}{b_j} = \alpha \quad (6)$$

TABLE IV
CORRELATION PARAMETERS OF THE LINEAR RELATIONSHIPS IN EQN. 1 BETWEEN THE LITERATURE DATA (ΔG_i) AND THE COMMON HYDROPHOBICITY SCALE OF PENICILLINS, f_{C6} OR f_{Common} , FROM TABLES II AND III (ΔG_j)

Ref.	Organic phase (stationary phase)	Aqueous phase (mobile phase)	Ionic form of antibiotic ^a	Correlated value ^b (ΔG_i)	Slope	Intercept	<i>n</i>	<i>r</i>	<i>s</i>	Included points ^c	Excluded points ^c
	<i>n</i> -Octanol	Water ^d	—	Log <i>P</i>	0.993	0.017	17	0.9976	0.061	2-5, 7, 14, 19, 21-27, 35, 37, 39	—
18	<i>n</i> -Octanol	Acetate buffer (pH 4.0)	—	Log <i>P^e</i>	0.838	1.297	7	0.9953	0.049	2, 12, 23, 24, 28, 29, 33	8, 30
19	<i>n</i> -Octanol	pH 3-4	Un-ionized form	Log <i>P^e</i>	0.772	1.438	7	0.9947	0.066	2, 7, 23-26, 33	—
23	<i>n</i> -Octanol	pH 3-4	Un-ionized form	Log <i>P^e</i>	0.751	1.364	8	0.9960	0.051	2, 23-25, 28-30, 33	—
23	<i>n</i> -Octanol-impregnated TLC plate	pH 3.0	—	$R_M^{e,f}$	0.779	-0.356	8	0.9958	0.055	2, 23-25, 28-30, 33	—
24	<i>n</i> -Octanol	pH 3-6, 0.15 <i>M</i> KCl	Un-ionized form	Log <i>P^e</i>	0.725	1.415	11	0.9953	0.069	2, 9, 10, 23-25, 28-31, 33	—
24	<i>n</i> -Octanol	pH 7.4, 0.15 <i>M</i> KCl	Anion	Log <i>P</i>	0.731	-2.098	6	0.9708	0.158	9, 10, 23, 25, 30, 31	—
25	<i>n</i> -Octanol	pH 7.4, 0.15 <i>M</i> KCl	Un-ionized form; estimated	Log <i>P</i>	0.735	1.413	12	0.9986	0.043	2, 4, 5, 9, 11, 23-25, 28-31	35
17	Isobutanol	pH 7.4, 0.15 <i>M</i> KCl	Anion	Log <i>P</i>	0.535	-0.411	11	0.9967	0.039	4, 5, 23-25, 28-31, 35, 36	—
24	Isobutanol	pH 7.4, 0.15 <i>M</i> KCl	Anion	Log <i>P^e</i>	0.434	-0.323	11	0.9791	0.088	2, 9, 10, 23-25, 28-31, 33	—
24	Isobutanol	pH 7.4, 0.15 <i>M</i> KCl	Anion	Log <i>P^e</i>	0.512	-0.393	9	0.9858	0.064	2, 23-25, 28-31, 33	9, 10
26	<i>n</i> -Butanol	0.5 <i>M</i> KCl, 37°C	Anion	Log <i>P</i>	0.352	-0.296	5	0.9701	0.102	1, 4, 5, 23, 29	—
27	Chloroform	Teorell buffer	Anion	Log <i>P</i>	1.306	0.506	6	0.9972	0.061	23, 28-30, 32, 33	—
28	Chloroform	0.1 <i>M</i> , 25°C	Un-ionized form	(Log <i>P</i> + p <i>K_a</i>)	1.208	3.318	5	0.9753	0.142	2, 23-25, 28	—
28	Chloroform	0.1 <i>M</i> , 25°C	Un-ionized form	(Log <i>P</i> + p <i>K_a</i>)	1.522	3.067	4	0.9955	0.059	2, 23, 24, 28	25
28	Chloroform	0.1 <i>M</i> , 25°C	Anion	Log <i>K_{ox}^g</i>	1.266	1.609	5	0.9713	0.161	2, 23-25, 28	—
28	Chloroform	0.1 <i>M</i> , 25°C	Anion	Log <i>K_{HAX}^h</i>	1.228	3.195	5	0.9529	0.203	2, 23-25, 28	—
28	Chloroform	0.1 <i>M</i> , 25°C	Un-ionized form	Log <i>K_{Ass}ⁱ</i>	-0.144	2.054	3	-0.9455	0.028	23, 25, 28	24
9	Silica gel 60 F ₂₅₄ ^m (Merck)	Acetate-veronal buffer + 20% CH ₃ OH, pH 7.0	Anion	R_M	0.614	-0.118	10	0.9844	0.129	2, 4, 5, 8, 11, 20, 28-30, 33	—
20	Silica gel G ^m	Extrapolated to 0% acetone, pH 7.4	Anion	R_M	0.776	0.166	8	0.9993	0.029	4, 6, 8, 23, 24, 28, 29, 32	5
21	Silica gel G ^m	Extrapolated to 0% acetone, pH 7.4	Anion	R_M	0.773	0.172	11	0.9991	0.030	2, 4, 6, 8, 23, 24, 28-30, 33, 34	—
21	Silica gel G ^m	Extrapolated to 0% acetone, pH 7.4	Anion	R_M^j	0.720	0.211	10	0.9975	0.057	1, 2, 4, 19, 21, 22, 27, 37-39	—
22	Silica gel G ^m	Extrapolated to 0% acetone, pH 9.4	Anion	R_M	0.710	0.129	10	0.9956	0.060	2, 4, 8, 23, 24, 28-30, 33, 34	—
22	Silica gel G ^m	Extrapolated to 0% acetone, pH 2.6	Un-ionized form	R_M	0.807	0.363	10	0.9810	0.142	2, 4, 8, 23, 24, 28-30, 33, 34	—

42	Silica gel 60 F ₂₅₄ ^m (Merck)	0.05 M phosphate buffer, pH 7.0	Anion	R_M	1.492	0.556	6	0.9814	0.138	4, 5, 13-16	-
43	HPTLC plates F ₂₅₄ ^m (Merck)	0.01 M KH ₂ PO ₄ + 61.5% CH ₃ OH + 7.7% CH ₃ CN, pH 4.1		R_M	0.258	-0.247	6	0.8325	0.132	2, 4, 23, 25, 28, 31	-
44	Silica gel layer ^m	Average of 22 mobile phases, pH \approx 5.0		R_M^f	0.445	-0.149	18	0.9855	0.088	2, 4, 5, 8, 9, 12, 18, 20, 23-25, 28-30, 32, 33, 36, 43	-
44	Silica gel layer ^m	Average of 22 mobile phases, pH \approx 5.0		R_M^f	0.412	-0.087	15	0.9981	0.029	2, 8, 9, 12, 18, 20, 23- 25, 28-30, 32, 33, 43	4, 5, 36
45	Silica gel HF ₂₅₄ ^m	Phthalate buffer + 20% acetone, pH 6.0; first elution		R_M	0.759	-0.468	18	0.9872	0.119	1, 2, 4, 5, 8, 12, 23-25, 28-30, 32-34, 36, 41, 47	6, 35
45	Silica gel HF ₂₅₄ ^m	As above, second elution		R_M	0.839	-0.762	18	0.9901	0.114	2, 4, 5, 8, 12, 23-25, 28-30, 32-34, 36, 41, 45, 47	6, 35
45	Silica gel HF ₂₅₄ ^m	As above, third elution		R_M	0.851	-0.925	19	0.9893	0.124	2, 4, 5, 8, 12, 23-25, 28-30, 32-34, 36, 41, 45-47	6, 35
25	Zorbax-ODS	0.035 M NH ₄ Cl + 30% CH ₃ OH	Anion	Log k	0.755	-0.380	13	0.9710	0.198	2, 4, 5, 9, 11, 23-25, 28-31, 35	-
25	Zorbax-ODS	0.035 M NH ₄ Cl; extrapolated to 0% CH ₃ OH, pH 7.4	Anion	Log k	0.712	1.000	10	0.9987	0.043	2, 4, 5, 9, 11, 23, 24, 29-31	-
36	Spherisorb-ODS	0.05 M phosphate buffer + 20% isopropanol, pH 7.25, 15°C	Anion	Log k , $t_0 = 1.8$	0.607	0.073	6	0.9939	0.058	2, 4, 5, 13, 23, 29	-
46	LiChrosorb RP-18	0.01 M sodium acetate + 20% CH ₃ CN, pH 3.15		Log t , $t_0 = 0$	0.492	0.638	5	0.9857	0.099	5, 13, 17, 20, 34	-
47	Ultrasphere-ODS	6 mM MOPS-TEA buffer + 40% CH ₃ OH, pH 6.7	Anion	Log t , $t_0 = 0$	-0.106	0.795	4	-0.2896	0.289	4, 8, 13, 20	-
48	RP-8, Brownlee Labs.	0.05 M phosphate buffer + 53% CH ₃ OH, pH 3.5		Log t , $t_0 = 0$	0.283	0.766	3	0.9938	0.032	2, 3, 23	-
50	μ Bondapak C ₁₈	0.1 M borate buffer + 0.6% cetyltri- methylammonium bromide + 23% <i>n</i> -propanol, pH 8.5	Anion	Log k , $t_0 = 2.5$	0.332	0.427	7	0.9995	0.001	4, 5, 28-30, 32, 41	-
50	RP-2, Brownlee Labs.	0.05 M phosphate buffer + 20% CH ₃ CN, pH 4.5		Log t , $t_0 = 0$	0.559	-0.827	3	0.9996	0.009	28-30	-

TABLE IV (continued)

Ref.	Organic phase (stationary phase)	Aqueous phase (mobile phase)	Ionic form of antibiotic ^a	Correlated value ^b (ΔG_i)	Slope	Intercept	<i>n</i>	<i>r</i>	<i>s</i>	Included points ^c	Excluded points ^c
51	Develosil-ODS-10	50% CH ₃ OH, pH 2.5		Log <i>k</i>	0.357	0.523	4	0.9997	0.006	2, 28-30	4, 5, 8, 35
52	Anion-exchange resin	0.02 M NaNO ₃ + 0.01 M borate buffer, pH 9.15	Anion	Log <i>k</i> , <i>t</i> ₀ = 4.7	0.741	-0.328	3	0.9993	0.019	2, 4, 23	—
53	RP-HPLC column	Linear gradient: 0.01 M NaH ₂ PO ₄ + 0.01 M EDTA + 16.5-31.5% CH ₃ OH		Log <i>t</i> , <i>t</i> ₀ = 0	0.427	0.837	4	0.9469	0.081	2, 3, 23, 33	—
54	Ultrasphere-ODS	0.01 M NaH ₂ PO ₄ + 15% CH ₃ CN, pH 4.7, 45°C		Log <i>k</i>	1.231	0.364	4	0.9862	0.201	2, 8, 13, 20	—
55	Bondapak C ₁₈	0.15 M buffer + 30% CH ₃ OH	Anion	Log <i>k</i>	0.784	0.470	4	0.9969	0.040	2, 4, 23, 24	—
56	Styrene-divinylbenzene copolymer	0.15 M buffer + 50% CH ₃ OH	Anion	Log <i>k</i>	0.996	0.660	5	0.9930	0.106	1, 2, 4, 23, 24	—
57	LiChrosorb RP	0.1 M phosphate buffer + 30% CH ₃ OH, pH 8.0	Anion	Log <i>k</i>	0.824	0.542	9	0.9598	0.181	2, 4, 5, 8, 12, 23, 35, 36, 40	—
58	Bondapak phenyl (Waters Assoc.)	0.01 M ammonium acetate, pH 7.0	Anion	Log <i>t</i> , <i>t</i> ₀ = 0	0.328	0.561	3	0.9836	0.121	8, 20, 34	—
59	Spherisorb S5-ODS	1 mM acetate buffer + 10% CH ₃ CN, pH ≈ 4.0		Log <i>k</i>	1.095	0.208	5	0.9921	0.124	2, 4, 5, 23, 28	—
59	Spherisorb S5-ODS	1 mM acetate buffer + 20% CH ₃ CN, pH ≈ 4.0		Log <i>k</i>	0.427	-0.330	4	0.9923	0.030	2, 23, 28, 34	—
60	Chromegabond C ₁₈	0.01 M KH ₂ PO ₄ + CH ₃ OH + CH ₃ CN		Log <i>k</i> , <i>t</i> ₀ = 3.2	0.689	-0.432	9	0.9926	0.078	2, 4, 5, 23, 28-30, 33, 34	—

61	μ Bondapak C ₁₈	0.1 M phosphate buffer + 10% CH ₃ OH, pH 7.0	Anion	Log <i>t</i> , <i>t</i> ₀ = 0	0.654	1.669	4	0.9912	0.066	20, 42-44	—
62	C ₈	Extrapolated to 0% CH ₃ CN		Log <i>k</i>	0.740	0.998	3	0.9991	0.018	28-30	33
62	C ₈	Extrapolated to 0% CH ₃ CN		Log <i>k</i> ^k	0.728	1.990	4	0.9991	0.024	28-30, 33	—
63	—	Water, 30°C		Log CMC ^l	-0.473	-0.189	6	-0.9644	0.091	2, 9, 23, 24, 29, 32	—
63	—	0.15 M KCl, 30°C		Log CMC ^l	-0.655	-0.166	6	-0.9895	0.067	2, 9, 23, 24, 29, 32	—
64	μ Bondapak C ₁₈	0.015 M phosphate buffer + 30% CH ₃ OH, pH 7.0	Anion	Log <i>t</i> , <i>t</i> ₀ = 0	0.491	0.826	6	0.9946	0.039	2, 4, 6, 28, 29, 32	5
65	Hypersil-ODS	0.01M Na ₂ HPO ₄ , extrapolated to 0% CH ₃ CN and pH 0, 28°C	Un-ionized form	Log <i>k</i> ^j	0.122	0.850	3	0.9983	0.002	29, 30, 32	—

^a The ionic form of antibiotic is given here when it was especially indicated in the original references or in cases when it was possible to define the ionic state from the partitioning conditions (pH of aqueous phase).

^b *P*, *k* and *t* are the partition coefficient, capacity factor and retention time of antibiotics, respectively; *t*₀ is retention time of the eluent (min).

^c The numbers correspond to those in Table I. Excluded points refer to antibiotics with additionally ionized side-chains under partition conditions or those which diverge sharply from established relationships.

^d Calculated in Appendix for the proper R_{CE} amides.

^e In these instances the hydrophilic partition value *f*_{CE} of -0.250 for methicillin was used. In all the other instances the lipophilic value of 0.385 was accepted (see Table II).

^f Data for the other mobile and stationary phases given in these papers correlated analogously.

^g *K*_{OX} is the coefficient of extraction by the tetrabutylammonium cation: $K_{OX} = [Q^+X^-]/([Q^+][X^-])$, where Q⁺ is the tetrabutylammonium cation and X⁻ is the penicillin anion.

^h *K*_{HAX} is the coefficient of extraction by dodecylammonium cation: $K_{HAX} = [HA^+X^-]/([HA^+][X^-])$, where HA⁺ is the dodecylammonium cation and X⁻ is the penicillin anion.

ⁱ *K*_{ASS} is the dimerization constant of protonated penicillin (see Scheme 1).

^j In this instance the data for C-3'-acetylcephalosporins were correlated.

^k In this instance the data for the {(1,4-dihydro-1-methyl-3-pyridinyl)carbonyl}methyl esters of the proper penicillins were correlated (see Table VIII).

^l CMC is critical micelle concentration (mol kg⁻¹) of the penicillins in aqueous solutions.

^m Impregnated with silicone oil or other reversed-phases.

TABLE V

CORRELATION MATRIX BETWEEN LOG k OF FOURTEEN CEPHALOSPORINS^a WITH DIFFERENT C-3 SUBSTITUENTS, NOS. 50, 51, 56, 57, 59, 70, 71, 72, 76, 77, 78, 85, 86 AND 88 ACCORDING TO TABLE I (TOP RIGHT PART OF THE TABLE), AND BETWEEN LOG k OF FIVE CEPHALOSPORINS WITH THE SAME C-3 SUBSTITUENT NOS. 50, 51, 56, 57 AND 59 (BOTTOM LEFT PART OF THE TABLE) ON DIFFERENT RP-HPLC COLUMNS

No. ^b	Column ^c	1	2	3	4	5	6	7	8	9	10	11	12	13	14	Methyl red adsorption value (mg/g) ^d
1	LiChrosorb RP-8, Hibar, 10 μ m	1	0.990	0.974	0.983	0.990	0.996	0.983	0.991	0.985	0.962	0.934	0.954	0.888	0.968	ND
2	LiChrosorb RP-8, 10 μ m	0.998	1	0.986	0.976	1.000	0.997	0.988	0.997	0.990	0.981	0.959	0.976	0.921	0.958	2
3	LiChrosorb RP-8, 5 μ m	0.994	0.998	1	0.984	0.986	0.987	0.998	0.989	0.960	0.951	0.913	0.937	0.866	0.916	2
4	LiChrosorb RP-8 ^{e,f} , 10 μ m	0.992	0.990	0.993	1	0.975	0.985	0.991	0.981	0.956	0.921	0.881	0.919	0.831	0.910	2
5	LiChrosorb RP-8 ^{e,f} , 10 μ m, 2 years later	0.998	1.000	0.998	0.989	1	0.997	0.987	0.997	0.990	0.979	0.956	0.974	0.915	0.955	2
6	LiChrosorb, RP-8 ^{e,f} , Hibar, 10 μ m	0.998	1.000	0.998	0.989	1.000	1	0.991	0.999	0.988	0.974	0.948	0.965	0.907	0.973	ND
7	LiChrosorb RP-8 ^{e,f} , 5 μ m	0.996	0.998	1.000	0.996	0.998	0.998	1	0.992	0.964	0.948	0.910	0.936	0.860	0.924	2
8	μ Bondapak C ₁₈ , 10 μ m	0.998	1.000	0.999	0.994	0.999	0.999	1.000	1	0.988	0.970	0.944	0.966	0.906	0.955	1
9	Nucleosil C ₁₈ , 10 μ m	0.999	0.998	0.993	0.989	0.998	0.998	0.995	0.997	1	0.981	0.973	0.989	0.951	0.973	ND
10	Nucleosil C ₈ , 10 μ m	0.985	0.987	0.977	0.957	0.986	0.988	0.976	0.982	0.988	1	0.991	0.984	0.961	0.967	13
11	Polygosil C ₈ , 10 μ m	0.978	0.981	0.970	0.948	0.980	0.981	0.968	0.975	0.984	0.998	1	0.991	0.987	0.956	15
12	R-Sil C ₁₈ LL, 10 μ m	0.992	0.993	0.986	0.976	0.995	0.993	0.986	0.990	0.997	0.992	0.993	1	0.982	0.952	92
13	Partisil ODS, 10 μ m	0.977	0.978	0.965	0.948	0.979	0.978	0.965	0.972	0.984	0.993	0.998	0.995	1	0.918	ND
14	Zorbax C ₈ ^f , 7 μ m	0.986	0.989	0.981	0.960	0.989	0.990	0.979	0.984	0.988	1.000	0.996	0.991	0.990	1	0.5

^a In all instances cephaloridine was excluded from the general cephalosporin set, its log k values being apparently outside the general relationships.

^b The numbers in the row correspond to those in the column. Columns with the same $b_{i(j)}$ value are separated by continuous lines.

^c If not stated otherwise, the data were taken from ref. 66. The mobile phase in all instances was 5% phosphate buffer containing 1.0–11.5% CH₃CN.

^d Data from ref. 67. This value characterizes the overall number of residual silanol groups in the columns.

^e Data from ref. 67. The mobile phase in all instances was 0.01 *M* phosphate buffer (pH 7.0) containing 8.5–12.0% CH₃CN.

^f In these instances the values of eluent retention times (t_0) reported in the original papers exceeded those for the most hydrophilic eluates or they were not reported at all, therefore the following values of t_0 were accepted: No. 4, 2.80 min; No. 5, 2.50 min; No. 6, 2.30 min; No. 7, 2.65 min; No. 14, 1.80 min. In all other instances t_0 values reported in ref. 66 were used.

where $a_{i(j)}$, $b_{i(j)}$ are related to eqns. 5 and α to eqn. 1. Indeed, as shown in Table V, columns inside one group have roughly the same number of non-end-capped silanol groups, and therefore $b_i/b_j \approx 1$. The

ratio a_i/a_j cannot noticeably differ from 1, as the reversed-phase was the same (bonded *n*-alkyl) and the eluent composition differed insignificantly in all instances. For columns from different groups, char-

acterized by large differences in the density of free silanol groups, $b_i/b_j \ll 1$ ($\gg 1$), and therefore the linear relationships in eqn. 1 are not observed in this instance. A small change in the composition of the eluent causes only a minor deviation of the ratios a_i/a_j and b_i/b_j from 1, and therefore, irrespective of the RP column properties, good correlations between $\log k_{\text{Eluent}_i}$ and $\log k_{\text{Eluent}_j}$ ($r > 0.99$) are obtained.

It is noteworthy that the amounts of free silanol groups listed for each column in ref. 67 (Table V) should be regarded only as an approximate characteristic of the silanophilic interaction ability of the stationary phase. Actually, the parameter $b_{i(j)}$ should be compared not with the total number of free silanol groups but rather with the proportion that readily interacts with analytes [69]. This is the probable reason why the poor correlation between $\log k$ on the Zorbax C₈ column and the columns inside the first group are observed.

Considering the cephalosporins with the same C-3 substituent, linear relationships (eqn. 1) between $\log k$ are observed for all the columns, independently of their division into separate groups (see the bottom left part of Table V). This demonstrates that if the C-3 radical is constant, the silanophilic interaction increment for different cephalosporins also appears

to be constant. In accordance with the case (a) this leads to the linear relationships in eqn. 1 for any mobile and stationary phases, irrespective of their $a_{i(j)}$ and $b_{i(j)}$ characteristics. However, this does not mean that C-3 substituents themselves interact with the free silanol groups. Most likely, the C-4 carboxyl anion, common to all the cephalosporins, is involved in such an interaction, and different C-3 substituents appear to create a corresponding microenvironment for this group. Charged C-3 substituents exert an especially strong effect. Cephaloridine was reported [67] to be the most sensitive to silanophilic interactions among the studied cephalosporins. Indeed, $\log k$ of cephaloridine sharply deviated from the linear dependence in almost all the eluate sets examined by us (see below). Large positive changes were observed even with a minor change in the mobile phase composition with a constant stationary phase. Ion-ion interactions, extremely sensitive to changes in the bulk medium properties (*i.e.*, in the organic co-solvent concentration in the eluent) appear to take place between the positively charged C-3' pyridinium substituent and the deprotonated C-4 carboxyl group.

The proposed interactions between the C-3 substituent and the C-4 carboxyl anion apparently make the chromatographic behaviour of cephalosporins

TABLE VI
STANDARD CEPHALOSPORIN HYDROPHOBICITY VALUES

No. ^{a,b}	f_{Common}	$f_{\text{C}^3}^c$	f_{Nuclei}^d	References which confirm f_{Common} value ^e
48	-0.801 (L) ^f	-0.800	-0.001	21, 22, 56, 72, 81
49	0.424 (L)	0.451	-0.027	21, 22
50	-0.101 (H, L)	-0.098	-0.003	21, 25, 45, 66, 71, 72, 78, 84
51	0.315 (H, L)	0.289	0.026	6, 9 ^g , 21, 22, 25, 37, 40, 45, 49, 54-56, 66, 71, 73-76, 79, 88
52	-0.050 (L)	-0.042	-0.008	21, 22
53	1.550 (L)	1.557	-0.007	21, 22
54	1.626 (H)	1.600 ^h	0.026	8
55	1.219 (L)	1.226	-0.007	21, 22
56	-0.420 (L)	-0.450 ^h	(0.030)	37, 49, 81
		-0.420 ⁱ		
57	-0.407 (L)	-0.407 ⁱ		40, 54, 66, 71, 74-77, 79, 80, 82, 86-88
58	1.936 (L)	1.943	-0.007	21, 22
59	-1.241 (L)	-1.242	0.001	9 ^g , 21, 22, 66, 71, 81, 84
60	-0.837 (H, L)	-1.460 ^h	(0.624)	6, 8, 9 ^g , 49, 81
		-0.837 ⁱ		
61	-0.698 (L)	-0.690	-0.008	21

(Continued on p. 22)

TABLE VI (continued)

No. ^{a,b}	f_{Common}	f_{C7}^c	f_{Nuclei}^d	References which confirm f_{Common} value ^e
62	-0.367 (L)	0.451	-0.818	21
63	-0.508 (L)	0.289	-0.797	72, 79
64	-1.230 (L)	-0.42 ⁱ	-0.810	37
65	-1.210 (L)	-0.407 ⁱ	-0.803	77, 86, 88
66	0.240 (L)	0.289	-0.049	21, 22
67	1.219 (L)	1.226	-0.007	21, 22
68	-1.110 (L)	-0.800	-0.310	56, 72, 81
69	0.107 (L)	0.451	-0.344	55, 56
70	-0.414 (H, L)	-0.098	-0.316	17, 25, 26, 45, 66, 71, 72, 74, 76, 77, 80, 83-85, 87, 88
71	-1.040 (H, L)	-0.743	-0.297	9 ^g , 17, 66, 74, 80
72	-0.288 (H, L)	-0.010	-0.278	17, 25, 45, 49, 71, 74, 83, 84, 86
73	-0.630 (L)	-0.407 ⁱ	-0.223	74, 82
74	-0.747 (L)	-0.959 ⁱ		9 ^g
75	-0.625 (H)	-0.837 ⁱ	0.212	6
76	-0.370 (H, L)	-0.959 ⁱ	0.589	6, 8, 9 ^g , 25, 37, 40, 49, 54-56, 66, 71, 73, 74, 76, 77, 80, 81, 84, 88
77	-0.546 (L)	-0.743	0.197	66, 71, 83
78	0.111 (H, L)	-0.060	0.171	8, 9 ^g , 40, 54, 66, 71, 73-76, 78, 79, 82
79	0.504 (L)	0.252 ^h	0.252	71, 74
80	0.060 (L)	-0.220	0.280	54, 73, 74, 80
81	-0.620 (H)	-0.837 ⁱ	0.217	6
82	-0.906 (H)	-0.822 ^h -1.136 ⁱ	(-0.084)	8
83	0.238 (L)			40, 85
84	-0.630 (L)	-0.060	-0.570	54
85	-0.404 (H, L)	-0.014 ⁱ	-0.390 ^k	8, 40, 66, 71, 75, 78, 79
86	-0.215 (H, L)	0.289	-0.504	8, 9 ^g , 54, 66, 71, 74-80, 82
87	-0.153 (L)	-0.010	-0.143	40, 85
88	-0.451 (L)	-0.098	-0.353	66, 71, 74, 76, 80, 87
89	-2.051 (L)	0.289	-2.340	26, 49, 81, 88
90	-1.279 ^j (L)	-1.125	-0.154 ^j	9 ^g , 40, 85

^{a,e,f,h,j} See footnotes *a*, *c*, *e*, *f* and *g*, respectively, in Table II.

^b The antibiotics with the same nuclei (*i.e.*, the same C-3 substituent except in the case of cefoxitin) are separated by horizontal lines.

^c If not stated otherwise, the f_{C7} values are taken from Table II.

^d For cephalosporins (except cefoxitin) f_{Nuclei} values represent relative hydrophobicities of the C-3 substituents. The mean f_{Nuclei} values for all the nuclei are given in Table VIII. The f_{Nuclei} values in parentheses were not taken into account when calculating the mean values.

^g In this instance the mean values of the data for 22 antibiotics from refs. 9-16 were correlated. The main part of these data (for sixteen solutes) was given in ref. 9.

ⁱ These f_{C7} values were calculated from reliable f_{Nuclei} values as follows: $f_{\text{C7}} = f_{\text{Common}} - f_{\text{Nuclei}}$.

^k Calculated from the f_{Nuclei} value of cefoxitin by postulating that the hydrophobic increment of 7-OCH₃ was the same as for penicillins (-0.113).

distinctly different from that of penicillins. For the latter silanophilic interactions may be expected always to be identical, as the surrounding of the C-3 carboxyl in their nuclei is always the same. Therefore, in this instance condition (a) for reducing the equation system 5 to eqn. 1 always applies irrespective of the $a_{i(j)}$ and $b_{i(j)}$ values. Hence any set of $\log k$ or R_M values will always correlate with the unified hydrophobicity scale. This is true, of course, only if no specific interactions between the stationary phase and the R_1 substituent are present and in the absence of an R_4 substituent. For cephalosporins the linear relationships in eqn. 1 between $\log k$ or R_M will be observed only on stationary phases with roughly the same number of free silanol groups. However, a unified set of $\log k$ or R_M values obtained by those linear transformations will not necessarily correlate with the common hydrophobicity scale. Probably this is the reason why up to now there has been no published evidence for the correlation between the chromatographic behaviour of cephalosporins and their water-organic solvent partition, whereas for penicillins such relationships have been reported on many occasions.

A unified cephalosporin hydrophobicity scale

As has been stated above, it is most convenient to choose octanol-water partition $\log P$ for the R_1 -substituent amides as standard conditions when reducing the literature data to a single hydrophobicity scale (Table VI). Table VII gives the correlation parameters of these transformations for each case. The zero value for a standard f_{Common} scale was chosen in order to correlate jointly data for penicillins and cephalosporins. In the previous section we have demonstrated that the linear relationships in eqn. 1 may be fulfilled even when the retention of cephalosporins is noticeably affected by silanophilic interactions. Therefore, reducing all RP chromatographic data to a common scale, we paid most attention to their ability to correlate well with the literature data, where silanophilic interactions were minimal. Such data include, especially, $\log k$ and R_M from refs. 21, 22, 40, 49, 75 and 84, where the corresponding conditions of the eluent composition were generally fulfilled (for the enumeration of the indications of an "ideal" eluent, see above), and also $\log k$ on the stationary phases from the first group in Table V.

Table VII shows that the corresponding values for cephalirin (56) and cephaloridine (89) nearly always diverged from the established relationships (eqn. 1). This is probably due to their extraordinary ability for silanophilic interactions, and so f_{Common} values for these antibiotics were calculated proceeding from the most reliable data from ref. 49. Deviation of the retentions of other antibiotics from the established relationships in Table VII is probably due to the protonation-deprotonation ability of their ionogenic R_1 substituents or to the inaccurate column void volumes determined in the original work; this, in turn, badly distorts the $\log k$ values for the most hydrophilic eluates. Generally, the results summarized in Table VII indicate that the published data on the partitioning of β -lactam antibiotics are well described by the common hydrophobicity scale. Therefore, the absence of linear relationships between f_{Common} and the calculated values of $\log P$ from ref. 8 or experimental values from ref. 5 is probably indicative of incorrect results in those studies.

As the total hydrophobicity of cephalosporins, like that of penicillins, is a sum of hydrophobic increments of the C-7 radical and nucleus, Table VI adduces the corresponding values of f_{C7} (taken generally from Table II) and f_{Nuclei} (calculated according to eqn. 4). To make it more convenient for use in calculations, the mean hydrophobicity values of f_{Nuclei} are summarized in Table VIII.

Obviously, using eqn. 4, one can calculate the value of f_{Common} for all β -lactam antibiotics that have the $f_{C6(C7)}$ value for the corresponding R_1 radical in Tables II and VI, and the f_{Nuclei} value for the corresponding nucleus in Table VIII. Compounds containing both a nucleus with the functional R_2 substituent and a non-typical R_1 radical, e.g., 7-amino-7-methoxycephalosporanic acid, form an exception, since in this instance the mutual intramolecular interactions of the variable fragments ought to be taken into account, and eqn. 4 cannot be applied. In all the other instances the variable molecular fragments are sufficiently distant from each other, and thus their intramolecular interactions may be neglected. Much care is needed in estimating hydrophobicity values of antibiotics with charged C-6(C-7) or C-3 radicals because of possible implications in their self-association (see the last section).

It is noteworthy that the $f_{C6(C7)}$ value may be

TABLE VII
CORRELATION PARAMETERS OF THE LINEAR RELATIONSHIPS IN EQN. 1 BETWEEN THE LITERATURE DATA (AG_i) AND COMMON HYDROPHOBICITY SCALE OF CEPHALOSPORINS AND PENICILLINS, f_{common} , FROM TABLES II, III AND VI (AG_i)

Ref.	Organic phase (stationary phase)	Aqueous phase (mobile phase)	Ionic form of antibiotic ^d	Correlated value ^b (AG_i)	Slope	Inter-cept	n	r	s	Included points ^c	Excluded points ^c
5	<i>n</i> -Octanol	0.2 M, pH 7.4	Anion ^d	Log <i>P</i>	-0.707	-2.683	6	-0.3232	1.880	50, 51, 70, 72, 76, 89	—
7, 8	<i>n</i> -Octanol	0.1 M glycine-HCl buffer, pH 2-3, or 0.1 M citrate buffer, pH 4.0	Un-ionized form	Log <i>P</i>	0.909 ^a	0.228	7	0.9921	0.108	54, 60, 76, 78, 82, 85, 86	49, 51, 80
8	<i>n</i> -Octanol	0.1 M glycine or citrate buffer, calculated	Un-ionized form	Log <i>P</i>	0.310	0.366	18	0.2529	0.964	49-51, 54, 57, 59, 60, 70, 73, 76, 78, 80, 82, 85, 86, 88-90	—
29	<i>n</i> -Octanol	0.2 M, pH 8.0	Anion ^d	Log <i>P</i>	0.414	-0.852	4	0.9991	0.019	50, 70, 72, 89	—
6	Isobutanol	0.02 M phosphate buffer + 0.9% NaCl, pH 7.4	Anion ^d	Log <i>P</i>	1.263	-0.869	7	0.9596	0.201	2, 4, 51, 60, 75, 76, 81	89
17	Isobutanol	pH 7.4, 0.15 M KCl	Anion	Log <i>P</i>	0.557	-0.439	14	0.9967	0.047	4, 5, 23-25, 28-31, 35, 36, 70-72	—
26	<i>n</i> -Butanol	0.5 M KCl	Anion ^d	Log <i>P</i>	0.465	-0.342	7	0.9608	0.171	1, 4, 5, 23, 29, 70, 89	—
9 ^e	Silica gel 60 F ₂₅₄ (Merck)	Acetate-veronal buffer + 20% CH ₃ OH, pH 7.0	Anion ^d	R_M	0.636	-0.123	19	0.9863	0.105	2, 4, 5, 8, 11, 20, 28-30, 33, 51, 59, 60, 71, 74, 76, 78, 86, 90	70, 80, 89
21	Silica gel G ⁱ	Extrapolated to 0% acetone, pH 7.4	Anion ^d	R_M	0.741	0.200	24	0.9978	0.047	2, 4, 6, 8, 23, 24, 28, 29, 30, 33, 34, 48-53, 55, 58, 59, 61, 62, 66, 67	89
22	Silica gel G ⁱ	Extrapolated to 0% acetone, pH 9.4	Anion ^d	R_M ^f	0.700	0.218	20	0.9887	0.100	2, 4, 8, 23, 24, 28, 29, 30, 33, 34, 48-53, 55, 58, 59, 66, 67	89
45	Silica gel HF ₂₅₄ ⁱ	Phthalate buffer + 5% acetone, pH 6.0		R_M	1.104	-0.005	4	0.9973	0.032	50, 51, 70, 72	56, 89
45	Silica gel HF ₂₅₄ ⁱ	Phthalate buffer + 20% acetone, pH 6.0		R_M	0.744	-0.438	22	0.9859	0.119	1, 2, 4, 5, 8, 12, 23-25, 28-30, 32-34, 36, 41, 47, 50, 51, 70, 72	6, 35, 56, 89
71	Silica gel ⁱ	15% ammonium acetate + 15% CH ₃ OH, pH 6.2		R_M ^f	0.943	0.593	14	0.9893	0.067	50, 51, 57, 59, 70-72, 76-79, 85, 86, 88	56, 89
72	Silica gel 60 F ₂₅₄ ⁱ (Merck)	25% CH ₃ OH		R_M	0.937	0.090	4	0.9830	0.090	50, 63, 68, 70	51, 48, 89
25	Zorbax-ODS	0.035 M NH ₄ Cl + 30% CH ₃ OH, pH 7.4	Anion ^d	Log <i>k</i>	0.551	-0.101	16	0.9753	0.113	2, 4, 9, 23-25, 28-31, 35, 50, 51, 70, 72, 76	5, 11, 89
37	Octadecylsilane	1 mM [(C ₄ H ₉) ₄]HSO ₄ + 1 mM [(C ₂ H ₅) ₄]OH + 5% CH ₃ CN		Log <i>k</i>	0.656	0.907	4	0.9695	0.128	51, 56, 64, 76	—

40	LiChrosorb RP-18	0.3 M Na ₂ HPO ₄ + Anion 15% CH ₃ OH, pH 8.0	Log k	1.132	1.485	8	0.9977	0.042	51, 57, 76, 78, 83, 85, 87, 90	—
49	μ Bondapak C ₁₈	0.1 M borate buffer + 0.6% cetyltri- methylammonium bromide + 23% <i>n</i> -propanol, pH 8.5	Log k, <i>t</i> ₀ = 2.5	0.333	0.437	13	0.9950	0.040	4, 5, 28-30, 32, 41, 51, 56, 60, 72, 76, 89	—
54	Ultrasphere-ODS	0.01 M NaH ₂ PO ₄ + 15% CH ₃ CN, pH 4.7	Log k	1.171	0.394	11	0.9826	0.118	2, 8, 13, 20, 51, 57, 76, 78, 80, 84, 86	56
54	Ultrasphere-ODS	0.01 M NaH ₂ PO ₄ + 15% CH ₃ CN, pH 4.0	Log k ^f	0.697	0.425	7	0.9968	0.021	51, 57, 76, 78, 80, 84, 86	56
55	Bondapak C ₁₈	0.15 M buffer + 30% CH ₃ OH	Log k	0.872	0.391	7	0.9924	0.062	2, 4, 23, 24, 51, 69, 76	70, 72, 89
55	Bondapak C ₁₈	0.15 M buffer + 20% CH ₃ OH	Log k	0.827	1.071	5	0.9825	0.059	2, 4, 51, 69, 76	70, 72, 89
56	Styrene-divinyl- benzene copolymer μ Bondapak C ₁₈	0.15 M buffer + 50% CH ₃ OH	Log k	0.954	0.744	10	0.9868	0.123	1, 2, 4, 23, 24, 48, 51, 68, 69, 76	70, 72
66	R-Sil C ₁₈ LL	5% phosphate buffer + 10% CH ₃ CN	Log k ^f , <i>t</i> ₀ = 1.50	0.869	1.153	13	0.9852	0.065	50, 51, 57, 59, 70-72, 76-78, 85, 86, 88	56, 89
66	Zorbax C ₈	5% phosphate buffer + 8% CH ₃ CN	Log k ^f , <i>t</i> ₀ = 2.20	0.874	0.931	13	0.9004	0.182	50, 51, 57, 59, 70-72, 76-78, 85, 86, 88	56, 89
66	RP-2 (Merck)	5% phosphate buffer + 1% CH ₃ CN 25% CH ₃ OH	Log <i>t</i> ^f , <i>t</i> ₀ = 0	0.765	1.160	13	0.9080	0.152	50, 51, 57, 59, 70-72, 76-78, 85, 86, 88	56, 89
72	μ Bondapak C ₁₈	5 mM acetate buffer + 25% CH ₃ OH, pH 4.5	Log k	1.151	0.068	4	0.9691	0.158	48, 50, 68, 70	51, 63, 89
73	μ Bondapak C ₁₈	0.02 M acetic acid + 30% CH ₃ OH, pH 3.2	Log <i>t</i> , <i>t</i> ₀ = 0	0.597	1.016	4	0.9869	0.034	51, 76, 78, 80	56, 89
74	μ Bondapak C ₁₈	0.01 M Titrisol- phosphate buffer + 0.4% cetyltri- methylammonium bromide + 35% CH ₃ CN, pH \approx 6.5	Log k, <i>t</i> ₀ = 3.1	0.898	0.652	12	0.9941	0.044	51, 57, 70-73, 76, 78-80, 86, 88	56
75	RP C ₁₈	Acetate buffer + 0.007 M H ₃ PO ₄ + 15% CH ₃ CN	Log <i>t</i> , <i>t</i> ₀ = 0	0.547	1.134	5	0.9890	0.030	51, 57, 78, 85, 86	80
76	C ₁₈	Stearic acid bonded to polysilicate	Log <i>t</i> , <i>t</i> ₀ = 0	0.860	0.829	7	0.9908	0.039	51, 57, 70, 76, 78, 86, 88	56
77	μ Bondapak C ₁₈	0.01 M acetate buffer + 15% CH ₃ OH, pH 4.8	Log k, <i>t</i> ₀ = 3.4	2.151	1.072	5	0.9956	0.092	57, 65, 70, 76, 86	—
78	Stearic acid bonded to polysilicate	0.2% (NH ₄) ₂ CO ₃ + 9% C ₂ H ₅ OH	Log k, <i>t</i> ₀ = 2.0	1.239	0.054	4	0.9849	0.086	51, 78, 85, 86	76, 80
79	μ Bondapak C ₁₈	0.01 M acetate buffer + 15% CH ₃ OH, pH 4.8	Log <i>t</i> , <i>t</i> ₀ = 0	1.287	1.646	6	0.9753	0.107	51, 57, 63, 78, 85, 86	76, 80

TABLE VII (continued)

Ref.	Organic phase (stationary phase)	Aqueous phase (mobile phase)	Ionic form of antibiotic ^d	Correlated value ^b (ΔG_i)	Slope	Inter- cept	<i>n</i>	<i>r</i>	<i>s</i>	Included points ^c	Excluded points ^c
80	Zorbax C ₈	0.05 M lithium citrate buffer + 23% CH ₃ OH, pH 3.0	Anion ^d	Log <i>k</i> , <i>t</i> ₀ = 1.27	1.013	0.827	7	0.9676	0.096	57, 70, 71, 76, 80, 86, 88	—
81	DEAE-Sephadex A-25 (Cl ⁻)	0.2 M sodium acetate, pH 8.0	Anion ^d	Log <i>k</i> ^g , <i>V</i> ₀ = 9.0	0.329	1.175	7	0.9739	0.048	48, 56, 59, 60, 68, 76, 89	51, 70, 72
82	μBondapak C ₁₈	0.5 M acetic acid + 13% CH ₃ CN		Log <i>t</i> , <i>t</i> ₀ = 0	1.015	1.412	4	0.9906	0.055	57, 73, 78, 86	56, 70, 76, 89
83	R-Sil C ₁₈ LL	0.05 M NaH ₂ PO ₄ + Anion 20% CH ₃ OH, pH 7.5		Log <i>k</i>	1.815	1.076	3	0.9996	0.009	70, 72, 77	—
84	μBondapak C ₁₈	0.03% (NH ₄) ₂ CO ₃ + 5% CH ₃ OH		Log <i>k</i> , <i>t</i> ₀ = 2.67	1.427	0.007	5	0.9955	0.069	50, 59, 70, 72, 76	51
85	RP-8	0.09 M K ₃ PO ₄ + 0.1 M [(C ₄ H ₉) ₄]HSO ₄ + 15% CH ₃ OH		Log <i>t</i> , <i>t</i> ₀ = 0	0.310	1.292	4	0.9467	0.083	70, 83, 87, 90	—
86	RP-8	0.02 M NaH ₂ PO ₄ + 23% CH ₃ OH, pH 4.5		Log <i>t</i> , <i>t</i> ₀ = 0	0.425	1.257	3	0.9422	0.107	57, 65, 72	—
87	Bondapak C ₁₈	0.15 M KH ₂ PO ₄ + Anion 18% CH ₃ OH, pH 6.5		Log <i>t</i> , <i>t</i> ₀ = 0	1.416	1.697	4	0.9979	0.018	5, 57, 70, 88	4
88	Radial-Pak C ₁₈	1 mM [(C ₄ H ₉) ₄]OH + 17% CH ₃ CN		Log <i>k</i> , <i>t</i> ₀ = 1.80	0.947	0.810	6	0.9978	0.058	51, 57, 65, 70, 76, 89	—

^{a,b,c,f,i} See footnotes *a*, *b*, *c*, *f* and *m*, respectively, in Table IV.

^d Zwitterionic form for the cephaloridine and cefsulodine.

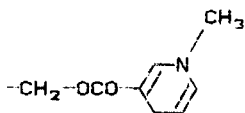
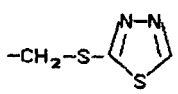
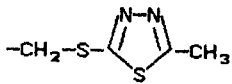
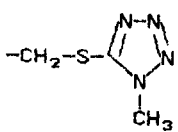
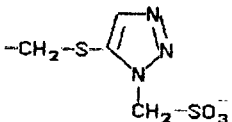
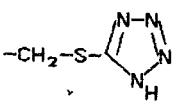
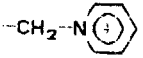

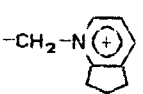
^e In this instance the mean values of the data for 22 antibiotics given in refs. 9–16 under the same conditions were correlated. The main part of these data (for sixteen solutes) is given in ref. 9.

^g In this instance the capacity factor *k* is expressed as follows: $k = (V - V_0)/V_0$, where *V* and *V*₀ are the elution volume of the antibiotic and the column void volume, respectively.

^h In this instance the correlation parameters depended strongly on included or excluded points.

TABLE VIII

STANDARD HYDROPHOBICITY VALUES FOR PENICILLIN AND CEPHALOSPORIN NUCLEI

Nucleus ^a	R ₂ ^b	R ₃	R ₄	f _{Nuclei} ^c
I	H	- ^d	-	0.00 (H, L)
I	OCH ₃	- ^d	-	-0.11 (L)
I	SCH ₃	- ^d	-	-0.03 (L)
I	H	H	-	3.51 ^e (H)
I	H	CH ₂ OAc	-	1.85 (L)
I	H	CH ₂ OOCC(CH ₃) ₃	-	2.47 (L)
I	H	C ₂ H ₄ N(C ₂ H ₅) ₂	-	1.37 (L)
I	H		-	0.88 ^f (L)
II	H	- ^d	H	-0.22 (L)
II	H	- ^d	CH ₃	-0.31 (H, L)
II	H	- ^d	CH ₂ OH	-0.81 (L)
II	H	- ^d	CH ₂ OAc	0.00 (H, L)
II	H	- ^d	CH ₂ OCONH ₂	-0.39 (H, L)
II	H	- ^d	CH ₂ N ₃	-0.03 (L)
II	H	- ^d		0.21 (H)
II	H	- ^d		0.59 (H, L)
II	H	- ^d		0.23 (H, L)
II	H	- ^d		-0.57 ^e (L)
II	H	- ^d		0.20 (L)
II	H	- ^d		-2.34 ^e (L)
II	H	- ^d		-0.15 ^e (L)
II	H	- ^d		ca. 0 ^{e-g} (H)

(Continued on p. 28)

TABLE VIII (continued)

Nucleus ^a	R ₂ ^b	R ₃	R ₄	f_{Nuclei}^c
II	H	— ^d	OCH ₃	−0.14 (L)
II	H	— ^d	Cl	−0.35 (L)
II	OCH ₃	— ^d	CH ₂ OCONH ₂	−0.50 (H, L)

^a I denotes penicillin and II denotes cephalosporin nuclei according to Table I.

^b The substituent designations correspond to those in Table I.

^c Here the f_{Nuclei} values are mean values of those from Tables III and VI. Letters in parentheses have the same meaning as in Table II.

^d C-3(4)-carboxyl anion.

^e Uncertain value (see text).

^f Calculated from ref. 62.

^g From ref. 70, where log P of cefotaxime was stated to be almost the same as for cefpirome.

calculated using the generally accepted additive scheme of Hansch and Leo [32]. Hence theoretically f_{Common} values may be calculated for all β -lactam antibiotics which have one of the nuclei listed in Table VIII. At the same time the Hansch and Leo method does not allow one to estimate the influence of the C-3 radical on the value of f_{Nuclei} . This may be due both to the extremely complex intramolecular H-polar interaction between fragments in the cephalosporin nucleus and their C-3 substituents and to the spatial interaction of the latter with the C-4 carboxyl anion.

The hydrophobicity scale of f_{Common} can describe not only the retention of β -lactam antibiotics in RP chromatography but also their behaviour in ion-exchange and gel chromatography, and their aggregation [critical micelle concentration (CMC) or K_{Ass}] in different aqueous and organic media (Tables IV and VII). The existence of such correlations becomes clear if we assume that the total free energy of the investigated process, $\Delta G_{i(j)}$, can be described by the eqn. 5, where $\Delta G_{\text{Non-hydroph}}$ represents the ability of antibiotics to undergo any non-hydrophobic interactions (*e.g.*, electrostatic), and $b_{i(j)}$ characterizes a corresponding property of the medium (*e.g.*, a dielectric constant). As the energy contribution of these non-hydrophobic interactions is constant for all the antibiotics studied, the system of eqns. 5 is simply reduced to linear dependence in eqn. 1.

Characteristics of partitioning of β -lactam antibiotics in various organic–water systems

The f_{Common} scale shows good correlations with the partitioning of penicillins and cephalosporins in both hydrophilic and lipophilic systems. However,

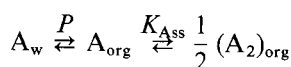
in a number of instances the correlation parameters obtained differ greatly from the expected values. Table IX compares the slopes of the correlations between different partitioning solvent systems for β -lactam antibiotics (α_1) and for various substances devoid of the β -lactam ring (α_2) from ref. 34. Such a discrepancy of these correlation slopes (especially for the octanol–water system) makes it impossible to apply the additivity schemes of Hansch and Leo [32] or Rekker [41] to calculate log P values of these antibiotics.

Earlier these methods were also considered to be inadequate for estimating log P values of penicillins. Attempts were made to explain this fact by various intramolecular interactions, *e.g.*, by shielding effects [23] or hydrogen bonding [31,89]. Meanwhile, the good correlations obtained in Tables IV and VII demonstrate that the observed effect is common for all β -lactams, and does not depend on particular intramolecular interactions in the antibiotic molecules. Moreover, the results in Table IX indicate that the ratio α_1/α_2 depends on the range of experimentally obtained log P values, which, in its turn, depend on the partitioning conditions, *e.g.*, the pH of the aqueous phase. All this is indicative of some secondary equilibrium processes taking place in organic–water systems in the course of partitioning of β -lactam compounds. Indeed, neutral penicillin molecules were shown to be capable of dimerization in chloroform [28] and butyl acetate [90]. The results in Table IX show that such dimerization is also typical of C-3(C-4) carboxyl anions. To describe the partitioning of β -lactam antibiotics, we adopted the following “minimal” scheme:

TABLE IX

DEPENDENCE OF SLOPE α IN EQN. 1 FROM TABLES IV AND VII ON THE PARTITION CONDITIONS

Ref.	Organic phase	Ionic form of antibiotic	Slope α_1 for β -lactam antibiotic ^a	Slope α_2 for non- β -lactam compounds ^b	Normalized slope, α_1/α_2	Range of $\log P_{\text{obs}}^e$	Predicted value of α_1/α_2^d
7, 8	<i>n</i> -Octanol	Un-ionized form	(0.8–1.8) ^e	1.000	(0.8–1.8) ^e	–0.7 ^f to +0.7	0.8–1.6
18	<i>n</i> -Octanol	Un-ionized form (pH 4.0)	0.838	1.000	0.838	1–3	0.8
19	<i>n</i> -Octanol	Un-ionized form	0.772	1.000	0.772	1–3	0.8
23	<i>n</i> -Octanol	Un-ionized form	0.751	1.000	0.751	1–3	0.8
24	<i>n</i> -Octanol	Un-ionized form	0.725	1.000	0.725	0–4	0.8
24	<i>n</i> -Octanol	Anion	0.731	1.000	0.731	0–4	0.8
6	Isobutanol	Anion	1.263	0.697	1.812	–2.0 to –0.2	1.6
17	Isobutanol	Anion	0.557	0.697	0.799	0–4	0.8
24	Isobutanol	Anion	0.512	0.697	0.735	0–1	0.8
26	<i>n</i> -Butanol	Anion	0.465	0.697	0.667	0–2	0.8
27	Chloroform	Anion	1.306	1.276	1.024	1–3	1.0
28	Chloroform	Un-ionized form	1.208	1.276	0.947	1–3	1.0
28	Chloroform	Anion + tetra-butylammonium	1.266	1.276	0.992	1–3	1.0

^a From Tables IV and VII.^b Data taken from ref. 34.^c Ranges of experimentally obtained $\log P_{\text{obs}}$ values which were given in the original references.^d Calculated assuming that $K_{\text{Ass}} \approx P^{-0.4}$ in Scheme 1.^e In this instance the slope depended strongly on the points included or excluded and varied from 0.8 to 1.8.^f Estimated range; in the original references only the recalculated values of $\log P$ were given.

Scheme 1.

where $P = [A_{\text{org}}]/[A_w]$ denotes the real partition coefficient, $K_{\text{Ass}} = [(A_2)_{\text{org}}]/[A_{\text{org}}]^2$ is the association constant, A_w and A_{org} are the neutral or the ionized antibiotic molecule, respectively, in aqueous or organic media, and $(A_2)_{\text{org}}$ designates the dimeric associates of antibiotics in an organic medium.

Apparently, the experimentally observed partition coefficient can be expressed as

$$P_{\text{obs}} = \frac{[A_{\text{org}}] + 2[(A_2)_{\text{org}}]}{[A_w]} \quad (7)$$

Generally, P_{obs} is not an independent thermodynamic value, as it depends on the solute concentration:

$$P_{\text{obs}} = P(1 + 2K_{\text{Ass}}[A_{\text{org}}]) \quad (8)$$

As the proposed dimerization should lead to energetically unfavourable partial solute desolva-

tion, it would be reasonable to assume the value of K_{Ass} to be proportional to the value of P^x , where x varies from -1 to 0 . In fact, the only available set of K_{Ass} values reported in the literature for penicillins in chloroform [28], as shown in Table IV, proved to be linearly related to $P^{-0.14}$. To interpret the results in Table IX, we assumed that in octanol and butanol K_{Ass} changes proportionally to $P^{-0.4}$. Accordingly, the following particular cases of a dependence between the real and observed partition coefficients can be distinguished:

(a) $[A_{\text{org}}] \gg [(A_2)_{\text{org}}]$ and $P_{\text{obs}} = P$;

(b) $[A_{\text{org}}] \ll [(A_2)_{\text{org}}]$ and $P_{\text{obs}} = 2P K_{\text{Ass}}[A_{\text{org}}]$.

The value of $[A_{\text{org}}]$ for each separate antibiotic under the experimental conditions might be varied absolutely arbitrarily. Nevertheless, all the authors of the reports dealing with partitioning emphasized that the total concentration of partitioned penicillins and cephalosporins in the system was kept constant. Therefore, we might assume that the total antibiotic concentration $[A]_{\text{Total}}$ was constant. Then, when $\log P_{\text{obs}} > 0$,

$$[A_{\text{org}}] \approx \left(\frac{[A]_{\text{Total}}}{2K_{\text{Ass}}} \right)^{0.5}$$

and hence

$$P_{\text{obs}} \approx P^{0.8} \sqrt{2[A]_{\text{Total}}}$$

and when $\log P_{\text{obs}} < 0$,

$$[A_{\text{org}}] \approx P [A]_{\text{Total}}$$

and hence

$$P_{\text{obs}} \approx P^{1.6} \cdot 2[A]_{\text{Total}}$$

Case (a) occurs in a chloroform medium, as here for different penicillins $\log K_{\text{Ass}} = 1.7\text{--}2.0$ [28]. This implies that in the most frequently used concentration range of $[A]_{\text{Total}}$ ($5 \cdot 10^{-5}\text{--}1 \cdot 10^{-3} M$), in the organic phase the dominant form of antibiotics is A_{org} , and $\alpha_1/\alpha_2 = 1.0$ (see Table IX). However, in octanol and butanol media the associated form of $(A_2)_{\text{org}}$ seems to prevail, so the α_1/α_2 value changes depend on the partition conditions, being 0.8 at $\log P_{\text{obs}} > 0$ and 1.6 at $\log P_{\text{obs}} < 0$.

Owing to the proposed β -lactam antibiotics association, it should apparently be impossible to predict $\log P_{\text{obs}}$ values for the antibiotics with charged C-6(C-7) or C-3 substituents. The point is that the K_{Ass} value for additionally charged antibiotics, besides their total hydrophobicity, will depend on additional electrostatic repulsion. Indeed, the partition coefficients of cephaloridine and carbenicillin in hydrophilic systems given in refs. 6 and 18 showed large positive deviations from the established dependences in Tables IV and VII.

It should be stressed that Scheme 1 for equilibrium partitioning is only a "minimal" model, as it takes no account of the acid-base equilibrium of antibiotics and their association in the aqueous phase [63], or the possible interactions between neutral and ionized solutes in the organic phase.

However, this is not of much significance, as any further elaboration of the partition model will certainly not interpret the results in Table IX any worse than Scheme 1 does. What is important here is the occurrence of secondary equilibrium processes demonstrating the non-stringency of the physical sense of $\log P_{\text{obs}}$ and, consequently, the conditionality of the most of the earlier investigations on β -lactam antibiotic partitioning. The partition data reported in refs. 5 or 7 and 8 can serve as an illustrative example thereof. The most probable reason for the disturbances of the linear dependence in these instances seems to result from the inconsistency of the experimental conditions, e.g., from variations in $[A]_{\text{Total}}$ in the partitioning system.

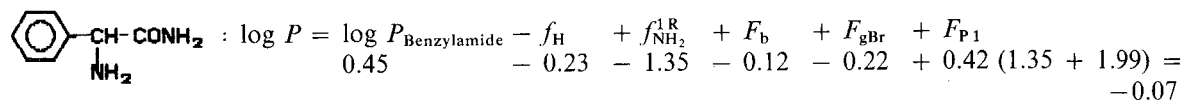
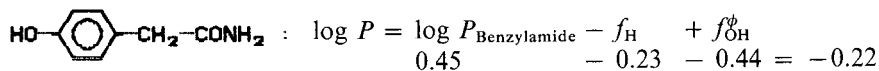
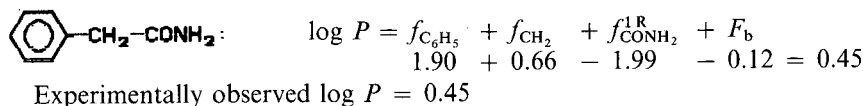
APPENDIX

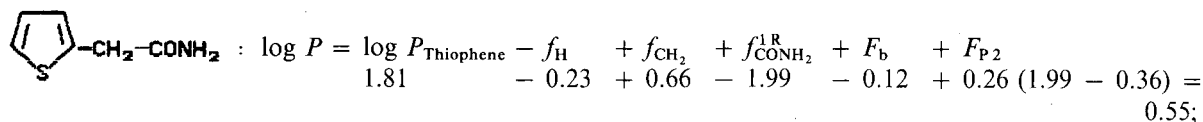
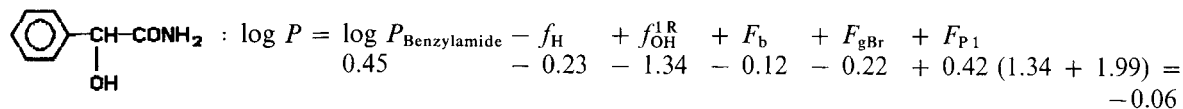
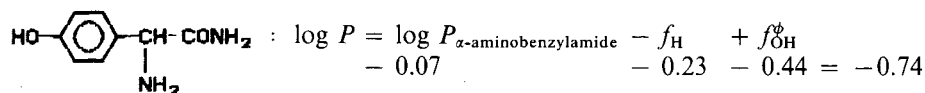
Calculation of log P in octanol-water system by the fragment method of Hansch and Leo [32]

The method is based on the following equation:

$$\log P = \sum_1^n a_n f_n + \sum_1^m b_m F_m \quad (9)$$

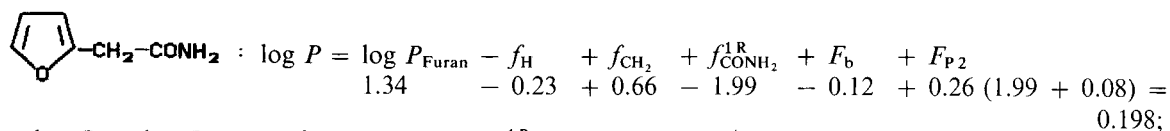
Here $\log P$ is expressed as a sum of constant fragment values (f_n) and other factors (F_m) affecting the partition coefficients of complex substances. Below we give the calculation of $\log P$ only for amides with a "well characterizable" structure. This means that all functional fragments in the amide molecule are separated each from other by isolating carbon atoms (sp^3) and charged groups are absent. Quantitative values of $\log P$, f_n , F_m and their particular designations have been taken from ref. 32.





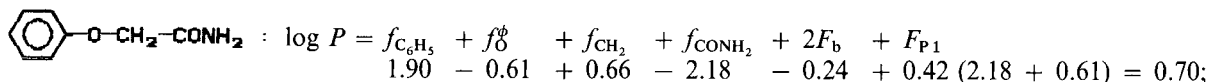
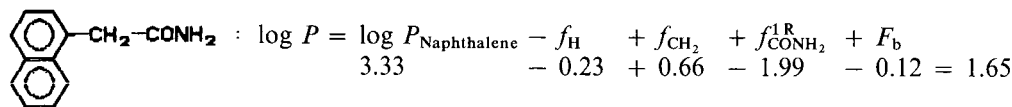
$$\log P = \log P_{\text{Thiophene}} - f_{\text{H}} + f_{\text{CH}_2} + f_{\text{CONH}_2}^{1\text{R}} + F_{\text{b}} + \frac{F_{\text{P2}}}{2}$$

$$1.81 \quad - 0.23 \quad + 0.66 \quad - 1.99 \quad - 0.12 \quad + 0.08 (1.99 - 0.36) = 0.26; \text{ accepted for correlations } \log P = 0.30$$



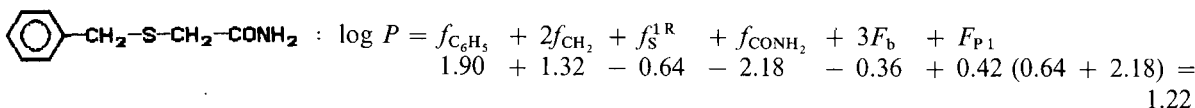
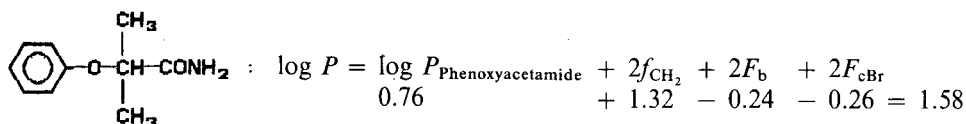
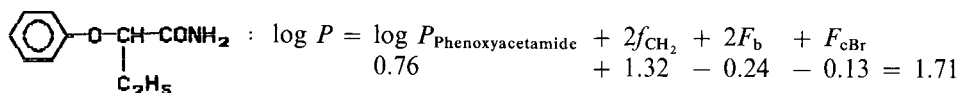
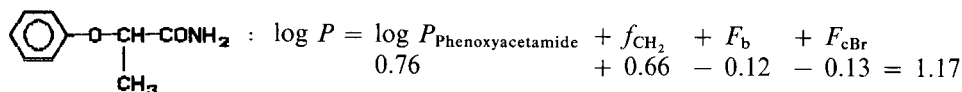
$$\log P = \log P_{\text{Furan}} - f_{\text{H}} + f_{\text{CH}_2} + f_{\text{CONH}_2}^{1\text{R}} + F_{\text{b}} + \frac{F_{\text{P2}}}{2}$$

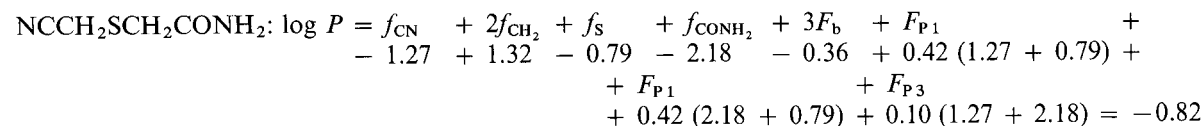
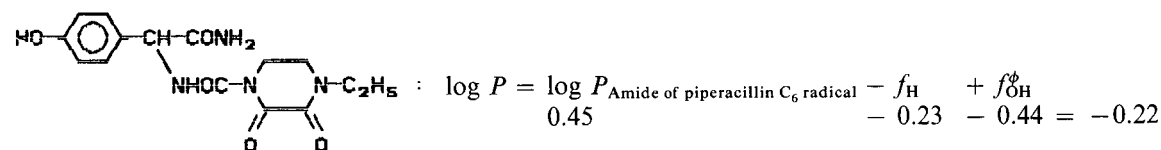
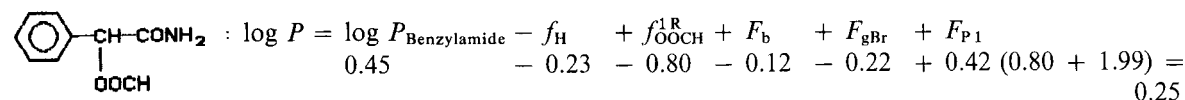
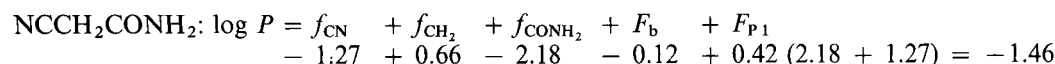
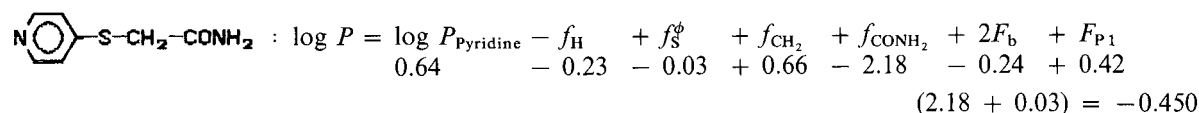
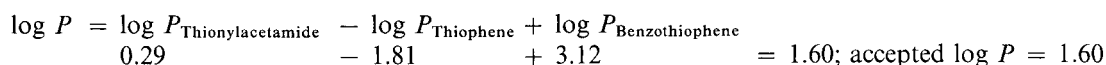
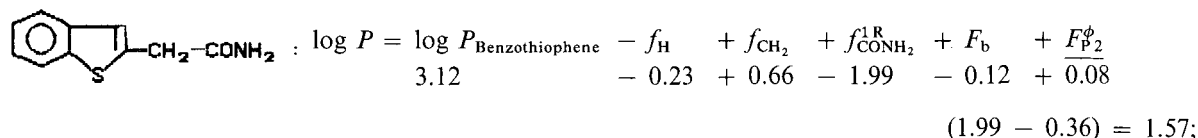
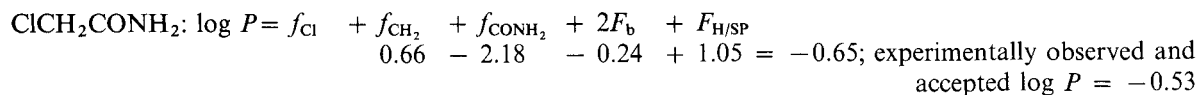
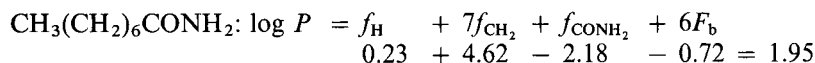
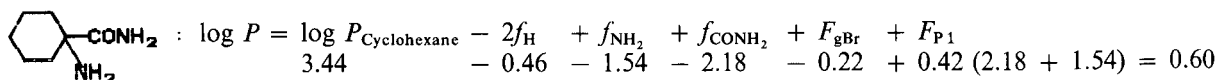
$$1.34 \quad - 0.23 \quad + 0.66 \quad - 1.99 \quad - 0.12 \quad + 0.08 (1.99 + 0.08) = -0.174; \text{ accepted } \log P = -0.07$$



$$\log P = f_{\text{C}_6\text{H}_5} + f_{\text{O}}^{\phi} + f_{\text{CH}_2} + f_{\text{CONH}_2}^{1\text{R}} + 2F_{\text{b}} + F_{\text{P1}}$$

$$1.90 \quad - 0.61 \quad + 0.66 \quad - 1.99 \quad - 0.24 \quad + 0.42 (1.99 + 0.61) = 0.81; \text{ experimentally observed and accepted } \log P = 0.76$$





As seen from Tables II, III and VI, inaccurately calculated $\log P$ values proved to be only those for cyanoacetamide and cyanomethylthioacetamide.

REFERENCES

- 1 C. Hansch and T. Fujita, *J. Am. Chem. Soc.*, 86 (1963) 1616.
- 2 C. Hansch, *J. Am. Chem. Soc.*, 85 (1963) 2817.
- 3 C. Hansch and E. W. Deutsh, *J. Med. Chem.*, 8 (1965) 705.
- 4 C. Hansch and A. R. Steward, *J. Med. Chem.*, 7 (1964) 691.
- 5 V. P. Irwin, J. M. Quigley and R. F. Timoney, *Int. J. Pharm.*, 34 (1987) 2416.
- 6 W. Zimmerman and A. Roselet, *Antimicrob. Agents Chemother.*, 12 (1977) 368.
- 7 H. Nikaido and E. Y. Rosenberg, *J. Bacteriol.*, 153 (1983) 232.

- 8 F. Yoshimura and H. Nikaido, *Antimicrob. Agents Chemother.*, 27 (1985) 84.
- 9 A. Yamaguchi, R. Hiruma and T. Sawai, *FEBS. Lett.*, 164 (1983) 389.
- 10 T. Sawai, K. Matsuba, A. Tamura and S. Yamagishi, *J. Antibiot.*, 32 (1979) 59.
- 11 A. Yotsuji, J. Mitsuyama, R. Hori, T. Yasuda, I. Saikawa, M. Inoue and S. Mitsuhashi, *Antimicrob. Agents Chemother.*, 32 (1988) 1097.
- 12 A. Yamaguchi, N. Tomiyama, R. Hiruma and T. Sawai, *FEBS. Lett.*, 181 (1985) 143.
- 13 R. Hiruma, A. Yamaguchi and T. Sawai, *FEBS. Lett.*, 170 (1984) 268.
- 14 J. Mitsuyama, R. Hiruma, A. Yamaguchi and T. Sawai, *Antimicrob. Agents Chemother.*, 31 (1987) 379.
- 15 T. Sawai, R. Hiruma, N. Kawana, M. Kaneko, F. Taniyasu and A. Inami, *Antimicrob. Agents Chemother.*, 22 (1982) 585.
- 16 A. Yamaguchi and T. Sawai, *J. Antibiot.*, 35 (1982) 1692.
- 17 A. Tsuji, E. Nakashima, J. Kogami and T. Yamana, *J. Pharm. Sci.*, 70 (1981) 768.
- 18 Å. Ryrfeldt, *J. Pharm. Pharmacol.*, 23 (1971) 463.
- 19 A. E. Bird and A. C. Marshall, *Biochem. Pharmacol.*, 16 (1967) 2275.
- 20 G. L. Biagi, M. C. Guerra, A. M. Barbaro, G. Cantelli-Forti and T. Rossi, *Boll. Soc. Ital. Biol. Sper.*, 51 (1975) 403.
- 21 G. L. Biagi, M. C. Guerra, A. M. Barbaro and M. F. Gamba, *J. Med. Chem.*, 13 (1970) 511.
- 22 G. L. Biagi, A. M. Barbaro and M. C. Guerra, *J. Chromatogr.*, 51 (1970) 548.
- 23 A. E. Bird and A. C. Marshall, *J. Chromatogr.*, 63 (1971) 313.
- 24 A. Tsuji, O. Kubo, E. Miyamoto and T. Yamana, *J. Pharm. Sci.*, 66 (1977) 1675.
- 25 T. Yamana, A. Tsuji, E. Miyamoto and O. Kubo, *J. Pharm. Sci.*, 66 (1977) 747.
- 26 L. Koprivic and E. Polla, *Acta Pharm. Jugosl.*, 27 (1977) 185.
- 27 H. H. Thijssen, *Arzneim.-Forsch.*, 28 (1978) 1065.
- 28 R. Modin and M. Schröder-Nielsen, *Acta Pharm. Suec.*, 8 (1971) 573.
- 29 V. P. Irwin, J. M. Quigley and R. F. Timoney, *Int. J. Pharm.*, 43 (1988) 187.
- 30 G. G. Nys and R. F. Rekker, *Eur. J. Med. Chem.*, 9 (1974) 361.
- 31 M. S. Tute, in N. J. Harper and A. B. Simmonds (Editors), *Advances in Drug Research*, Vol. 6, Academic Press, London, 1971, p. 1.
- 32 C. Hansch and A. J. Leo, *Substituent Constant for Correlation Analysis in Chemistry and Biology*, Wiley, New York, 1979.
- 33 R. Collander, *Acta Chem. Scand.*, 5 (1951) 774.
- 34 A. J. Leo, *Adv. Chem. Ser.*, No. 114 (1972) 51.
- 35 P. Seiler, *Eur. J. Med. Chem.*, 9 (1974) 473.
- 36 J. Martin, R. Mendez and A. Negro, *J. Liq. Chromatogr.*, 11 (1988) 1707.
- 37 E. Crombez, W. Van Den Bossche and P. De Moerloose, *J. Chromatogr.*, 169 (1979) 343.
- 38 W. Melander, J. Stoveken and C. Horváth, *J. Chromatogr.*, 199 (1980) 35.
- 39 K. E. Bij, C. Horváth, W. R. Melander and A. Nahum, *J. Chromatogr.*, 203 (1981) 65.
- 40 M. C. Rouan, F. Abadie, A. Leclerc and F. Juge, *J. Chromatogr.*, 275 (1983) 133.
- 41 R. F. Rekker, *The Hydrophobic Fragmental Constant*, Elsevier, Amsterdam, 1977.
- 42 S. Okuno, I. Maezawa, Y. Sakuma, T. Matsushita and T. Yamaguchi, *J. Antibiot.*, 41 (1988) 239.
- 43 A. A. Khier, G. Blaschke and M. El Sadek, *Anal. Lett.*, 17 (1984) 1667.
- 44 S. Hendrickx, E. Roets, J. Hoogmartens and H. Vanderhaeghe, *J. Chromatogr.*, 291 (1984) 211.
- 45 G. M. Overliet, *Pharm. Weekbl.*, 109 (1974) 537.
- 46 K. Borner, H. Lode and A. Elvers, *Antimicrob. Agents Chemother.*, 22 (1982) 949.
- 47 M. A. Riegel and P. P. Ellis, *J. Chromatogr.*, 424 (1988) 177.
- 48 M. Le Belle, K. Graham and W. L. Wilson, *J. Pharm. Sci.*, 66 (1979) 555.
- 49 F. Barbato, C. Grieco, A. Silipo and A. Vittoria, *Farmaco*, 34 (1979) 233.
- 50 G. Lauriault, M. J. Le Belle and A. Vilim, *J. Chromatogr.*, 246 (1982) 157.
- 51 T. Nakagawa, A. Shibukawa and T. Uno, *J. Chromatogr.*, 239 (1982) 695.
- 52 K. Tsuji and J. H. Robertson, *J. Pharm. Sci.*, 64 (1975) 1542.
- 53 M. E. Rogers, M. W. Adlard, G. Saunders and G. Holt, *J. Liq. Chromatogr.*, 6 (1983) 2019.
- 54 G. Nygard and S. K. W. Khalil, *J. Liq. Chromatogr.*, 7 (1984) 1461.
- 55 F. Salto, J. G. Prieto and M. T. Alemany, *J. Pharm. Sci.*, 69 (1980) 501.
- 56 F. Salto and J. G. Prieto, *J. Pharm. Sci.*, 70 (1981) 994.
- 57 D. Westerlund, J. Carlqvist and A. Theodorsen, *Acta Pharm. Suec.*, 16 (1979) 187.
- 58 T. Annesley, K. Wilkerson, K. Matz and D. Giacherio, *Clin. Chem.*, 30 (1984) 908.
- 59 M. Margosis, *J. Chromatogr.*, 236 (1982) 469.
- 60 G. T. Briguglio and C. A. Lau-Cam, *J. Assoc. Off. Anal. Chem.*, 67 (1984) 228.
- 61 A. E. Bird, C.-H. Charsley, K. R. Jennings and A. C. Marshall, *Analyst (London)*, 109 (1984) 1209.
- 62 E. Pop, W.-M. Wu and N. Bodor, *J. Med. Chem.*, 32 (1989) 1789.
- 63 D. Attwood and S. P. Agarwal, *J. Pharm. Pharmacol.*, 36 (1984) 563.
- 64 R. H. Rumble and M. S. Roberts, *J. Chromatogr.*, 342 (1985) 436.
- 65 C. T. Hung, J. K. C. Lim and A. R. Zoest, *J. Chromatogr.*, 425 (1988) 331.
- 66 I. Wouters, S. Hendrick and E. Roets, *J. Chromatogr.*, 291 (1984) 59.
- 67 I. Wouters, S. Hendrick, E. Roets, J. Hoogmartens and H. Vanderhaeghe, *ACS Symp. Ser.*, 297 (1986) 68.
- 68 C. Horváth, W. Melander and I. Molnár, *J. Chromatogr.*, 125 (1976) 129.
- 69 S. H. Unger, P. S. Cheung, G. H. Chiang and J. R. Cook, in W. J. Dun, J. H. Block and R. S. Pearlman (Editors), *Partition Coefficients. Determination and Estimation*, Pergamon Press, New York, 1986, p. 69.
- 70 W. Dürckheimer and E. Schrunner, in J. Ishigami (Editor), *Recent Advances in Chemotherapy, Proceedings of the 14th International Congress on Chemotherapy, (Antimicrobial Sect., 1)*, University of Tokyo Press, Tokyo, 1985, p. 51.

- 71 J. H. Hoogmartens, E. E. Roets and H. J. Vanderhaeghe, *J. Assoc. Off. Anal. Chem.*, 64 (1981) 173.
- 72 T. Okumura, *J. Liq. Chromatogr.*, 4 (1981) 1035.
- 73 T. Fuji, Y. Arai, A. Kubota, N. Mizushima, Y. Machida and T. Nagai, *Yakuzaigaku*, 46 (1986) 119.
- 74 S. Ting, *J. Assoc. Off. Anal. Chem.*, 71 (1988) 1123.
- 75 C. Y. Chan, K. Chan and G. L. French, *J. Antimicrob. Chemother.*, 18 (1986) 537.
- 76 L. A. Danzer, *Clin. Chem.*, 29 (1983) 856.
- 77 R. L. Yost and H. Derendorf, *J. Chromatogr.*, 341 (1985) 131.
- 78 A. Csiba, H. Graber, *Acta Pharm. Hung.*, 53 (1983) 241.
- 79 A. M. Brisson and J. B. Fourtillan, *J. Chromatogr.*, 223 (1981) 393.
- 80 D. J. Miner, in S. H. Y. Wong (Editor), *Therapeutic Drug Monitoring and Toxicology by Liquid Chromatography*, Marcel Dekker, New York, 1984, p. 269.
- 81 G. Tortolani and E. Romagnoli, *J. Chromatogr.*, 120 (1976) 149.
- 82 E. M. McCormick, R. M. Echols and T. G. Rosano, *Antimicrob. Agents Chemother.*, 25 (1984) 336.
- 83 E. Crombez, B. Van Der Weken, W. Van Den Bossche and P. De Moerloose, *J. Chromatogr.*, 173 (1979) 165.
- 84 M. A. Carrol, E. R. White, Z. Jancsik and J. E. Zaremba, *J. Antibot.*, 30 (1977) 397.
- 85 J. B. Lecaillon, M. C. Rouan, C. Souuppart, N. Febvre and F. Juge, *J. Chromatogr.*, 228 (1982) 257.
- 86 L. Hakim, *J. Chromatogr.*, 424 (1988) 111.
- 87 J. S. Leeder, M. Spino, A. M. Tesoro and S. M. MacLeod, *Antimicrob. Agents Chemother.*, 24 (1983) 720.
- 88 F. M. Demotes-Mainard, G. A. Vincon, C. H. Jarry and H. C. Albin, *J. Chromatogr.*, 336 (1984) 438.
- 89 H. H. W. Thijssen, *Eur. J. Med. Chem.*, 16 (1981) 449.
- 90 G. S. Libinson, *Antibiotiki*, 27 (1982) 68.

CHROM. 23 507

(2*R*,3*R*)-Dicyclohexyl tartrate as a chiral mobile phase additive

Eva Heldin*, N. Hang Huynh and Curt Pettersson

Department of Analytical Pharmaceutical Chemistry, Biomedical Centre, Uppsala University, Box 574, S-751 23 Uppsala (Sweden)

(First received April 19th, 1991; revised manuscript received May 27th, 1991)

ABSTRACT

The enantiomers of acids, esters and amino alcohols of moderate hydrophobicity containing two hydrogen bonding functions were separated in underivatized form using (2*R*,3*R*)-dicyclohexyl tartrate (DCHT) in phosphate buffer (pH 3) as mobile phase and porous graphitic carbon (Hypercarb) as stationary phase. The retention of the solutes can be controlled by the concentration of DCHT in the mobile phase without affecting the enantioselectivity. A low pH in the mobile phase gave optimum enantioselectivity for both acidic and basic solutes. DCHT, which is water soluble up to 0.5 mM, has a high affinity for the graphitic carbon phase when using phosphate buffer as the mobile phase. It seems to be adsorbed on the support as a monolayer as changes in the concentration of the mobile phase have only a minor influence on the amount adsorbed (0.14 mmol/g support). Addition of acetonitrile to the mobile phase in higher amounts decreased the amount of DCHT adsorbed on the carbon support and also decreased the retention and the stereoselectivity.

INTRODUCTION

The separation of enantiomers is of particular interest in the biomedical field as it has been shown that the enantiomeric forms of a drug may have different biological activities [1]. A number of chiral solid phases using different principles for enantiomeric recognition [2] are now commercially available.

A chiral mobile phase additive that is dynamically coated on an achiral solid phase may be used as an alternative to covalently bound stationary phases. The technique is flexible and permits screening for new chiral selectors and reversals of the retention order of enantiomers [3]. Lindner *et al.* [4] and Davankov *et al.* [5,6] have demonstrated the optical resolution of amino acids using ligand-exchange chromatography after coating of the support with *N*-alkyl-*L*-amino acids. The use of chiral crown ethers dynamically coated on C₁₈ material for the resolution of the enantiomers of amino acids and amines has been presented by Shinbo *et al.* [7]. A liquid ester of tartaric acid [(2*R*,3*R*)-di-*n*-butyl tartrate (DBT)] coated on silica-based reversed-phase

materials has been used as the chiral stationary phase in the liquid-liquid chromatography (LLC) of amino alcohols [8,9]. Esters of tartaric acid dissolved in organic solvents have also been applied as stationary phases [10].

The studies with DBT dissolved in organic solvents indicated that the solutes were adsorbed on the support [10]. High separation factors were observed for some ephedrine analogues when using a support with a minimum [11] number of polar groups, namely porous graphitic carbon, Hypercarb.

The aim of this study was to evaluate the stereoselective properties of a hydrophobic chiral selector, (2*R*,3*R*)-dicyclohexyl tartrate (DCHT) dynamically coated on Hypercarb.

EXPERIMENTAL

Apparatus

The pump used was a Beckman (Fullerton, CA, USA) Model 114 M. Detection was performed at 254 nm using a SpectroMonitor 3100 (Milton Roy, Riviera Beach, FL, USA); the injector was a Rheodyne (Berkeley, CA, USA) Model 7120 with a 20- μ l

loop. The injector, column and solvent reservoir were kept at 25°C using a thermostat HETO type 02 PT 923 TC water-bath (Birkerød, Denmark).

Column equilibration

The columns were equilibrated by pumping the mobile phase containing the selector. The equilibration was followed by recording the absorbance of the eluent at 195 nm. The breakthrough volume was used to calculate the amount of DCHT adsorbed on the support. The studies carried out under various conditions were performed during the first day after the breakthrough had been observed.

Capacity factors (k') were calculated on the assumption that sodium nitrate is unretained. The separation factor is given as $\alpha = k'_2/k'_1$.

Columns

The Hypercarb columns were either obtained prepacked in 100 × 4.7 mm I.D. stainless-steel columns from Shandon (Astmoor, UK) or packed in the laboratory by a slurry technique in stainless-steel columns (100 × 3.0 mm I.D.). Chloroform was used as the slurry liquid and *n*-hexane as packing liquid. After thorough washing with chloroform and methanol, the columns were tested in a system with a mobile phase consisting of 3.8 M acetonitrile–phosphate buffer (pH 2.8) (20:80, v/v). (*R*)- and (*S*)-mandelic acid, phenol, racemic atropine, racemic 2-amino-1-(4-nitrophenyl)propanol and racemic 2-amino-1-[spiro(cyclopropane-1,1'-inden)-3'-yl]ethanol were used as test solutes. The columns were rinsed with 100 ml of ethyl acetate followed by 150 ml of dioxane or dioxane–methanol (25:75) after each chromatographic system. The column performance was checked regularly using the 3.8 M acetonitrile–phosphate buffer (pH 2.8) (20:80) mobile phase described above.

μ Bondapak phenyl material was packed according to procedures described earlier [9].

Capcell PAK C₁₈ SG 120 (5- μ m particles) was a kind gift from Professor Nabuo Tanaka (Kyoto Institute of Technology) and was obtained packed in a stainless-steel column (250 × 4.6 mm I.D.).

Chemicals

Acetonitrile (LiChrosolv), methanol (Li-Chrosolv), ethyl acetate (analytical-reagent grade) and

phenol (analytical-reagent grade) were from E. Merck (Darmstadt, Germany) and isopropanol (HPLC grade) and dioxane (HPLC grade) from Lab Scan (Dublin, Ireland). (2*R*,3*R*)-Dicyclohexyl tartrate was synthesized according to procedures described earlier [10]. The solutes used are presented in Table I. All other chemicals were of analytical-reagent grade and were used without further purification.

RESULTS AND DISCUSSION

Support

Previous liquid–liquid chromatographic studies [10] with DBT as chiral selector showed that the separation factors were highest when using graphitic carbon as support. The lower separation factors obtained with chemically modified silica as support (*e.g.*, μ Bondapak phenyl) might be due to an achiral retention, *e.g.*, by residual silanols. End-capping of the material has become the usual way of treating residual silanols but these materials still show polar properties [12]. A polymer-coated silica (Capcell PAK C₁₈), suitable for protonated amines in regular chromatographic systems [13], was therefore included in this study (Table II).

Addition of DCHT to the mobile phase gave reduced retention and improved peak symmetry for the enantiomeric solutes with all supports. In agreement with previous observations [10], the enantioselectivity was much higher using graphitic carbon as the support (Table II). Calculations of the coverage of DCHT on the supports based on the stated area of underivatized silica particles and of the carbon phase showed that the two hydrophobic supports, Capcell PAK and Hypercarb, had about a tenfold higher coverage than μ Bondapak. Despite this fact, the peak symmetry and separation factors were similar on the two silica-based supports. It might be that the conformation adopted by DCHT depends on the three-dimensional structure of the packing material. In addition, the polar groups in DCHT, probably needed for the chiral interaction with the solutes, may interact with residual silanols on the silica support. In contrast, the interaction between DCHT and graphitic carbon is of apolar character and does not involve the polar groups of DCHT.

TABLE I
SOLUTES

No.	Name	Source ^a
1	(1 <i>R</i> ,2 <i>S</i>)-N-Methylephedrine	Fluka
2	(1 <i>S</i> ,2 <i>R</i>)-N-Methylephedrine	Fluka
3	(1 <i>R</i> ,2 <i>R</i>)-Pseudoephedrine	Sigma
4	(1 <i>S</i> ,2 <i>S</i>)-Pseudoephedrine	Sigma
5	(1 <i>R</i> ,2 <i>S</i>)-Ephedrine · HCl	Fluka
6	(1 <i>S</i> ,2 <i>R</i>)-Ephedrine · HCl	Merck
7	(1 <i>R</i> ,2 <i>S</i>)-Norephedrine · HCl	Serva
8	(1 <i>S</i> ,2 <i>R</i>)-Norephedrine · HCl	Janssen
9	Racemic 2-amino-1-(4-methanesulphonamido-phenyl)ethanol	Leo
10	Racemic 2-amino-1-(4-nitrophenyl)-ethanol · HCl	Leo
11	Racemic 2-amino-1-(3-nitrophenyl)-ethanol · HCl	Leo
12	Racemic 2-amino-1-(3-nitrophenyl)-propanol	Leo
13	Racemic 2-amino-1-(2,4-dichlorophenyl)ethanol	Leo
14	Racemic 2-amino-1-[1,1-dimethylinden-3-yl]ethanol	Kabi
15	Racemic 2-amino-1-[spiro(cyclopropane-1,1'-inden)-3'-yl]ethanol	Kabi
16	Racemic 3-phenyllactic acid	Fluka
17	(-)-Phenyllactic acid	Fluka
18	(<i>R</i>)-Mandelic acid	Fluka
19	(<i>S</i>)-Mandelic acid	Fluka
20	Racemic 3-hydroxy-4-methoxy-mandelic acid	Fluka
21	Racemic tropic acid	Sigma
22	(<i>R</i>)-2-Phenylpropionic acid	Sigma
23	(<i>S</i>)-2-Phenylpropionic acid	Sigma
24	(2 <i>S</i> ,3 <i>S</i>)-2-Benzoyloxy-1,3,4-butanetriol	Janssen
25	(2 <i>R</i> ,3 <i>S</i>)-2-Benzoyloxy-1,3,4-butanetriol	Janssen
26	(<i>R</i>)-Phenyl-1,2-ethanediol	Janssen
27	(<i>S</i>)-Phenyl-1,2-ethanediol	Janssen
28	(<i>R</i>)-2-Phenylpropanol	Janssen
29	(<i>S</i>)-2-Phenylpropanol	Janssen
30	(<i>R</i>)-Ethyl mandelate	Aldrich
31	(<i>S</i>)-Ethyl mandelate	Aldrich
32	Racemic homatropine	Merck
33	Racemic N-methylhomatropine	Merck
34	Racemic atropine	Merck
35	(<i>S</i>)-Atropine	Sigma
36	Racemic N-methylatropine	Merck
37	Racemic ipratropine	Draco

^a Leo (Helsingborg, Sweden); Draco (Lund, Sweden); Kabi (Stockholm, Sweden); Serva (Heidelberg, Germany); Janssen Chimica (Beerse, Belgium); Fluka (Buchs, Switzerland); E. Merck (Darmstadt, Germany); Sigma (St. Louis, MO, USA); Aldrich (Milwaukee, WI, USA).

Solute structure and stereoselectivity

Graphitic carbon dynamically modified with DCHT can separate the enantiomers of amines, acids and non-protolytic solutes (Tables III–V). An example is given in Fig. 1, which shows the separation of the enantiomers of homatropine (**32**). Complete resolution was obtained within 10 min using a flow-rate of 1.0 ml/min.

Amines. A higher enantioselectivity was observed (Table III) for the primary amine norephedrine (**7** and **8**) than for the corresponding secondary amine [ephedrine (**5** and **6**)] and the tertiary amine [N-methylephedrine (**1** and **2**)]. Similar observations have been made in liquid–liquid chromatographic studies with DBT as selector [9]. As has been concluded earlier [9], the amine function in these ephedrine analogues is most likely needed for the interaction with the selector. In contrast to what was seen in the liquid–liquid studies, a methyl substituent on the α -carbon slightly decreased the enantioselectivity (e.g., **11** and **12** in Table III). In the adsorption systems the substituents in the aromatic ring also seem to be of importance for chiral discrimination (see Table III, **7–13**), possibly owing to steric effects and/or the changed electron configuration [14].

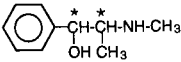
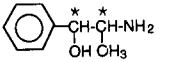
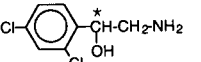
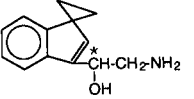
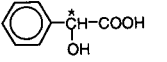
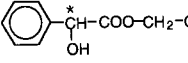
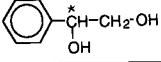
Included in Table III are two solutes with similar indene structures (**14** and **15**). Exchange of two methyl substituents on carbon one for a cyclic dimethylene group, giving the molecule a more rigid structure, drastically increased the stereoselectivity.

Acidic and non-protolytic solutes. The separation of enantiomers of hydroxy acids is presented in Table IV. With a mobile phase of pH 3 the acids are present mainly in uncharged form. The pK_a of mandelic acid is 3.4 [15]. The enantioselectivity was favoured by a hydroxyl group directly attached to the chiral carbon [mandelic acid (**18** and **19**) and tropic acid (**21**)]. Substitution in the aromatic ring seems to improve the stereoselectivity [e.g., 3-hydroxy-4-methoxymandelic acid (**20**)].

Table V shows the retention and the stereoselectivity of some esters of mandelic acid and tropic acid at pH 3. Homatropine (**32**), which is a tropanyl ester of mandelic acid (**18** and **19**), is separated with higher enantioselectivity than mandelic acid and ethyl mandelate (**30** and **31**). Atropine (**34** and **35**), which is a tropanyl ester of tropic acid (**21**), shows a lower separation factor than homatropine (**32**). Substitu-

TABLE II
SOLID SUPPORTS

Mobile phase: 0.31 mM DCHT in phosphate buffer (pH 2.8) ($I = 0.1$). $asf_{10\%}$ = Asymmetry factor measured at 10% of the height.

Solute	Support									
	Hypercarb ($9.9 \cdot 10^{-7}$ mol/m ²) ^b			μ Bondapak phenyl ($7.0 \cdot 10^{-8}$ mol/m ²) ^b			Capcell PAK C ₁₈ ($6.6 \cdot 10^{-7}$ mol/m ²) ^b			
	k'_1	α	$asf_{10\%}$	k'_1	α	$asf_{10\%}$	k'_1	α	$asf_{10\%}$	
5,6		0.09	>1.00	1.9	1.20	1.03	1.2	0.90	1.04	1.2
7,8		0.07	>1.00	2.2	0.96	1.04	1.3	0.79	1.04	1.3
13 ^a		5.90	1.41	2.8	12.0	1.0	—	15.2	1.00	1.4
15 ^a		11.8	1.76	3.5	14.9	1.0	—	13.8	1.00	1.4
18,19		2.08	1.08	1.8	2.04	1.01	1.9	1.75	1.02	1.8
30,31		4.43	1.13	1.3	12.0	1.00	—	11.2	1.01	3.1
26,27		1.02	1.07	1.4	2.18	1.03	—	2.06	1.02	1.4

^a The solute is injected as the racemic only.

^b Amount of DCHT adsorbed.

tion on the nitrogen affects the selectivity, probably owing to steric effects as a bulky substituent [ipratropine (**37**)] was less favourable than a methyl group [N-methylatropine (**36**)]. The higher stereoselectivity obtained for the tropanyl esters may be due to spatial fitting. It seems unlikely that the nitrogen in the tropane function takes part in any hydrogen bonding as stereoselectivity was obtained for the quaternary ammonium compounds (**33**, **36** and **37**).

Among the aprotic solutes in Table V, the diol 1-phenyl-1,2-ethanediol (**26** and **27**) gave about the same enantioselectivity as mandelic acid (**18** and **19**).

The enantiomers of 2-phenyl-1-propanol (**28** and **29**) containing one hydrogen-accepting/donating group only were not separated.

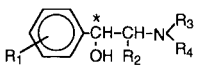
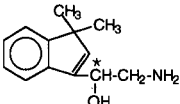
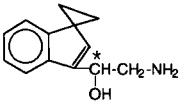
Control of retention and stereoselectivity

Influence of pH. The stereoselectivity of both acids and bases (amino alcohols) was favoured by a low pH in the mobile phase (Fig. 2). As could be expected, neither the retention nor the stereoselectivity of the aprotic solutes was affected by pH.

An increase in pH was followed by an enhanced retention of the amino alcohols (Fig. 2). If the

TABLE III
SOLUTE STRUCTURE AND STEREOSELECTIVITY FOR AMINO ALCOHOLS

Solid support: Hypercarb. Mobile phase: 0.25 mM DCHT in phosphate buffer (pH 2.8) ($I = 0.1$).

Solute					k'_1	α
	R ₁	R ₂	R ₃	R ₄		
1,2	H	CH ₃	CH ₃	CH ₃	0.16	1.04
3,4	H	CH ₃	CH ₃	H	0.13	1.10
5,6	H	CH ₃	CH ₃	H	0.15	1.16
7,8	H	CH ₃	H	H	0.13	1.22
9	<i>p</i> -NHSO ₂ CH ₃	H	H	H	0.51	1.41
10	<i>p</i> -NO ₂	H	H	H	1.13	1.20
11	<i>m</i> -NO ₂	H	H	H	0.92	1.19
12	<i>m</i> -NO ₂	CH ₃	H	H	1.20	1.17
13	<i>o,p</i> -di-Cl	H	H	H	7.61	1.42
14					7.69	1.00
15					15.8	1.76

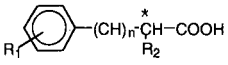
retention (k') is regarded as a retention composed of two different mechanisms, one chiral (k'_{chir}) and one without stereoselectivity (k'_{achir}), the separation factor is given by

$$\alpha_{+/-} = \frac{k'_{\text{chir}(+)} + k'_{\text{achir}}}{k'_{\text{chir}(-)} + k'_{\text{achir}}} \quad (1)$$

The increased retention with increase in pH is the

TABLE IV
SOLUTE STRUCTURE AND STEREOSELECTIVITY FOR ACIDS

Solid support: Hypercarb. Mobile phase as in Table III.

Solute				k'_1	α
	R ₁	R ₂	n		
16,17	H	OH	1	7.68	1.10
18,19	H	OH	0	2.69	1.08
20	<i>m</i> -OH, <i>p</i> -OCH ₃	OH	0	2.85	1.12
21	H	CH ₂ OH	0	3.22	>1.0 ^a
22,23	H	CH ₃	0	25.0	1.00

^a Two columns.

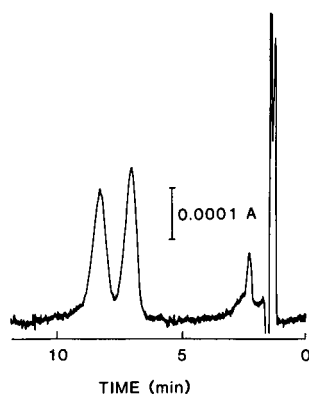


Fig. 1. Resolution of homatropine. Support: Hypercarb. Mobile phase: 0.063 mM DCHT and 0.13 M isopropanol in phosphate buffer (pH 2.8) ($I = 0.1$).

result of an increased retention as base. This binding seems to have an achiral character as it gives rise to a lower α and, according to the equation above, this is the effect of an increase in k'_{achir} .

Atropine (**34** and **35**) and homatropine (**32**) were affected differently to the bases discussed above. An increased retention was observed at higher pH, but

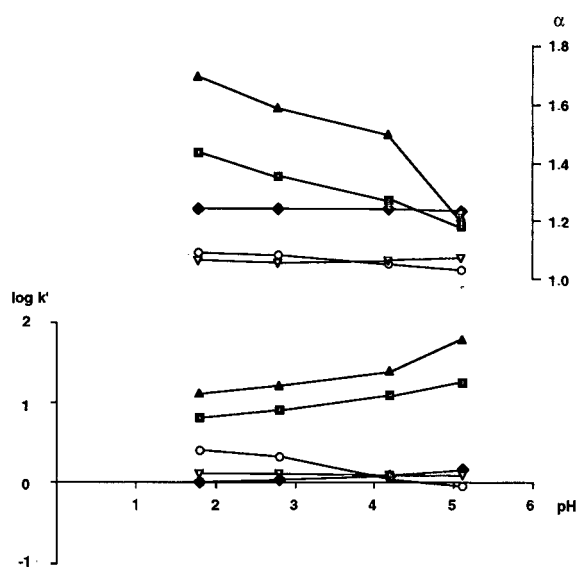


Fig. 2. Influence of pH on the capacity factor for the first-eluted peak (k'_1) and the separation factor (α). Mobile phase: 0.25 mM DCHT and 0.13 M isopropanol in phosphate buffer ($I = 0.1$). Solutes: \blacktriangle = racemic 2-amino-1[spiro(cyclopropane-1,1'-inden)-3'-yl]ethanol; \blacksquare = racemic 2-amino-1-(2,4-dichlorophenyl)ethanol; \blacklozenge = homatropine; ∇ = 1-phenyl-1,2-ethanediol; \circ = mandelic acid.

the stereoselectivity was not affected. This is in accordance with the hypothesis that the nitrogen is not involved in the hydrogen bonding between selector and solute.

The acidic solutes were less retained at higher pH and at the same time a decreased stereoselectivity was observed (Fig. 2). It is likely that is the uncharged acid that takes part in the chiral interaction.

Influence of DCHT concentration. In mobile phases containing DCHT and 0.13 M isopropanol in phosphate buffer (pH 3), the retention could be regulated by the concentration of DCHT without a significant effect on the stereoselectivity (Figs. 3 and 4). Only small changes in adsorption of DCHT were obtained within the concentration range studied (see Fig. 5) and it is therefore likely that the amount of DCHT adsorbed was close to a monolayer. Assuming a monolayer, the area occupied by each

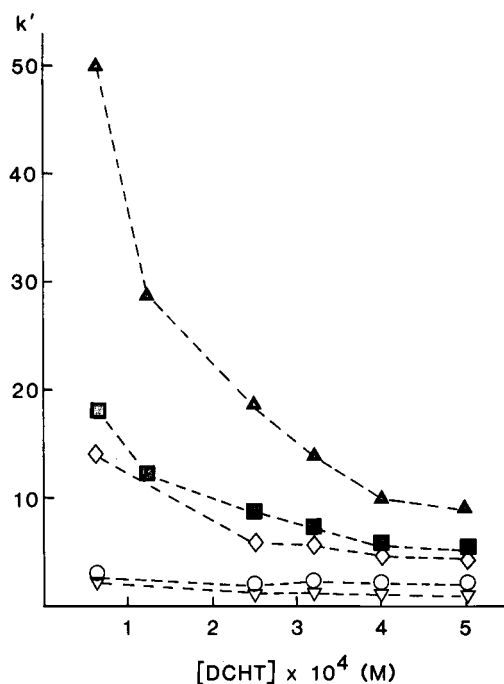


Fig. 3. Influence of DCHT concentration on the capacity factor for the first-eluted enantiomer (k'_1). Mobile phase: DCHT and 0.13 M isopropanol in phosphate buffer (pH 2.8) ($I = 0.1$). Solutes: \blacktriangle = racemic 2-amino-1[spiro(cyclopropane-1,1'-inden)-3'-yl]ethanol; \blacksquare = racemic 2-amino-1-(2,4-dichlorophenyl)ethanol; \blacklozenge = (*R*)-ethanol mandelate; ∇ = (*R*)-1-phenyl-1,2-ethanediol; \circ = (*R*)-mandelic acid.

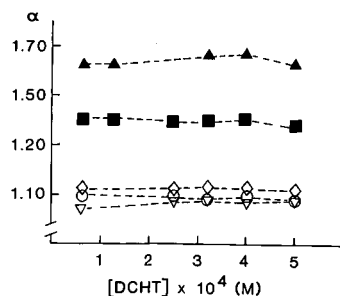


Fig. 4. Influence of DCHT concentration on the separation factor (α). Conditions as in Fig. 3.

molecule of DCHT was around 170 \AA^2 . Further, the high loading of DCHT even at low concentrations implies a high affinity of DCHT for the graphitic carbon.

However, increased concentrations of DCHT gave a decreased retention (Fig. 3). The process responsible for this decrease has so far not been elucidated, but it seems to be without influence on the ratio between chiral and achiral retention (see eqn. 1) as the separation factor is not altered.

Influence of organic modifier. A low content of a hydrogen donor such as isopropanol or a hydrogen acceptor such as acetonitrile had no significant effect on the amount of DCHT adsorbed on Hypercarb. However, the retention and the stereoselectivity for most of the solutes were affected (see Table VI).

When the concentration of acetonitrile was in-

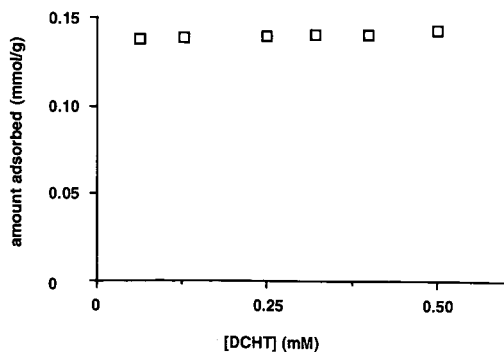


Fig. 5. Influence of DCHT concentration on the adsorption of DCHT. Conditions as in Fig. 3.

creased from 0.95 to 3.8 *M*, the amount of DCHT adsorbed was decreased by 60% (Table VI). Simultaneously, a decrease in both retention and stereoselectivity was observed. The lower stereoselectivity is probably due to the smaller amount of DCHT adsorbed, giving a higher proportion of achiral retention (see eqn. 1). On increasing the concentration of DCHT in the mobile phase containing 3.8 *M* acetonitrile, a higher loading of DCHT was obtained (Fig. 6), the retention was lower (Fig. 7) and the stereoselectivity was improved (Fig. 8). These results strongly support the assumption of a negative influence of achiral retention. The highest stereoselectivities observed were still lower than the separation factors achieved with mobile phases without acetonitrile.

TABLE V

SOLUTE STRUCTURE AND STEREOSELECTIVITY FOR APROTIC SOLUTES AND HYDROXY ESTERS

Solid support: Hypercarb. Mobile phase as in Table III.

Solute	Structure	k'_1	α
24,25		3.42	1.01
26,27		1.43	1.08
28,29		14.2	1.0
30,31		6.13	1.13
	R ₁ R ₂		
32	OH H	1.21	1.26
33	OH CH ₃	0.87	1.25
34,35	CH ₂ OH H	1.42	1.21
36	CH ₂ OH CH ₃	1.07	1.19
37	CH ₂ OH CH(CH ₃) ₂	1.35	1.15

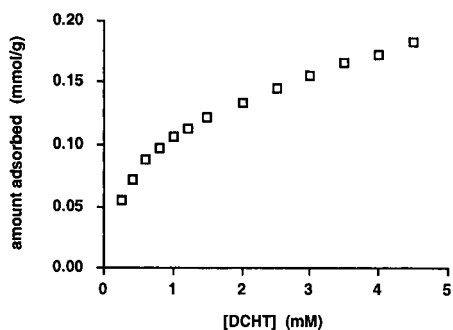


Fig. 6. Influence of DCHT concentration on the adsorption of DCHT with acetonitrile in the mobile phase. Mobile phase: DCHT and 3.6 M acetonitrile in phosphate buffer (pH 2.8) ($I = 0.1$).

Stability and reproducibility of chromatographic systems

The stability of a system with Hypercarb as support was studied for 6 days (1500 column volumes). The capacity factors (Fig. 9) and separation factors (Fig. 10) of the enantiomers of uncharged solutes were stable, whereas a 10–14% increase in retention was observed for the amino alcohols. The prolonged retention is probably due to

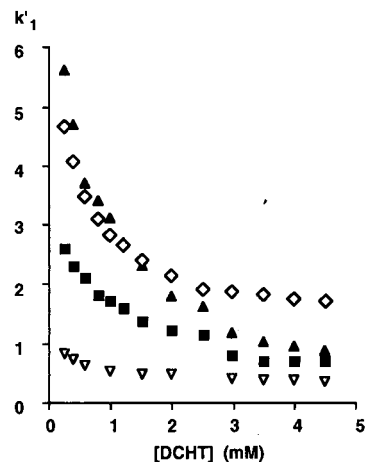


Fig. 7. Influence of DCHT concentration on the capacity factor for the first-eluted enantiomer with acetonitrile in the mobile phase. Conditions as in Fig. 6. Solutes: ▲ = racemic 2-amino-1[spiro(cyclopropane-1,1'-inden)-3'-yl]ethanol; ■ = racemic 2-amino-1-(2,4-dichlorophenyl)ethanol; ◆ = homatropine; ◇ = (*R*)-ethyl mandelate; ▽ = (*R*)-1-phenyl-1,2-ethanediol.

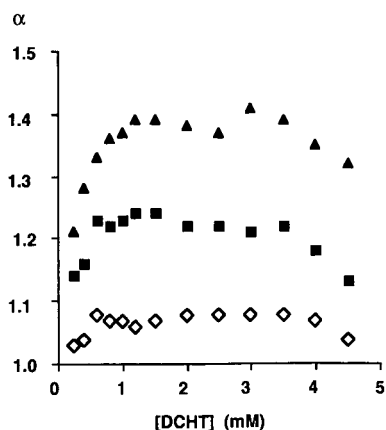


Fig. 8. Influence of DCHT concentration on the stereoselectivity with acetonitrile in the mobile phase. Conditions as in Fig. 6. The α values for 1-phenyl-1,2-ethanol could not be determined at enhanced concentrations of acetonitrile and are therefore not given.

hydrolysis giving monocyclohexyl tartrate, which may act as a counter ion.

Good agreement for retention and stereoselectivity (Table VII) was observed on applying the chromatographic system to three different batches of graphitic carbon.

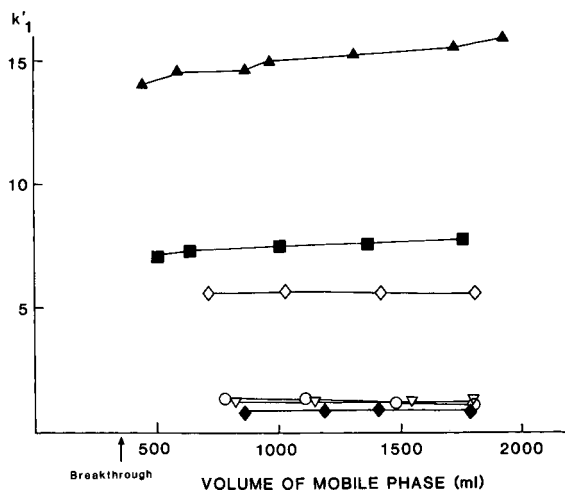
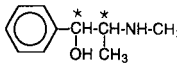
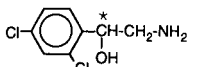
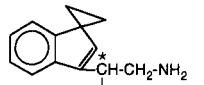
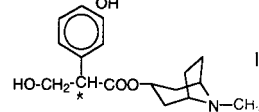
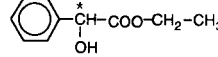
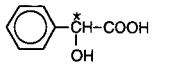
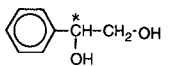


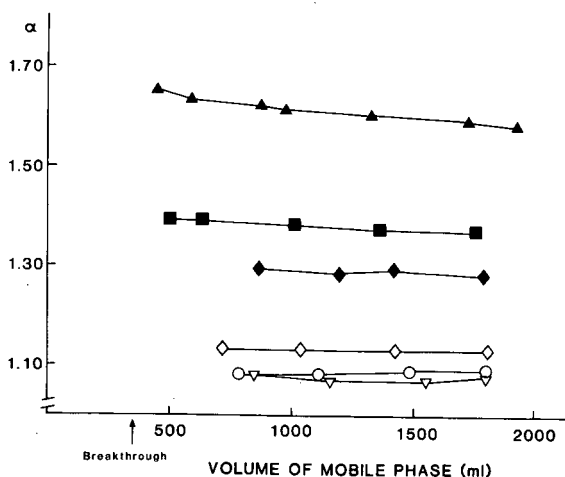
Fig. 9. Stability of chromatographic system: capacity factor (k'_1). Mobile phase: 0.32 mM DCHT and 0.13 M isopropanol in phosphate buffer (pH 2.8) ($I = 0.1$). Solutes: ▲ = racemic 2-amino-1[spiro(cyclopropane-1,1'-inden)-3'-yl]ethanol; ■ = racemic 2-amino-1-(2,4-dichlorophenyl)ethanol; ◆ = homatropine; ◇ = (*R*)-ethylmandelate; ▽ = (*R*)-1-phenyl-1,2-ethanediol; ○ = (*R*)-mandelic acid.

TABLE VI

ORGANIC MODIFIERS

Mobile phase: organic modifier and 0.25 mM DCHT in phosphate buffer (pH 2.8).

Solute	— (0.13 M) 0.137 ^a		Isopropanol (0.95 M) 0.142 ^a		Acetonitrile (1.9 M) 0.144 ^a		Acetonitrile (3.8 M) 0.124 ^a		Acetonitrile 0.057 ^a	
	<i>k'</i> ₁	α	<i>k'</i> ₁	α	<i>k'</i> ₁	α	<i>k'</i> ₁	α	<i>k'</i> ₁	α
5,6 	0.15	1.16	0.28	1.13	0.36	1.06	0.27	1.04	0.17	1.00
13 	7.6	1.42	8.8	1.39	9.4	1.39	—	—	—	—
15 	15.8	1.76	18.7	1.62	14.2	1.57	13.9	1.55	5.5	1.23
34,35 	1.4	1.21	1.2	1.21	2.4	1.15	1.9	1.13	1.2	1.0
30,31 	6.1	1.13	6.0	1.12	7.0	1.11	6.8	1.10	5.4	1.04
18,19 	2.6	1.08	1.9	1.09	1.6	1.09	1.6	1.08	1.2	1.03
26,27 	1.4	1.08	1.2	1.07	1.3	1.05	1.2	1.02	0.99	1.01

^a Amount of DCHT adsorbed (mmol/g).Fig. 10. Stability of chromatographic system: separation factor (α). Conditions as in Fig. 9.

CONCLUSIONS

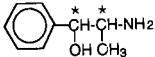
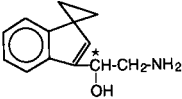
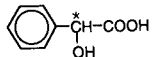
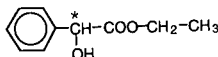
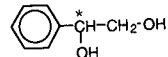
The enantiomers of amino alcohols, acids, hydroxy esters and diols were separated by using DCHT dynamically adsorbed on graphitic carbon. All the separated solutes contained at least two hydrogen-bonding functions. The character of the hydrogen-bonding groups and the presence of bulky groups are important for chiral recognition. For example, the stereoselectivity increased in the order mandelic acid < ethyl mandelate < homatropine.

Among the amino alcohols, where at least one point of interaction is provided by the nitrogen, the separation factor increased with decreasing degree of substitution on the nitrogen, *i.e.*, methylephedrine < ephedrine < norephedrine.

TABLE VII

REPRODUCIBILITY OF CHROMATOGRAPHIC SYSTEM

Mobile phase: 0.25 mM DCHT and 1.9 M acetonitrile in phosphate buffer (pH 2.8) ($I = 0.1$).

Solute	Hypercarb column (batch No.)					
	99		100		102	
	k'_1	α	k'_1	α	k'_1	α
7,8 	0.22	1.14	0.21	1.14	0.20	1.16
15 	14.2	1.56	15.5	1.49	14.5	1.56
18,19 	1.8	1.07	1.7	1.08	1.6	1.07
30,31 	7.0	1.10	6.6	1.10	6.8	1.10
26,27 	1.3	1.04	1.2	1.02	1.2	1.02

ACKNOWLEDGEMENTS

We are grateful to Professor Douglas Westerlund for his interest in this project. This work was supported by the Swedish Natural Science Research Council. Research grants from the Swedish Academy of Pharmaceutical Sciences and the I.F. Foundation for Pharmaceutical Research are gratefully acknowledged.

REFERENCES

- 1 E. J. Ariëns, *Med. Res. Rev.*, 6 (1986) 451.
- 2 A. M. Krstulovic (Editor), *Chiral Separations by HPLC: Application to Pharmaceutical Compounds*, Ellis Horwood, Chichester, 1989; and references cited therein.
- 3 C. Pettersson, A. Karlsson and C. Gioeli, *J. Chromatogr.*, 407 (1987) 217.
- 4 W. Lindner, J. LePage, G. Davies, D. Seitz and B. L. Karger, *J. Chromatogr.*, 185 (1979) 323.
- 5 V. A. Davankov, A. S. Bochkov, A. A. Kurganov, P. Roumeliotis and K. K. Unger, *Chromatographia*, 13 (1980) 677.
- 6 V. A. Davankov, A. S. Bochkov and Yu. P. Belov, *J. Chromatogr.*, 218 (1981) 547.
- 7 T. Shinbo, T. Yamabuchi, K. Nishimura and M. Sugiura, *J. Chromatogr.*, 405 (1987) 145.
- 8 C. Pettersson and H. W. Stuurman, *J. Chromatogr. Sci.*, 22 (1983) 441.
- 9 C. Pettersson, E. Heldin and H. W. Stuurman, *J. Chromatogr. Sci.*, 28 (1990) 413.
- 10 E. Heldin, K.-J. Lindner, C. Pettersson, W. Lindner and R. Rao, *Chromatographia*, in press.
- 11 J. H. Knox and B. Kaur, in P. R. Brown and R. A. Hartwick (Editors), *High Performance Liquid Chromatography*, Wiley, New York, 1989, p. 205.
- 12 D. C. Leach, M. A. Stadalius, J. S. Berus and L. R. Snyder, *LC GC Int.*, 1 (1988) 88.
- 13 Y. Ohtsu, Y. Shiojima, T. Okumura, J.-I. Koyama, K. Nakamuro, O. Makata, K. Kimata and N. Tanaka, *J. Chromatogr.*, 481 (1989) 147.
- 14 B. J. Bassler and R. A. Hartwick, *J. Chromatogr. Sci.*, 27 (1989) 162.
- 15 G. Kortüm, W. Vogel and K. Andrussov, *Dissociation Constants of Organic Acids in Aqueous Solution*, Butterworths, London, 1961, p. 410.

Adsorption and elution of bovine γ -globulin using an affinity membrane containing hydrophobic amino acids as ligands

Min Kim, Kyoichi Saito* and Shintaro Furusaki

Department of Chemical Engineering, Faculty of Engineering, University of Tokyo, Hongo 7-3-1, Tokyo 113 (Japan)

Takeshi Sato

Department of Neurology, Juntendo University School of Medicine, Hongo 2-1-1, Tokyo 113 (Japan)

Takanobu Sugo and Isao Ishigaki

Takasaki Radiation Chemistry Research Establishment, Japan Atomic Energy Research Institute, Watanuki, Takasaki, Gunma 370-12 (Japan)

(First received September 24th, 1990; revised manuscript received March 20th, 1991)

ABSTRACT

A hollow-fibre affinity membrane containing hydrophobic amino acids as ligands was prepared by the radiation-induced grafting of glycidyl methacrylate onto a porous polyethylene hollow fibre and subsequent coupling with phenylalanine (Phe) or tryptophan (Trp). The densities of the Phe and Trp ligand of the resulting affinity membrane were 0.4 and 0.4 mol/kg, respectively. The Trp-containing affinity membrane exhibited a higher amount of adsorbed bovine γ -globulin (BGG) than the Phe-containing membrane. To evaluate the adsorption behaviour of the membrane, the BGG-containing buffer solution was permeated from the inside to the outside of the Trp-containing hollow-fibre affinity membrane through the ligand-immobilized pores. The breakthrough curves as a function of effluent volume coincided irrespective of the flow-rate, *i.e.* the residence time (55–220 s) of the solution across the membrane (thickness 0.83 mm), as a result of negligible mass transfer resistance. A series of chromatographic procedures, (adsorption–washing–elution) was repeated twice and a satisfactory quantitative elution was attained. The reproducible profile of the flux and the protein concentration assured a quantitative cycle of chromatography using the affinity membrane containing Trp as a ligand.

INTRODUCTION

Affinity ligands can be classified into biospecific and pseudobiospecific ligands [1]. Amino acids, especially hydrophobic amino acids, belong to the group of pseudobiospecific ligands. Phenylalanine (Phe)- or tryptophan (Trp)-containing immunoadsorbents based on polyvinyl alcohol beads have been used for rheumatism and myasthenia gravis therapy [2,3]. In addition, Phe has been used as a ligand for the purification of serum proteins [4,5] and enzymes [4,6].

Membrane-based affinity chromatography was proposed by Brandt *et al.* in 1988 [7]. The technique

has advantages over conventional bead-based chromatography for the following two reasons: (1) the module charged with hollow fibres requires a much lower operating pressure than a bead-packed bed; and (2) as the biomolecule to be determined can be directly transported by convection to the ligand immobilized on the inner surface of the microporous membrane, faster adsorption onto the affinity membrane can be attained. Brandt *et al.* [7] demonstrated the efficient isolation of fibrinogen and IgG with gelatin- and protein A-containing affinity membranes. However, details of the preparation of affinity membranes and properties such as ligand density and pore structure were not described.

Functional materials have been developed by applying radiation-induced graft polymerization. These include a packing material for the selective recovery of uranium from sea water [8], a chelating hollow-fibre membrane for the collection of cobalt ultrapure water [9] and affinity membranes for the separation of biomolecules from biological fluids [10]. Radiation-induced grafting is a useful technique as it is applicable to various kinds and arbitrary shapes of polymers.

In this study, affinity membranes based on polyethylene hollow fibres were prepared and hydrophobic amino acid-bovine γ -globulin (BGG) were selected as an affinity pair. The objectives of the study were three-fold: (1) to compare the effectiveness of the Phe and Trp ligands with respect to the adsorption isotherm and kinetics; (2) to clarify the breakthrough features by varying the inlet concentration and flow-rate of the feed; and (3) to examine the adsorption-elution cycle using an affinity membrane.

EXPERIMENTAL

Preparation of Phe- and Trp-containing affinity membranes

Hollow-fibre affinity membranes containing Phe and Trp as ligands were prepared by the radiation-induced grafting of glycidyl methacrylate (GMA) onto a porous polyethylene hollow fibre, followed by coupling of the epoxide group produced with L-Phe and L-Trp. The commercially available hollow fibre (Asahi Chemical Industry, Japan) was used as a base polymer for grafting. This hollow fibre has been used industrially for microfiltration. The inner and outer diameters of this hollow fibre are 2.02 and 3.28 mm, respectively. The hollow fibre is made of polyethylene with a nominal pore diameter of $2 \cdot 10^{-7}$ m and a porosity of 71%. The details of grafting and coupling have been described elsewhere [11]. The resulting hollow fibres containing Phe and Trp as ligands were referred to as Phe-T and Trp-T fibres, respectively; T denotes tubular. The degree of GMA grafting and coupling efficiency were about 120 and 12–13%, respectively:

$$\text{degree of GMA grafting} = 100[(W_1 - W_0)/W_0]$$

$$\text{Coupling efficiency for Phe-T fibre } (X_p)$$

$$W_2 = W_0 + (W_1 - W_0)[X_p(142 + 165) + (1 - X_p)(142 + 18)]/142$$

$$X_p = [142(W_2 - W_0)/(W_1 - W_0) - 160]/147$$

Coupling efficiency for Trp-T fibre (X_t)

$$W_2 = W_0 + (W_1 - W_0)[X_t(142 + 204) + (1 - X_t)(142 + 18)]/142$$

$$X_t = [142(W_2 - W_0)/(W_1 - W_0) - 160]/186$$

where W_0 , W_1 and W_2 are the weights of a starting fibre, GMA-grafted fibre and the Phe-T or Trp-T fibres, respectively. The values 142, 165, 204 and 18 are the molecular weights of GMA, Phe, Trp and water. The ligand density was calculated as:

$$\text{ligand density for Phe-T fibre} = X_p(W_1 - W_0)/142/W_2$$

$$\text{ligand density for Trp-T fibre} = X_t(W_1 - W_0)/142/W_2$$

The chemical structures of the Phe-T and Trp-T fibres are illustrated in Fig. 1.

The dimensions of the resulting hollow fibres were measured using a microscope and a scale. The specific surface area of the dried hollow fibre was determined using Quantasorb (Yuasa Ionics, Japan) according to the BET method. The apparent density of the hollow fibre was calculated by dividing the dry weight by the wet volume.

Adsorption isotherm

The adsorption isotherm of BGG onto the Phe-T and Trp-T fibres was measured by the batchwise

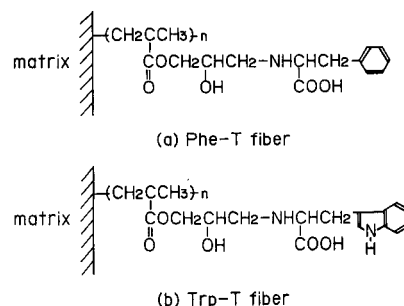


Fig. 1. Chemical structure of the affinity membrane containing Phe or Trp as a ligand.

method. The prescribed weight of each hollow fibre was immersed in the protein solution. BGG was purchased from Sigma (St. Louis, MO, USA; No. G5009, Cohn Fraction II, III) and was used as received. A phosphate-buffered saline (PBS) solution was prepared by dissolving powdered Dulbecco's PBS (Nissui Pharmaceutical, Japan) in water. BGG was dissolved in the PBS buffer solution [pH 7.4; ionic strength (I) = 0.19], the concentration of which ranged from 1 to 4 g/l. Contact for 24 h allowed the system to attain equilibrium. The amount of BGG adsorbed onto the hollow fibre was calculated from the decrease of BGG concentration in the solution. BGG was determined by UV spectroscopy (at 280 nm).

Membrane affinity chromatography

Fig. 2a shows the experimental apparatus for the adsorption and elution of proteins using the hollow-fibre affinity membrane. The 12-cm-long hollow fibre was set in a U-shaped configuration. The protein solution in the syringe was fed at a constant flow-rate ranging from 0.010 to 0.040 l/h. The BGG solution was applied to the inside of the hollow-

fibre affinity membrane and was permeated to the outside through the pores around which the ligand was immobilized. The effluent dropping from the outside of the membrane was collected continuously and the BGG concentration of each fraction was determined. After 30 ml of the effluent had crossed the membrane, the feed solution was switched to the buffer solution to rinse the membrane. After rinsing with 20 ml, 20 ml of the eluate were fed through at the same flow-rate. The eluate was a mixture of 1 M sodium chloride solution and 50% ethylene glycol [4]. This adsorption–washing–elution cycle was repeated once more. In each procedure, the concentration of BGG was determined.

To examine the specificity of the Trp-T fibre to serum proteins, a mixture of BGG and bovine serum albumin (BSA) in PBS buffer was permeated across the membrane at a constant flow-rate of 0.030 l/h. The inlet concentrations of BGG and BSA were both 1 g/l. Each concentration in the effluent was determined by liquid chromatography with a Asahipak GS-520H column (Asahi Chemical Industry, Japan). All experiments were performed at 303 K.

Flux measurement

The initial filtration pressure of the Trp-T fibre was $3.0 \cdot 10^3$ N/m² at a flow-rate of 0.040 l/h. The flow-rate changes during the chromatographic procedures as a result of protein adsorption and elution. To examine the change in flow-rate of the hollow-fibre affinity membrane, a series of solutions, *i.e.* the BGG-containing buffer, the buffer and the eluate, were permeated across the Trp-T fibre at a constant filtration pressure of $1.0 \cdot 10^4$ N/m². The experimental apparatus is shown schematically in Fig. 2b. The flow-rate of each solution dropping from the outside of the membrane was measured. The flux, u_i , was calculated by dividing the flow-rate by the inner surface area of the membrane:

$$u_i = (\text{flow-rate})/\pi d_i L$$

where L is the length and d_i the inner diameter of the hollow fibre.

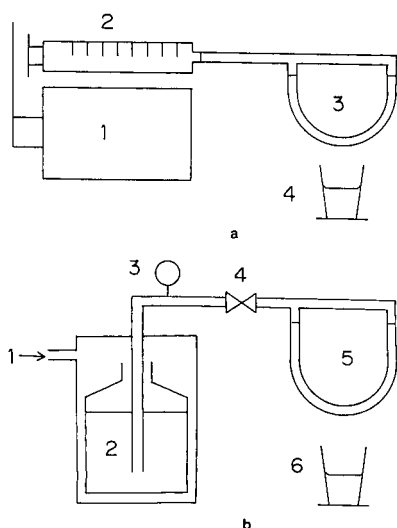


Fig. 2. Experimental apparatus for membrane chromatography. The solution was forced to permeate across the hollow-fibre membrane. (a) At constant flow-rate: 1 = syringe infusion pump; 2 = syringe; 3 = hollow-fibre membrane; 4 = measuring cylinder. (b) At constant filtration pressure: 1 = nitrogen cylinder; 2 = feed tank; 3 = pressure gauge; 4 = valve; 5 = hollow-fibre membrane; 6 = measuring cylinder.

RESULTS AND DISCUSSION

Properties of Phe-T and Trp-T fibres

The physical properties of Phe-T and Trp-T fibres are summarized in Table I. The physical properties of the two affinity membranes were similar. The pure water flux and specific surface area of the Trp-T fibre were about 75 and 60% of those of the starting hollow fibre, respectively. The 120% degree of GMA grafting and 12.3% coupling efficiency of Trp gave a ligand density of 0.40 mol/kg. As the apparent density was 0.35 kg (dry)/l (wet), the ligand density per kg was converted into 0.14 mol/l (wet), which is two orders of magnitude greater than that of commercial affinity beads. For example, the ligand density of the commercial affinity bead containing Trp is 0.003 mol/l [12]. The remaining epoxide group is quantitatively converted on coupling into a diol group [13]. The diol group renders the polymer surface hydrophilic and prevents non-selective adsorption [13], whereas the coupled Phe and Trp adsorb BGG pseudospecifically. Both the inner and outer diameters of the hollow-fibre affinity membrane increased by chemical modification compared with the starting hollow fibre. The membrane thickness corresponds to the bed height when the hollow-fibre affinity membrane is regarded as a packed bed charged with affinity beads.

Adsorption isotherms

Fig. 3 shows the adsorption isotherms of BGG onto the Phe-T and Trp-T fibres. The Trp-T fibre

TABLE I
PROPERTIES OF THE PHE-T AND TRP-T FIBRES

Property	Phe-T	Trp-T	Starting hollow fibre
Degree of GMA grafting (%)	120	120	—
Coupling efficiency (%)	12.8	12.3	—
Ligand density (mol/kg)	0.40	0.40	—
Inner diameter (mm)	2.43	2.43	2.02
Outer diameter (mm)	3.96	4.08	3.28
Specific surface area (m ² /g)	13.0	13.9	23.9
Apparent density (kg/l)	0.36	0.35	0.24
Porosity (—)	0.60	0.60	0.71
Pure water flux ^a (m/h)	0.090	0.090	0.12

^a At a filtration pressure of $1.0 \cdot 10^4$ N/m².

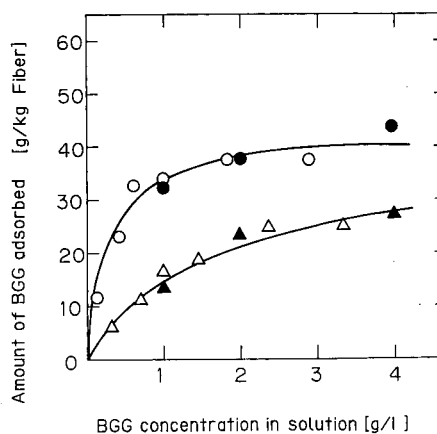


Fig. 3. Adsorption isotherms of BGG on the affinity membranes. The Phe-T (triangles) or Trp-T (circles) fibre was contacted with the BGG-containing buffer solution at 303 K by the batch mode (open symbols) and the breakthrough mode (closed symbols).

bound more BGG than the Phe-T fibre. The reason for this difference is unclear. The data were correlated with a Langmuir-type equation and the saturation capacities of the Phe-T and Trp-T fibres were calculated to be 36 and 49 g/kg, respectively. The saturation capacity of the affinity membrane was determined from the specific surface area when the ligand was in excess of the protein [11].

Affinity chromatography with hollow-fibre membrane

By varying the BGG concentration of the feed, the breakthrough curves (BTCs) were determined. Fig. 4a and b show the BTCs for the Phe-T and Trp-T fibres, respectively. As expected from the isotherm results, the Trp-T fibre exhibited more favourable characteristics than the Phe-T fibre. The amount of BGG adsorbed onto the membrane in equilibrium with the inlet concentration can be calculated by the following integration:

$$q_0 = \int_0^{V_s} (C_0 - C) dV/W$$

where C_0 , C and q_0 are the concentrations of the feed and effluent and the amount of the protein adsorbed in equilibrium with C_0 . V and W are the effluent volume and the weight of the membrane, respectively. V_s is the effluent volume for which concentration reaches C_0 . The results of this integra-

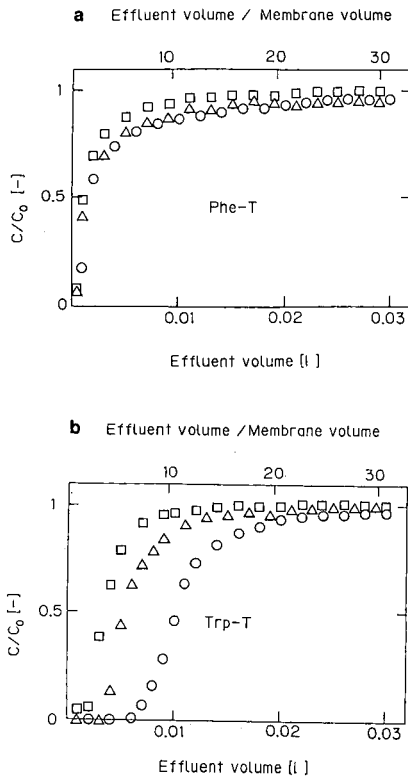


Fig. 4. BTCs as a function of inlet concentration. (a) Phe-T fibre; (b) Trp-T fibre. The BGG solution was applied to the inside of the 12-cm-long hollow fibre at a constant flow-rate of 0.02 l/h. The BGG concentration of the effluent dropping from the outside across the hollow fibre was determined as a function of the effluent volume. C_0 : (○) 1; (△) 2; and (□) 4 g/l.

tion were inserted into Fig. 3. The isotherm data calculated from the BTC analysis agreed with the data determined by the batchwise method. Although the flow-rate can interfere with adsorption on the polymer surface due to the deformation of protein by shear stress [14,15], the flow-rate in the pores did not affect the adsorption capacity in this instance. The shear stress on the surface of the straight pore can be calculated from the following [16]:

$$\text{shear stress} = \Delta P r_p / (2L_p)$$

where ΔP is the filtration pressure and r_p and L_p are the radius and length of the pore, respectively. When the filtration pressure was $3.0 \cdot 10^3 \text{ N/m}^2$, the shear stress was calculated to be about 0.2 N/m^2 at

most, assuming that r_p was $1.0 \cdot 10^{-4} \text{ mm}$ and L_p is the thickness of the Trp-T fibre (0.83 mm). This stress is too small to damage the protein.

Fig. 5 shows the BTCs of the Trp-T fibre as a function of the flow-rate of the feed. The upper abscissa in Fig. 5 represents the “membrane volume” corresponding to the bed volume, which is defined as:

$$\text{membrane volume} = (\text{effluent volume}) / (\text{membrane volume})$$

The change in the flow-rate indicates the variation of the residence time of the solution across the membrane. The flow-rate can be converted into the mean residence time, t_r :

$$t_r = \varepsilon(d_0^2 - d_i^2) / 4d_i u_i$$

where d_i and d_0 are the inner and outer diameters of the hollow-fibre affinity membrane, respectively. The porosity of the hollow fibre, ε , can be determined from measurement of its water content. When the flow-rate varied from 0.010 to 0.040 l/h, the residence time ranged from 55 to 220 s. As a result, the residence time caused almost no difference in the BTC. This was indicative of the negligible mass transfer resistance. A rectangular line for an ideal BTC is shown in Fig. 5, where the ideal breakthrough point, t_i , was calculated from the following:

$$t_i = (d_0^2 - d_i^2) \rho_a q_0 / 4u_i d_i C_0$$

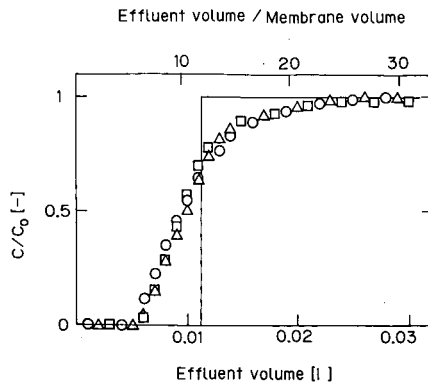


Fig. 5. BTCs of the Trp-T fibre as a function of flow-rate. The BGG solution was fed at a feed concentration of 1 g/l. Flow-rate: (○) 0.01; (△) 0.02; and (□) 0.04 l/h.

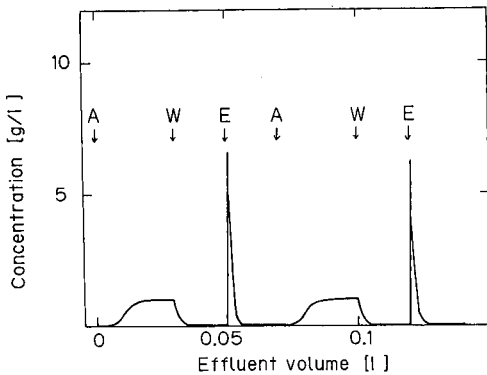


Fig. 6. Concentration change of BGG in membrane affinity chromatography. The adsorption–washing–elution cycle using the 12-cm-long Trp-T fibre was repeated twice at a constant flow-rate of 0.030 l/h. The symbols A, W and E designate adsorption, washing and elution, respectively. $C_0 = 1$ g/l.

where ρ_a is the apparent density of the affinity membrane. The dispersion in the BTC was obtained. This is due to the distribution in the pore length of the membrane, *i.e.* the residence time distribution of the solution across the membrane.

Fig. 6 shows the concentration change of BGG with effluent volume during the chromatographic procedures of adsorption, washing and elution. The mass balance was almost satisfied for the BGG and Trp-T fibre affinity system. Moreover, the repeated

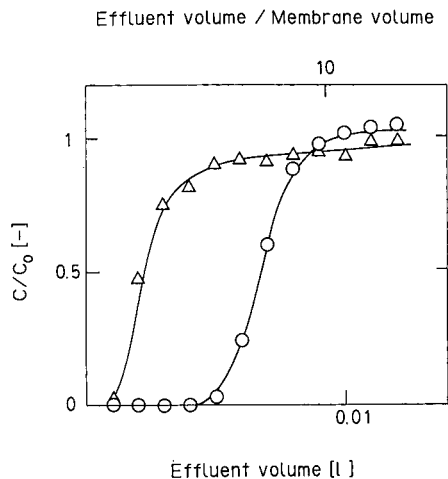


Fig. 7. BTC of the Trp-T fibre for the mixture of (○) BGG and (△) BSA. The inlet concentrations were both 1 g/l. Flow-rate = 0.03 l/h.

use of the affinity membrane showed a similar chromatographic performance. With an eluate of 1 M sodium chloride solution and 50% ethylene glycol, the peak and average concentrations of BGG were to 7 and 5.5 g/l, respectively.

A BTC for the mixture of BGG and BSA is shown in Fig. 7. BSA had a faster breakthrough behaviour than BGG at the same concentration of 1 g/l due to the higher specificity of the Trp-T fibre to BGG.

Flux consideration

Fig. 8 shows the variation of the flux under a constant filtration pressure of $1.0 \cdot 10^4$ N/m² during affinity membrane chromatography. As the adsorption of BGG onto the pore surface of the Trp-T fibre proceeded, the flux gradually decreased. Switching to the feed of the viscous eluate caused the flux to decrease irrespective of protein elution. The viscosities of the PBS buffer and eluate were determined to be $0.94 \cdot 10^{-3}$ and $2.81 \cdot 10^{-3}$ N/m² s, respectively. The viscosity ratio of the buffer to the eluate, 0.33, did not agree with the reciprocal of the flux ratio, 0.24. This is due to the difference in the interaction between the graft chain immobilized on the membrane and the solution permeating through its pores [17]; the eluate of 1 M sodium chloride solution and 50% ethylene glycol will cause the graft chain to swell.

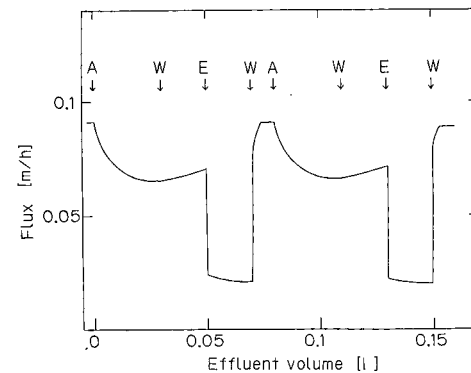


Fig. 8. Flux change in membrane affinity chromatography. The adsorption–washing–elution cycle using the 12-cm-long Trp-T fibre was repeated twice at a constant filtration pressure of $1.0 \cdot 10^4$ N/m². $C_0 = 1$ g/l. The flow-rate of the effluent was determined and was converted into the flux. The symbols are the same as those used in Fig. 6.

The affinity membrane recovered the initial flux by washing with PBS buffer. The reproducible profile in the flux and the protein concentration indicates that a stable cycle is possible in chromatography using an affinity membrane containing a hydrophobic amino acid as a ligand.

SYMBOLS

C	concentration in the effluent (g/l)
C_0	concentration in the feed (g/l)
d_i	inner diameter of the affinity hollow fibre (cm)
d_o	outer diameter of the affinity hollow fibre (cm)
L	fibre length (cm)
L_p	pore length (cm)
ΔP	filtration pressure (N/m ²)
q_0	amount of protein adsorbed per kg of the affinity membrane in equilibrium with C_0 (g/kg)
r_p	pore radius (cm)
t_i	ideal breakthrough time (s)
t_r	mean residence time (s)
u_i	flux based on the inner surface area of the hollow fibre (cm/s)
V	volume of the effluent (l)
V_s	volume of the effluent with a concentration which reaches C_0 (l)
W_0	weight of the starting fibre (kg)
W_1	weight of the GMA grafted fibre (kg)
W_2	weight of the Phe- or Trp-T fibre (kg)
X_p	coupling efficiency for Phe-T fibre
X_t	coupling efficiency for Trp-T fibre
ε	porosity of the affinity hollow fibre
ρ_a	apparent density of the affinity hollow fibre (kg/l)

ACKNOWLEDGEMENTS

The authors thank Kazuo Toyomoto and Takeru Uchida of the Industrial Membrane Division and Gel Separation Department of Asahi Chemical Industry for their help in providing the starting hollow fibre and the liquid chromatography column.

REFERENCES

- 1 M. A. Vijayalaskshmi, *Trends Biotechnol.*, 17 (1989) 71.
- 2 Z. Yamazaki and N. Yamawaki, *Jpn. J. Artif. Organs*, 12 (1983) 895.
- 3 T. Sato, M. Anno, K. Arai, N. Yamawaki, T. Kuroda and K. Inagaki, *Prog. Artif. Organs*, 4 (1983) 719.
- 4 B. H. J. Hofstee, *Biochem. Biophys Res. Commun.*, 63 (1975) 618.
- 5 G. J. Doellgast and A. G. Plaut, *Immunochemistry*, 13 (1976) 135.
- 6 M. H. Gething, B. E. Davidson and T. A. A. Dopheide, *Eur. J. Biochem.*, 71 (1976) 317.
- 7 S. Brandt, R. A. Goffe, S. B. Kessler, J. L. O'Connor and S. E. Zale, *Biotechnology*, 6 (1988) 779.
- 8 K. Saito, K. Uezu, T. Hori, S. Furusaki, T. Sugo and J. Okamoto, *AIChE J.*, 34 (1988) 411.
- 9 K. Saito, M. Ito, H. Yamagishi, S. Furusaki, T. Sugo and J. Okamoto, *Ind. Eng. Chem. Res.*, 28 (1989) 1812.
- 10 H. Iwata, K. Saito, S. Furusaki, T. Sugo and J. Okamoto, *Biotechnol. Progress*, in press.
- 11 M. Kim, K. Saito, S. Furusaki, T. Sugo and I. Ishigaki, *J. Chromatogr.*, in press.
- 12 *Catalogue*, Sigma Chemical St. Louis, MO, 1990, p. 1453.
- 13 M. Kim, K. Saito, S. Furusaki, T. Sugo and J. Okamoto, *J. Membrane Sci.*, 56 (1991) 289.
- 14 R. G. Lee and S. W. Kim, *J. Biomed. Mater. Res.*, 8 (1974) 251.
- 15 S. E. Charm and B. L. Wong, *Biotechnol. Bioeng.*, 12 (1970) 1103.
- 16 R. B. Bird, W. E. Stewart and E. N. Lightfoot, *Transport Phenomena*, Wiley, New York, 1960, p. 45.
- 17 S. Tsuneda, K. Saito, S. Furusaki, T. Sugo and I. Ishigaki, *J. Membrane Sci.*, submitted for publication.

Determination of picomole amounts of lipoxins C₄, D₄ and E₄ by high-performance liquid chromatography with electrochemical detection

Frank-Peter Gaede*, Matthias Kirchner, Dieter Steinhilber and Hermann J. Roth

Pharmaceutical Institute, University of Tübingen, Auf der Morgenstelle 8, W-7400 Tübingen (Germany)

(First received February 26th, 1991; revised manuscript received May 8th, 1991)

ABSTRACT

A method for the sensitive determination of the sulphopeptide lipoxins (LXs) C₄, D₄ and E₄ by high-performance liquid chromatography with subsequent electrochemical detection is described. The best results were obtained when the analysis was carried out with the solvent system methanol–water–trifluoroacetic acid (66:34:0.008, v/v/v). The acquired half-wave potentials were different for all investigated compounds: +1.18 V for LXC₄, +1.3 V for LXD₄ and +1.25 V for LXE₄. The detection limits of LXC₄, LXD₄ and LXE₄, based on a signal-to-noise ratio of 3:1, were found to be 200–700 fmol. Although sulphopeptide lipoxins possess a high molar absorptivity, electrochemical detection still is three times more sensitive than ultraviolet detection.

INTRODUCTION

Lipoxins (LXs), which are arachidonic acid metabolites formed by the interaction of the 5- and 15-lipoxygenase pathways, have been shown to exhibit various biological activities. LXA₄ leads to superoxide anion generation and the degranulation of human neutrophils, promotes chemotaxis, contracts lung parenchymal stripes and activates protein kinase C *in vitro*. LXA₄ and LXB₄ inhibit natural killer cell activity [1].

(15S)-Hydroxy-5,6-epoxy-7,9,13-*trans*-11-*cis*-eicosatetraenoic acid has been suggested to be a common intermediate in the biosynthesis of LXA₄ and LXB₄ in human granulocytes [2]. LXA₄ has been found in extracts from human eosinophils stimulated with the ionophore A23187 and arachidonic acid [3]. Moreover, human eosinophils contain considerable amounts of glutathione-S-transferase [4]. This enzyme catalyses the conjugation of glutathione to another well known allylic epoxide, LTA₄, leading to the sulphopeptide leukotrienes (LTs) LTC₄, LTD₄ and LTE₄. Combining the 5- and

15-lipoxygenase with the glutathione-S-transferase pathway, it has been shown that human eosinophils can release amino acid containing lipoxins. Owing to the similar biosynthetic route of these compounds to LXA₄ and LXB₄, and in accordance with the nomenclature of leukotrienes, the trivial names LXC₄, LXD₄ and LXE₄ were suggested [5] (structures given in Fig. 1).

The method of choice for the qualitative determination of lipoxins is separation by high-performance liquid chromatography (HPLC) with ultraviolet (UV) detection [6]. The conjugated tetraene system shows a typical absorbance maximum at 301 nm and a molar absorptivity of 50 000 [2]. The new lipoxins C₄, D₄ and E₄ present a bathochromic shift to 307 nm. A method has been reported [7] for the highly sensitive determination of oxidizable compounds, such as lipoxins, using HPLC and subsequent electrochemical detection (ED). In this paper the application of this technique to the new lipoxins is described, including a study of the electrochemical behaviour of these compounds under certain chromatographic conditions.

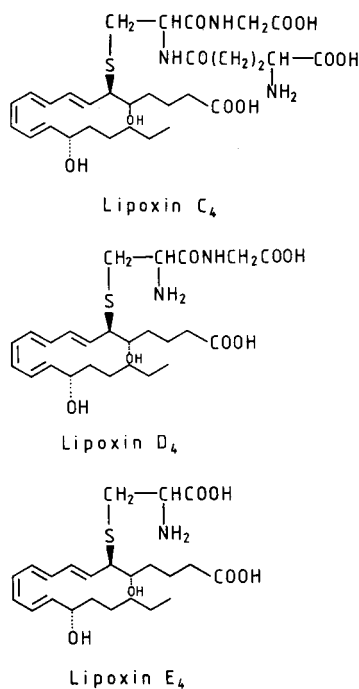


Fig. 1. Structures of the sulphopeptide lipoxins.

EXPERIMENTAL

Materials

LTC₄, LTD₄ and LTE₄ were obtained from Paesel (Frankfurt, Germany). Soybean lipoxygenase, trifluoroacetic acid (TFA) and Ca²⁺ ionophore A23187 (free acid) were purchased from Sigma (St. Louis, MO, USA), phosphate-buffered saline (PBS) buffer PM 16 without Ca²⁺, Mg²⁺ and phenol red from Serva (Heidelberg, Germany), methanol (Li-Chrosolv) and lithium chloride from Merck (Darmstadt, Germany) and alumina powder (0.3 μm), lithium perchlorate and sodium borohydride from Fluka (Buchs, Switzerland). Water used for the mobile phase was freshly distilled. All other chemicals used were of analytical-reagent grade.

The concentration of the stock solutions of lipoxins in methanol were established with a Beckman DU-50 spectrophotometer by measuring the UV absorption at 307 nm. A molar absorptivity of 50 000 was used for the calculations.

Preparation of lipoxin standards

The lipoxin standards were prepared according to the method of Örning and Hammarström [8].

LTD₄ and LTE₄ (2.5 μg) were incubated with 20 μg of soybean lipoxygenase (2500 U) in 1 ml of PBS buffer (9.55 g/l, see under Materials), pH 7.4, at room temperature with vigorous shaking. A 100-μg mass of soybean lipoxygenase was used to transform LTC₄. The UV spectrum was scanned (from 250 to 350 nm every 10 min. The reaction was finished when no further increase in absorption at 307 nm was observed. To stop the enzyme activity, 500 μl of pure methanol were added; 10 mg of sodium borohydride were then dissolved in the incubation mixture to reduce the hydroperoxides formed. This preparation was kept at room temperature for 15 min. The addition of 1 ml of PBS buffer (9.55 g/l) was necessary to reduce the methanol content to less than 30% to obtain better recoveries during the solid-phase extraction. Finally the solution was acidified to pH 6 with 1 M hydrochloric acid, extracted and analysed as described in the following section.

Extraction procedure

Using the method reported by Steinhilber and Roth [5], Baker C₁₈ disposable columns were conditioned with 2 ml of 100% methanol, 2 ml of water, 2 ml of a 0.1% aqueous EDTA solution and again with 2 ml of water. The samples were then applied to the columns and washed with 3 ml of water and 3 ml of 25% methanol. Finally, the lipoxins were eluted with 100% methanol. The extract was evaporated to dryness under a stream of nitrogen and resuspended in a small volume of methanol. Aliquots of this solution were injected into the HPLC apparatus.

Apparatus

The HPLC equipment consisted of a Waters Assoc. 460 electrochemical detector with a thin-layer glassy carbon electrode assembly, a Waters 481 variable-wavelength UV detector, a Waters 590 pump and a Waters U6K injector. Both detector outputs were connected to an IEEE interface of a Maxima 820 workstation. All data were acquired and processed with the Maxima full control software.

To restore sensitivity to the glassy carbon elec-

trode, its surface was pretreated with a dichromate-sulphuric acid and alumina slurry, as previously reported [9]. All potentials applied were referred to a Ag/AgCl electrode filled with 3 M lithium chloride in 65% aqueous methanol.

Column and mobile phase

The separations were carried out using a Waters Radial-Pak cartridge (100 × 5 mm I.D.) packed with 4- μ m Novapak C₁₈ material obtained from Waters (Eschborn, Germany). The solvent system was methanol-water-TFA (66:34:0.008, v/v/v). A flow-rate of 1.2 ml was used. All experiments were carried out at ambient temperature.

RESULTS AND DISCUSSION

The mobile phase most commonly used to separate lipoxygenase products by reversed-phase HPLC is either acetonitrile-water with TFA or methanol-water containing TFA. Although an excellent separation of the lipoxins can be achieved with the former mobile phase, this solvent system was not suitable for ED owing to a high background current. These findings are in agreement with previously published data [10]. To prevent interaction between the cations and the amino acid containing eicosanoids, a few workers have proposed the addition of EDTA to the mobile phase [11]. This substance was not applicable to ED because it leads to an increase in the background current. For the best electrochemical results the analysis was carried out with a solvent system using only methanol-water-TFA as reported previously [7]. To obtain a low background current and retention times for optimal separation ($\alpha = 1.14$) of the lipoxins, a solvent mixture containing 66% aqueous methanol and 1 mM TFA was applied. Fig. 2 shows a characteristic chromatogram of LXC₄, LXD₄ and LXE₄ standards, obtained as described. Owing to the preparation method, bulk impurities were eluted in front of the lipoxins but they did not influence the determination.

Hydrodynamic voltammograms of LXC₄, LXD₄ and LXE₄ are presented in Fig. 3. At +1.45 V a maximum response was obtained for all lipoxins. The half-wave potentials were different for all compounds investigated: +1.18 V for LXC₄, +1.3 V for LXD₄ and +1.25 V for LXE₄. In contrast,

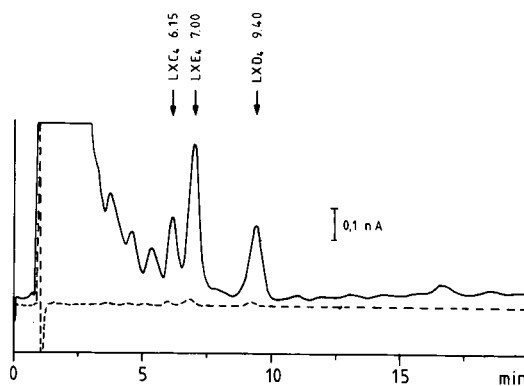


Fig. 2. HPLC-ED (solid line) and HPLC-UV (broken line) profiles of sulphopeptide lipoxins. Eluent, methanol-water (66:34, v/v) containing 1 mM TFA; flow-rate, 1.2 ml/min; applied potential, +1.35 V (versus Ag/AgCl); UV detection, 308 nm; injection volume, 15 μ l containing 5 ng of each lipoxin.

LXC₄, LXD₄ and LXE₄ showed an identical electrochemical response (89 ± 2.25 nA s) per 100 μ M injected. In subsequent experiments a potential of +1.35 V was used.

With the aim of finding a mobile phase with a low background current and a high sensitivity, various concentrations of TFA (0.1–1 mM) and lithium perchlorate (0–3 mM) were used. Both compounds strongly affected the elution of every lipoxin (data not shown). Generally, increasing concentrations of both additives decreased the retention times. In a few instances LXC₄ and LXE₄ were co-eluted. Only

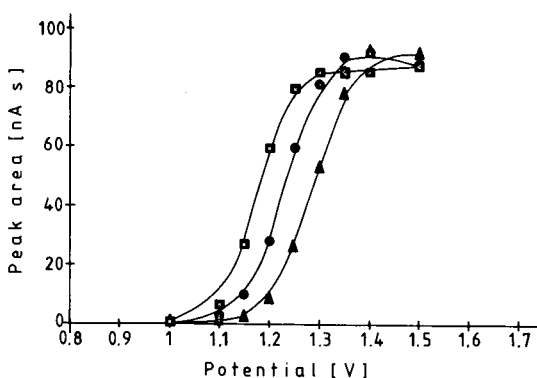


Fig. 3. Hydrodynamic voltammograms of LXC₄ (■), LXD₄ (▲) and LXE₄ (●), each corresponding to 100 μ M of lipoxin.

TABLE I
MEANS OF PEAK AREAS

Injected (ng)	Peak area (mean \pm S.D., $n = 3$) (nA s)		
	LXC ₄	LXD ₄	LXE ₄
1	1.74 \pm 0.29	2.84 \pm 0.47	4.03 \pm 0.62
10	11.47 \pm 0.17	23.32 \pm 1.52	28.12 \pm 1.63
20	21.95 \pm 0.74	41.02 \pm 0.55	51.00 \pm 0.82
50	54.37 \pm 2.50	106.17 \pm 1.43	139.17 \pm 1.65

a slight rise in electrochemical response was observed when the background current increased to 19 nA. The best results with respect to chromatographic resolution and electrochemical response were achieved with a mobile phase containing 66% aqueous methanol and 1 mM TFA. This solvent mixture established a stable baseline and a typical background current of 5–8 nA, thus allowing measurements at a sensitivity of 100 pA full scale.

Data obtained under these conditions are giving as means \pm S.D. of the areas (in nA s), corresponding to the amount of each lipoxin injected (Table I). Table II presents the equations of these graphs and the correlation coefficients for the peptido-lipoxins,

TABLE II
EQUATIONS CORRESPONDING TO THE CALIBRATION GRAPHS AND CORRELATION COEFFICIENT FOR THE LIPOXINS

Equation is defined as $y = ax + b$, where y is the peak area and x is the amount (ng) of sample; r is the correlation coefficient.

Lipoxin	t_R (min)	Equation	r
LXC ₄	6.15	$y = 1.074x + 0.641$	1.0000
LXD ₄	9.40	$y = 2.098x + 0.857$	0.9995
LXE ₄	7.00	$y = 2.776x - 0.503$	0.9990

which were obtained by calculating the results shown in Table I by the least-squares method. The detection limits of LXC₄, LXD₄ and LXE₄, based on a signal-to-noise ratio of 3:1, were 100–500 pg (200–700 fmol).

This method shows that HPLC with ED allows sensitive detection even at high potentials. In spite of the fact that sulphopeptide lipoxins are very sensitive to variations in the mobile phase, relatively small amounts of LXC₄, LXD₄ and LXE₄ can be detected. Although peptido-lipoxins possess a high molar absorptivity, ED still is three times more sensitive than UV detection.

ACKNOWLEDGEMENTS

This work is a part of a doctoral thesis (F.-P. Gaede; referee H. J. Roth, 1991). The authors thank the Fonds der Chemischen Industrie (Frankfurt a.M., Germany) for supporting this study and Dr. C. Müller for critical reading of the manuscript.

REFERENCES

- 1 B. Samuelsson, S.-E. Dahlen, J. A. Lindgren, C. A. Rouzer and C. N. Serhan, *Science*, 237 (1987) 1171.
- 2 C. N. Serhan, K. C. Nicolaou, S. E. Webber, C. A. Veale, S.-E. Dahlen, T. J. Puustinen and B. Samuelsson, *J. Biol. Chem.*, 261 (1986) 16340.
- 3 C. N. Serhan, U. Hirsch, J. Palmblad and B. Samuelsson, *FEBS Lett.*, 217 (1987) 242.
- 4 P. Borgeat, B. Fruteau de Lacroix, H. Rabinovitch, S. Picard, P. Braquet, J. Hebert and M. Laviolette, *J. Allergy Clin. Immunol.*, 74 (1984) 310.
- 5 D. Steinhilber and H. J. Roth, *FEBS Lett.*, 255 (1989) 143.
- 6 D. Steinhilber, T. Herrmann and H. J. Roth, *J. Chromatogr.*, 493 (1989) 361.
- 7 T. Herrmann, D. Steinhilber and H. J. Roth, *J. Chromatogr.*, 428 (1988) 237.
- 8 L. Örnning and S. Hammarström, *FEBS Lett.*, 153 (1983) 253.
- 9 T. Herrmann, D. Steinhilber and H. J. Roth, *J. Chromatogr.*, 416 (1987) 170.
- 10 J. Knospe, D. Steinhilber, T. Herrmann and H. J. Roth, *J. Chromatogr.*, 442 (1988) 444.
- 11 J. Verhagen, *J. Chromatogr.*, 378 (1986) 208.

Chromatographic fractionation of nucleic acids using microcapsules made from plant cells

Andres Jäschke and Dieter Cech*

Department of Chemistry, Humboldt University, Invalidenstrasse 42, O-1040 Berlin (Germany)

Rudolf Ehwald

Department of Biology, Humboldt University, Invalidenstrasse 42, O-1040 Berlin (Germany)

(Received March 27th, 1991)

ABSTRACT

The chromatographic fractionation of nucleic acids and oligodeoxyribonucleotides on a vesicular packing (VP) material has been investigated. As the VP material consists of microcapsules with a negatively charged ultrafiltration membrane, the experiments were focused on permeation chromatography in aqueous buffers of different ionic compositions. The adsorption of oligonucleotides and nucleic acids by the VP material occurring at pH values below 7 and especially in the presence of divalent cations, was negligible in neutral or weakly alkaline buffers. In such buffers the separation principle is based only on the permeation of polyanions into the stationary liquid within the vesicles. Polydisperse samples may be separated into an excluded peak fraction (at 40% of bed volume), fractions with intermediate elution volumes and a permeating peak fraction (at 95% of bed volume). The ratio between these fractions can be varied gradually by changing the salt concentration. Using defined oligonucleotides the maximum chain length for permeation into the whole stationary phase was smaller than the minimum chain length for complete exclusion. Both values were dependent on the salt concentration and pH. They could be varied gradually and reversibly over a wide range by altering the magnesium chloride concentration from 0 to 10 mM. In contrast to ion-exclusion effects known from gel permeation chromatography, in vesicle permeation chromatography there is no salt effect on the elution volume of the permeable fraction. Preparative applications for the fractionation of oligodeoxyribonucleotides and nucleic acids are presented.

INTRODUCTION

Microcapsules are widely used for the immobilization of enzymes, microorganisms and mammalian tissues as well as for the encapsulation of drugs. In addition, there are a variety of potential applications as chromatographic supports. Microcapsules consisting of the intact primary cell wall of higher plants have been successfully applied as a chromatographic material [1]. This vesicular packing (VP) material was shown to be suitable for a new type of exclusion chromatography. In contrast to gel permeation chromatography (GPC), the separation mechanism is not based on a size-dependent distribution within a matrix, but on permeation through a thin ultrafiltration membrane into a large stationary liquid volume. Hence, vesicle chromatography (VC) is a

chromatographic form of membrane separation rather than a subtype of GPC. Whereas in GPC the fractionation range is extended to more than one order of magnitude in terms of molecular weight, a very small fractionation range was observed in VC. Molecules with small differences in molecular size may be separated by a large difference in elution volume. The maximum Stokes' diameter for permeation into the whole stationary liquid volume of standard VP materials was determined using calibrated dextrans to be 5.6 nm [2]. Not only the size and shape of a molecule, but also its charge governs the permeability through membranes. Negatively charged proteins with Stokes' diameters normally allowing permeation (pepsin and ovalbumin) were excluded from the VP material [2]. It is assumed that electrostatic interactions between the proteins and

TABLE I
 OLIGODEOXYRIBONUCLEOTIDE SEQUENCES (DIRECTION 5' → 3')

Chain length	Sequence
2	CC
3	AAC
4	GAT G
5	AAC TC
6	CCG AAC
7	ACA CAT C
8	ACA CAT GC
9	CGC GTT CCA
11	CTA GAC ATA TG
14	CTT TCA AGA TCC CC
17	TAG CAT CAA CCG CAG CC
20	GTT GAA GGA TCA ACA TTT TG
23	GTC GAC CAA TGG GGT GGC TTT GC
25	CCG GTC TGA GAG GAT GGC CGG CCA C
28	ATC TAG AAT GTG GGG GGG GCT CCC AAC A
33	GGA GGA GGC CCC TTA GGA GCT TGT CGG GGT TGA
36	CGT CAG CTC GTG CCG TGA GGT GTT GGG TTA AGT CCC
40	CGA CCG TTC CCG GTT CCA ATA TCA TGG TCG TGT CCA GGCA
45	AGC TTA GAA CTG AAG GCC AGC TTC ACG GGC AGC ATC TGC CAG TGC
50	CTG GGC GCA ACT CGC CTG GTG GTA CAT CGT ACC CCG CGT CAC ATT TAT GC
59	GCT GTG GGT AAA GCT GTC GCT GAA CGC GCT CTG GAA AAA GGC ATC AAA GAT GTA TCC TT
70	GTC ACC TGC AGT CTA GAT CTA ACA CCG TGC GTC TTG ACT ATT TTA CCT CIG GCG GTC ATA ATG GTT GCA G

the negatively charged cell wall matrix cause this exclusion. Compared with proteins, nucleic acids and oligonucleotides have an extremely high charge density. Therefore, electrostatic interactions with the cell wall should be more important than for proteins. Thus, nucleic acids and oligonucleotides promised to be suitable for systematic studies of the effect of charge in VC. This work considers the influence of salt concentration and pH value on separation.

EXPERIMENTAL

DNA from calf thymus and from herring sperm, adenosine, 2',3'-uridinemonophosphate (2',3'-UMP) and 2',3'-cytidinemonophosphate (2',3'-CMP) were obtained from Serva. RNA (not further specified) and tRNA^{val} were from Boehringer Mannheim. Plasmid pKK 161-8 [3] was a gift from Dr. R. K. Hartmann (Freie Universität Berlin, Berlin, Germany).

Oligonucleotides were synthesized on an Applied Biosystems 380A oligonucleotide synthesizer following the phosphoramidite strategy. The sequences are listed in Table I. The raw products were purified by reversed-phase high-performance liquid chromatography on ODS Hypersil. The dimethoxytrityl groups were removed by treatment with 80% acetic acid. Oligonucleotides with a chain length greater than ten were desalted on NAP 10 columns (Pharmacia) and shorter oligonucleotides on self-packed Sephadex G 10 columns. Water was removed by using a Speed Vac concentrator (Savant). The oligonucleotides, nucleotides and nucleic acids were dissolved in the appropriate buffer to give an absorbance (A_{260}) of 1 unit in a 200- μ l volume.

All other reagents were of analytical-reagent grade and were obtained from Serva and Biomol.

The VP material described by Ehwald *et al.* [1], commercially available from Serva ("Vesipor") and from Permselect ("Permselect"), was used. Furthermore, alkali-treated VP material with an increased separation limit was tested.

For chromatographic use, the VP material was swollen for 5 min in distilled water. It was then titrated with one buffer component to the desired pH. The pH value should be equal to that of the buffer used in the chromatographic separation. This step was followed by extensive washing using a high

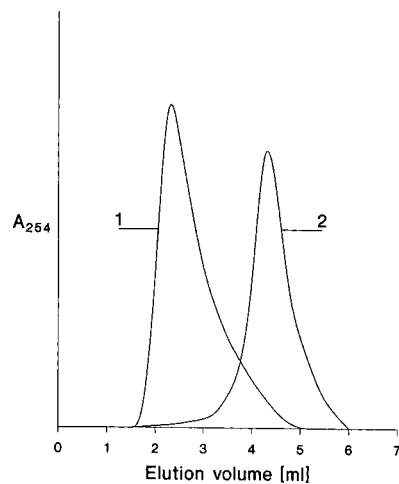


Fig. 1. Vesicle chromatography of RNA at 0 and 20 mM magnesium chloride. Column dimensions, 25 \times 16 mm; sample volume, 50 μ l; flow-rate, 0.8 ml/min. Column equilibration, sample dissolution and elution with: (1) 1 mM Tris-HCl, pH 7.5; and (2) 1 mM Tris-HCl, pH 7.5, 20 mM magnesium chloride.

salt buffer (desired pH, 200 mM magnesium chloride, 500 mM sodium chloride) and finally with the appropriate buffer for chromatography. Short glass columns (injection syringes with an I.D. of 16 mm) were packed conventionally. For the preparative fractionation, an Econo column (Bio-Rad) was

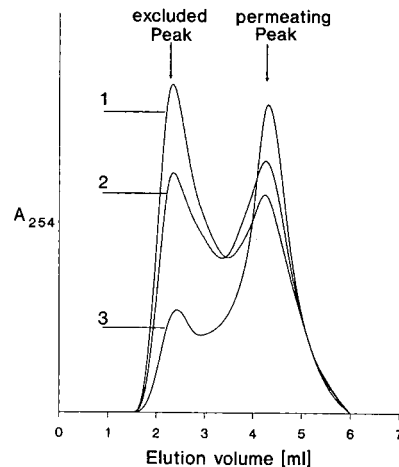


Fig. 2. Vesicle chromatography of RNA at different concentrations of magnesium chloride. Conditions as in Fig. 1. Buffer composition: (1) 1 mM Tris-HCl, pH 7.5, 0.2 mM magnesium chloride; (2) 1 mM Tris-HCl, pH 7.5, 1 mM magnesium chloride; and (3) 1 mM Tris-HCl, pH 7.5, 3 mM magnesium chloride.

used. The packing material was covered with filter paper. After equilibration, at least 0.04 A_{260} units of the sample were loaded onto the column. The flow-rate was gravity-controlled and maintained in the range 0.2–0.5 ml $\text{cm}^{-2} \text{min}^{-1}$. For the chromatographic separation of oligonucleotides, a peristaltic pump (Minipuls 2, Gilson) was used running at a constant flow-rate. Unless otherwise indicated, the experiments were carried out at pH 7.5.

The chromatograms were recorded using an LKB 2238 Uvicord S II spectrometer operating at 254 nm.

RESULTS

At pH 7.5, peak elution volumes of nucleotides or nucleic acids larger than one packing volume have not been observed, indicating that the elution behaviour was determined only by permeation and not by adsorption.

Ribonucleic acid from yeast, a technical product with a broad molecular weight distribution, showed an elution behaviour which was remarkably dependent on the magnesium chloride concentration (Figs. 1 and 2). At low salt concentration (Fig. 1, line 1) one peak was observed leaving the column with the void volume (about 40% of the total packing volume). Most RNA molecules were obviously excluded. If magnesium chloride was present at a concentration of 20 mM in the buffer and the sample, the peak appeared with the total permeation

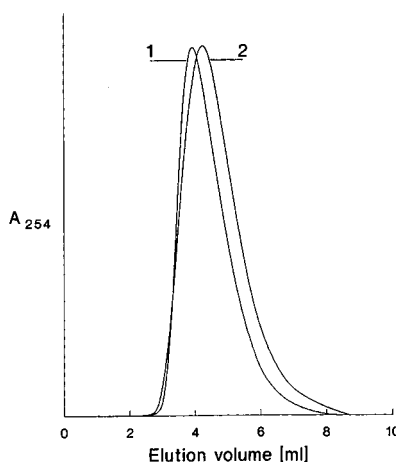


Fig. 3. Chromatography of RNA using destroyed VP material. Conditions as in Fig. 1. The material was destroyed using a swinging mill, until no intact cellular structures were detected under a microscope (magnification 200 \times). Buffers: (1) 1 mM Tris-HCl, pH 7.5; and (2) 1 mM Tris-HCl, pH 7.5, 20 mM magnesium chloride.

volume (90–95% of the packing volume, Fig. 1, curve 2). Fig. 2 shows the chromatograms of the same RNA preparation at magnesium chloride concentrations of 0.2, 1 and 3 mM. The addition of 0.2 mM magnesium chloride led to the appearance of a minor permeating peak (Fig. 2, curve 1). About 70% of the sample components were still excluded.

TABLE II

PERMEATION BEHAVIOUR OF NUCLEIC ACIDS, OLIGONUCLEOTIDES AND NUCLEOTIDES AT MAGNESIUM CHLORIDE CONCENTRATIONS OF 0 AND 20 mM IN 1 mM TRIS-HCl, pH 7.5

Sample	Molecular weight	Permeation at 0 mM MgCl_2	Permeation at 20 mM MgCl_2
2',3'-CMP	323	Permeating ^c	Permeating
2',3'-UMP	324	Permeating	Permeating
RNA from yeast ^a	< 15 000	Excluded ^d (Fig. 1)	Permeating (Fig. 1)
DNA from herring sperm ^a	< 15 000	Excluded	Permeating
tRNA ^{val} from <i>Escherichia coli</i>	\approx 30 000	Excluded	Excluded
DNA from calf thymus	\approx 5 000 000 ^b	Excluded	Excluded
Plasmide pKK 161-8	\approx 3 000 000	Excluded	Excluded

^a Technical products, best referred to as crude mixtures of oligonucleotides.

^b Value represents an average of a broad molecular weight distribution.

^c "Permeating" refers to an elution volume at peak maximum of 90–95% of the packing volume.

^d "Excluded" refers to an elution volume of about 40%.

Increasing the magnesium chloride concentration to 1 mM (line 2) resulted in an increase in the permeating fraction (about 55% of the sample) and a decrease in the excluded fraction. Only a small part of the sample was excluded at a concentration of 3 mM (line 3).

After mechanical rupture of its vesicular structure, the cell wall preparation showed a totally different chromatographic behaviour (Fig. 3). With the same RNA as used in Figs. 1 and 2, one peak was observed, the location of which was influenced slightly by the magnesium chloride concentration. A group separation into excluded and permeating molecules did not occur.

Chromatography with intact VP material at different magnesium chloride concentrations was carried out using a variety of nucleotides and nucleic acids. Table II gives a summary of the results obtained.

The nucleotides 2',3'-CMP and 2',3'-UMP were too small to be excluded and permeated through the membranes into the whole stationary volume at all salt concentrations. Similar to RNA from yeast, (technical) DNA from herring sperm exhibited a chromatographic behaviour influenced by the salt concentration. Larger molecules such as tRNA, plasmides or highly polymerized DNA from calf thymus were excluded in all instances. The ionic influence on the permeability is not specific for magnesium salts, as shown with sodium and calcium chlorides. The concentration of monovalent cations

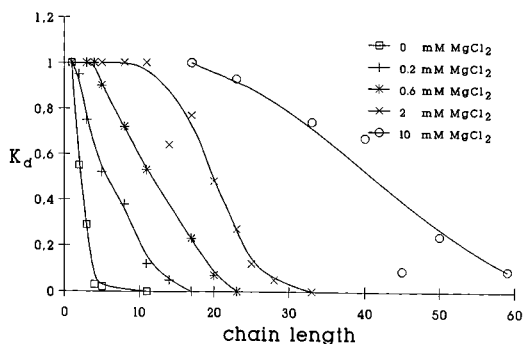


Fig. 4. Relationship between K_d value and chain length at different magnesium chloride concentrations. Column, 60 × 16 mm, standard VP titrated to pH 7.5; Sample, 0.04 A_{260} unit each; flow-rate, 0.3 ml/min; buffer, 1 mM Tris-HCl, pH 7.5; magnesium chloride concentrations as indicated in the figure.

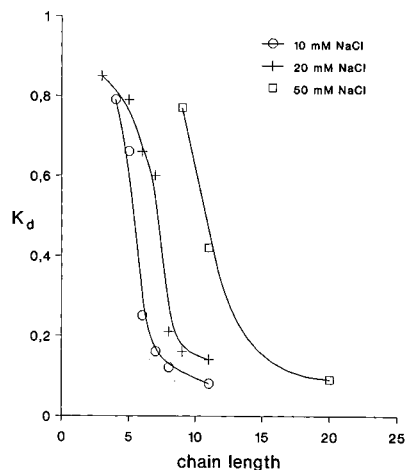


Fig. 5. Relationship between K_d value and chain length at different sodium chloride concentrations. Conditions as in Fig. 4; sodium chloride concentrations as indicated in the figure.

necessary for permeation is much higher; 3 mM magnesium chloride led to permeation of most RNA molecules (see Fig. 2), whereas 50 mM sodium chloride was required for a similar chromatogram in the absence of magnesium chloride (data not shown).

To obtain a more precise knowledge of the relationships between molecular size and permeability, purified monodisperse synthetic oligonucleotides were chromatographed at different magnesium chloride concentrations (for sequences, see Table I). At certain salt concentrations, oligonucleotide peaks appeared between the exclusion and the permeation volume, *i.e.* within the fractionation range. Fig. 4 shows the relationships between the chain length of the oligonucleotides and the apparent volumetric distribution coefficients (K_d values) at pH 7.5.

The permeation is strongly dependent on the magnesium chloride concentration. In the absence of magnesium chloride only adenosine was eluted with the whole packing volume (apparent K_d value close to unity), whereas the K_d values of the di- and trinucleotide were in the range 0–1. Even oligonucleotides with a chain length greater than 3 were excluded. With increasing magnesium chloride concentrations the exclusion limit rose and the frac-

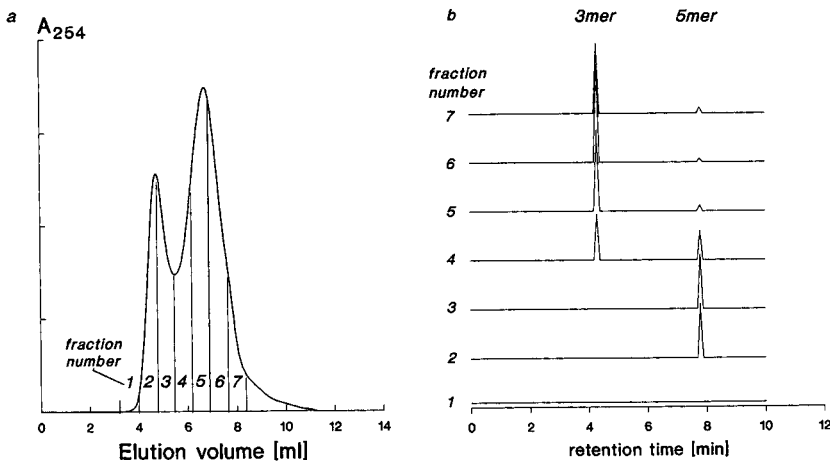


Fig. 6. Preparative fractionation of a mixture of the trinucleotide d(AAC) and the pentanucleotide d(AAC TC). (a) Chromatogram. Column, 115 × 10 mm standard VP material, titrated to pH 7.5; sample, 2 A_{260} units of the mixture; flow-rate, 80 μ l/min; buffer, 1 M Tris-HCl, pH 7.5, 0.1 M magnesium chloride. (b) Anion-exchange chromatograms of the fractions collected in (a). Column, Mono Q; gradients, 0–100% B in 25 min (A = 10 mM sodium hydroxide; B = 1.2 M sodium chloride in A); flow-rate, 1 ml/min.

tionation range became more extended. In the presence of 10 mM magnesium chloride, a comparatively broad fractionation range was found from a chain length of 25–60 nucleotides. Similar curves were found using calcium chloride instead of magnesium chloride (not shown). With the monovalent

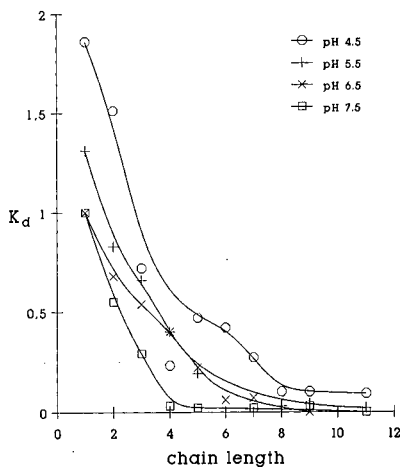


Fig. 7. Relationships between K_d value and chain length at different pH values. Column, 60 × 16 mm, standard VP material, titrated to the appropriate pH; sample, 0.04 A_{260} units each; flow-rate, 0.3 ml/min. Buffers, pH 7.5: 1 M Tris-HCl; pH 6.5: 1 mM 2-(*N*-morpholino)ethanesulphonic acid buffer; pH 5.5: 1 mM phosphate buffer; and pH 4.5: 1 mM acetate buffer.

cations Na^+ and K^+ a dependence of permeation limits and K_d values on the salt concentration was also observed, but much higher concentrations were required to give comparable effects to divalent cations. Fig. 5 shows the relationships between K_d values and sodium chloride concentration.

Generally, intermediate K_d values were dependent on flow-rate and bed length. They increased with the residence time of the sample on the bed. Peaks of oligonucleotides with intermediate K_d values were broader than those with K_d values of 0 or 1.

The counterion-controlled permeability of oligonucleotides can be used for preparative fractionations. Fig. 6a shows the separation of a trimer from a pentamer. The eluted fractions were collected and analysed for their composition by anion-exchange chromatography; the chromatograms are presented in Fig. 6b. The fractions of the first peak were free from trinucleotide. Owing to tailing of the excluded peak, the trimer peak was contaminated with small amounts of the pentamer.

Fig. 7 shows the relationships between chain length and K_d value at different pH values in the absence of magnesium chloride. Apparently, at lower pH values, larger molecules permeate into the inner volumes of the vesicles. However, at pH 4.5 and 5.5 some smaller molecules, which were obviously retarded by adsorption, exhibited K_d values

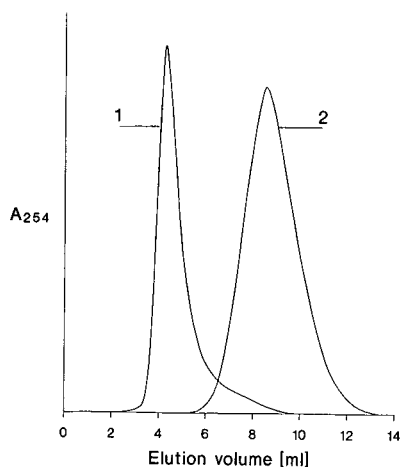


Fig. 8. Chromatography of tRNA^{val} on a VP material with a size limit for permeation of 10 nm. Column, 50 × 16 mm, sodium carbonate-treated VP material, titrated to pH 7.5; sample, 0.01 A_{260} unit of tRNA^{val}; flow-rate, 0.3 ml/min. Buffers: (1) 1 mM Tris-HCl, pH 7.5; and (2) 1 mM Tris-HCl, pH 7.5, 20 mM magnesium chloride.

significantly greater than 1.0. In the presence of 5 mM magnesium chloride a decrease of the pH to values below 7 resulted in strong or even total adsorption of the oligonucleotides. At pH 6.5 a broad peak over more than one bed volume appeared, whereas the oligonucleotides were totally adsorbed at pH 4.5 and 5.5, respectively.

The counterion-dependent barrier function of the vesicle membrane for RNA was also observed using a VP material with increased separation limits. This VP material was obtained by treatment of the vesicular plant cell wall preparation with sodium carbonate [2], leading to de-esterification and controlled partial decomposition of polygalacturonic acid (unpublished results). As an example, a VP material with a size limit for the permeation of neutral macromolecules close to 10 nm (determined as described by Ehwald *et al.* [2]) was used for the investigation of the elution behaviour of tRNA^{val}. This molecule was too large for permeation with standard VP materials (see Table II). With the modified VP material a dependence of the permeability of this tRNA on the salt concentration was found. The tRNA was completely excluded at pH 7.5 in the absence of magnesium chloride, but was totally permeable with 20 mM magnesium chloride (Fig. 8).

DISCUSSION

The stationary phase built by the packing particles investigated here consists of thin vesicle membranes (negatively charged purified plant cell walls) and liquid enclosed within the vesicles. The vesicle membranes are considered to be cation-exchange membranes with a high charge density. Non-esterified carboxyl groups are present at high concentrations (0.7 mval/g dry material) in the pectin component. This component (a network of polygalacturonans) is responsible for sizing the neutral macromolecules [2] and also determines the size- and environment-dependent permeability of polyanions. The vesicular structure of the VP material is essential for efficient group separations and for the dependence of the elution volumes on the salt concentration. Comparison of Figs. 1, 2 and 3 shows the importance of the free stationary liquid inside the VP material for the fractionation result.

Permeation chromatography with this material is dominated by membrane permeation between the mobile phase and the enclosed liquid. As the enclosed liquid comprises about 95% of the volume of the packing particle, the partial exclusion of polyanions from the negatively charged cell wall matrix has an insignificant effect on the elution behaviour, as long as it does not prevent the fast equilibration of the enclosed liquid volume with the mobile phase. Indeed, polyanions were eluted with a K_d value of 1 below a critical chain length (Fig. 4). This is a remarkable difference compared with the GPC of anions on negatively charged porous or gel-like support materials, where the K_d values of all anions are reduced at low ionic strength due to the Donnan equilibrium.

The results of this work show that the permeability of the vesicle membrane for nucleic acids depends on both their chain length and ion environment factors. The most important of these factors are salt concentration and the type of cations. Weakening of the electrostatic repulsion by Mg^{2+} ions may be traced back to (1) the well known Debye-Hückel screening interactions which reduce the field strength in the surroundings of the polyanion proportional to the ionic strength and (2) charge reduction by localized binding of the cations to the polyanion (counterion condensation) [4]. Generally, the latter effect is more efficient with divalent cations

than with monovalent ions. This might explain the need for the much higher sodium chloride concentrations to give comparable effects to magnesium chloride (compare Figs. 4 and 5).

In addition, permeation through the microcapsule membranes may be influenced by enlargement of the molecular dimensions of the nucleic acids at low salt concentrations as a result of intramolecular phosphate repulsion [5].

Considering the size limit of permeation of the investigated VP material for neutral dextran molecules (Stokes' diameter of 5.6 nm) or proteins (molecular weight 35 000 dalton) [2], the effective exclusion of a nucleotide tetramer by the VP material in the absence of Mg^{2+} ions (Fig. 4) is a striking result. The electrostatic repulsion between the polyanion and the vesicle membrane is obviously strong enough to prevent diffusional exchange of the oligonucleotide with the enclosed liquid phase, at least for the given separation time. The combined effect of size and electrostatic exclusion of polyanions from the charged membrane matrix may be described by the concept of Dubin *et al.* [6], who analysed the thickness, X_E , of an electrical barrier around a charged particle in pores with equally charged surfaces. X_E may be added to the Stokes' radius of the molecule or subtracted from the radius of the pore to describe the liquid space fraction accessible for diffusion of the charged molecule within the charged particle. Values of X_E have been determined empirically by comparison of the molecular radii estimated by size-exclusion chromatography of polyanions on porous glass with those derived from the intrinsic viscosity at different salt concentrations. Concerning this concept, the critical thickness of the electrical barrier X_E which prevents the permeation of a polyanion through the cell wall is the difference between the critical Stokes' radius for the exclusion of neutral polymers and the Stokes' radius of the polyanion. In addition to the qualitative aspect of polyanion exclusion from the matrix (impermeability of the membrane) there is also, at X_E values below the critical value, a quantitative aspect, *i.e.* decreased permeability. The latter is a consequence of the decreased concentration and mobility of permeable polyanions in the negatively charged matrix. This might explain why intermediate K_d values were dependent on flow-rate and bed length. As the separation time and bed length were

not sufficient to reach the diffusional equilibrium, the intermediate K_d values refer to the given experimental conditions. They do not only reflect an excluded portion of the stationary liquid volume, but also (or mainly?) the limited permeability of the vesicle membrane.

Peak broadening by limited diffusion is the most serious problem for the application of counterion-dependent size fractionation of oligonucleotides and nucleic acids by VC. Between the excluded and permeable fraction a kinetically influenced fractionation range has to be taken into account. The investigations with synthetic oligonucleotides show its dependence on the salt concentration. The correlation between K_d and the chain length is not ideal, as the permeability is influenced by the size, shape and charge of the oligonucleotide. The net charge does depend not only on the chain length, but also on the base composition. In addition, base pairing may lead to secondary structures with different hydrodynamic properties, *e.g.*, the investigated 14mer oligonucleotide seems to behave differently from its neighbours (Fig. 4).

As the dissociation of the pectin carboxyl groups depends on the pH value, the permeability of polyanions through the cell walls should also be influenced by the proton concentration. Furthermore, owing to the protonation of adenine and cytosine (pK_a around 4.5), the influence of the sequence-dependent charge might be of functional relevance. Fig. 7 shows that the K_d values of the oligonucleotides are varied by the pH value, but to a different extent.

Whereas all the effects described at pH 7.5 can be discussed as pure permeability effects, additional adsorption phenomena must be considered at pH values below 7. K_d values far above 1 clearly indicate an additional retention (Fig. 7). Therefore, it is not possible to decide unequivocally whether the influence illustrated in Fig. 7 derives from increased permeability or from a retention due to adsorption phenomena.

The polydisperse RNA and DNA samples which were excluded in one instance and permeable in the other, undergo systematic changes in their chromatographic behaviour between magnesium chloride concentrations of 0 and 20 mM (Fig. 2). In contrast to conventional gel chromatography media, it is not the location of the peak maximum, but the ratio

between the excluded and permeating peak that is varied by the salt concentration. The opportunity to vary the exclusion limit of the VP material over a wide range allows the adaption of the separation conditions to the respective separation problem. Alkali-treated VP materials with irreversibly increased separation limits are also susceptible to reversible adjustment of their permeability for larger polyanions by the salt concentration. This is of special interest for the fractionation of naturally occurring nucleic acids.

The dependence of the fractionation result in VC on the kind and concentration of salts and the pH value should not only apply to nucleic acids. Any other anionic polyelectrolyte should be influenced in a similar way. Therefore, aqueous VC might develop into a useful tool for polyelectrolyte fractionation and characterization.

ACKNOWLEDGEMENTS

Part of this work was supported by a grant from the Senatsverwaltung für Wissenschaft und Forschung (Berlin, Germany). The authors are indebted to Professor Dr. V. A. Erdmann, Freie Universität Berlin, and his co-workers for support of this work and fruitful cooperation. The authors sincerely thank Dr. R. Bald, Dr. J. P. Fürste and S. Schulze for the synthesis of oligonucleotides and critical discussions.

REFERENCES

- 1 R. Ehwald, G. Fuhr, M. Olbrich, H. Göring, R. Knösche and R. Kleine, *Chromatographia*, 28 (1989) 561.
- 2 R. Ehwald, P. Heese and U. Klein, *J. Chromatogr.*, 542 (1991) 239.
- 3 J. Brosius, *Gene*, 27 (1984) 151.
- 4 G. S. Manning, *Q. Rev. Biophys.*, 11 (1978) 179.
- 5 A. H. Rosenberg and F. W. Studier, *Biopolymers*, 7 (1969) 765.
- 6 P. L. Dubin, C. M. Speck and J. I. Kaplan, *Anal. Chem.*, 60 (1988) 895.

Determination of chlorotriazines in aqueous environmental samples at the ng/l level using preconcentration with a cation exchanger and on-line high-performance liquid chromatography

V. Coquart and M.-C. Hennion*

École Supérieure de Physique et Chimie de Paris, Laboratoire de Chimie Analytique, 10 Rue Vauquelin, 75231 Paris Cedex 05 (France)

(First received July 31st, 1990; revised manuscript received May 28th, 1991)

ABSTRACT

On-line precolumn sample handling was applied to preconcentrate chlorotriazines in aqueous samples prior to their high-performance liquid chromatographic separation. Chlorotriazines are ionizable compounds (pK_a between 1.6 and 2) and a strong cation exchanger is used for their concentration. As the direct percolation of large aqueous sample volumes through a cation-exchange precolumn is impossible owing to the high concentrations of inorganic cations in natural waters, a two-step preconcentration has to be carried out. First, triazines are trapped in their neutral form by direct percolation of the aqueous sample through a first precolumn packed with the copolymer-based PRP-1 sorbent. In the second step, the PRP-1 precolumn is coupled to a second precolumn packed with a cation exchanger. A small volume of deionized water–acetonitrile mixture at pH 1 allows the triazines to be desorbed from the PRP-1 precolumn and concentrated on the cation exchange–acetonitrile mixture in their protonated form. The content of the cation exchange precolumn is analysed on-line using an acetonitrile–water gradient. As the PRP-1 precolumn also acts as a powerful filter to many neutral interferents, detection limits are below the 10 ng/l level in drinking water.

INTRODUCTION

The extensive use of chlorotriazines as selective herbicides in agriculture and their relatively high persistence [1] imply that these compounds are now present in the environment. Contamination of surface and groundwater and of sediments by the most commonly applied chlorotriazine herbicides, simazine and atrazine, has been reported [2–6]. In European countries, the drinking water ordinance demands a limited concentration of 0.5 $\mu\text{g/l}$ (ppb) for the sum of all pesticides and 0.1 $\mu\text{g/l}$ with respect to each compound [7]. Sensitive analytical methods are required to detect such low concentrations, including a preconcentration step before the analysis. Reported detection limits of chlorotriazines obtained by UV detection at 220 nm are between 0.5 and 5 ng. Therefore, determinations at levels below

0.1 $\mu\text{g/l}$ require the preconcentration of 100–500-ml water samples.

Sample enrichment based on liquid–solid sorption techniques has been shown to be a good alternative to liquid–liquid extractions. Off-line procedures with prepacked cartridges and subsequent gaschromatographic (GC), GC–mass spectrometric or high-performance liquid chromatographic (HPLC) analyses have been described [8–15]. On-line enrichment analysis has some advantages, especially when applied to trace analysis. For example, selectivity can be increased by coupling several precolumns packed with different sorbents in series [16]. On-column technology requires the precolumn dimensions and packing to be adapted to those of the analytical column and the precolumns to be packed with a small-granule sorbent in order to avoid band broadening of analytes during their

transfer from the precolumn to the analytical column [17]. Grob and Li [18] have described an on-line atrazine preconcentration coupled with GC analysis [18].

Octadecylsilica can be used for the concentration of chlorotriazines but breakthrough occurs rapidly for the more polar simazine. Chlorotriazines are more retained by PRP-1 copolymer [19,20]. This sorbent could be used alone for chlorotriazine preconcentration, but the desired detection limit could not be reached, owing to many interfering peaks present in the matrix of natural aqueous samples and also concentrated by this sorbent, giving rise to a noise baseline.

A solution to reducing the number of matrix components concentrated together with chlorotriazines is to use a selective sorbent such as a cation exchanger, as chlorotriazines are ionizable compounds (pK_a between 1.6 and 2). Their direct concentration on a cation exchanger from water samples has not been reported. One reason is that a pH lower than 0.5 is necessary for their complete ionization in water and it is known that some triazines are not stable at very low pH. Another reason is that it is not possible to percolate large volumes of water samples through a cation exchanger owing to the high concentration of inorganic cations in natural waters. In previous work dealing with determination of polar aniline derivatives in water, we showed that direct percolation could be avoided by carrying out a two-step extraction, which consists of first trapping the analytes in their neutral form by PRP-1 sorbent and subsequent transfer to a cation exchanger in their protonated form [21]. The application of this procedure to chlorotriazines requires very acidic conditions for the transfer to the cation exchanger, so that the analyte stability has to be assessed. In the literature, there is one example of the use of a cartridge prepacked with a silica-based cation exchanger, which was not used as a cation exchanger but under strictly anhydrous conditions that involved complete removal of water and consequently off-line preconcentration [3].

EXPERIMENTAL

Apparatus

On-line percolation of water was performed with a Chromatem pump (Touzart et Matignon, Paris,

France). Precolumn elutions and analyses were carried out with a Varian Model (Palo Alto, CA, USA) 5060 liquid chromatograph equipped with a UV 200 variable-wavelength spectrophotometer and a Coulochem Model 5100 electrochemical detector (ESA, Bedford, MA, USA). Precolumn and analytical column switching was effected with two Rheodyne valves (Berkeley, CA, USA). Quantitative measurements of peak areas were provided by a CR3A integrator-computer from Shimadzu (Kyoto, Japan).

Stationary phases and columns

The analytical column was a 15 cm \times 4.6 mm I.D. stainless-steel column prepacked with spherical 5- μ m Nucleosil C₁₈ octadecylsilica (Macherey, Nagel & Co., Düren, Germany). Samples were preconcentrated on a 15 mm \times 3.2 mm I.D. precolumn prepacked with 7- μ m PRP polystyrene-divinylbenzene polymer (Brownlee Columns; Applied Biosystems, San Jose, CA, USA). The cation-exchange precolumn was a 10 mm \times 2 mm I.D. stainless-steel precolumn available from Chrompack (Middelburg, Netherland) which was packed manually with BC-X8 sulphonic acid-type resin-based cation exchanger (15–20 μ m) (Benson, Reno, NV, USA) using a thick slurry and a microspatula.

Chemicals

HPLC-grade acetonitrile was purchased from Rathburn (Walkerburn, UK) and methanol from Prolabo (Paris, France). LC-grade water was prepared by purifying demineralized water in a Milli-Q filtration system (Millipore, Bedford, MA, USA). Other chemicals were obtained from Prolabo, Merck or Fluka (Buchs, Switzerland).

Stock solutions of selected solutes were prepared by weighing and dissolving them in methanol. LC-grade water samples were spiked with these solutions at the μ g/l or ng/l level. The final standard solutions did not contain more than 0.5% methanol.

Procedure

The experimental set-up is described in ref. 18. The following procedure was adopted.

(1) Percolation of a natural water sample adjusted to a pH between 6 and 8 (if necessary) through the PRP-1 precolumn via the percolation pump at a flow-rate of 10 ml/min.

(2) Flushing the PRP-1 precolumn with 2 ml of LC-grade water via the same pump at a flow-rate of 1 ml/min. The 2-ml volume was measured with a 5-ml burette.

(3) Transfer of the cationic compounds to the exchanger precolumn. The PRP-1 precolumn was coupled with the 10-mm long cation-exchange precolumn and 3 ml of a mixture containing 25% of acetonitrile and water acidified to pH 1 with perchloric acid were percolated through the two precolumns in series with the same pump and flow-rate as in (2).

(4) Flushing of the two precolumns with 2 ml of LC-grade water as in (2).

(5) Backflush desorption from the cation exchanger to the C₁₈ analytical column by an acetonitrile gradient with lithium perchlorate-perchloric acid (0.05 M) at pH 4 via the gradient HPLC pump with the experimental conditions described in Fig. 14.

(6) Regeneration of the PRP-1 precolumn with 10 ml of pure acetonitrile and then with 20 ml of LC-grade water at a flow-rate of 10 ml/min.

(7) Regeneration of the exchanger precolumn with 25 ml of 10⁻³ M perchloric acid at a flow-rate of 10 ml/min;

Drinking water samples were analysed without any filtration. River water samples were filtered over a glass-fibre filter (Whatman GF/F).

RESULTS AND DISCUSSION

Table I reports the characteristics of the four chlorotriazines tested. In the first step of the concentration procedure, analytes are adsorbed under

neutral conditions and the maximum water sample volume that can be percolated through the PRP-1 precolumn depends on their retention in water. In the second step, they are desorbed from the PRP-1 sorbent at pH 1, which is the lowest recommended pH for this sorbent. As simazine and atrazine are only partially ionized at pH 1, their desorption from the PRP-1 sorbent, their fixation on the cation exchanger and their stability have to be carefully assessed.

Preconcentration on the PRP-1 precolumn

Chlorotriazines are well retained by the PRP-1 sorbent in their neutral form. Breakthrough volumes higher than 500 ml were measured on a 15 mm × 3.2 mm I.D. precolumn packed with the PRP-1 copolymer for the four chlorotriazines according to the procedure described in ref. 19. A consequence is that a conventional on-line analysable precolumn can be used and the sample volume can be increased to 500 ml for the first step of the preconcentration procedure.

Desorption from PRP-1 and transfer to the cation exchanger

Desorption and transfer of protonated solutes are carried out at the same time by flushing the two precolumns in series with a solution named in this work "transfer solution" and consisting of a few millilitres of deionized water adjusted to pH 1 and a certain amount of acetonitrile. This transfer solution must allow the complete desorption of solutes from the PRP-1 precolumn and their fixation by the cation-exchange precolumn. The first point can be verified by on-line analysis of the PRP-1 precol-

TABLE I
CHARACTERISTICS OF 2-CHLORO-1,3,5-TRIAZINES

Compound	Abbreviation	Substituent in position		pK _a
		2-	4-	
Simazine	S	-NHC ₂ H ₅	-NHC ₂ H ₅	1.65
Atrazine	A	-NHC ₂ H ₅	-NHCH(CH ₃) ₂	1.68
Propazine	P	-NHCH(CH ₃) ₂	-NHCH(CH ₃) ₂	1.85
Terbutylazine	T	-NHC ₂ H ₅	-NHC(CH ₃) ₃	1.95

umn, and the second by knowing the breakthrough volumes of solutes dissolved in the transfer solution on the cation-exchange precolumn.

The breakthrough volumes on the cation-exchange precolumn depends mainly on the ionization state of the solute. They were not measured directly but were estimated in the following way: 5-ml transfer solutions made of pure water at pH 1 and 1.5 were spiked with 0.5 μg of each chlorotriazine and percolated directly through the cation-exchange precolumn, which was subsequently analysed on-line. By comparing the results with those of a 0.5- μg loop injection, breakthrough volumes were found to be lower than 5 ml at pH 1.5 (60% of atrazine protonated) and larger than 5 ml at pH 1 (82% of atrazine protonated).

These results imply that it is possible to retain the compounds on the small cation-exchange precolumn. However, as seen above, the transfer solution must also contain a certain amount of organic solvent for the desorption from PRP-1. The effect of the transfer solution composition was studied by using the whole procedure: a 50-ml LC-grade water sample spiked with 10 $\mu\text{g}/\text{l}$ of chlorotriazines at pH 6 was preconcentrated through the PRP-1 precolumn; the two precolumns were flushed with transfer solutions having different compositions (reported in Table II) and each precolumn was analysed separately on-line. Recoveries were calculated by comparison with a 0.5- μg direct injection onto the ana-

lytical column, as described above, for both precolumns. Experiments were first made at pH 1.5. With a 5-ml transfer solution made of water at pH 1.5 and 20% of acetonitrile, simazine and atrazine were completely desorbed from PRP-1 but not propazine and terbutylazine. On adding more acetonitrile (25%), the desorption was still not complete for the two late-eluted triazines, but there was only a 20–25% loss. The volume was then decreased to 3 ml (line 3 in Table II) and the recoveries increased on the cation exchanger, being above 75% for all compounds except terbutylazine. A lower pH was then necessary. With 5 ml of water at pH 1 and 25% of acetonitrile, no compound was left on the PRP-1 precolumn but there was still a beginning of elution from the cation-exchange precolumn. On decreasing the volume to 3 ml, all recoveries were above 85% owing to a small breakthrough from the cation-exchange precolumn for simazine and atrazine and an incomplete desorption for the two late-eluted compounds. It is not necessary to know these recoveries accurately because all the quantitative analyses are made by spiking water samples and preconcentrating them via the whole method, but in trace analysis it is important to have the highest possible amount on the precolumn. This composition of the transfer solution (3 ml, pH 1 and 25% of acetonitrile) was selected for the final procedure.

Chlorotriazines are stable during the acidic transfer, as the recoveries reported above were calculated

TABLE II

EFFECT OF TRANSFER SOLUTION ON THE DESORPTION FROM THE PRP-1 PRECOLUMN AND ON THE ADSORPTION ON THE CATION-EXCHANGE PRECOLUMN

Recoveries (%) calculated on the PRP-1 precolumn (R_a) and on the cation-exchange precolumn (R_b) by comparison between a 0.5- μg direct injection and the preconcentration of a 50-ml of LC-grade water sample spiked with 10 $\mu\text{g}/\text{l}$ of each compound via the whole procedure; mean values from triplicate measurements.

Transfer solution			Compound							
Acetonitrile concentration (%)	pH	Volume (ml)	S		A		P		T	
			R_a	R_b	R_a	R_b	R_a	R_b	R_a	R_b
			20	1.5	5	0	65	0	70	40
25	1.5	5	0	60	0	70	20	50	25	75
25	1.5	3	0	83	0	87	25	75	50	50
25	1	5	0	70	0	80	0	90	0	100
25	1	3	0	88	0	91	5	90	10	85

by comparing peak areas with those obtained by a direct 20- μ l injection of standard solution in methanol. The 10–15% loss of simazine and atrazine could be due to a certain instability, but is also easily explained by incomplete retention by the cation exchanger owing to their partial ionization. This is confirmed by an increase in the transfer solution volume (line 4), which increases the breakthrough of these two analytes. Terbutylazine has the highest pK_a value and is more ionized at pH 1, so that the observed recovery is 100% when it is completely desorbed from the PRP-1 precolumn (line 4). These experiments just indicate that chlorotriazines are stable during the 3 min necessary for the transfer. Their stability was also observed at pH 1 for a period of up to 30 min in the experiments described above (direct percolation through the cation exchanger). Stability over a longer period was not studied.

Desorption from the cation exchanger

In order to have detection limits as low as those obtained by direct injections, band broadening is undesirable when analysing the solutes preconcentrated on the cation exchange precolumn by the analytical mobile phase. Fig. 1a shows the chromatogram obtained on injecting 0.5 μ g directly onto the analytical column with a 20- μ l loop with UV detection at 230 nm (close to the maximum absorbance of chlorotriazines) and Fig. 1b shows the chromatograms obtained on preconcentrating and analysing on-line a 500-ml drinking water sample spiked with 0.1 μ g/l of each compound. Considering the chlorotriazine peaks, no band broadening is observed: the peak heights differ only because of the different amounts injected (0.5 and 0.05 μ g, respectively) and the 85–90% recoveries. Therefore, the precolumn–column coupling is correct and chlorotriazine desorption is rapid under the chromatographic conditions selected. Some aniline derivatives were included in the standard solution to ensure the good working of an electrochemical detector, which was in series with the UV detector. Chlorotriazines are not oxidizable and cannot be detected electrochemically. Nevertheless, as we can expect some aniline derivatives to be also concentrated by

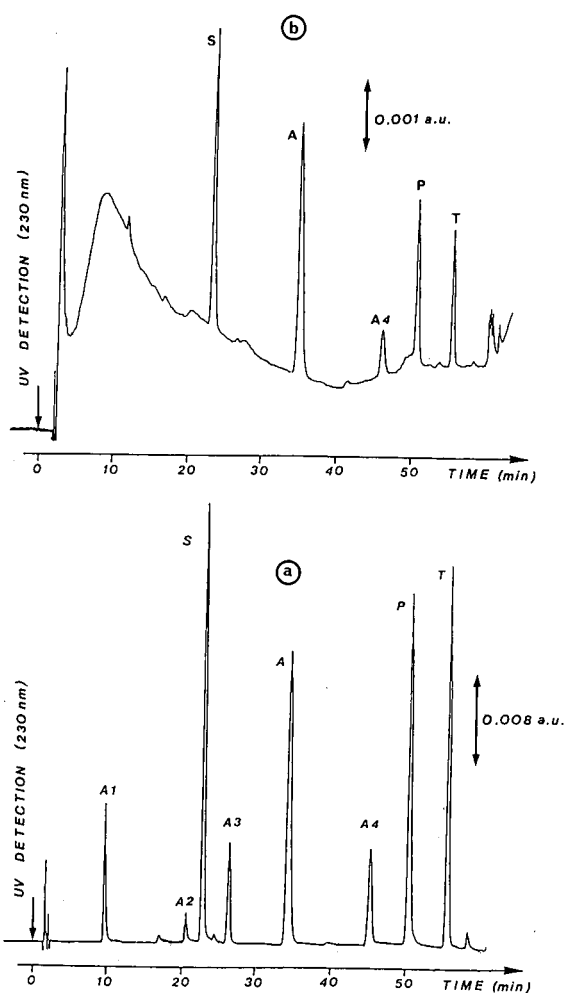


Fig. 1. (a) Direct 20- μ l loop injection of each chlorotriazine reported in Table I and of four aniline derivatives (A1 = 3-chloro-4-methoxyaniline, A2 = 3-chloro-4-methylaniline, A3 = 4-isopropylaniline, A4 = 3,4-dichloroaniline). (b) Chromatogram corresponding to the on-line elution of the cation-exchange precolumn after preconcentration of a 500-ml drinking water sample spiked with 0.1 μ g/l of each compound. Analytical column, 15 cm \times 0.46 cm I.D. packed with 5- μ m Nucleosil C₁₈; mobile phase, acetonitrile gradient with a 0.05 M solution of perchloric acid–lithium perchlorate at pH 4 at a flow-rate of 1.5 ml/min; gradient 15% to 23.5% acetonitrile from 0 to 20 min, 25.3% from 20 to 35 min and up to 46% at 60 min; UV detection at 230 nm, preconcentration at pH 6 through a 15 mm \times 3.2 mm I.D. precolumn packed with 7- μ m PRP-1, transfer to 10 mm \times 2 mm I.D. precolumn packed with 15–20- μ m BC-X8 cation exchanger with 3 ml of perchloric acid (pH 1) containing 25% of acetonitrile.

the procedure and to interfere in the analysis, the use of the two detectors helps to identify chlorotriazine with a peak at 230 nm and the absence of a peak with the electrochemical detector.

Detection limits and application to drinking water samples

The chromatogram in Fig. 1b indicates that the determination at the 0.1 $\mu\text{g/l}$ level required by the EEC ordinance is easy and that the detection limits are much lower. The baseline contains very little background, owing to an efficient removal of neutral interferents left on the PRP-1 precolumn and the absence of cationic interfering material detected at 230 nm. The detection limits and the linearity of solute peak height or surface response were assessed by adding increasing amounts to 500 ml of LC-grade and drinking water samples and by using the whole preconcentration and on-line analysis procedure. Owing to this baseline quality, it is possible to use a more sensitive range of the UV detector and increase the peak heights. The calibration graphs for the chlorotriazines with UV detection at 230 nm were linear ($r = 0.998$ with six data points) over the whole range tested (0.02–1 ng/l). The repeatability ranged between 3 and 8% (relative standard deviation) ($n = 4$) at the 0.1 $\mu\text{g/l}$ level. Detection limits were calculated for a signal-to-noise ratio of 3 and were 3 ng/l for simazine and atrazine and 5 ng/l for terbutylazine and propazine when 500-ml samples were analysed. Therefore, the analysis of a 100-ml sample is sufficient for monitoring drinking waters with detection limits of 15 ng/l for atrazine and simazine, which allows accurate determinations at the 0.1 $\mu\text{g/l}$ level. Nevertheless, it could be of interest to handle 500-ml samples to detect lower concentrations, *e.g.*, for metabolite studies. Fig. 2a illustrates the low detection limits obtained with real samples. This sample was not spiked and simazine and atrazine were detected at 10 and 15 ng/l concentrations, respectively. In Fig. 2b, a 500-ml sample of the same drinking water was spiked with 2 ng/l of each compound.

Interferent filter effect of the PRP-1 precolumn: application to river water samples

Compared with other methods, the low detection limits obtained here with drinking water sample are due to the efficient removal of many neutral

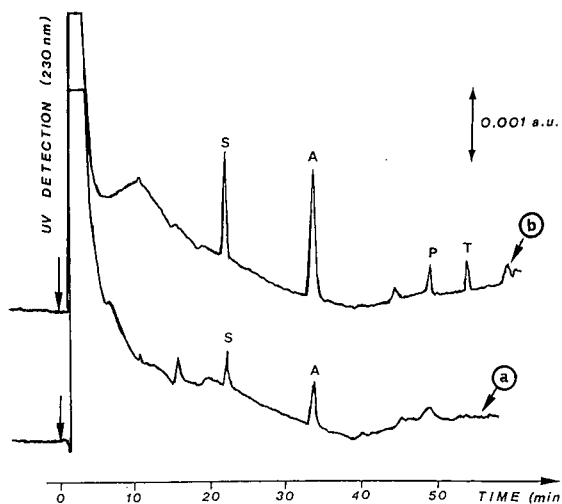


Fig. 2. Preconcentration and on-line analysis of a 500-ml drinking water sample from Paris, April 1990: (a) non-spiked; (b) spiked with 20 ng/l of each compound. Experimental conditions as in Fig. 1b.

interferences by the PRP-1 precolumn. This is more noticeable when analysing river waters with more complex matrices than those of drinking waters. Fig. 3 shows the analysis of a non-spiked 500-ml sample of water from the river Seine, taken in Paris at the end of April. The transfer solution contained 25% of organic solvent, both ionic and some neutral compounds are desorbed from the PRP-1 precolumn, and, as the cation-exchange precolumn is a styrene-divinylbenzene polymer-based sorbent, we can expect the retention of some neutral aromatic organic compounds together with the ionic compounds. However, the baseline obtained in Fig. 3 on eluting the cation-exchange precolumn is free from interferents and is similar to that obtained on analysing drinking water samples, showing that the neutral organics desorbed by the 25% acetonitrile content are not recovered on the cation-exchange precolumn. Therefore, the trapping of ionic chlorotriazines is very selective under the selected experimental conditions. This also indicates that the matrix of the river Seine does not contain many ionizable compounds showing absorption at 230 nm and having polarities similar to those of chlorotriazines. The electrochemical response, not represented here, does not show the presence of oxidizable com-

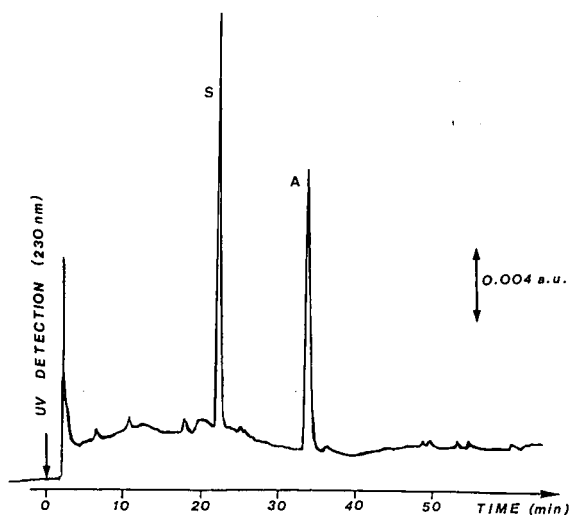


Fig. 3. Preconcentration and on-line analysis of a non-spiked 500-ml sample taken from the river Seine, Paris, April 1990. On-line analysis of the cation-exchange precolumn. Experimental conditions as in Fig. 1b.

pounds. This sample contained 0.7 and 0.8 ng/l of simazine and atrazine, respectively.

CONCLUSIONS

The on-line preconcentration and analysis of aqueous environmental samples carried out with two precolumns allows chlorotriazine determinations at very low levels without pretreatment of the samples. This method is sensitive, selective and can be easily automated. The identity of compounds is reinforced by the fact that the solutes are ionizable, by their retention time, their UV response at 230 nm and the absence of electrochemical response. Compared with other methods, the detection limits are lower and the handling of a 100-ml sample produces accurate determinations at the 0.1 ng/l level. However, the main conclusion of this work is that when looking for trace compounds, a low level can be obtained only with efficient removal of interfer-

ences and selective trapping of the relevant compounds, rendering the precolumn selection and coupling the most important step of the methodology.

ACKNOWLEDGEMENT

The Compagnie Générale des Eaux and the Syndicat des Eaux de l'Île-de-France are thanked for having supported part of this work.

REFERENCES

- 1 D. Barcelo, *Chromatographia*, 25 (1988) 928.
- 2 P. Subra, M.-C. Hennion, R. Rosset and R. W. Frei, *Int. J. Environ. Anal. Chem.*, 37 (1989) 45.
- 2 M. Battista, A. Di Corcia and M. Marchetti, *Anal. Chem.*, 61 (1989) 935.
- 4 A. Di Corcia, M. Marchetti and R. Samperi, *J. Chromatogr.*, 405 (1987) 357.
- 5 E. A. Hogendoorn and C. E. Goewie, *J. Chromatogr.*, 475 (1989) 432.
- 6 D. Gröhlich and W. Meier, *J. High Resolut. Chromatogr.*, 12 (1989) 340.
- 7 *EEC Drinking Water Guideline*, 80/779/EEC, EEC No. L229/11-29, EEC, Brussels, August 30th, 1980.
- 8 M. Battista, A. Di Corcia and M. Marchetti, *J. Chromatogr.*, 454 (1988) 233.
- 9 A. Ramsteiner, *J. Chromatogr.*, 465 (1989) 410.
- 10 W. J. Günther and A. Kettrup, *Chromatographia*, 28 (1989) 209.
- 11 I. G. Ferris and B. M. Haigh, *J. Chromatogr. Sci.*, 25 (1987) 170.
- 12 F. Mangani and F. Bruner, *Chromatographia*, 17 (1983) 377.
- 13 M. Popl, Z. Voznakova, V. Tatar and J. Strnadova, *J. Chromatogr. Sci.*, 21 (1983) 39.
- 14 Y. Xu, W. Lorentz, G. Pfister, M. Bahadir and K. Farle, *Fresenius' Z. Anal. Chem.*, 325 (1986) 377.
- 15 V. Pacakova, K. Stulik and M. Prihoda, *J. Chromatogr.*, 442 (1988) 147.
- 16 M. W. F. Nielen, U. A. Th. Brinkman and R. W. Frei, *Anal. Chem.*, 57 (1985) 806.
- 17 C. E. Goewie, M. W. F. Nielen, R. W. Frei and U. A. Th. Brinkman, *J. Chromatogr.*, 301 (1984) 325.
- 18 K. Grob, Jr., and Z. Li, *J. Chromatogr.*, 473 (1989) 423.
- 19 P. Subra, M.-C. Hennion, R. Rosset and R. W. Frei, *J. Chromatogr.*, 456 (1988) 121.
- 20 S. Coppi and A. Betti, *J. Chromatogr.*, 472 (1989) 406.
- 21 M.-C. Hennion, P. Subra, V. Coquart and R. Rosset, *Fresenius' Z. Anal. Chem.*, 339 (1991) 488.

Quality control of cured epoxy resins

Determination of residual free monomers (*m*-xylylenediamine and bisphenol A diglycidyl ether) in the finished product

P. Paseiro Losada

Universidad de Santiago de Compostela, Facultad de Farmacia, Departamento de Química Analítica, Nutrición y Bromatología, Área de Nutrición y Bromatología, 15706 Santiago de Compostela (La Coruña) (Spain)

S. Paz Abuín

Gairesá, Departamento de Investigación, Lago-Valdoviño (La Coruña) (Spain)

L. Vázquez Odériz, J. Simal Lozano and J. Simal Gándara*

Universidad de Santiago de Compostela, Facultad de Farmacia, Departamento de Química Analítica, Nutrición y Bromatología, Área de Nutrición y Bromatología, 15706 Santiago de Compostela (La Coruña) (Spain)

(First received January 31st, 1991; revised manuscript received May 28th, 1991)

ABSTRACT

A simultaneous method for extracting residual bisphenol A diglycidyl ether (BADGE) and *m*-xylylenediamine (*m*-XDA) from finished epoxy resins cured with different equivalent ratios of these raw materials (1:1, 1:2 and 1:3) has been developed. Extraction is based on refluxing epoxy-amine formulations in a chloroform-methanol (25:75) mixture for 10 h and quantification is carried out by reversed-phase high-performance liquid chromatography with fluorescence detection, directly for BADGE and previous precolumn derivatization with fluorecamine for *m*-XDA. The relative standard deviation for BADGE chromatography at 200 µg/l was 3.4% and for *m*-XDA derivatization-chromatography 5.7%, the detection limit 5 µg/l for BADGE and 20 µg/l for *m*-XDA and the recovery for six spiked concentrations of 200 µg/l was 98.9 ± 6.5% for BADGE and 89.3 ± 6.0% for *m*-XDA.

INTRODUCTION

The first commercial epoxy resins were obtained by a condensation reaction between epichlorohydrin and bisphenol A [1]. This reaction leads to the diglycidyl ether of bisphenol A and, depending on the epichlorohydrin to bisphenol A molar ratios and the reaction conditions, products of different molecular weights are obtained as indicated in Fig. 1, where *n* is the degree of condensation.

A liquid epoxy resin of low molecular weight has

a structure derived from two molecules of epichlorohydrin and one molecule of bisphenol A. Higher molecular weights increase the viscosity of the epoxy resins and solid products are obtained. However, these products are soluble, fusible and without remarkable mechanical and chemical properties. To be converted into insoluble and thermosetting products, the epoxy resins need to undergo reaction with other chemical intermediates, so-called curing agents, which must be of high functionality (at least three) with good hydrogen-releasing activity to ob-

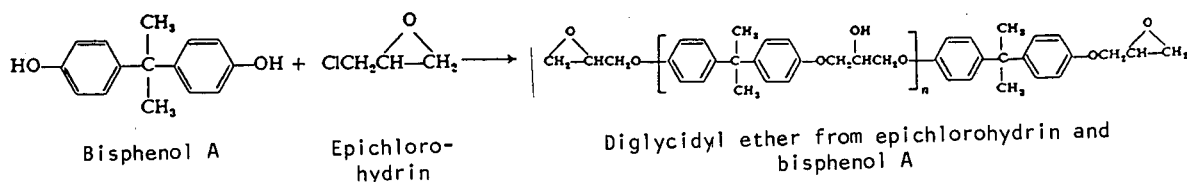


Fig. 1. General reaction forming epoxy resins of the bisphenol A type.

tain a highly cross-linked structure owing to the high reactivity of the hydrogen donor. Amine compounds are most commonly used in epoxy formulations [2].

The degree of toxicity of epoxy compounds depends mainly on the fractional concentration of unreacted epoxy groups. Epoxy compounds are alkylating agents and they have specific cytotoxic actions in tissues with high rates of cell division. Bisphenol A diglycidyl ether [2,2-bis(4-hydroxyphenyl)propanebis(2,3-epoxypropyl) ether (BADGE) causes sensitization of surface tissues, probably owing to the presence of by-product impurities which are toxic. Hardeners probably play a major role. *m*-Xylylenediamine (1,3-benzenedimethanamine) (*m*-XDA) is toxic by inhalation, in contact with the skin and if swallowed. It is necessary to bear in mind that many aromatic amines have been shown to produce toxic effects on animals, *e.g.*, liver, kidney and bone marrow damage [3].

Epoxy-based solution coatings are used many applications. Our interest is centred on their use for lacquer coatings on food cans and food storage vessels [4,5]. Because of their toxicity it is necessary to control the unreacted products to prevent their migration into food.

BADGE (oligomer of molecular weight 340) is contained in list 7 of the Scientific Committee for Food (SCF) 19th Report [6], which includes substances for which some toxicological data exist but for which an admissible daily ingest (ADI) or tolerable daily ingest (TDI) could not be established. The additional specified information should be furnished. The Committee recognizes that priorities will have to be set because of the large number of substances mentioned. The criteria for setting these priorities should include, for example, availability of analytical methods, data on exposure (*e.g.*, usage, extent of migration) and hydrolysis data. *m*-XDA is contained in list 8, which includes sub-

stances for which no or only scant and inadequate data were available.

A recent EEC Directive [7] established as the specific migration limit in food or in food simulants a level of 0.02 mg/kg for BADGE and 0.05 mg/kg for *m*-XDA, and set also for BADGE the maximum permitted concentration of the residual substance in the material or article at 1 mg/kg.

Many papers [8–11] have been devoted to aspects of the control of food packaging because of its possible contamination of foods by migration of additives and free monomers. Test conditions (10 days at 40°C) have been approved to determine this transfer of residuals, but it is possible to detect them in the final product fairly rapidly.

The American Society for Testing and Materials (ASTM) include test methods which cover the determination of the epoxy content in the epoxy resins [12]. However, gel permeation chromatography (GPC) permits the coarse separation of epoxidic oligomers [13–17], although the best resolution has been achieved using reversed-phase partition techniques, commonly using ultraviolet detection [18–24]. We have determined BADGE by reversed-phase high-performance liquid chromatography (RP-HPLC) with fluorescence detection because of its higher sensitivity, in a similar manner to that reported previously [25].

Low-level detection techniques to determine *m*-XDA based on HPLC with both electrochemical and fluorescence detection have also been reported [26]. We decided to use the latter because of its greater simplicity.

EXPERIMENTAL AND RESULTS

Apparatus

A Perkin-Elmer DSC/7 differential scanning calorimeter, a Perkin-Elmer FT-IR 1720/X Fourier transform infrared spectrometer, a Spectra-Physics

SP8700 XR extended-range LC pump, a Spectra-Physics SP8750 organizer, a Perkin-Elmer PE LS 40 fluorescence detector, a Spectra-Physics SP4290 integrator and SP WINNER software V. 4.00, a Crison microPH 2002 pH meter and an Agimatic heater were used.

Polyester membrane (47 mm × 0.4 μm) was obtained from Nuclepore and glass material from Afora.

Reagents

Water purified with a Milli-Q system (Millipore) was used throughout. Helium (N-48) from SEO was used for degassing the mobile phases. Analytical-reagent grade chemicals were used unless indicated otherwise.

Acetonitrile, methanol and chloroform (LiChrosolv) were obtained from Merck and tetrahydrofuran and fluorescamine from Carlo Erba.

Phosphate buffer (1/15 M, pH 8) was prepared as follows: solution A was 0.9073 g of KH_2PO_4 (Merck) in 100 ml of water, solution B was 11.87 g of $\text{Na}_2\text{HPO}_4 \cdot 2\text{H}_2\text{O}$ (Merck) in 1 l of water, and 37 ml of solution A were mixed with 963 ml of solution B and the mixture was filtered through 0.4-μm filter and adjusted to pH 8 with solution A.

A stock solution of *m*-XDA (purity 99%) (Aldrich) containing exactly 500 mg of *m*-XDA in 100 ml of water was prepared under a nitrogen atmosphere with silica gel as desiccant to avoid carbonation. It was stored in the dark in a refrigerator.

Bisphenol A diglycidyl ether was obtained as Epikote 828 from Shell, purified (>99%) by Shell for Gairesa Industry. A product of similar purity can be obtained as described by Paz Abvín *et al.* [27]. A stock solution was prepared containing exactly 500 mg of BADGE in 100 ml of tetrahydrofuran. It was stored in the dark in a refrigerator.

Chromatographic conditions

A stainless-steel column (15 cm × 5 mm I.D.) packed with 5-μm Pecosphere CRT C_{18} RC was used. Guard columns (C_{18}) were used in order to protect the packing in the analytical columns. For injection, the 50-μl loop in a Rheodyne valve was filled with a Hamilton syringe. The eluent flow-rate was 1 ml/min.

Elution was carried out as follows. Gradient elu-

tion for BADGE consisted of a 5-min linear gradient from acetonitrile–water (30:70) (30% acetonitrile) to 55% acetonitrile, 5-min isocratic elution at 55% acetonitrile, a 5-min linear gradient to 75% acetonitrile and 5 min isocratic elution at 75% acetonitrile. Isocratic elution for derivatized *m*-XDA was performed with phosphate buffer (1/15 M, pH 8)–water–methanol (16:34:50).

For detection, the attenuation factor was 16 with auto-zero, and the response was 4 [equivalent RC (98% FS) response time 2.8 s]. The excitation wavelengths were 275 nm for BADGE and 395 nm for derivatized *m*-XDA and the emission wavelengths were 300 nm for BADGE and 480 nm for derivatized *m*-XDA. The photomultiplier voltage was 750 V.

The integrator attenuation was 4.

Procedure

Before starting the extraction, the details of the curing conditions are very important. Epoxy–amine formulations that have not completely cured contain large amounts of soluble compounds, so it is necessary to predetermine the optimum curing conditions, that is, the time and temperature characteristics for each epoxy–amine equivalent ratio. The time and temperature of curing for a 1:1 equivalent ratio in this reaction was stated to be 10 min at 110°C [27]. Following the same technique, employing differential scanning calorimetry and Fourier transform IR techniques, we found that 16 min at 80°C for a 1:2 and 90 min at 50°C for a 1:3 equivalent ratio produced fully cured resins.

A sample of about 200 mg of the epoxy–amine formulation was treated as follows. The sample was transferred into a 100-ml conical flask and 20 ml of chloroform–methanol (25:75) were added. A reflux column was fitted and the sample was maintained at reflux for 10 h. The mixture was filtered into a 50-ml volumetric flask. The conical flask was washed with methanol and the washings were filtered into the 50-ml flask. Finally, methanol was added to the mark.

For formulations with BADGE to *m*-XDA ratios of 1:2 and 1:3, free BADGE may be directly determined in this solution. If the ratio is 1:1, it is necessary to dilute 25-fold with methanol (2 ml in 50 ml) before chromatographic analysis.

Free *m*-XDA at a BADGE to *m*-XDA ratio of

1:1 is determined by diluting the refluxed solution 25-fold with water (2 ml in 50 ml), derivatizing with fluorescamine and chromatographic analysis. Pre-column derivatization was performed as follows. A 2-ml volume of the solution was pipetted into a screw-topped tube and 0.4 ml of phosphate buffer (1/15 M, pH 8) was added. A 20- μ l volume of a solution of fluorescamine in acetone ((2 mg/ml) was added and the mixture was stirred for 1 min and allowed to stand for 10 min before injection. For formulations with BADGE to *m*-XDA ratios of 1:2 and 1:3, this new solution was further diluted with water 10-fold (10 ml in 100 ml) and 100-fold (1 ml in 100 ml), respectively, before derivatization.

Chromatograms obtained in this way are shown for BADGE and *m*-XDA in Fig. 2.

Calibration

Working solutions with concentrations of 1000 μ g/l were prepared from the stock solutions of BADGE and *m*-XDA using stepwise dilution steps of 50-fold (1 ml in 50 ml) and 100-fold (1 ml in 100 ml), respectively, with methanol or water.

Aliquots of 1, 2.5, 5, 10, 20 and 40 ml of the BADGE working solution were pipetted into 50-ml volumetric flasks and made up to the mark with methanol to give concentrations of 20 μ g/l (limit of quantification of the calibration line) to 800 μ g/l (at higher levels the detector signal is saturated under the chromatographic conditions). These six new solutions were utilized to construct the BADGE calibration graph (Fig. 3).

Aliquots of 2.5, 5, 10, 15 and 25 ml of the *m*-XDA working solution were pipetted into 50-ml volumetric flasks and made up to the mark with water. These five solutions and a sample of the working solution were derivatized according to the described procedure and chromatographed to construct the *m*-XDA calibration graph (Fig. 3).

External standard chromatograms for BADGE and *m*-XDA are shown in Fig. 4.

Calculations

The free BADGE content in the cured epoxy resin was calculated from the equation

$$R = \frac{CF}{200W}$$

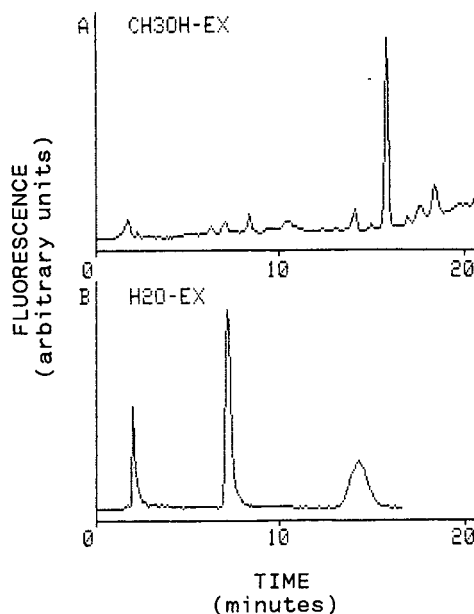


Fig. 2. Chromatograms obtained following the described procedure independently of the raw material ratio in the epoxy resin: (A) BADGE; (B) derivatized *m*-XDA. The late peak results from the reaction of two molecules of fluorescamine with each amine group in *m*-XDA [29].

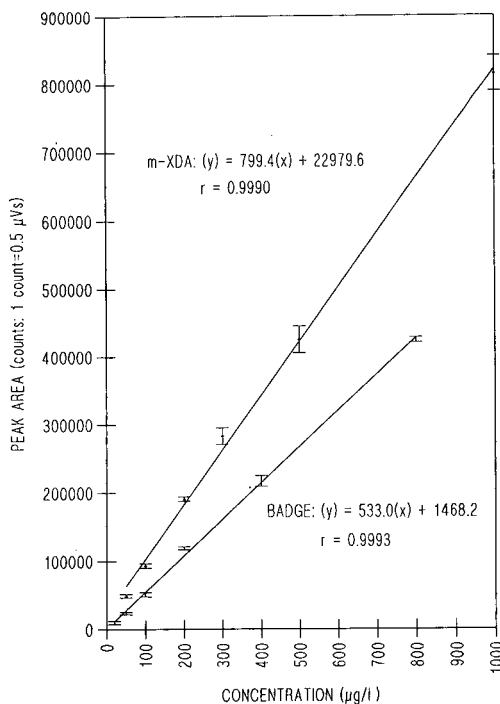


Fig. 3. Calibration graphs for BADGE and *m*-XDA.

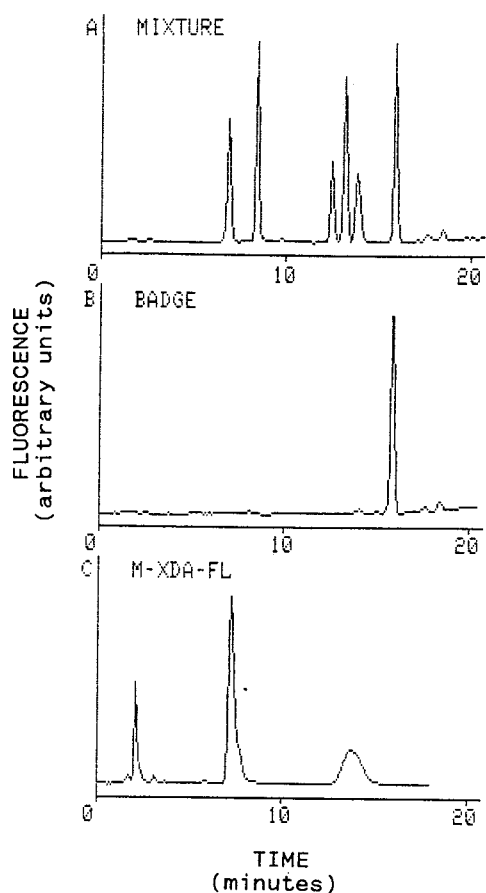


Fig. 4. External standard chromatograms: (A) mixture of, in order of elution, bisphenol F, bisphenol A, three Bisphenol F diglycidyl ether isomers and bisphenol A diglycidyl ether; (B) BADGE; (C) derivatized *m*-XDA.

where R is the free BADGE content (%) in the cured epoxy resin, C is the concentration ($\mu\text{g/l}$) given by the calibration line, F is a factor, being 25 for a BADGE to *m*-XDA ratio of 1:1 or 1 for a ratio of 1:2 or 1:3, and W is the weight utilized of cured epoxy resin (mg) utilized in the procedure.

The free *m*-XDA content in the cured epoxy resin was calculated from the same equation, but now R is the *m*-XDA content (%) and F is 25 for a BADGE to *m*-XDA ratio of 1:1, 250 for a ratio of 1.2 and 2500 for a ratio of 1:3.

Chromatographic precision (including the derivatization for *m*-XDA)

A single specimen with a fortified BADGE concentration of $200 \mu\text{g/l}$ in methanol was chromatographed six times, giving a relative standard deviation of 3.4%. A single specimen containing $200 \mu\text{g/l}$ of *m*-XDA in water was derivatized and chromatographed six times, giving a relative standard deviation of 5.7%.

Recovery and precision

A 1-ml volume of the stock solution of BADGE in tetrahydrofuran was diluted to 100 ml with methanol, and 0.5 ml of the stock solution of *m*-XDA in water was diluted to 100 ml with methanol. Then 5 or 10 ml of the solution containing $250 \mu\text{g}$ of BADGE or *m*-XDA, respectively, were mixed with 5 ml of chloroform in a conical flask. Refluxing, filtration and washing steps were carried out as in the described procedure and then the methanol solution (50 ml) was diluted 25-fold (2 ml in 50 ml) using methanol to determine BADGE and water to determine *m*-XDA. The final concentration in both solutions is *ca.* $200 \mu\text{g/l}$. The results are given in Table I. Table II gives the results of the determination of free levels of BADGE and *m*-XDA in two different kinds of epoxy-amine resin formulations at BADGE to *m*-XDA equivalent ratios of 1:1, 1:2 and 1:3.

Detection limit

The lowest concentration of BADGE observable at a signal-to-noise ratio of 3 was $5 \mu\text{g/l}$ and the corresponding concentration of *m*-XDA was $20 \mu\text{g/l}$. These results were verified experimentally by spiking a blank at these levels.

DISCUSSION

Chloroform-methanol (25:75) was used to extract BADGE and *m*-XDA from cured epoxy resins. Chloroform was chosen by Kwei [28] for vapour sorption studies because of the extensive swelling of highly cross-linked network structures, but a higher proportion of methanol was found necessary in order to prevent the high reactivity of *m*-XDA towards humidity and its tendency to form carbonates.

TABLE I
RESULTS OF RECOVERY EXPERIMENTS FOR BADGE AND *m*-XDA

BADGE			<i>m</i> -XDA		
Added (μg)	Found (μg)	Recovery (%)	Added (μg)	Found (μg)	Recovery (%)
250	262	104.8	250	218	87.2
	248	99.2		234	93.6
	226	90.4		217	86.8
	237	94.8		248	99.2
	270	108.0		214	85.6
	241	96.4		208	83.2
Average		98.9			89.3
Relative standard deviation (%)		6.5			6.0

TABLE II
RESULTS OF DETERMINATIONS OF RESIDUAL FREE LEVELS OF BADGE AND *m*-XDA IN CURED EPOXY RESINS

BADGE to <i>m</i> -XDA equivalent ratio	First resin		Second resin	
	BADGE (%)	<i>m</i> -XDA (%)	BADGE (%)	<i>m</i> -XDA (%)
1:1	0.047	0.19	0.098	—
1:2	0.007	1.23	0.001	0.84
1:3	—	2.88	—	6.21

CONCLUSIONS

The proposed method for the determination of free residual BADGE and *m*-XDA in cured epoxy resins has very good precision. The accuracy is excellent for BADGE and adequate for *m*-XDA in comparison with other methods [26].

This method for the quality control of epoxy resins is not time consuming and is quicker than the migration assays performed on food-simulating solvents. Further, it has an appropriate limit of detection. It can therefore be recommended for determining BADGE monomer and *m*-XDA hardener in epoxy resins with different ratios of these raw materials.

ACKNOWLEDGEMENT

This work was supported by Gairesa Industry, Lago-Valdoviño (La Coruña), Spain.

REFERENCES

- 1 L. Henry and K. Neville, *Handbook of Epoxy Resins*, McGraw-Hill, New York, 1982.
- 2 J. I. Kroschwitz, *Polymers: An Encyclopedic Sourcebook of Engineering Properties*, Wiley, New York, 1987.
- 3 C. A. May, *Epoxy Resins. Chemistry and Technology*, Marcel Dekker, New York, 1988.
- 4 P. A. Tice and J. D. McGuinness, *Food Additives Contam.*, 4 (1987) 267–276.
- 5 P. A. Tice, *Food Additives Contamin.* 5 (1988) 373–380.
- 6 *Second Addendum to the First of the Scientific Committee for Food on Certain Monomers and Other Starting Substances to be Used in the Manufacture of Plastic Materials Intended to Come into Contact with Foodstuffs*, III/851/86-EN, Rev. 2, 19th Series of SCF Reports, Scientific Committee for Food, DGIII, Brussels, 1987, pp. 104–125.
- 7 Commission Directive (23 February 1990) Relating to Plastic Materials and Articles Intended to Come into contact with Foodstuffs (90/129/EEC), *Off. J. Eur. Commun.*, No. L 75/19, March 21 (1990).
- 8 M. J. Shepherd, *Food Chem.*, 8 (1982) 129–145.
- 9 J. R. Bell, *Food Chem.* 8 (1982) 157–168.
- 10 W.-D. Bieber, W. Freitag, K. Figge, C. G. vom Bruck and L. Rossi, *Food Chem. Toxicol.*, 22 (1984) 737–742.

- 11 L. Rossi, *Food Additives Contamin.* 5 (1987) 21–31.
- 12 *Standard Test Methods for Epoxy Content of Epoxy Resins*, ASTM Committee on Standards, D 1652-88, ASTM, Philadelphia, PA, 1988.
- 13 W. Heitz, *J. Chromatogr.*, 53 (1970) 37–49.
- 14 E. A. Eggers and J. S. Humphrey, Jr., *J. Chromatogr.*, 55 (1971) 33–44.
- 15 J. J. Kirkland and P. E. Antle, *J. Chromatogr. Sci.*, 15 (1977) 137–147.
- 16 R. V. Vivilecchia, B. G. Lightbody, N. Z. Thimot and H. M. Quinn, *J. Chromatogr. Sci.*, 15 (1977) 424–433.
- 17 J. Russel, *J. Liq. Chromatogr.*, 11 (1988) 383–394.
- 18 W. A. Dark, E. C. Conrad and L. W. Crossman, Jr., *J. Chromatogr.*, 91 (1974) 247–260.
- 19 F. P. B. van der Maeden, M. E. F. Biemond and P. C. G. M. Janssen, *J. Chromatogr.*, 149 (1978) 539–552.
- 20 S. A. Mestan and C. E. M. Morris, *JMS Rev. Macromol. Chem. Phys.*, C24 (1984) 117–172.
- 21 D. Noël, K. C. Cole, J. J. Hechler, A. Chouliotis and K. C. Overbury, *J. Appl. Polym. Sci.*, 32 (1986) 3097–3108.
- 22 D. Noël, K. C. Cole and J. J. Hechler, *J. Chromatogr.*, 447 (1988) 141–153.
- 23 B. Crathorne, C. P. Palmer and J. A. Stanley, *J. Chromatogr.*, 360 (1986) 266–270.
- 24 M.-L. Henriks-Eckerman and T. Laijoki, *Analyst* (London), 113 (1988) 239–242.
- 25 P. Paserio Losada, P. López Mahía, L. Vázquez Odériz, J. Simal Lozano and J. Simal Gándara, *J. Assoc. Off. Anal. Chem.*, in press.
- 26 U. Baumann and B. Marek, *Mitt. Geb. Lebensmittelunters. Hyg.*, 71 (1980) 468–483.
- 27 S. Paz Abuín, M. Pazos Pellín and L. Núñez, *J. Appl. Polym. Sci.*, 41 (1990) 2155–2167.
- 28 T. K. Kwei, *J. Polym. Sci.*, 1 (1963) 2977–2988.
- 29 J. Simal Gándara, P. Paseiro Losada and P. López Mahía, in preparation.

Prediction of retention in gas–liquid chromatography using the UNIFAC group contribution method

II. Polymer stationary phases

Gareth J. Price*[☆]

School of Chemistry, University of Bath, Claverton Down, Bath BA2 7AY (UK)

Michael R. Dent

Department of Chemistry, City University, Northampton Square, London EC1V 0HB (UK)

(Received February 13th, 1991)

ABSTRACT

The UNIFAC group contribution method and its free volume modified version have been used to calculate thermodynamic activity coefficients and hence specific retention volumes for a number of solutes at infinite dilution in a range of polymeric gas–liquid chromatographic stationary phases including Carbowax and several of the OV series of methyl silicones. Specific retention volumes and partition coefficients have been calculated and used to predict relative retentions and the order of elution of the solutes, and these were compared to corresponding experimental values. However, although in some cases the results were predicted to within a few percent of their experimental values, in general the agreement is not good enough to give a reliable predictive method for a range of solvents and so reinforces the conclusions from work on low-molecular-weight stationary phases that the wider application of group contribution methods awaits future developments.

INTRODUCTION

In an attempt to develop a method for the prediction of retention in gas–liquid chromatography (GLC) stationary phases, a previous paper [1] described the application of the UNIFAC group contribution method to a number of low-molecular-weight phases such as squalane and dinonyl phthalate. The aim was to use the predictions to simplify the choice of a suitable system for a particular analysis from the vast number of available possibilities. Systems were characterised in terms of specific retention volumes [2], V_g^0 , and it was found that, in most cases, although the absolute values of V_g^0 were

not accurately predicted, that the correct order of elution was obtained. However, very wide discrepancies were found with polar stationary phases such as N-methyl pyrrolidone.

The majority of GLC analyses currently performed use stationary phases developed over the past decade or so based on polymeric materials. These have been found to give excellent results and allow the use of higher analysis temperatures due to their lower volatility. They have been widely used in capillary columns. This paper continues our earlier work by applying our methods to a range of polymer stationary phases including the OV and Carbowax series of materials.

The basis of the method arises from the use of GLC to measure thermodynamic properties of solution [2]. For instance, the activity coefficient of a

* Formerly of City University, London, UK.

volatile solute at infinite dilution in a low-molecular-weight liquid stationary phase, γ_1^∞ , is given by:

$$\gamma_1^\infty = 273.15 R/V_g^0 P_1^0 M_2 \quad (1)$$

where R is the gas constant, M_2 is the molecular weight of the stationary phase liquid, P_1^0 is the saturated vapour pressure of the solute at the column temperature and V_g^0 is the specific retention volume of the solute *i.e.* the retention volume per gram of stationary phase fully corrected to standard temperature and pressure. However, when considering polymers, this definition is often complicated by lack of an accurate value for M_2 . Thus, the activity coefficients are usually defined on a weight fraction rather than mole fraction concentration basis. [3]. Thus,

$$\Omega_1^\infty = 273.15 R/V_g^0 P_1^0 M_1 \quad (2)$$

where M_1 is now the molecular weight of the volatile solute. The validity of GLC measurements of thermodynamics in polymer systems was not confirmed until well after that in low-molecular-weight systems, particularly with silicone polymers [4], but there is now ample evidence that, under the correct experimental conditions, GLC does provide valid results [5].

The UNIFAC method was developed by Fredenslund and co-workers [6,7] to allow the prediction of phase equilibria and other thermodynamic properties of solution in liquid mixtures. This is a group contribution method which splits the molecules comprising the solution into a number of well defined functional groups. The thermodynamic activities of these groups are then summed using previously calculated and tabulated values of a selection of properties. Thus, only relatively few parameters are needed and, since only pure component properties such as densities and molecular weights are needed, this makes the method particularly attractive as it may be used in systems where little or no experimental data is available, as would be the case for a new GLC analysis. The full method has been described elsewhere and is merely summarized here.

The basic technique assumes two contributions to the thermodynamic activity in solution. The combinatorial (or entropic) part, a_1^C , accounting for

differences in size and shape between the molecules in solution, is calculated using an expression derived from statistical mechanical treatments using tabulated values of parameters calculated from the Van der Waals volumes and surface areas. The second, residual (or enthalpic) contribution to the activity, a_1^R , accounting for energetic interactions in solution, is defined in terms of inter-group interaction parameters which have been calculated by minimizing differences between UNIFAC and experimental vapour-liquid equilibrium results for a large number of binary systems. These two contributions were found to be adequate for small molecules solutions but, when working with polymer solutions an extra contribution, a_1^{FV} , to the solvent activity arising from the well known free volume differences between polymers and solvents must be considered as shown by Oishi and Prausnitz [8].

The overall activity of the volatile component in the solution is thus given by:

$$\ln a_1 = \ln a_1^C + \ln a_1^R + \ln a_1^{FV} \quad (3)$$

Roth and Novak [9] applied the original UNIFAC method to a number of systems and concluded that "(it) can be used merely to give a rough estimation of relative retentions" while Price and Ashworth [10] found that a single result from GLC could be used to improve the predictive ability of UNIFAC for polymer solutions. In the previous paper, this method was applied to stationary phases such as squalane, dinonyl phthalate and similar compounds. In this paper, we present a comparison of UNIFAC results for a number of volatile solutes with high quality thermodynamic measurements to gauge the accuracy of our method followed by a systematic approach to a number of analytical systems including methyl silicone polymers with varying phenyl substitution that comprise the OV series of phases and also, as a rather more polar phase, polyethylene oxide, often known as Carbowax.

RESULTS

Analytical GC is usually performed with the solute being analysed effectively at infinite dilution. Since a value of zero concentration cannot be used in the UNIFAC equations, a solute weight fraction of $1 \cdot 10^{-6}$ was used to simulate infinite dilution.

The use of lower concentrations was found to have negligible effect on the results. The UNIFAC activity of the solute was calculated using the appropriate equations [1] in a BASIC program written for the IBM-PC and converted to an activity coefficient by dividing by the weight fraction. Values of the specific retention volume were calculated from Eqn. 2 using this Ω_1^∞ value and physical property data from literature sources [11]. Values have been calculated using both the original treatment and with the free volume correction proposed for polymer solutions. These will be designated "uni" and "uni-fv" respectively. The deviation of the predictions from the experimental results was calculated according to

$$\Delta V_g^0(\%) = 100\{[V_g^0(\text{uni}) - V_g^0(\text{exptl.})]/V_g^0(\text{exptl.})\} \quad (4)$$

so that a negative value indicates that UNIFAC underestimates the specific retention volume. The results are also shown graphically by plots of the experimental retention volume *versus* the corresponding UNIFAC value which would, if the predictions were perfect, lie on the diagonal straight line on the graphs.

Poly(isobutylene) (PIB)

PIB, although little used as a GC stationary phase, has been used in a number of thermodynamic studies so that it gives a good basis of comparison with our UNIFAC results. Oishi and Prausnitz [8]

applied the method to solutions of PIB in pentane, cyclohexane and benzene and found that solvent activities could be predicted to 24–38% with UNIFAC but to within 3–8% using the free volume correction. However, these results were at high solvent concentrations and any inaccuracies in the method would be expected to be magnified at infinite dilution. Table I lists the specific retention volumes [12] of a number of volatile solutes in PIB at 298 K together with the corresponding values from the UNIFAC treatments. The original UNIFAC gives very poor prediction of these values but, as would be expected, those from the version including the free volume treatment are much closer to experimental results although they are not as good as those found with solutions of higher concentrations. The values are plotted in Fig. 1 which clearly shows that there are large deviations from experimental.

Of perhaps more interest to the chromatographer than the absolute retention volumes are the relative retention volumes of a series of solutes. The values of the solutes considered here are shown in Table II along with the order in which they would elute. This shows that although the order of elution is reasonably well predicted there are some notable exceptions, hexane being swapped with chloroform and cyclohexane with benzene. Thus, it would appear that UNIFAC has limited usefulness with this stationary phase.

TABLE I
SPECIFIC RETENTION VOLUMES OF SOLUTES IN POLY(ISOBUTYLENE) AT 298 K

Solute	V_g^0 (cm ³ g ⁻¹)			Deviation, ΔV_g^0 (%)	
	Expt.	uni	uni-fv	uni	uni-fv
Pentane	54.8	151.0	58.5	176.0	6.8
Hexane	184.0	439.9	204.1	139.0	10.9
Heptane	575.3	1263.6	596.6	119.6	3.7
Octane	1781.1	3665.6	1849.0	105.8	3.8
Cyclohexane	338.8	756.5	440.3	123.3	29.9
Benzene	405.1	628.3	313.4	55.1	-22.6
Toluene	1062.1	1738.1	962.9	63.7	-9.3
Dichloromethane	137.2	172.5	80.2	20.5	-41.5
Chloroform	262.9	330.4	162.9	25.7	-38.0
Carbon tetrachloride	387.4	695.5	321.5	79.5	-17.0

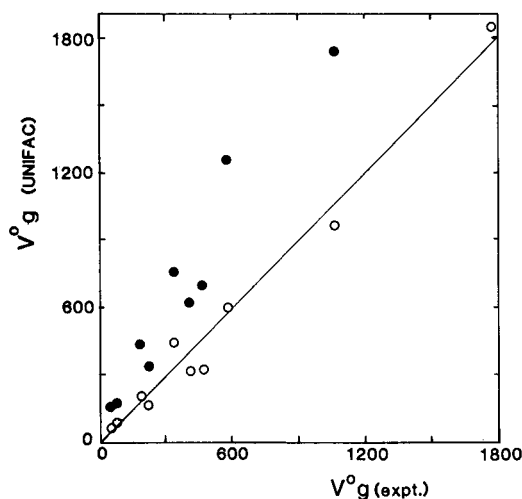


Fig. 1. Plot of experimental *versus* UNIFAC specific retention volumes for solutes in poly(isobutylene) at 298 K. ● = uni; ○ = uni-fv.

Poly(dimethyl siloxane) (PDMS)

PDMS, in addition to being the first in the series of OV analytical stationary phases, has been well studied from a thermodynamic point of view by a number of workers [4,5,12]. Table II lists the specific retention volumes of a number of solutes in this polymer at 298 K together with the predicted values from the UNIFAC treatments. One point that should perhaps be noted is that the UNIFAC interaction parameter for the siloxane SiO group are

based on a rather limited data set [13] so that they carry a fair degree of uncertainty. In particular, UNIFAC interaction parameters are not available for SiO with several of the necessary functional groups such as those including the chloroalkanes. Thus, comparisons in terms of relative values will be more valid than the absolute results.

With this polymer, there is much less difference in the predicted retention volumes from the two UNIFAC variations, the average differences from experimental being 8.6% for the original UNIFAC and 6.6% if the free volume modification is included. The relative retention volumes and order of elution are shown in Table IV. In this case, both UNIFAC treatments predict the correct order of elution for the seven solutes involved. Fig. 2 also shows that the results for PDMS are much closer to experiment than was the case with PIB.

The OV series

The base polymer of this series of stationary phases is PDMS, originally known as OV-1 although a lower-molecular-weight version, OV-101 is now more common. Other phases have been prepared by replacing one or more of the methyl groups with other functionalities including phenyl, trifluoromethyl, cyanopropyl etc. to give a range of materials with varying polarity, basicity etc. It was of interest to apply UNIFAC to these phases since they are in common use. However, as noted above, there are a limited range of UNIFAC interaction

TABLE II

RELATIVE RETENTION VOLUMES OF SOLUTES IN POLY(ISOBUTYLENE) AT 298 K

Solute	Expt. V^0_g ($\text{cm}^3 \text{g}^{-1}$)	Relative retention volume			Elution order		
		Expt.	uni	uni-fv	Expt.	uni	uni-fv
Pentane	54.8	1	1	1	1	1	1
Hexane	184.0	3.3	2.9	3.5	3	4	4
Heptane	575.3	10.5	8.4	10.2	8	8	8
Octane	1781.1	32.5	24.3	31.6	10	10	10
Cyclohexane	338.8	6.2	5.0	7.5	5	7	7
Benzene	405.1	7.4	4.1	5.4	7	5	5
Toluene	1062.1	19.4	14.5	16.5	9	9	9
Dichloromethane	137.2	2.5	1.1	1.4	2	2	2
Chloroform	262.9	4.8	2.2	2.8	4	3	3
Carbon tetrachloride	387.4	7.1	4.6	5.5	6	6	6

TABLE III

SPECIFIC RETENTION VOLUMES OF SOLUTES IN POLY(DIMETHYL SILOXANE) AT 298 K

Solute	V_g^0 (cm ³ g ⁻¹)			Deviation, ΔV_g^0 (%)	
	Expt.	uni	uni-fv	uni	uni-fv
Pentane	77.4	81.4	70.2	5.3	-9.3
Hexane	219.5	226.3	204.9	3.1	-6.6
Heptane	604.7	619.9	590.9	2.5	-2.3
Octane	1633.5	1714.9	1641.9	4.9	0.5
Cyclohexane	390.4	470.2	465.7	20.4	11.3
Benzene	359.1	434.5	414.7	20.9	15.5
Toluene	1053.4	1084.7	1064.2	3.0	1.0

TABLE IV

RELATIVE RETENTION VOLUMES OF SOLUTES IN POLY(DIMETHYL SILOXANE) AT 298 K

Solute	Expt. V_g^0 (cm ³ g ⁻¹)	Relative retention volume			Elution order		
		Expt.	uni	uni-fv	Expt.	uni	uni-fv
Pentane	77.4	1	1	1	1	1	1
Hexane	219.5	2.8	2.8	2.9	2	2	2
Heptane	604.7	7.8	7.6	8.4	5	5	5
Octane	1633.5	21.1	21.0	23.4	7	7	7
Cyclohexane	390.4	5.0	5.8	6.6	4	4	4
Benzene	359.1	4.6	5.3	5.9	3	3	3
Toluene	1053.4	13.6	13.3	15.2	6	6	6

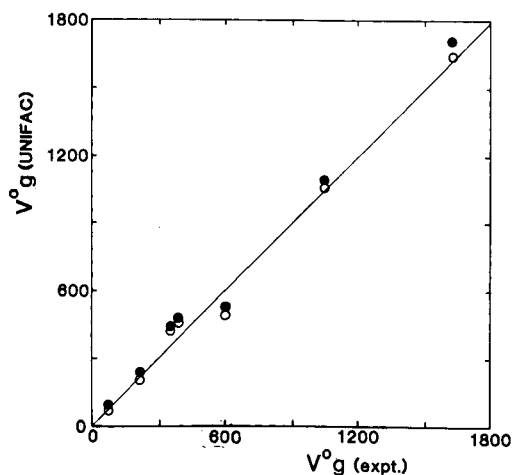


Fig. 2. Plot of experimental *versus* UNIFAC specific retention volumes for solutes in poly(dimethyl siloxane) at 298 K. ● = uni; ○ = uni-fv.

parameters available so that only a series with varying phenyl content could be considered. The compounds studied were OV-101, OV-3, OV-7, OV-11 and OV-17 having 0, 10, 20, 35 and 50% phenyl substitution respectively.

Parcher *et al.* [14] measured the retention of five solutes in these stationary phases at 66, 100 and 150°C and the results, along with the UNIFAC predictions, are shown in Tables V–VII. The densities of the polymers at 20°C were taken from the manufacturers' data sheets and those at higher temperatures estimated from the thermal expansion coefficient of PDMS.

In these systems, the free volume modified UNIFAC yields considerably less accurate predictions of retention volume than the original treatment and hence the relative retention volumes are also further away from experiment. However, it is noticeable

TABLE V
RELATIVE RETENTION VOLUMES FOR SOLUTES IN OV PHASES AT 66°C

Solute	Expt. V_g^0 ($\text{cm}^3 \text{g}^{-1}$)	Deviation, ΔV_g^0 (%)		Relative retention volume			Elution order		
		uni	uni-fv	Expt.	uni	uni-fv	Expt.	uni	uni-fv
<i>OV-101 (0% phenyl)</i>									
Pentane	21.4	5.7	-24.7	1	1	1	1	1	1
Hexane	48.4	4.8	-18.1	2.3	2.2	2.4	2	2	2
Heptane	108.2	4.0	-12.9	5.1	5.0	5.6	4	4	4
Octane	240.4	3.5	-9.8	11.3	11.0	2.8	5	5	5
Benzene	75.2	24.6	13.5	3.5	4.4	5.1	3	3	3
<i>OV-3 (10% phenyl)</i>									
Pentane	18.8	12.0	-17.2	1	1	1	1	1	1
Hexane	43.3	9.2	-13.4	2.3	2.2	2.4	2	2	2
Heptane	98.8	6.5	-10.6	5.3	5.0	5.6	4	3	3
Octane	222.8	4.3	-9.3	11.9	10.9	12.7	5	5	5
Benzene	83.7	26.3	15.1	4.5	5.3	6.2	3	4	4
<i>OV-7 (20% phenyl)</i>									
Pentane	17.3	11.9	-20.8	1	1	1	1	1	1
Hexane	40.3	7.6	-18.5	2.3	2.2	2.4	2	2	2
Heptane	92.6	3.5	-6.9	5.4	4.9	5.5	4	3	3
Octane	211.0	-0.5	-7.3	12.2	10.7	12.6	5	5	5
Benzene	92.4	24.4	10.8	5.3	6.2	7.2	3	4	4
<i>OV-11 (35% phenyl)</i>									
Pentane	13.9	19.4	-18.5	1	1	1	1	1	1
Hexane	32.9	13.1	-18.8	2.4	2.2	2.4	2	2	2
Heptane	75.5	7.8	-18.8	2.4	4.8	5.4	4	4	4
Octane	171.6	3.0	-19.4	12.3	10.2	12.2	5	5	5
Benzene	97.9	23.8	5.4	7.0	7.5	8.8	3	3	3
<i>OV-17 (50% phenyl)</i>									
Pentane	11.5	24.5	-21.9	1	1	1	1	1	1
Hexane	26.6	19.4	-20.3	2.3	2.2	2.3	2	2	2
Heptane	60.1	14.7	-18.5	5.2	4.6	5.4	4	4	4
Octane	135.8	9.4	-20.2	11.8	9.8	11.9	5	5	5
Benzene	93.8	28.4	4.0	8.1	8.6	10.3	3	3	3

that the free volume results underestimate V_g^0 while the uncorrected values are overestimated. The two treatments give the same elution order and this in general agrees with experiment, although in some cases benzene is predicted to elute in the wrong place. The results are also displayed in Fig. 3.

Poly(ethylene oxide)

Two determinations of V_g^0 in poly(ethylene oxide) have been published, one on a low-molecular-weight ($1 \cdot 10^4$) sample [15] and the other on a higher-molecular-weight polymer ($4 \cdot 10^6$) [16]. The results are shown in Table VIII and a considerable

molecular weight dependence can be seen. This is reflected in the UNIFAC calculations through the density of the polymer and the values of this parameter were those used in the experimental work. Results from the two UNIFAC treatments are compared with experimental in Tables VIII and IX. The agreement with experimental results is very variable with some excellent prediction for some probes such as toluene and xylene but very poor for others such as chloroform and cyclohexane. This is also shown by the scatter of the results in Fig. 4. In general, the free volume corrected results are superior but even these are not in sufficient agreement with experi-

TABLE VI
RELATIVE RETENTION VOLUMES FOR SOLUTES IN OV PHASES AT 100°C

Solute	Expt. V_g^0 ($\text{cm}^3 \text{g}^{-1}$)	Deviation, ΔV_g^0 (%)		Relative retention volume			Elution order		
		uni	uni-fv	Expt.	uni	uni-fv	Expt.	uni	uni-fv
<i>OV-101 (0% phenyl)</i>									
Pentane	9.9	0.1	-45.3	1	1	1	1	1	1
Hexane	20.2	-2.7	-39.0	2.0	2.0	2.1	2	2	2
Heptane	38.4	-0.2	-26.9	3.9	3.9	4.4	4	4	4
Octane	74.4	-0.3	-21.9	7.5	7.5	8.9	5	5	5
Benzene	29.0	21.9	4.0	2.9	3.7	4.3	3	3	3
<i>OV-3 (10% phenyl)</i>									
Pentane	8.4	10.2	-31.6	1	1	1	1	1	1
Hexane	16.9	8.2	-25.1	2.0	2.0	2.1	2	2	2
Heptane	33.6	6.2	-19.5	4.0	3.8	4.4	4	3	3
Octane	65.9	4.7	-16.6	7.9	7.4	8.9	5	5	5
Benzene	30.4	27.0	9.8	3.6	4.5	5.3	3	4	4
<i>OV-7 (20% phenyl)</i>									
Pentane	7.9	8.5	-38.5	1	1	1	1	1	1
Hexane	16.1	4.9	-33.5	2.0	2.0	2.1	2	2	2
Heptane	32.3	1.0	-29.7	4.1	3.8	4.4	3	3	3
Octane	64.6	-3.4	-29.8	8.2	7.3	8.8	5	5	5
Benzene	33.8	23.9	3.5	4.3	5.2	6.2	4	4	4
<i>OV-11 (35% phenyl)</i>									
Pentane	6.5	14.8	-39.1	1	1	1	1	1	1
Hexane	13.3	9.8	-35.9	2.0	1.9	2.1	2	2	2
Heptane	26.4	5.8	-31.7	4.1	3.7	4.3	3	3	3
Octane	53.1	-0.3	-33.9	8.2	7.0	8.5	5	5	5
Benzene	34.5	25.6	0.5	5.3	6.1	7.4	4	4	4
<i>OV-17 (50% phenyl)</i>									
Pentane	5.5	18.2	-47.9	1	1	1	1	1	1
Hexane	11.5	10.6	-48.5	2.0	1.9	2.1	2	2	2
Heptane	22.4	7.4	-41.5	4.1	3.6	4.2	3	3	3
Octane	44.1	2.2	-42.0	8.0	6.7	8.3	5	4	4
Benzene	34.3	27.2	7.3	6.2	7.0	8.6	4	5	5

mental to allow their use in a predictive manner. Table IX shows this in terms of the predicted relative retention volumes and the generally poor predicted elution order of the solutes.

DISCUSSION

Taken overall, the predicted retention volumes from the free volume modified UNIFAC method are closer to the experimental results suggesting that it is indeed useful for polymer solutions. However, the deviations of the infinite dilution results discussed here in most cases are wider than those at

higher solvent concentrations discussed by other workers. For the poly(isobutylene) values, it is interesting that the compounds where the biggest differences between the two treatments occur are with the alkane solutes. In solutions of PIB (a polyalkane) with these compounds, there is assumed to be zero enthalpic interaction in UNIFAC whereas there is a small mixing enthalpy in these system [17]. Thus, there are clearly deficiencies in the UNIFAC model even for these straightforward solutions. It also suggests that, as would be expected from current usage [18], the expression for the combinatorial (entropic) contribution to the solvent activity does

TABLE VII

RELATIVE RETENTION VOLUMES FOR SOLUTES IN OV PHASES AT 150°C

Solute	Expt. V_g^0 ($\text{cm}^3 \text{g}^{-1}$)	Deviation, ΔV_g^0 (%)		Relative retention volume			Elution order		
		uni	uni-fv	Expt.	uni	uni-fv	Expt.	uni	uni-fv
<i>OV-101 (0% phenyl)</i>									
Pentane	3.9	2.4	-70.4	1	1	1	1	1	1
Hexane	6.6	1.4	-50.5	1.7	1.8	1.9	3	3	2
Heptane	11.1	-1.6	-40.5	2.9	3.0	3.5	4	4	4
Octane	18.5	2.2	-32.8	4.8	5.0	6.2	5	5	5
Benzene	9.0	-12.9	-211.1	2.3	1.1	1.3	2	2	3
<i>OV-3 (10% phenyl)</i>									
Pentane	3.5	1.4	-66.0	1	1	1	1	1	1
Hexane	6.0	3.7	-48.0	1.7	1.8	1.9	2	3	3
Heptane	10.3	2.5	-40.4	2.9	3.0	3.5	4	4	4
Octane	17.4	1.2	-35.1	5.0	5.0	6.2	5	5	5
Benzene	9.4	-114.4	-196.2	2.7	1.3	1.5	3	2	2
<i>OV-7 (20% phenyl)</i>									
Pentane	3.1	-3.7	-67.4	1	1	1	1	1	1
Hexane	5.5	4.0	-53.2	1.8	1.8	1.9	2	3	3
Heptane	9.5	1.3	-46.7	3.0	3.0	3.4	3	4	4
Octane	16.2	-1.7	-43.3	5.2	4.9	6.1	5	5	5
Benzene	9.8	-113.4	-205.3	3.2	1.4	1.7	4	2	2
<i>OV-11 (35% phenyl)</i>									
Pentane	2.6	9.0	-71.2	1	1	1	1	1	1
Hexane	4.6	7.8	-58.8	1.7	1.8	1.9	2	3	2
Heptane	8.0	3.3	-55.0	3.1	2.9	3.4	3	4	4
Octane	13.7	3.3	-53.1	5.2	4.7	5.9	5	5	5
Benzene	9.9	-107.3	-218.6	7.0	7.5	8.8	4	2	3
<i>OV-17 (50% phenyl)</i>									
Pentane	2.4	5.8	-98.4	1	1	1	1	1	1
Hexane	4.2	5.4	-80.9	1.7	1.7	1.9	2	2	2
Heptane	7.1	1.1	-75.6	2.9	2.8	3.3	3	4	4
Octane	12.1	4.0	-73.7	5.0	4.5	5.7	5	5	5
Benzene	10.0	-107.8	-252.3	4.2	1.9	2.3	4	3	3

not completely describe the situation in polymer solutions. These points have been addressed in a number of modifications to the UNIFAC combinatorial and free volume model [7,13,19,20] and we intend to investigate these in a forthcoming paper.

Many of the results showing greatest deviation from experimental are those involving polar solvents such as alcohols. This may well be due to the inability of the UNIFAC interaction parameters to describe such polar intermolecular forces. Additionally, doubts have been expressed [21] as to use of small molecule interaction parameters for polymer solutions since the restricted conformations of

the chain may prevent some interactions. A related factor may be that these interaction parameters may not describe infinite dilution conditions with sufficient accuracy for use in chromatography. Recently, parameters have been derived solely from infinite dilution data [22,23] and it is intended to explore the use of these for predicting retention volumes.

Thus, on the basis of these results, the same conclusion must be drawn as was the case with low-molecular-weight stationary phases, that at its present stage of refinement, the UNIFAC methods cannot be used to predict chromatographic behaviour

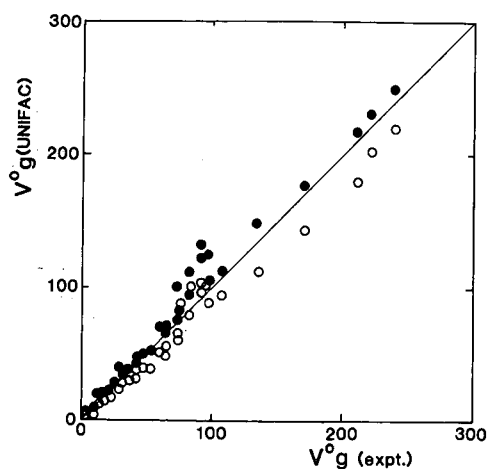


Fig. 3. Plot of experimental *versus* UNIFAC specific retention volumes for solutes in OV polymers at 66 and 100°C. (Some points have been omitted for clarity.) ● = uni; ○ = uni-fv.

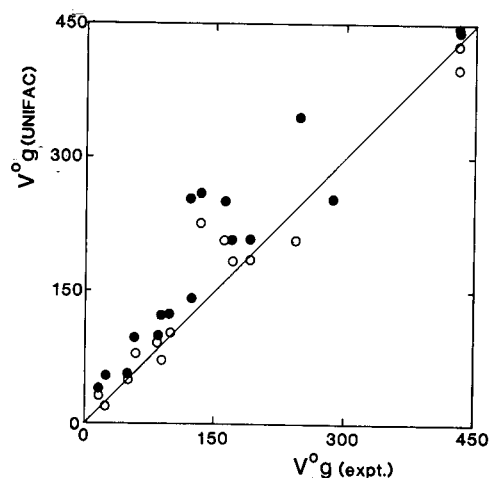


Fig. 4. Plot of experimental *versus* UNIFAC specific retention volumes for solutes in poly(ethylene oxides) at 343 K. ● = uni; ○ = uni-fv.

TABLE VIII

SPECIFIC RETENTION VOLUMES OF SOLUTES IN POLY(ETHYLENE OXIDE) AT 70°C

Solute	V_g^0 (cm ³ g ⁻¹)			Deviation, ΔV_g^0 (%)	
	Expt.	uni	uni-fv	uni	uni-fv
A ^a Water	283.9	254.8	0.1	-10.3	-
1-Butan-ol	431.6	444.4	401.3	3.0	-7.0
Chloroform	124.0	253.6	141.0	104.5	13.7
1,1,2-Trichloroethane	643.2	322.8	300.6	-49.8	-53.3
Benzene	89.4	123.2	70.1	37.8	-21.2
Toluene	173.6	209.2	185.8	20.5	7.0
<i>O</i> -Xylene	430.6	448.0	426.9	4.0	-0.8
Acetone	50.4	56.3	48.9	11.8	-2.8
Butanone	86.7	101.4	90.5	16.9	4.3
Butyl acetate	246.0	346.4	209.2	40.8	-14.9
B ^b Heptane	17.9	37.1	30.0	107.7	68.0
Decane	134.6	261.8	233.1	94.5	73.2
Benzene	100.0	123.2	102.9	23.2	2.9
Toluene	192.6	209.2	185.5	8.6	-3.7
Cyclohexane	22.9	53.2	20.8	132.1	-9.2
Chloroform	162.1	253.6	208.4	56.4	28.6
Ethyl acetate	62.7	95.8	77.4	52.7	23.4

^a Results from ref. 16. Polymer molecular weight = $4 \cdot 10^6$, density = 1.175 g cm^{-3} .

^b Results from ref. 15. Polymer molecular weight = 10 000, density = 1.085 g cm^{-3} .

TABLE IX

SPECIFIC RETENTION VOLUMES OF SOLUTES IN POLY(ETHYLENE OXIDE) AT 70°C

Solute	Expt. V_g^0 ($\text{cm}^3 \text{g}^{-1}$)	Relative retention volume			Elution order		
		Expt.	uni	uni-fv	Expt.	uni	uni-fv
^a Water	283.9	5.6	4.5	—	7	6	—
1-Butan-ol	431.6	8.6	7.9	8.2	9	9	8
Chloroform	124.0	2.5	4.5	2.9	4	5	4
1,1,2-Trichloroethane	643.2	12.8	5.7	6.1	9	7	7
Benzene	89.4	1.8	2.2	1.4	3	3	2
Toluene	173.6	3.4	3.7	3.8	5	4	5
<i>O</i> -Xylene	430.6	8.5	7.9	8.7	8	10	9
Acetone	50.4	1	1	1	1	1	1
Butanone	86.7	1.7	1.8	1.8	2	2	3
Butyl acetate	246.0	4.9	6.1	4.7	6	8	6
^b Heptane	17.9	1	1	1.4	1	1	2
Decane	134.6	7.5	7.1	11.2	5	7	7
Benzene	100.0	5.6	3.3	5.0	4	4	4
Toluene	192.6	10.8	5.6	8.9	7	5	5
Cyclohexane	22.9	1.3	1.4	1	2	2	1
Chloroform	162.1	9.1	6.8	10.0	6	6	6
Ethyl acetate	62.7	3.5	2.6	3.7	3	3	3

^a Results from ref. 16. Polymer molecular weight = $4 \cdot 10^6$, density = 1.175 g cm^{-3} .

^b Results from ref. 15. Polymer molecular weight = 10000, density = 1.085 g cm^{-3} .

with any degree of certainty. Whether the adaptations developed will improve its predictive use will be the subject of a future communication.

REFERENCES

- G. J. Price and M. R. Dent, *J. Chromatogr.*, 483 (1989) 1.
- J. R. Conder and C. L. Young, *Physicochemical Measurement by Gas Chromatography*, Wiley, Chichester, 1977.
- D. Patterson, Y. Tewari, H. P. Schreiber and J. E. Guillet, *Macromolecules*, 4 (1971) 356.
- R. Lichtenthaler, J. M. Prausnitz, C. Su, H. P. Schreiber and D. Patterson, *Macromolecules*, 7 (1984) 136.
- A. J. Ashworth, C. Chien, D. Furio, D. M. Hooker, M. Kopecki, R. J. Laub and G. J. Price, *Macromolecules*, 17 (1984) 1090.
- A. Fredenslund, R. L. Jones and J. M. Prausnitz, *AIChE J.*, 21 (1975) 1086.
- A. Fredenslund, J. Gmehling and P. Rasmussen, *Vapour-Liquid Equilibria Using UNIFAC*, Elsevier, Amsterdam, 1977.
- T. Oishi and J. M. Prausnitz, *Ind. Eng. Chem. Process Des. Dev.*, 17 (1978) 333.
- M. Roth and K. Novak, *J. Chromatogr.*, 258 (1983) 23.
- G. J. Price and A. J. Ashworth, *Polymer*, 28 (1987) 2105.
- Selected Values of the Properties of Hydrocarbons*, TRC Data Project, Texas A&M University, College Station, TX 1967.
- G. J. Price, J. E. Guillet and J. H. Purnell, *J. Chromatogr.*, 369 (1986) 273.
- M. Gottlieb and M. Herskowitz, *Macromolecules*, 14 (1981) 1468.
- J. F. Parcher, J. R. Hansborough and A. M. Koury, *J. Chromatogr.*, 16 (1978) 183.
- M. Galin, *Polymer*, 24 (1983) 865.
- Y. H. Chang and D. C. Bonner, *J. Appl. Polym. Sci.*, 19 (1975) 2439.
- A. Rodrigues and D. Patterson, *J. Chem. Soc. Faraday II.*, 78 (1982) 501.
- P. J. Flory, *Discuss. Faraday Soc.*, 49 (1970) 7.
- A. Bekker, D. E. Knox and S. E. Sund, *J. Solution Chem.*, 16 (1987) 435.
- U. Weidlich and J. Gmehling, *Ind. Eng. Chem. Res.*, 26 (1987) 1372.
- L. A. Belfiore, A. A. Parwardhan and T. G. Lenz, *Ind. Eng. Chem. Res.*, 27 (1988) 284.
- A. Sarius, K. Gerstenberger, F. Hradsky, W. Hauthal and H. Freydanck, *Chem. Tech. (Leipzig)*, 36 (1984) 159.
- J. C. Bastos, M. E. Soares and A. G. Medina, *Ind. Eng. Chem. Res.*, 27 (1988) 1269.

Determination of sulphur and nitrogen gases by gas chromatography on polystyrene porous polymer columns

Gianrico Castello* and Giuseppina D'Amato

Istituto di Chimica Industriale, Università, C.so Europa 30, 16132 Genova (Italy)

(First received January 8th, 1991; revised manuscript received May 16th, 1991)

ABSTRACT

The performance of various Chromosorb Century Series porous polymer bead stationary phases for the simultaneous determination of sulphur and nitrogen gaseous compounds was investigated. The separation at different temperatures of H₂S, COS, SO₂, N₂O, NO, NO₂, CO₂, H₂O, NH₃, CH₄, C₂H₂, C₂H₄, C₂H₆ and C₃H₈ was carried out over wide concentrations ranges using thermal conductivity and helium ionization detectors. Retention times and retention index values on polystyrene and styrene-divinylbenzene polymers (Chromosorb 101, 102, 103 and 106) are given. The effect of contamination of the sample and of the system, contamination of the carrier gas, adsorption and reaction of the sample and area losses due to the integration method on the accuracy of determinations at low concentrations was investigated.

INTRODUCTION

The gas chromatographic (GC) determination of sulphur and nitrogen gases (H₂S, COS, SO₂, NH₃, N₂O, NO, NO₂) has previously been carried out by many workers with different detectors and stationary phases [1–33]. From the early commercial availability of porous polymer beads (PPBs), these polymeric phases were considered a good choice for the determination of reactive gases, owing to their low polarity [34,35] and good stability [36–47]. Previous studies on the determination of trace amounts of these gases by using a Porapak Q column and a helium detector were published in 1969 [48]. Surprisingly, for some years the application of porous polymers to the simultaneous determination of trace amounts of sulphur and nitrogen gases was neglected, probably owing to the difficulty of operating the helium detector under routine conditions, as it is very sensitive to carrier gas impurities and to microscopic leakages in the pneumatic circuit. On the other hand, the flame photometric detector, which is very sensitive to sulphur compounds, does not permit the determination of nitrogen compounds.

More recently, the introduction of detectors stable and sensitive enough to reach the ppm range under routine conditions (amplified micro thermal conductivity detectors) led to the application in industry of GC methods for the simultaneous determination of sulphur and nitrogen gases in samples of different origin and concentration (process and exhaust gases, controlled atmosphere for metallurgy and electronics, environmental monitoring, etc.).

Industrial and environmental applications often require automatic sampling and computerized data handling, and sometimes yield poorly reproducible results in the analysis of low-concentration samples, which is generally ascribed to adsorption or decomposition phenomena taking place in the sampling system or in the column [2,13,49,50].

Many types of PPBs with different polarities have been used and various advantages were claimed for particular applications. It therefore seemed useful to compare under reproducible conditions the performances of the various PPBs available, and to investigate the effects of different phenomena on the accuracy of analyses at low concentrations.

In the work described here, the Chromosorb Century Series (Johns-Manville, Denver, CO, USA)

porous polymers, the polarity and batch-to-batch reproducibility of which have been investigated previously [51], were tested for the separation of sulphur and nitrogen gases, the performances of polystyrene types mainly being considered.

EXPERIMENTAL

Stainless-steel, glass and PTFE columns (3 m × 2.4 mm I.D.) were filled with Chromosorb Century Series types 101, 102, 103, 104, 105, 106, 107 and 108 (80–100 mesh) and conditioned at 150°C for 4 days or more under a helium flow. The samples contained different amounts of the following compounds, diluted in helium: H₂S, COS, SO₂, N₂O, NO, NO₂, CO₂, CH₄, C₂H₂, C₂H₄, C₂H₆, C₃H₈ and H₂O. The alkanes permitted the measurement of the Kováts retention index, while ethylene, CO₂ and acetylene were used in order to evaluate the polarity of the columns, following the procedure suggested previously [52,53].

Samples at different concentrations were prepared by mixing in PTFE or Mylar bags different amounts of pure gases, delivered from glass syringes of various volumes (1–100 ml). The sampling systems, tubings, sample loops, etc., were made of PTFE or nylon and, when metal or glass connections were unavoidable, they were deactivated by silanization. Low-concentration samples were prepared by using the exponential dilution flask technique [54,55], by starting from an initial concentration of 100 or 200 ppm and going down to the ppb^a level, until memory effects, vacancy chromatography and other non-linear phenomena were observed (see below).

The analyses were carried out at different temperatures ranging from 30 to 100°C. All of the test compounds were examined over the whole temperature range, in steps of 20°C in the range 30–70°C and of 15°C for higher temperatures. Slowly eluting compounds (H₂O, SO₂, NH₃ and COS) on more polar columns were mainly studied in the range 70–100°C, where their elution times are shorter and the resulting peaks more symmetrical.

An amplified-output thermal conductivity detectors installed in a Model 3700 gas chromatograph

(Varian, Palo Alto, CA, USA) was used for most of the analyses. The conditions were as follows: detector block temperature, 120°C; detector filament temperature, 300°C; detector filament current, 340 mA; and sensitivity range, 0.05. At the highest sensitivity range it permitted the detection of 0.1–0.2 ppm of O₂, N₂, CH₄, CO, CO₂, C₂H₄, C₂H₆, C₂H₂ [56], NO, N₂O and H₂S. A lower sensitivity to SO₂, H₂O, NH₃ and NO₂ was observed, mainly owing to unfavourable peak shapes or longer retention times. In order to investigate the behaviour of the column at the lowest sample concentrations, with respect of memory effects and vacancy chromatography phenomena, a helium detector (Varian), originally designed for installation on the Varian Model 1532 trace gas analyser and modified to fit the Model 3700, was also used in some experiments and operated at a voltage of $-400 \text{ V} \pm 10 \text{ mV}$ [48,57,58].

Pure-grade helium, further purified through a molecular sieves trap immersed in liquid nitrogen for the analyses of low-concentration samples with helium detection (HeD) and highly amplified thermal conductivity detection (TCD) and for calibration with the exponential dilution flask, was used as the carrier gas, at a flow-rate of 22 cm³/min, kept constant by proper adjustment after equilibration of the column at each temperature. This carrier gas flow-rate was selected because previous experiments showed that it corresponds to the minimum of the Van Deemter–Jones plot, *i.e.*, the highest column efficiency. The maximum HeD sensitivity was not achieved at this flow-rate, because the sub-ppb range required about 60 cm³/min of pure helium, but a sensitivity in the 2–10 ppb concentration range was sufficient for the planned experiments.

Integration of the peaks was carried out by using different integration devices and data systems, or by manual triangulation and height/width measurements, in order to investigate the effect of integration methods on the accuracy at low concentration.

RESULTS AND DISCUSSION

The adsorption or decomposition phenomena often indicated as the cause of the anomalous response of reactive gases on porous polymer columns were found to be a real problem for polar compounds on some polymers. The producer re-

^a Throughout this article, the American billion (10⁹) is meant.

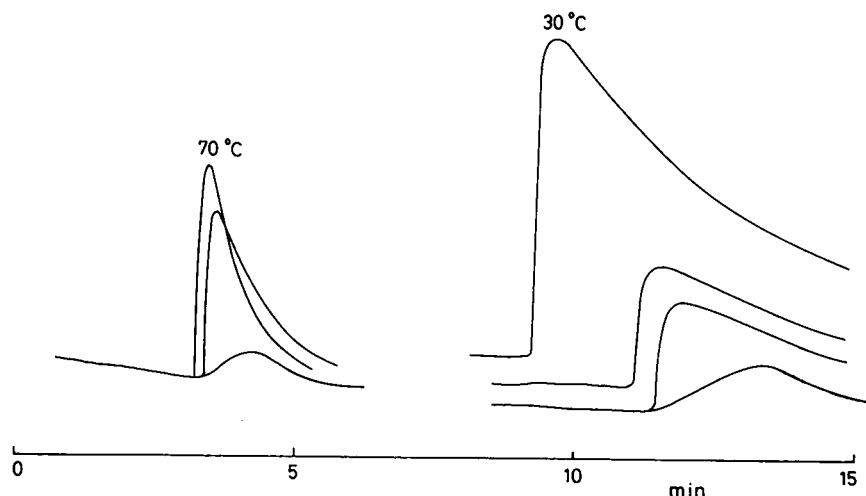


Fig. 1. Asymmetry of NH₃ peak at various concentrations (from 100 to 3000 ppm) on a Chromosorb 103 column at 30°C and 70°C. Carrier gas flow-rate, 22 cm³/min. Thermal conductivity detector.

ports the possible reaction of SO₂ with Chromosorb 101, 102, 104 and 106 [59,60]; this was found to be true at high temperatures but of minor importance at room temperature. On the other hand, very high retention times were observed for sulphur gases on acrylic polymers (Chromosorb 104, 105, 107 and 108) with respect to those of nitrogen compounds, making the simultaneous determination of these compounds impracticable. Very long retention times and peak asymmetry up to the sudden rise of the elution front followed by a near-zero slope of the peak tails, giving a step aspect to the chromatogram, were observed, making quantitative analysis unreliable. Reaction of nitrogen oxides with the polymer, resulting in sample disappearance, formation of decomposition products, yellowing of the polymer beads and changes in retention times of non-reactive compounds after the injection of large reactive samples were also observed on acrylic polymers. From a practical point of view, Chromosorb 101, 102, 103 and 106 [all styrene-divinylbenzene or polystyrene polymers with pore diameters ranging from 50 Å (type 106) to 85 Å (type 102) and 3500 Å (types 101 and 103)] were found to be suitable for the routine analysis of samples containing both sulphur and nitrogen gases. Peak asymmetry was observed for some compounds on these stationary phases at high concentrations of samples (see Figs. 1-3). Therefore, the retention values were measured by

injecting very small amounts of tail-forming compounds, in order to operate in a reasonably linear region of the partition isotherm.

Tables I and II show the retention times, t'_R (adjusted with respect to the elution time of hydrogen coincident under these conditions with that of the helium carrier gas), and the retention index values measured on these columns at different temperatures. Figs. 4 and 5 show the linear changes in the retention index values as a function of the reciprocal of absolute column temperature. The correlation

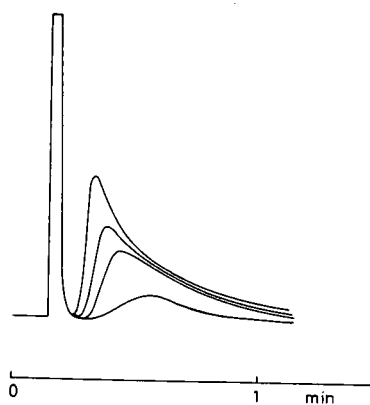


Fig. 2. Asymmetry of NO₂ peak at various concentrations (from 100 to 500 ppm) on a Chromosorb 106 column at 30°C. Carrier gas flow-rate, 22 cm³/min. Thermal conductivity detector.

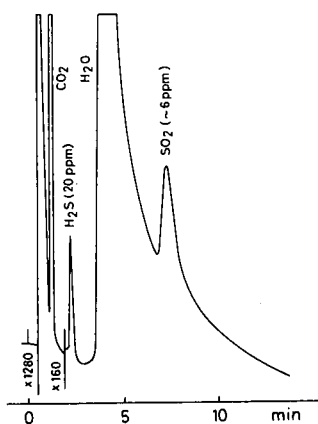


Fig. 3. Asymmetry of water peak and its interference with SO_2 . Analysis of sulphur-polluted exhaust gases from a chemical plant. Helium detector; carrier gas flow-rate, $22 \text{ cm}^3/\text{min}$; temperature, 100°C ; sample amount, 0.5 cm^3 .

coefficients, calculated at five temperatures for compounds whose analysis can be carried out in the range $30\text{--}100^\circ\text{C}$, and at three temperatures for compounds that require the range $70\text{--}100^\circ\text{C}$, were better than 0.98 for all of the compounds, except

H_2O , NH_3 and SO_2 , for which unsymmetrical peaks led to uncertainty in the retention times at the lowest temperatures and to correlation coefficients depending on the column and ranging between 0.90 and 0.96.

Different slopes for different compounds were observed, leading to peak coincidence at some temperatures and to elution order inversions. Changes of the I values as a function of polymer batch or column ageing were observed for polar compounds, mainly H_2O and NH_3 . The graph for Chromosorb 101 in Fig. 1 shows with near parallel lines the minimum, the average and the maximum values observed for these compounds during the experiments. Average values are given in Tables I and II.

The most suitable column for the separation of a given gas mixture can be selected on the basis of the reported values and graphs. Generally, severe interference of the H_2O peak with SO_2 , NH_3 and COS was observed with wet samples, and inversion of the elution order of the pairs $\text{N}_2\text{O}\text{--}\text{NO}$ and $\text{C}_2\text{H}_2\text{--}\text{C}_2\text{H}_4$ with temperature took place on some columns. The previously observed dependence of retention times

TABLE I

ADJUSTED RETENTION TIMES, t'_R (min), AND RETENTION INDICES, I , ON CHROMOSORB 101 AND 102 COLUMNS AT VARIOUS TEMPERATURES

Gas	Chromosorb 101				Chromosorb 102					
	30°C		70°C		30°C		70°C		100°C	
	t'_R	I	t'_R	I	t'_R	I	t'_R	I	t'_R	I
CH_4	0.41	100	0.30	100	0.71	100	0.38	100	0.27	100
C_2H_2	4.13	192	1.26	194	6.75	189	2.29	184	1.10	181
C_2H_4	3.45	184	1.11	186	7.43	193	2.39	186	1.13	182
C_2H_6	5.09	200	1.37	200	8.96	200	3.18	200	1.54	200
C_3H_8	36.41	300	6.11	300	76.94	300	14.35	300	5.46	300
CO_2	1.64	155	0.60	145	2.78	154	1.17	152	0.63	149
COS	21.15	272	4.81	284	38.92	268	8.99	269	3.70	269
H_2S	12.21	244	3.63	265	21.09	240	5.49	236	2.35	233
SO_2	58.38	324	8.81	324			13.63	297	7.85	329
NH_3^a	12.77	247	4.48	279			11.86	287	7.38	324
N_2O	2.45	171	0.98	178	3.61	164	1.53	165	0.85	166
NO	2.57	173	0.88	171	4.84	176	1.25	156	0.57	143
NO_2	1.72	157	0.64	150	3.39	161	0.95	143	0.45	130
H_2O^a	25.89	283	6.72	306			10.64	280	7.25	322

^a For NH_3 and H_2O average values are given (see text).

TABLE II

ADJUSTED RETENTION TIMES, t'_R (min), AND RETENTION INDICES, I , ON CHROMOSORB 103 AND 106 COLUMNS AT VARIOUS TEMPERATURES

Gas	Chromosorb 103						Chromosorb 106					
	30°C		70°C		100°C		30°C		70°C		100°C	
	t'_R	I	t'_R	I	t'_R	I	t'_R	I	t'_R	I	t'_R	I
CH ₄	0.35	100	0.28	100	0.14	100	1.76	100	0.83	100	0.54	100
C ₂ H ₂	3.91	195	1.08	200	0.46	204	18.11	185	5.25	183	2.68	181
C ₂ H ₄	3.17	187	0.87	184	0.37	186	17.04	183	5.39	184	2.88	185
C ₂ H ₆	4.39	200	1.07	200	0.44	200	27.7	200	7.70	200	3.91	200
C ₃ H ₈	23.97	300	4.04	300	1.41	300			39.56	300	15.80	300
CO ₂	1.59	160	0.54	149	0.22	141	6.84	150	2.49	149	1.42	149
COS	18.25	284	3.65	292	1.38	298			21.93	264	8.18	253
H ₂ S	12.43	261	3.64	292	1.67	315	41.60	216	10.93	221	5.69	227
SO ₂	3.40	190	1.55	228	1.05	274			21.50	263	9.04	260
NH ₃ ^a	13.94	268	4.12	301	1.88	325			17.80	251	6.59	237
N ₂ O	2.77	174	1.07	200	0.55	219	9.66	162	3.35	162	1.87	163
NO	2.20	172	0.71	169	0.20	166	6.89	150	2.52	151	1.49	151
NO ₂	0.53	116	0.34	114	0.16	113	1.14	84	0.82	99	0.50	105
H ₂ O ^a	18.30	284	4.32	305	1.78	320			19.3	256	9.09	260

^a For NH₃ and H₂O average values are given (see text).

on polymer batch and column ageing [51,61] may give different results under other experimental conditions. This may change the temperature where the retention times of compounds showing inversion of

elution order are coincident. Moreover, as the peak widths depend on the column length and efficiency and, for low concentrations, on the volume of sample injected to permit good sensitivity, a change in the temperature interval is possible before and after the crossing point where peak separation is too small. A check of the true performance of the column used with authentic samples is therefore necessary to confirm the identification when closely eluting compounds are analysed.

If the required separation cannot be obtained with any of the pure stationary phases, a tailor-made column obtained by homogeneously mixing suitable amounts of two different Chromosorb types, calculated by interpolation of the retention times or retention indices on the two pure phases, can achieve the desired result [62,63]. Mixing of different types of porous polymers is sometime precluded by electrostatic effects that glue the small beads in clusters that are difficult to pour into the column, but it was experimentally checked that Chromosorb 101, 102, 103 and 106, probably owing to their similar chemical composition, can be mixed together in any ratio. Series connection of different lengths of columns filled with pure phases is also possible, but in this

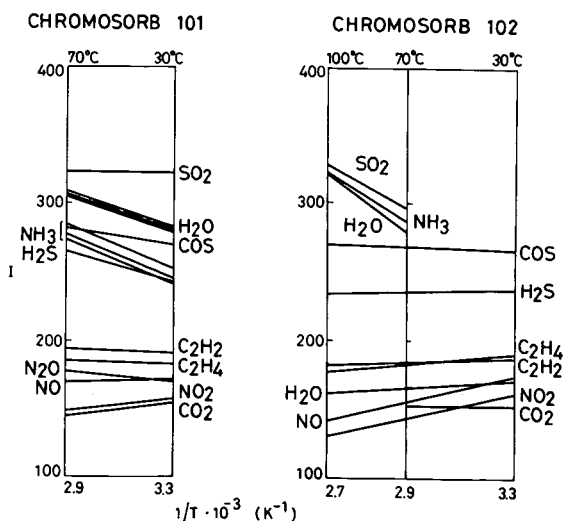


Fig. 4. Retention indices on Chromosorb 101 and 102 at different temperatures. On Chromosorb 101 the maximum, average and minimum values for H₂O and NH₃ are given.

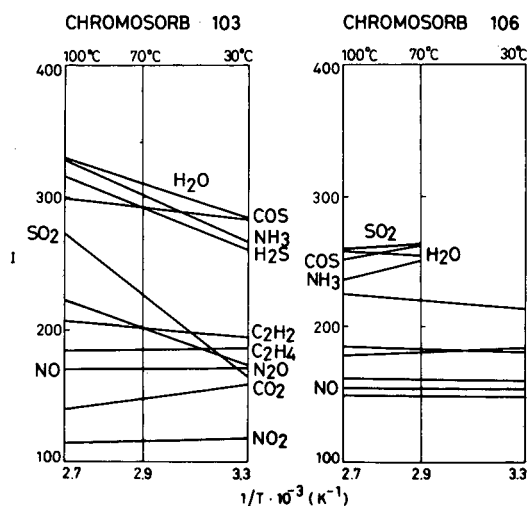


Fig. 5. Retention indices on Chromosorb 103 and 106.

instance the prevailing effect of the upstream column, working at higher pressure, must be taken into account in the calculation of the phase ratios.

Accuracy at low concentration

As mentioned in the Introduction, a reason for the limited application of GC to routine and automated analysis of sulphur and nitrogen gas mixtures at low concentrations is the scatter of the results, often attributed to reaction or decomposition phenomena. These effects, when present, are often negligible with respect of other causes of anomalous or reduced response. Different kinds of deviations from linearity of the plots of peak area vs. sample amount were observed during calibration runs extended down to low concentrations, and can be summarized and ascribed to different phenomena, illustrated in Fig. 6 with various lines plotted on a log-log scale, in order to emphasize the behaviour at low concentrations. As Fig. 6 is intended to show graphically the different behaviours connected with various phenomena, the units are not specified as they can change under different conditions and with different detectors. The data used for this plot were obtained with the helium detector and the abscissa values are therefore in the ppb range, the area values being expressed as integration counts at an electrometer range of 10^{-11} A/mV ($\times 10$ attenuation with respect of the maximum sensitivity of the system). Lines A-F in Fig. 6 can be described as follows.

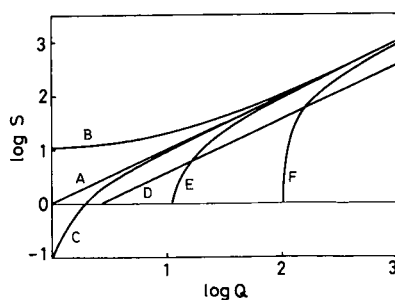


Fig. 6. Effects of different phenomena on quantitative results at low concentration. S = Peak area (integration counts); Q = concentration of the component in the sample injected (ppb). Lines: (A) ideal response; (B) system contamination; (C) vacancy chromatography; (D) adsorption and reaction; (E, F) area losses due to integration. For full explanation, see text.

(A) Theoretical response, with area S linearly proportional to amount Q .

(B) Memory effect, when adsorbed amounts of previous samples of higher concentration are released into further less concentrated or zero samples, yielding a "blank" area value. With the samples analysed in this work, memory effects were found for sulphur gases, mainly SO_2 , with glass or metal columns and connections. This effect was strongly reduced by using PTFE tubing and PTFE-lined sampling systems.

(C) Vacancy chromatography effect, due to the presence in the carrier gas of traces of the compound to be analysed. When the concentration of the sample decreases below the carrier contamination, a "plug" of contaminated carrier is replaced with a cleaner gas volume and this results in a negative peak. When the pressure in the carrier line at the sampling valve is equal to that in the sample line, no peak is observed when the concentrations of the carrier and of the sample are the same. This "zero area" point moves up and down along Q axis depending on the pressure difference between the carrier and sample streams. Vacancy chromatography phenomena were often observed when using the helium detector at high sensitivity and were strongly reduced by purification of the carrier gas and accurate checking for any possible leakage.

(D) Adsorption in the system proportional to the partial pressure of the compound in the system (*i.e.*, to the concentration in the sample). The straight line on a linear scale has a slope smaller than 1; on

a logarithmic scale as in Fig. 6 it is parallel to line A in the concentration range where the adsorption is proportional to concentration, while approximating line A at high concentrations when active adsorbing sites become saturated. With sulphur and nitrogen gases this effect was observed on polar Chromosorb types.

Important reasons for the deviation from linearity are not connected with the chromatographic system (injector, column, stationary phase, detector) but depend on the electronic procedures used for peak area integration. The peak detection algorithms of currently used data systems are activated by the increase in the first derivative of the signal (*i.e.*, by its slope) as a function of time. Narrow and symmetrical peaks are detected early and the integrated area closely approximates the true value. Large and tailing peaks, characteristic of NH_3 , H_2O and SO_2 , are detected later, when their slope changes appreciably with respect of that of the baseline. Some integrators can partially compensate for the delayed peak detection by re-examining some "bunches" of data, collected before the peak detection point, until a zero difference between contiguous values, *i.e.*, a baseline condition, is found. This correction fails, or is less efficient, on the peak tail, and therefore non-symmetrical peaks are more prone to "area loss" than symmetrical peaks. By decreasing the amount of sample, flatter peaks with smaller initial and final slopes are formed, and appreciable deviation from linearity are observed. Referring to Fig. 6, two curves were found as follows.

(E) Integration area losses at low concentration with symmetrical peaks, when the integration defect is due only to the delay of the slope sensitivity system in detecting the start and end of peaks having the same slope.

(F) Integration area losses at low concentration with non-symmetrical or tailing peaks, when the slope at the peak end is much smaller than at the peak start.

Plots E and F in Fig. 6 were obtained by standard integration programs that automatically increase the slope sensitivity when the width of a detected peak is 50% greater than that of the previous peak. This system often fails to detect peaks having a shape different from that of others previously appearing in the chromatogram. Of course, by programming the slope sensitivity or peak detection

parameters as a function of retention time or, better, by adjusting these values just before the elution of non-symmetrical peaks, the area loss can be substantially reduced and reasonable accuracy achieved. The results shown here seems to confirm that often the area losses responsible for inaccurate results in the determination of polar or reactive compounds are not due to decomposition or absorption in the column but depend on improper adjustment of the integration systems. At the lowest concentrations only, memory effects and vacancy chromatography may influence the quantitative results.

The minimum detectable level of each compound obviously depends on the detector used and on the occurrence or lack of vacancy or blank phenomena. As an example, the detection limit in absence of these phenomena of all the present compounds with universal detectors is in the region of 10^{-5} g with TCD and 10^{-11} g with HeD. By using flame photometric detection, the detection limit for sulphur is 10^{-9} g.

ACKNOWLEDGEMENT

This work was supported by the Ministero dell'Università e della Ricerca Scientifica e Tecnologica, Italy.

REFERENCES

- 1 J. Janak and M. Rusek, *Chem. Listy*, 48 (1954) 397.
- 2 S. A. Greene and H. Pust, *Anal. Chem.*, 29 (1957) 1541.
- 3 D. H. Szulczewski and T. Higuchi, *Anal. Chem.*, 29 (1957) 1541.
- 4 E. M. Graven, *Anal. Chem.*, 31 (1959) 1197.
- 5 M. Lefort and X. Tarrago, *J. Chromatogr.*, 2 (1959) 218.
- 6 D. H. Smith and E. Clarke, *Proc. Soil Sci. Soc. Am.*, 24 (1960) 111.
- 7 L. Marvillet and J. Tranchant, in *Proceedings of the 3rd Symposium on Gas Chromatography, Edinburgh, 1960*, Butterworths, London, 1960, pp. A9-A19.
- 8 A. B. Trenwith, *J. Chem. Soc.*, (1960) 3722.
- 9 B. Jay and R. Wilson, *J. Appl. Phys.*, 15 (1960) 298.
- 10 R. Aubeau and L. Champeix, *J. Chromatogr.*, 6 (1961) 209.
- 11 R. R. Sakada, R. G. Rinker, R. F. Cuffel and W. H. Corcoran, *Anal. Chem.*, 33 (1961) 32.
- 12 H. Hall, *Anal. Chem.*, 34 (1962) 64.
- 13 R. Bethea and F. Adams, *J. Chromatogr.*, 10 (1963) 1.
- 14 M. E. Morrison, R. G. Rinker and W. H. Corcoran, *Anal. Chem.*, 36 (1964) 2256.
- 15 J. P. Melia, *J. Inorg. Nucl. Chem.*, 27 (1965) 95.
- 16 C. T. Hodges and R. F. Matson, *Anal. Chem.*, 37 (1965) 1065.
- 17 J. M. Trowell, *Anal. Chem.*, 37 (1965) 1152.

- 18 G. S. Beskova and V. S. Filipov, *Zavod. Lab.*, 38 (1972) 154.
- 19 R. W. Jenkins, Jr., C. H. Cheek and V. J. Linnenbom, *Anal. Chem.*, 38 (1966) 1257.
- 20 V. R. Huebner, H. G. Eaton and J. H. Chaudet, *J. Gas Chromatogr.*, 4 (1966) 121.
- 21 H. Veening and G. D. Dupré, *J. Gas Chromatogr.*, 4 (1966) 153.
- 22 A. T. Dietrich, R. P. Bult and J. M. Ramaradhya, *J. Gas Chromatogr.*, 4 (1966) 241.
- 23 M. E. Morrison and W. H. Corcoran, *Anal. Chem.*, 39 (1967) 255.
- 24 R. N. Dietz, *Anal. Chem.*, 40 (1968) 1576.
- 25 R. M. Bethea and M. C. Meador, *J. Chromatogr. Sci.*, 7 (1969) 655.
- 26 P. W. H. Schnessler, *J. Chromatogr. Sci.*, 7 (1969) 763.
- 27 W. L. Thornsberry, Jr., *Anal. Chem.*, 43 (1971) 452.
- 28 R. K. Stevens, J. D. Mulik, A. E. O'Keefe and K. J. Krost, *Anal. Chem.*, 7 (1971) 827.
- 29 R. Patrick, T. Schrodt and R. Kermoda, *J. Chromatogr. Sci.*, 9 (1971) 381.
- 30 D. H. Bollman and D. M. Mortimore, *J. Chromatogr. Sci.*, 10 (1972) 523.
- 31 F. Bruner, A. Liberti, M. Possanzini and I. Allegrini, *Anal. Chem.*, 44 (1972) 2070.
- 32 F. Bruner, P. Cicciolelli and F. di Nardo, *J. Chromatogr.*, 99 (1974) 661.
- 33 G. Castello, *Relata Techn.*, 9 (1979) 38.
- 34 G. Castello and G. D'Amato, *J. Chromatogr.*, 254 (1983) 69.
- 35 G. Castello and G. D'Amato, *J. Chromatogr.*, 269 (1983) 153.
- 36 F. I. H. Tunstall, *Chromatographia*, 1 (1968) 477.
- 37 E. L. Obermiller and G. O. Charlier, *J. Chromatogr. Sci.*, 7 (1969) 580.
- 38 J. R. Birk, C. M. Larsen and R. G. Wilbourn, *Anal. Chem.*, 42 (1970) 273.
- 39 B. Turner, *Research Notes 11/70*, Varian Aerograph, Walnut Creek, CA, 1970, p. 10.
- 40 A. Lüssan and H. G. McAdie, *J. Chromatogr. Sci.*, 8 (1970) 731.
- 41 M. D. Lattue, H. D. Axelrod and J. P. Lodge, Jr., *Anal. Chem.*, 43 (1971) 1113.
- 42 C. W. Quinlan and J. R. Kittrel, *J. Chromatogr. Sci.*, 10 (1972) 691.
- 43 O. Grubner and A. S. Goldin, *Anal. Chem.*, 45 (1973) 944.
- 44 L. Kremer and L. D. Spicer, *Anal. Chem.*, 45 (1973) 1963.
- 45 T. L. C. de Souza, D. C. Lane and S. P. Bhatia, *Anal. Chem.*, 47 (1975) 543.
- 46 T. L. C. de Souza, *J. Chromatogr. Sci.*, 22 (1984) 470.
- 47 G. Castello, G. D'Amato and M. Nicchia, *J. Chromatogr.*, 521 (1990) 99.
- 48 G. Castello and S. Munari, *Chim. Ind.*, 51 (1969) 469.
- 49 J. M. Trowell, *J. Chromatogr. Sci.*, 9 (1971) 253.
- 50 O. Grubner, J. J. Lynch, J. W. Cares and W. A. Burgess, *Am. Ing. Hyg. Assoc. J.*, 33 (1972) 201.
- 51 G. Castello and G. D'Amato, *J. Chromatogr.*, 349 (1985) 189.
- 52 G. Castello and G. D'Amato, *J. Chromatogr.*, 212 (1981) 261.
- 53 G. Castello and G. D'Amato, *J. Chromatogr.*, 242 (1982) 25.
- 54 J. E. Lovelock, in R. Scott (Editor), *Gas Chromatography 1960*, Butterworths, London, 1960, p. 26.
- 55 C. H. Hartmann and K. P. Dimick, *J. Gas Chromatogr.*, 6 (1966) 163.
- 56 M. Elser and H. Kern, presented at the *International Symposium on Microchemical Techniques, Davos, May 1977; Application Notes No. 11*, Varian, Zug, 1978.
- 57 C. H. Hartmann and K. P. Dimick, *J. Gas Chromatogr.*, 4 (1966) 163.
- 58 C. H. Hartmann and K. P. Dimick, *Technical Bulletin No. 118-65*, Varian Aerograph, Walnut Creek, CA, 1966.
- 59 S. B. Dave, *I&EC Product Res. Develop.*, 14 (1975) 85.
- 60 *Chromosorb Century Series Porous Polymer Supports*, Johns-Manville, Denver, CO, 1980.
- 61 G. Castello and G. D'Amato, *J. Chromatogr.*, 248 (1982) 391.
- 62 G. Castello and G. D'Amato, *Ann. Chim. (Rome)*, 69 (1979) 541.
- 63 R. Mindrup, *J. Chromatogr. Sci.*, 16 (1978) 380.

Synthesis of novel selenium-containing choline and acetylcholine analogues and their quantitation using a pyrolysis–gas chromatography–mass spectrometry assay

A. V. Terry, Jr.

College of Pharmacy, University of South Carolina, Columbia, SC 29208 (USA)

Louis A. Silks III, R. B. Dunlap and J. D. Odom

Department of Chemistry, University of South Carolina, Columbia, SC 29208 (USA)

J. W. Kosh*

College of Pharmacy, University of South Carolina, Columbia, SC 29208 (USA)

(First received February 5th, 1991; revised manuscript received May 22nd, 1991)

ABSTRACT

Methods for the synthesis and quantitation of the novel choline analogues, selenonium choline and acetylselenonium choline, are described. An assay procedure utilizing pyrolysis–gas chromatography–mass spectrometry (Py–GC–MS) with cold trapping was developed with deuterated d_4 -selenonium choline and d_4 -acetylselenonium choline as internal standards. The selenonium compounds were ion-pair extracted from tissue with dipicrylamine, washed with 2-butanone, and pyrolyzed prior to GC–MS analysis. The compounds were monitored using selected ion monitoring at m/z 122 and m/z 125 for the non-deuterated and deuterated compounds, respectively. The assay had a sensitivity of 20 pmol of compound taken through the assay and was linear through 20 nmol.

INTRODUCTION

The role of choline in cholinergic neurotransmission has been studied using a number of analogues of choline and acetylcholine. Those compounds studied include alkyl side chain derivatives [1] (homocholine and β -methylcholine), and quaternary nitrogen alkyl derivatives [2] (monoethylcholine, diethylcholine, triethylcholine, and pyroliidinium-choline). A third group of choline analogues has been synthesized utilizing isosteric quaternary nitrogen replacements with a positive cationic feature. Examples include phosphocholine and arsenocholine [3], stibocholine [4], sulfocholine [5], and silicocholine and carbocholine [6]. A number of these choline analogues appear to qualify as cholinergic false transmitters [2–9], and can prevent acetylcholinesterase inhibitor toxicity [10].

Data indicate that some choline analogues exist naturally in living organisms including propionylcholine [11,12], arsenocholine [13–15], and arsenobetaine [16]. Selenium, like arsenic, is abundant in the earth's mantle [17] and is found in various food products [18]. Several selenoamino acids have been reported incorporated into proteins including selenocystine, selenocysteine, and selenomethionine [19]. Although selenobetaine does not occur naturally, it is extensively metabolized in male rats [16].

Because of the structural similarity of selenonium choline [$(\text{CH}_3)_2\text{Se}^+\text{CH}_2\text{CH}_2\text{OH}$, selenocholine] to choline, and the possibility that selenonium choline might occur in nature as well as act as a cholinergic false transmitter, it was of interest to undertake its synthesis and to develop a method for its quantitation.

Quantitation of choline or its analogues by gas

chromatography (GC) or GC–mass spectrometric (MS) methods is problematic because of their cationic and non-volatile properties and therefore must be demethylated using either chemical or pyrolytic procedures. Pyrolysis (Py)–GC–MS has proven useful in the identification and quantitation of many substances which are difficult to chromatograph such as paints, polymers, matrix trapped plasticizers, and bacteria [20], as well as choline and acetylcholine [21,22].

This work, therefore, describes the synthesis of the novel choline analogues selenonium choline and acetylselenonium choline and their quantitation using a Py–GC–MS assay. Although the name selenocholine appears in the literature [23], selenium was utilized in that study as an oxygen replacement for the alcohol functionality (*i.e.*, a selenol) of choline, rather than for the quaternary nitrogen function.

METHODS

Spectroscopic studies

NMR spectra were recorded as C^2HCl_3 solutions, unless otherwise noted, on either a Bruker AM-300 (7.05 T) or a Bruker AM-500 (11.70 T) spectrometer. Resonance frequencies on the AM-300 are 1H (300.133 MHz), ^{13}C (75.427 MHz), and ^{77}Se (57.19 MHz). On the AM-500, resonance frequencies are 1H (500.13 MHz), ^{13}C (125.767 MHz), and ^{77}Se (95.314 MHz). Chemical shifts for ^{13}C [referenced with respect to internal C^2HCl_3 (δ 77.0 ppm)] and 1H are reported in parts per million (ppm) relative to tetramethylsilane. The ^{77}Se chemical shifts are reported in ppm relative to a 60% C^2HCl_3 solution of dimethyl selenide [24]. All spectra were acquired at ambient probe temperature in 5-mm tubes. Typically, for ^{77}Se spectra 100–1000 scans were acquired using a pulse angle of 35° (90° pulse = 15.4 ms on the AM-500) and a recycle time of 2.2 s. A sweep width of 50 000 Hz and 64K data points resulted in a digitization of 1.7 Hz.

Infrared spectra were recorded on a Perkin-Elmer Fourier transform spectrometer as C^2HCl_3 solutions or neat unless otherwise noted. Mass spectra (including exact masses) were obtained on a VG 705Q mass spectrometer.

Reagents and chemicals

Elemental selenium was obtained from Alfa Products as a gray powder (100 mesh) and used without further purification. Bromoethanol was obtained from Aldrich, distilled, and stored over 4-Å molecular sieves before use. Iodomethane and methyllithium were obtained from Aldrich, and used without further purification. $[1-^2H_2][2-^2H_2]$ -bromoethanol was obtained from Cambridge Isotopes, and used without further purification. The concentration of methyllithium reagents in commercial solutions was determined by titration of diphenylacetic acid to the yellow end point [25]. Tetrahydrofuran (THF) was distilled from sodium–benzophenone prior to use.

Preparation of 2-(methylselenenyl)ethanol (1). Elemental selenium (6.50 g; 82.3 mmol) and 100 ml of dry THF were added to a flame-dried 250-ml 3-neck flask, which was purged with nitrogen and fitted with a septum, a gas inlet, a ground glass stopper and a magnetic stir bar. Under nitrogen, methyl lithium was added dropwise at $0^\circ C$ to the stirred Se–THF suspension. As the addition reached the end-point (1.0 equivalent), the dark brown suspension lightened to give a white suspension (if a more dilute solution was employed the resulting lithium methyl selenolate was a clear yellow solution). Stirring was continued for an additional 5 min, and the temperature was subsequently lowered to $-78^\circ C$. 2-Chloroethanol (5.51 ml; 82.3 mmol) was then added dropwise and stirring was continued for 1 h at $-78^\circ C$. The mixture was then allowed to warm to ambient temperature and stirring was continued for an additional hour. The reaction mixture was then filtered through a pad of SiO_2 (EM Science; 230–400 mesh) and all volatiles were removed *in vacuo*. The crude material was then subjected to flash column chromatography (SiO_2 , 230–400 mesh) using a diethyl ether–hexane (30:70) mixture. Purified yield, 57%. Infrared (in cm^{-1}): 3670 (m), 3616 (s), 3475 (s), 2933 (s), 2976 (s), 1604 (m), 1468 (s), 1430 (s), 1392 (s), 1380 (s), 1341 (s), 1290 (s), 1255 (s), 1197 (s), 1181 (s), 1047 (s). NMR (in ppm): 1H , δ 1.77 {s, 3H [1H – ^{77}Se satellites, J (1H – ^{77}Se) = 10.5 Hz]}, 2.46 (t, J = 6.7 Hz, 2H), 3.53 (m, 2H), 3.64 (t, J = 5.7 Hz, 1H (O–H)); ^{13}C , 61.0, 28.1 [J (^{13}C – ^{77}Se) = 61.6 Hz], 3.96 [J (^{13}C – ^{77}Se) = 62.3 Hz]; ^{77}Se , δ 34.

Preparation of 2-(dimethylselenonium)ethanol iodide, selenonium choline (2). Compound **1** (6.54 g; 47.1 mmol) was placed in a 100-ml single-neck round bottom flask fitted with a septum and containing a magnetic stir bar. The flask was chilled to -78°C and iodomethane was added dropwise. The mixture was slowly warmed to ambient temperature and stirring was continued for about 8 h. The resulting oil was washed three times with 50-ml portions of diethyl ether. All volatile materials were then removed *in vacuo* to yield 11.56 g (87%) of a viscous yellow oil. Infrared (in cm^{-1}): 3355 (s), 3011 (s), 2920 (m), 2876 (m), 1620 (w), 1417 (m), 1295 (m), 1270 (m), 1209 (w), 1142 (m), 1063 (s), 1010 (m), 984 (m). NMR (in ppm): ^1H [in dimethyl sulfoxide (DMSO-d_6)], δ 2.79 (s, 6H), 3.50 (m, 2H), 3.80 (dd, $J = 5.1$ Hz, 5.3 Hz, 2H), 5.24 (t, $J = 4.7$ Hz, 1H); ^{13}C (in DMSO-d_6), δ 57.0, 44.1, 21.5 [$J(^{13}\text{C}-^{77}\text{Se}) = 53$ Hz]; ^{77}Se (in DMSO-d_6), δ 285 ppm. Elemental analysis calculated for $\text{C}_4\text{H}_{11}\text{OSe}^+$: C, 17.10; H, 3.95; Se, 28.10. Found: C, 17.20; H, 3.99; Se, 28.47.

Preparation of 2-(methylselenenyl)-[1- $^2\text{H}_2$]-[2- $^2\text{H}_2$]ethanol (3). Compound **3** was prepared using a procedure identical to that used to prepare **1** except that [1- $^2\text{H}_2$][2- $^2\text{H}_2$]bromoethanol was employed. The purified yield was 67%. NMR: ^1H (DMSO-d_6), 81.90 (s, 3H), 2.50 (s, 1H, OH).

Preparation of 2-(dimethylselenonium)-[1- $^2\text{H}_2$]-[2- $^2\text{H}_2$]ethanol iodide (4). Compound **4** was prepared from **3** using a procedure identical to that used to prepare **2**. The purified yield was 70%. NMR: ^1H (DMSO-d_6), δ 2.73 (s, 6H), 3.40 (s, 1H, OH).

Demethylation experiment

Compound **2** (100 mg) was placed in a single-neck 100-ml round bottom flask equipped with a high vacuum stopcock. The flask was attached to a high vacuum system, evacuated, and subjected to dynamic vacuum for 18 h. Volatile materials that evolved from the solid over this period were collected in a trap at -196°C . These materials were then placed in an NMR tube, dissolved in C^2HCl_3 and a ^1H spectrum obtained. The major compound was shown to be CH_3I (δ 2.15) by comparison to a ^1H NMR spectrum of a known sample of CH_3I in C^2HCl_3 (δ 2.13).

Quantitation of selenonium choline and acetylselenonium choline

Synthesis of the acetyl esters of d_0 - and d_4 -selenonium choline was required for the construction of a standard curve used to quantitate selenonium choline and acetylselenonium choline. Amounts of 5 μmol each of d_0 - or d_4 -selenonium choline dissolved in acetonitrile were added to 10-ml assay tubes and evaporated to dryness with nitrogen. Further, the tubes were desiccated under vacuum for 5 min and the residue dissolved in 2 ml of 12.5 mM silver *p*-toluenesulfonate-acetonitrile solution. An aliquot of 100 μl of doubly distilled acetylchloride was added, the solution vortexed briefly, and left at room temperature for 30 min. The tube was then evaporated to dryness under nitrogen and desiccated under vacuum for 5 min. The dried compound was reconstituted in 1 ml of sodium acetate buffer (0.05 M, pH 4) and used without further purification.

Standard curves for selenonium choline and acetylselenonium choline were prepared using 2.5 nmol of d_4 -selenonium choline and d_4 -acetylselenonium choline as internal standards along with various amounts of unlabelled selenonium choline and acetylselenonium choline. Acetonitrile-1 M formic acid (85:15, v/v) (2 ml) was then added and the supernatant transferred to a 10-ml screw-capped conical centrifuge tube. Diethylether was added, vortexed, and centrifuged for 2 min. The organic phase was then aspirated and residual ether and acetonitrile evaporated under nitrogen at 70°C for 5 min. The selenonium compounds were ion-pair extracted by adding 2 ml of 2 mM dipicrylamine in dichloromethane (DCM) and 0.5 ml of tris(hydroxymethyl)-methylaminopropanesulfonic acid (TAPS) buffer (pH 9.2). The mixture was immediately vortexed for 2 min and centrifuged. The upper aqueous layer was aspirated and the DCM layer was transferred to another tube, evaporated under a stream of nitrogen, and desiccated under vacuum for 5 min. Silver *p*-toluenesulfonate (5 mM) in acetonitrile (0.5 ml) was added plus 50 μl of doubly distilled propionyl chloride. The solution was then vortexed, and left at room temperature for 10 min. The tube was then evaporated to dryness under nitrogen and desiccated under vacuum for 5 min. The residue was dissolved in 250 μl of sodium acetate buffer (0.05 M, pH 4) and washed twice with 500 μl of 2-butanone.

The aqueous layer was then evaporated to dryness with nitrogen at 50°C and desiccated under vacuum for 5 min. The sample was then dissolved in an acetonitrile–water mixture (90:10, v/v), vortexed, and briefly kept on ice until analyzed by Py–GC–MS. For the assay of tissue, the procedure was the same as described above except that the tissue was homogenized in formic acid–acetonitrile with an internal standard using a glass Elvehjem apparatus and PTFE pestle. After centrifugation at 26 000 *g* for 20 min, the supernatant was decanted and processed as above.

The prepared samples were analyzed by Py–GC–MS using a Hewlett-Packard gas chromatograph (5890)–mass spectrometer (5970) and a Stabilwax column (Restek, 30 m × 0.25 mm I.D., 0.5- μ m phase). Helium was used as the carrier gas at a head pressure of 5 p.s.i. and a linear flow velocity of 25 cm/s. Samples were pyrolyzed (Pyroprobe 122, Chemical Data Systems) using a quartz tube, for 10 s at 325°C. The pyrolysis interface temperature was 150°C, and the ramp setting was off. The pyrolysis products were trapped on the column by a CO₂ cold trapping attachment (see Fig. 1). Liquid CO₂ was supplied to the cold trapping area of the column from a CO₂ syphon cylinder controlled with a

hand-operated valve. The 1/8 in. copper supply line terminated in a brass “T” fitting which served to deflect the CO₂ to maximize the cooled area and to support a 10-cm stainless-steel tube column jacket. The column jacket was necessary to prevent column breakage from CO₂ pressure surges.

After pyrolysis of the sample and cold trapping for 3 min, the oven door was closed and the oven heating ramp initiated. The initial oven temperature was 30°C, and was increased at 30°C/min to 200°C and held for 2.5 min. To prevent late eluting pyrolysis products from contaminating the next run, the oven temperature was further increased by 30°C/min to 225°C and held for 5.0 min. GC was operated in the splitless mode and the injector purge initiated at 3 min. The mass spectrometer was operated at 68 eV ionization energy, a filament current of 220 μ A, an ion source temperature of 200°C and a vacuum of $5 \cdot 10^{-5}$ torr. Selected ion monitoring was chosen for sample analysis using *m/z* 122 ([CH₃-Se-CH=CH₂]⁺) and *m/z* 125 ([CH₃-Se-C²H=C²H₂]⁺) which corresponded to the base peaks for the d₀- and d₄-compounds, respectively (see Fig. 2). Quantitation was based on the d₀/d₄ ratios of the corrected areas and referenced to a standard curve. Areas were corrected and samples

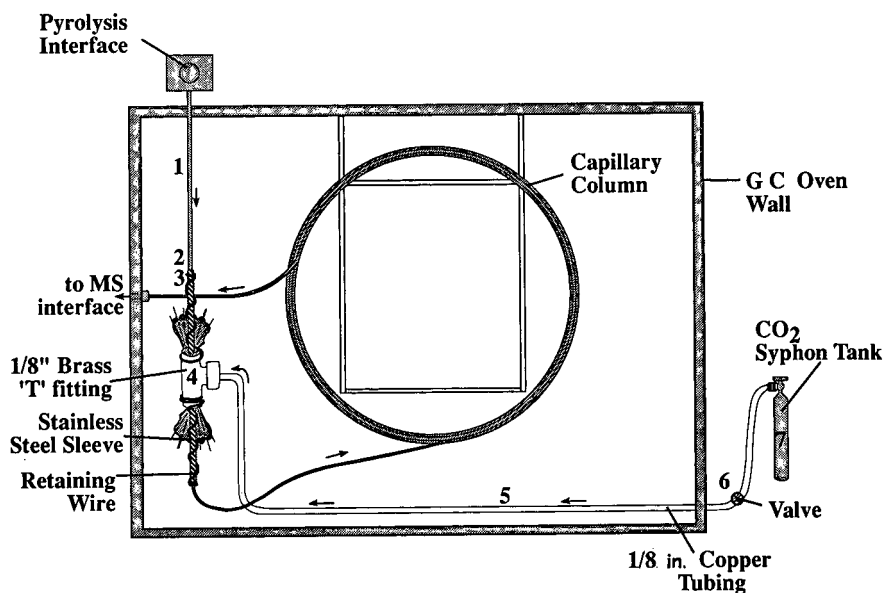


Fig. 1. Diagram of the CO₂ cold trapping apparatus. Key: 1 = capillary column, 2 = stainless-steel sleeve, 3 = retaining wire, 4 = 1/8 in. brass “T” fitting, 5 = 1/8 in. copper tubing, 6 = hand-operated control valve, 7 = CO₂ syphon tank.

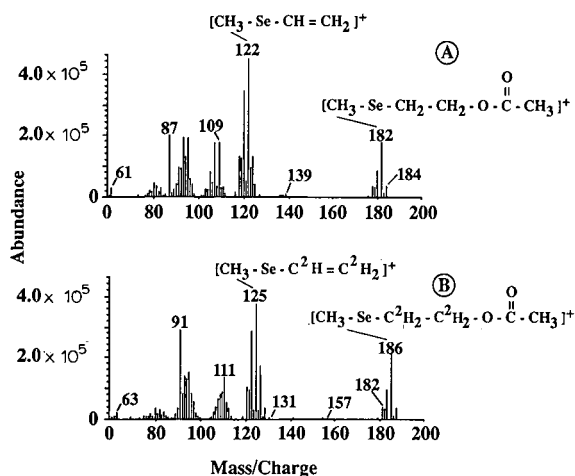


Fig. 2. Mass spectra of (A) d_0 - and (B) d_4 -acetylselenium choline. The selenium compounds were subjected to the complete assay protocol and analyzed by Py-GC-MS. Data were obtained using the HP5890/5970 GC-MS system operated in the "scan" mode.

automatically quantitated through the use of a matrix-based Pascal program written by the authors for the Hewlett-Packard system.

RESULTS AND DISCUSSION

The purpose of the present study was to synthesize the novel choline analogue selenium choline and to develop a method to quantitate this analogue and its acetyl ester in biological tissue. A thorough spectroscopic characterization of the products synthesized according to the procedures detailed in the Methods section leaves no doubt that selenium choline and the deuterated (d_4) analogue can be prepared in good yield (49.6% and 49%, respectively) with analytical purity. Proof of synthesis of these analogues is provided in Fig. 3. An exact mass peak using the glycerin $m/z = 185$ peak as a reference gave a mass of the parent 155 peak of 154.9972 for selenium choline. The calculated mass for $C_4H_{11}O^{80}Se$ was 154.9975. The most intense peak in the parent ion envelope for d_4 -selenium choline was m/z 159. During the vacuum desiccation of this analogue at room temperature, spontaneous demethylation of selenium choline iodide was found to occur with evolution of methyl iodide.

The quantitation of selenium choline and ace-

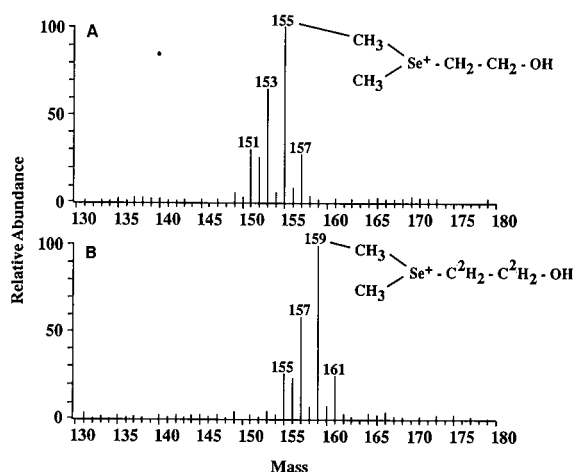


Fig. 3. Fast atom bombardment (FAB) spectra (positive ion) of (A) d_0 - and (B) d_4 -selenium choline. Spectra were obtained following a standard static procedure using a VG 705Q mass spectrometer and data system.

tylselenium choline was accomplished using a Py-GC-MS procedure. Briefly, the selenium compounds were ion-pair extracted from tissue samples, and selenium choline was converted to the propionyl ester (Fig. 4). The acetyl and propionyl esters were then pyrolyzed and quantitated. It was necessary to propionylate selenium choline in order to adequately resolve the peak areas representing acetylselenium choline and selenium choline. Several washes with 2-butanone were necessary to remove contaminating background due to dipicrylamine (DPA) used in the ion-pairing step. The column adopted for routine use was a Stabilwax column; however, HP20, and HP5 columns were also found to give satisfactory results. The assay procedure appears to be compatible with the column choice since over 300 injections have been made without decrements in performance. Since the selenium compounds are positively charged, demethylation was necessary to allow volatilization and GC separation. Chemical demethylation was initially tried using the following agents: lithium butylselenolate, hexamethyldisilazane, lithium diisopropylamide mono(tetrahydrofuran), lithium bis(trimethylsilyl)amide, lithium phenylselenolate and sodium thiophenoxide. Chemical demethylation was not quantitative for any of the reagents tried.

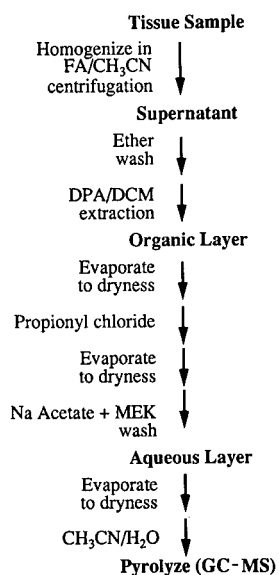


Fig. 4. Flow chart for assay of selenium choline and acetylselenium choline. Internal standards (d_4 -selenium choline and d_4 -acetylselenium choline) are added prior to homogenization. An aliquot of $2 \mu\text{l}$ of final extract is utilized for Py-GC-MS analysis. Abbreviations used are: FA = formic acid; MEK = methyl ethyl ketone; 2-butanone, DPA = dipicrylamine, DCM = dichloromethane.

Although sodium thiophenoxide was the most active, only 10% demethylation was observed. Quantitative demethylation of the selenium compounds could only be obtained using pyrolysis. A similar problem has been reported with arsenocholine and related compounds [15].

Due to large void volumes in the pyrolysis interface, it was necessary to cold trap the demethylated selenium compounds on the column prior to initiating the oven temperature program. The authors constructed a simple apparatus (see Fig. 1) at very low cost to achieve the cold trapping effect. A hand valve with low mass was necessary to allow control of CO_2 release and to minimize heat sink effects that would occur with a typical two stage pressure regulator. Also, a key part of the design is the stainless-steel tubing used to encase the column to minimize column breakage due to pressure surges. Although the temperature control of the cold trapped area was variable, little effect was observed on peak retention times and areas.

Fig. 2 illustrates representative mass spectra ob-

tained on the HP5870 mass spectrometer for d_0 - and d_4 -acetylselenium choline. Fragmentation patterns for the acetyl and propionyl esters were identical and only the acetyl ester is presented here. The peaks m/z 182 and 186 correspond to the molecular ion of the demethylated d_0 - and d_4 -acetyl esters, respectively. The most abundant peaks in the mass spectra for the acetyl ester were m/z 122 for the d_0 -variant and m/z 125 for the d_4 -variant. The m/z 122 peak corresponds to the olefinic ion $[\text{CH}_3\text{-Se-CH}=\text{CH}_2]^+$ for the d_0 -compound and m/z 125 corresponds to the ion $[\text{CH}_3\text{-Se-C}^2\text{H}=\text{C}^2\text{H}_2]^+$. Other prominent ions were: m/z 109 and 95 for the d_0 -compounds and m/z 111 and 91 for the d_4 -variant. The peaks m/z 87 and 91 correspond to the fragments $[\text{CH}_2\text{-CH}_2\text{-O-CO-CH}_3]^+$ and $[\text{C}^2\text{H}_2\text{-C}^2\text{H}_2\text{-O-CO-CH}_3]^+$ for the d_0 - and d_4 -compounds, respectively.

Fig. 5 illustrates the linearity of the standard curve obtained for selenium choline (as the propionyl ester) and acetylselenium choline. Excellent linearity with low standard error was observed from 20 pmol (1.6 pmol injected) through 20 nmol for both selenium compounds. Plotted points

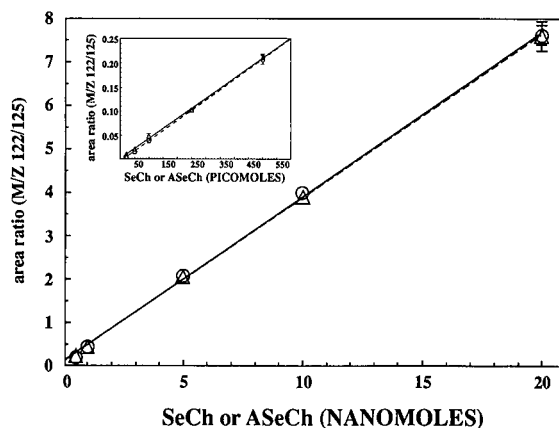


Fig. 5. Standard curves for selenium choline and acetylselenium choline. Known quantities of selenium analogues with 2.5 nmol of internal standard (d_4 -selenium variants) were processed using the described assay protocol and analyzed by Py-GC-MS. Areas of the m/z 122 and 125 ions were corrected as described in Methods and the ratio of m/z 122/125 plotted versus the d_0 -selenium analogue concentration. The large graph demonstrates the linearity of 0.5 to 20 nmol quantities and the inset 20 to 500 pmol quantities of d_0 -selenium analogues. ○ = Acetylselenium choline (ASeCh); △ = selenium choline (SeCh).

represent the ratio of the corrected areas of the d_0 - and d_4 -compounds for each selenium compound. Peak areas were corrected for isotopic spillover between m/z 122 and m/z 125 using a matrix calculation procedure similar to that used for the analysis of choline and acetylcholine [26]. The necessity for area corrections can be seen by inspection of a representative matrix table used in the calculations (Table I). The spillover from the m/z 122 ion into the m/z 125 ion area was usually low (5–8%), whereas the spillover from the m/z 125 ion into the m/z 122 ion area was higher and ranged from 16 to 17%. For the mixture of both compounds the m/z 125 ion area was typically 90–95% of the m/z 122 ion area. Generally one set of matrix tubes was analyzed and used as the basis for area corrections for each set of experimental samples (12–16 tubes).

Fig. 6 illustrates a representative selected ion monitoring (SIM) tracing of a 20 pmol sample (1.6 pmol injected) of selenium and acetylselenium choline processed in the presence of brain tissue and taken through the assay. Complete resolution and good separation (approximately 0.5 min) of the selenium analogues were observed. Peak widths at half-height usually ranged from 0.03 to 0.05 min for peaks in this concentration range. The peak for the propionylated ester (selenium choline) eluted after, and was usually larger than, the acetyl ester peak. The difference in peak areas for the same quantity of each ester is a pattern which is also seen in the GC–MS assay for choline and acetylcholine (data not presented). Table II illustrates the preci-

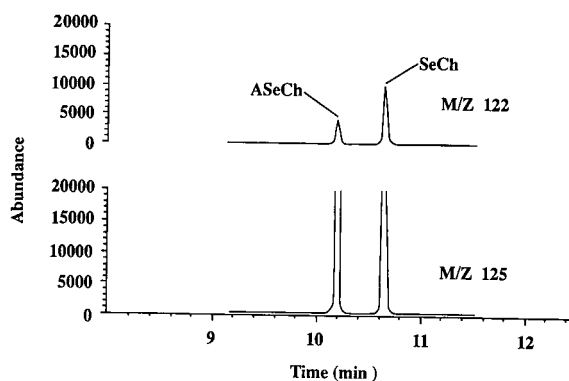


Fig. 6. Representative selected ion chromatogram of acetylselenium choline and selenium choline. The selenium compounds were taken through the Py–GC–MS assay in the presence of 100 mg of mouse brain tissue. The top tracing corresponds to 20 pmol of d_0 -analogues and the bottom tracing corresponds to 2.5 nmol of d_4 -internal standards.

sion of the assay and recovery of the selenium compounds in the presence of brain tissue. Considering the inherent problems associated with pyrolysis techniques [27], the data obtained show reasonable accuracy with slightly more variation at the lower concentrations of analogue. The presence of mouse brain tissue produced only marginal effects on the accuracy and precision of the method. The assayed values for selenium choline were generally lower than theoretical in the absence of tissue, and higher than theoretical in the presence of tissue. The assayed values for acetylselenium choline

TABLE I

REPRESENTATIVE NORMALIZED AREA CONTRIBUTIONS BETWEEN MASS 122 AND MASS 125 IONS

Assay tubes containing only d_0 -, or d_4 -, or a mixture of d_0 - + d_4 -selenium choline and acetylselenium choline were processed according to the assay protocol and subjected to Py–GC–MS analysis. The areas obtained during selected ion monitoring analysis for m/z 122 and m/z 125 were normalized by dividing each area by the largest value obtained. The normalized areas were subsequently used in matrix calculations to provide corrected area values for the experimental samples.

Acetylselenium choline			Selenium choline		
Analogue	m/z		Analogue	m/z	
	122	125		122	125
d_0	1.0	0.07961	d_0	1.0	0.06562
d_4	0.16692	1.0	d_4	0.16645	1.0
$d_0 + d_4$	1.0	0.93483	$d_0 + d_4$	1.0	0.94651

TABLE II

ASSAY REPRODUCIBILITY IN THE PRESENCE AND ABSENCE OF BRAIN TISSUE

Known quantities of selenium choline and acetylselenium choline were homogenized in formic acid-acetonitrile in the presence and absence of 100 mg of mouse brain tissue. The samples were then processed according to the assay protocol and subjected to Py-GC-MS analysis.

Compound	Added (pmol)	Observed			
		Control (pmol)		Brain tissue (pmol)	
		(mean \pm S.E.) ^a	<i>n</i>	(mean \pm S.E.)	<i>n</i>
Selenium choline	20.0	18 \pm 1.5	9	25 \pm 6	7
	100.0	94 \pm 3	5	102 \pm 4	6
	1000.0	1000 \pm 70	6	990 \pm 20	6
Acetylselenium choline	20.0	27 \pm 1	11	23 \pm 1	8
	100.0	111 \pm 4	6	103 \pm 6	6
	1000.0	1040 \pm 40	6	1000 \pm 10	6

were generally higher than theoretical in the absence and presence of tissue. The majority of the values shown in Table II were well within the standard error of the standard curve points (Fig. 5).

ACKNOWLEDGEMENTS

The authors wish to thank Mrs. Emily F. Wilingham for her expertise in the preparation of this manuscript and Dr. Julian H. Fincher, Dean of the College of Pharmacy for his generous support provided for supplies and equipment. This research was also supported by grant NSF, No. BNS-8515929 to J. W. K.

REFERENCES

- R. M. Dick, J. J. Freeman and J. W. Kosh, *Life Sci.*, 36 (1985) 1183.
- B. Collier, P. Boksa and S. Lovat, in F. Tucek (Editor), *Progress in Brain Research, Vol. 49, The Cholinergic Synapse*, Elsevier, Amsterdam, 1979, p. 107.
- A. D. Welch and M. H. Roepke, *J. Pharmacol. Exp. Ther.*, 55 (1935) 118.
- E. M. Meyer, R. J. Barnett and J. R. Cooper, *J. Neurochem.*, 39 (1982) 321.
- L. Frankenberg, G. Heimburger, C. Nilsson and B. Sorbo, *Eur. J. Pharmacol.*, 23 [1] (1973) 37.
- P. T. Henderson, E. J. Ariens, B. W. J. Ellenbroek and A. M. Simonis, *J. Pharm. Pharmacol.*, 20 (1968) 26.
- R. Hunt and R. R. Renshaw, *J. Pharmacol. Exp. Ther.*, 25 (1925) 315.
- R. Hunt and R. R. Renshaw, *J. Pharmacol. Exp. Ther.*, 48 (1933) 51.
- B. Hedlund, H. Norin, A. Christakopoulos, P. Alberts and T. Bartfai, *J. Neurochem.*, 39 (1982) 871.
- T. A. Patterson, A. V. Terry, Jr., and J. W. Kosh, *Br. J. Pharmacol.*, 97 (1989) 451.
- R. J. Banister, V. P. Whittaker and S. Wijesundera, *J. Physiol. (London)*, 121 (1953)-55.
- S. O'Regan, *J. Neurochem.*, 39 (1982) 764.
- H. Norin, A. Christakopoulos, L. Rondahl, A. Hagman and S. Jacobsson, *Biomed. Environment. Mass Spectrom.*, 14 (1987) 117.
- H. Norin and A. Christakopoulos, *Chemosphere*, 11 (1982) 287.
- H. Norin, R. Ryhage, A. Christakopoulos and M. Sandstrom, *Chemosphere*, 12 (1983) 299.
- S. J. Foster, R. J. Kraus and H. E. Ganther, *Arch. Biochem. Biophys.*, 247 (1986) 12.
- R. P. Beliles, in L. J. Casarett and J. Doull (Editors), *Toxicology: The Basic Science of Poisons, Metals*, Macmillan, New York, 1975, p. 454.
- C. S. Reddy and A. W. Hayes, in A. W. Hayes (Editor), *Principles and Methods of Toxicology, Food Borne Toxicants*, Raven Press, New York, 1989, p. 67.
- J. D. Odom, *Structure and Bonding*, 54 (1983) 1.
- C. J. Wolf, M. A. Grayson, D. L. Fanter, *Anal. Chem.*, 52 (1980) 348 A.
- R. L. Polak and P. C. Molenaar, *J. Neurochem.*, 32 (1979) 407.
- P. I. A. Szilagyi, P. E. Schmidt, J. P. Green, *Anal. Chem.*, 40 (1968) 2009.
- W. H. H. Gunther and H. G. Mautner, *J. Med. Chem.*, 7 (1964) 229.

- 24 N. P. Luthra, R. B. Dunlap and J. D. Odom, *J. Mag. Reson.*, 52 (1983) 318.
- 25 W. G. Kofron and Baclawski, *J. Org. Chem.*, 41 (1976) 1879.
- 26 D. J. Jenden, M. Roch and R. A. Booth, *Anal. Biochem.*, 55 (1973) 438.
- 27 J. Q. Walker, *Chromatographia*, 5 (1972) 547.

Gas chromatographic–mass spectrometric determination of ethyl carbamate as the xanthylamide derivative in Italian aqua vitae (grappa) samples

Claudio Giachetti*, Alessandro Assandri and Giovanni Zanolo

Istituto di Ricerche Biomediche "A. Marxer", RBM SpA, P.O. Box 226, 10015 Ivrea (To) (Italy)

(First received February 5th, 1991; revised manuscript received June 3rd, 1991)

ABSTRACT

A selective reaction of ethyl carbamate (urethane) and methyl urethane (urethylane), as internal standard, with xanthidrol was effected to detect urethane after extraction from Italian aqua vitae (grappa) samples. The xanthylamides formed were determined by gas chromatography–mass spectrometry in the selected ion monitoring mode on an apolar DB 5 silica column. The linearity of the method was tested from 10 to 1000 $\mu\text{g/l}$, with a detection limit of 1 $\mu\text{g/l}$.

INTRODUCTION

Initial studies on urethane in alcoholic beverages indicated that it is formed as a result of a reaction between diethyl pyrocarbonate (DEPC) and beverages containing naturally occurring amounts of ammonia [1]. DEPC had been widely used as an antimicrobial additive until 1972. Successive studies by Ough [2–4], however, demonstrated that urethane occurred naturally in fermented foods and beverages and that the addition of DEPC to wines minimally affected the amount of urethane produced.

As urethane is carcinogenic [5], it became essential to ensure that products for human consumption, including alcoholic beverages, contained minimum levels of the substance. In 1986 the Department of Health and Welfare in Canada issued [16] guidelines limiting the levels of ethyl carbamate in wines, distilled spirits, fruit brandies and liqueurs.

Reported urethane assays are based on gas chromatographic (GC) separation and detection with Hall electrolytic conductivity detectors in the nitrogen mode [6–9]. In conjunction with this technique, mass spectrometric (MS) detection was used for confirmation or for direct quantitative evaluations [10–12]. Urethane has also been determined by GC

using nitrogen–phosphorus thermionic detection after a methylation reaction [13] or using two-dimensional GC and flame ionization detection [14].

This paper describes a further assay procedure based on a selective reaction of urethane with xanthidrol and GC–MS measurement of the xanthylamide formed. The method was applied to the determination of urethane in twenty samples of the Italian grape distillate aqua vitae (grappa). The results obtained (values ranging from 70 to 400 $\mu\text{g/l}$) confirmed the sensitivity and accuracy of the method.

EXPERIMENTAL

Chemicals

Xanthidrol, urethane, urethylane and the solvents used, all of analytical-reagent grade, were supplied by Fluka (Buchs, Switzerland).

Authentic xanthylurethane and xanthylurethylane were synthesized by dissolving 250 mg of xanthidrol in 3 ml of glacial acetic acid with 250 mg of either ethyl carbamate or methyl carbamate, gently warmed in a water-bath at 37°C. The resulting solutions were allowed to stand for 20 min in the same bath, then cooled to obtain crystals. These were re-

crystallized from dioxane–water (1:1, v/v) and dried at 70°C for 15 min [15].

The following solutions were prepared: 0.1 mg/ml xanthidrol in glacial acetic acid, 0.1 and 0.01 mg/ml urethane in ethyl acetate and 0.01 mg/ml urethylane in ethyl acetate.

Extraction procedure

The grappa sample (10 ml) was washed twice with *n*-pentane (5 ml), vortex mixed for 1 min and the solvent discarded each time. After addition of sodium chloride (200 mg) and urethylane standard solution (25 μ l), the sample was extracted with dichloromethane–ethyl acetate (95:5, v/v) (10 ml) by vortex mixing for 20 s and shaking for 10 min. The sample was then briefly centrifuged at 625 g, the organic phase transferred to another tube containing anhydrous sodium sulphate and the aqueous phase re-extracted twice with dichloromethane–ethyl acetate (90:10, v/v) (5 ml). All the dehydrated extracts were evaporated under a stream of nitrogen in a water-bath at 37°C until the volume was reduced to 10–20 μ l. Xanthidrol standard solution (0.1 ml), glacial acetic acid (0.1 ml) and water (0.3 ml) were then added to this solution. After mixing, the sample was left in a warm bath (37°C) for 20 min, cooled with a further 0.6 ml of ice-cold water and re-extracted with dichloromethane–ethyl acetate (90:10, v/v) (5 ml) by shaking for 5 min. After centrifugation, the organic layer was removed and evaporated to dryness under nitrogen. The residue

was redissolved in two drops of ethyl acetate, mixed with 50–100 μ l of *n*-hexane and 1 μ l was injected for analysis.

Quantification

Standard amounts of urethane in the range 10–1000 ng were added to tubes containing 10 ml of ethanol–water (50:50, v/v). A 250-ng amount of urethylane was added as internal standard and then the mixture was subjected to the extraction procedure and reaction with xanthidrol as described above. Quantification was based on the peak-area ratios of xanthyl urethane to xanthyl urethylane versus added amounts. The resulting calibration graphs and linear regressions are shown in Fig. 1. Each point is the mean value from triplicate analyses.

Gas chromatography–mass spectrometry (GC–MS)

A Hewlett-Packard quadrupole mass spectrometer (Model 5970 B) connected with a Carlo Erba HRGC 5300 Mega Series gas chromatograph was used. GC was performed on a 15 m \times 0.24 mm I.D. fused-silica capillary column coated with DB 5 (film thickness 0.25 μ m) (J&W Scientific, Folsom, CA, USA) preinserted in a retention-gap silica column (1 m). The oven was programmed from 150°C (held for 1 min) to 180°C at 30°C/min, then to 205°C at 3.5°C/min, and finally to 260°C (held for 5–10 min) at 30°C/min. The injector and interface were maintained at 250°C. The sample injection was splitless

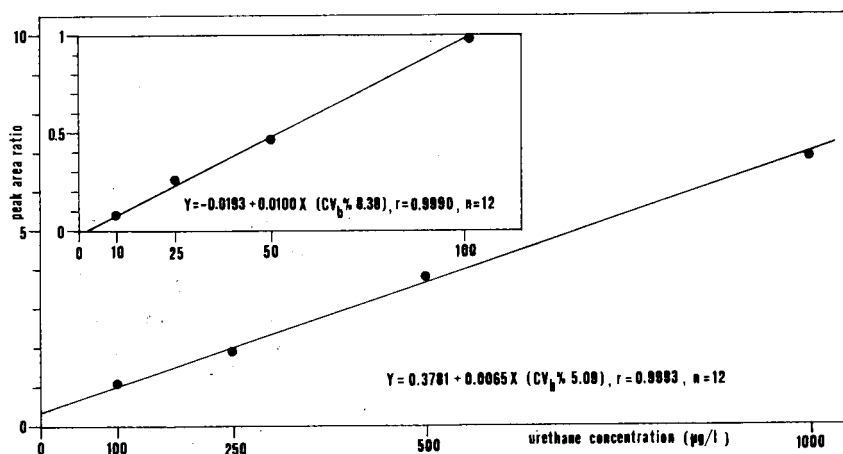


Fig. 1. Calibration graphs for the determination of urethane in grappa samples.

(30 s), splitting ratio 1:10. The carrier gas was helium at a flow-rate of 1.5 ml/min. Mass spectra were obtained in the scanning mode using positive-ion electron impact (EI) ionization (70 eV). Data processing on selected ion monitoring (SIM) mode acquisition was performed on a Hewlett-Packard 59970 C Chem Station.

Data acquisition

The peak areas of xanthylurethane or xanthylurethylane were obtained from the peaks at the m/z 76, 77, 90, 152, 181, 182, 195, 196, 197, 222, 240, 241, 255 and 269 in the mass chromatogram with SIM mode acquisition, using a time window from 6 to 8 min. A 100- μ s dwell time was applied to each ion monitored. The resulting voltage was 1.8 kV and the scan time was 0.6 cycles per second. Mass calibration was relative to external lock, from perfluorotributylamine.

RESULTS AND DISCUSSION

One of the reactions in organic chemistry that can be used to identify amides is that with xanthidrol. In fact, we easily succeeded in obtaining high yields of xanthylamides (>95%) by reacting urethane and urethylane with an excess of reagent (the molar equivalent ratios being 1:2.22 and 1:2.64, respectively). The crystalline products obtained when analyzed by GC-MS gave rise to the fragmentation spectra shown in Fig. 2.

Under electron impact both xanthylurethane and xanthylurethylane undergo a common fragmentation involving the alkylamide side-chains (Fig. 3). The high relative intensities of the m/z 196 and 181 peaks suggest a possible direct cleavage of the amide bond ($M-59$, $M-73$) with further loss of the remaining amino group. Alternatively, fragmentation might proceed stepwise through dealkylation ($M-29$, $M-15$) followed by CO_2 loss. Interestingly, the presence of the m/z 152 peak could be explained by the highly stable structure proposed in Fig. 3 which may be derived from m/z 181 by the loss of formaldehyde. The use of methylurethane (urethylane) as a suitable internal standard was suggested by the fact that the product is not a natural constituent of alcoholic beverages nor is it formed during their distillation process, and it retains the same chemical characteristics as urethane.

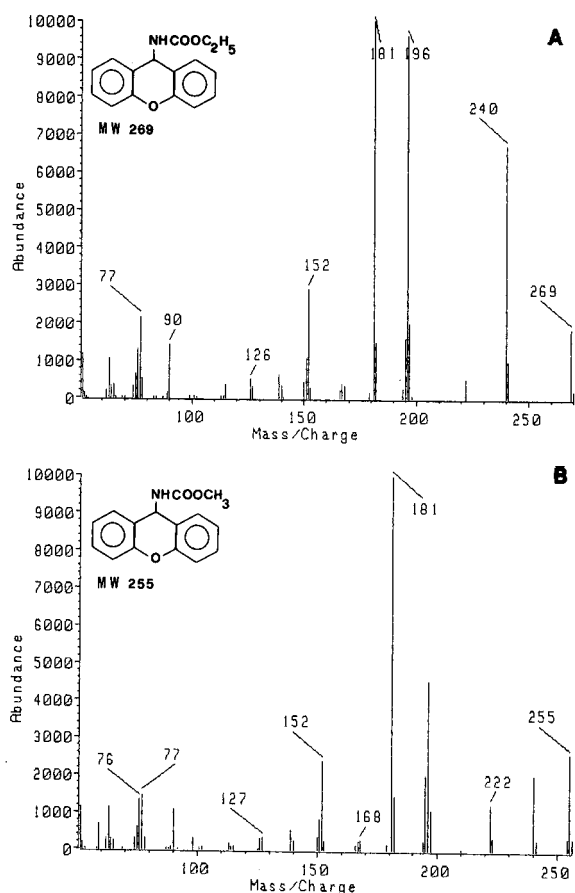


Fig. 2. GC-EI-MS of (A) xanthylurethane and (B) xanthylurethylane. MW = Molecular weight.

The application of such a highly selective reaction and detection method to the determination of urethane in grappa samples provided several advantages. The reaction products are simple to obtain, easily extractable and are more stable at high temperature than the underivatized compounds (urethane, m.p. 48°C; xanthylurethane, m.p. 169°C; urethylane, m.p. 54°C; xanthylurethylane, m.p. 193°C). As a consequence, xanthylamides do not decompose in the injection port and are not adsorbed on active sites such as on a contaminated liner, as could happen with other co-extracted polar compounds. The increased lipophilicity and thermal stability of the two derivatives permit both the use of a short apolar column, which reduces the analysis times, and the selection of a higher temperature

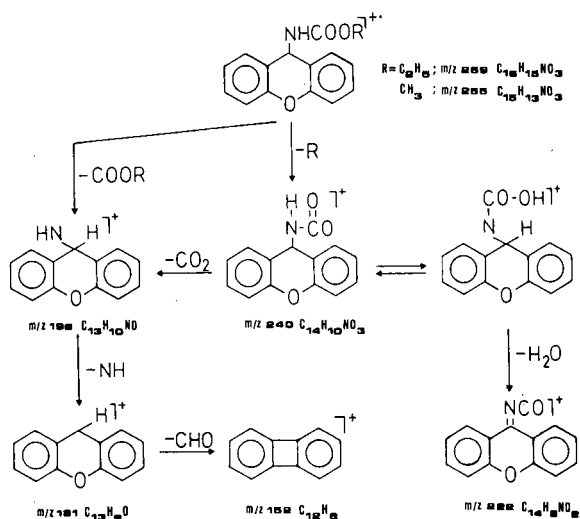


Fig. 3. Proposed fragmentation pattern of the xanthyl derivatives of urethane and urethylane.

to elute the compounds in a relatively free zone of possible interfering peaks.

In the extraction procedure, dichloromethane-ethyl acetate was extremely effective (the absolute recoveries ranged from 85% to 95%) in recovering urethane and urethylane from aqueous ethanol solutions, which could be considered as equivalent to distilled spirit, so that large amounts of solvents were not needed and minimal analytical apparatus was used. In addition, the washing with *n*-pentane was effective in eliminating heavy compounds such as waxes and esters usually present in these samples.

The final results obtained can be exemplified by the chromatograms depicted in Fig. 4, recorded for qualitative evaluations (scan mode), and Fig. 5, effected with SIM mode acquisition for quantitative analysis. The linearity from 10 to 100 and from 100 to 1000 $\mu\text{g/l}$ (Fig. 1) was tested and intra- and inter-assay tests were performed. At the two concentrations chosen (100 and 500 $\mu\text{g/l}$), the intra-assay test, carried out on ten samples analysed in one day, showed average recoveries of 95.4% and 98.6% with relative standard deviations (R.S.D.s) of 12.5% and 4.9%, respectively. Similarly, three samples a day for 10 days were analysed for the inter-assay test, obtaining average recoveries of 94.1% and 103.5% with R.S.D.s of 14.7% and 6.6%, respectively.

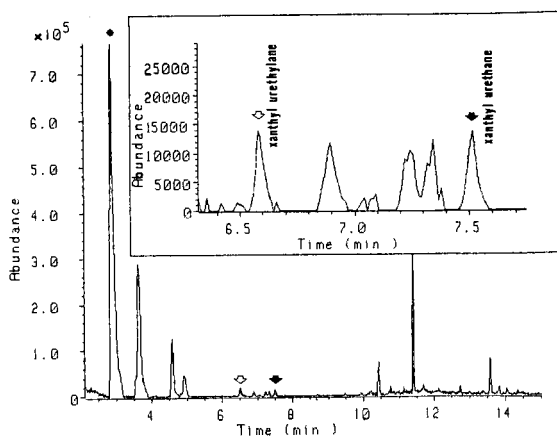


Fig. 4. Total ion current chromatogram (scan mode acquisition) from m/z 50 to 280 for qualitative analysis of an aqua vitae (grappa) sample, extracted, derivatized and further spiked with xanthylamides standard. The peak marked with an asterisk is unreacted xanthidrol.

Concentrations of $\mu\text{g/l}$ were considered presumptive evidence for the presence of urethane, even though the sensitivity could be increased to 1 $\mu\text{g/l}$ when only the m/z 181 ion is considered (signal-to-noise 2:1). Under the above conditions, the urethane concentration found in 20 grappa samples ranged from 70 to 400 $\mu\text{g/l}$. Excluding some samples from batches of home-made grappa, the average value was 87 $\mu\text{g/l}$, which is consistent with the

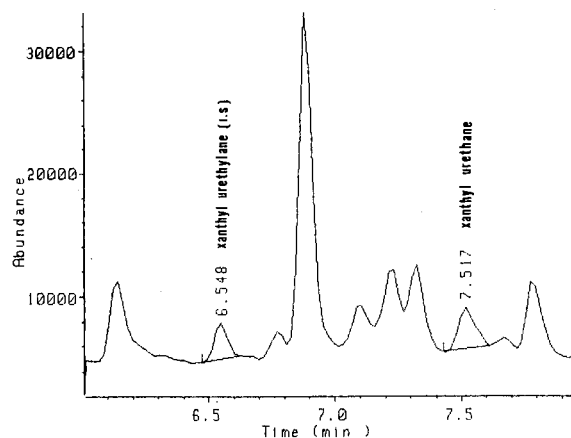


Fig. 5. Typical chromatographic trace (SIM mode acquisition) for the determination of urethane in an aqua vitae (grappa) sample extracted and derivatized. The amount found is 130 $\mu\text{g/l}$.

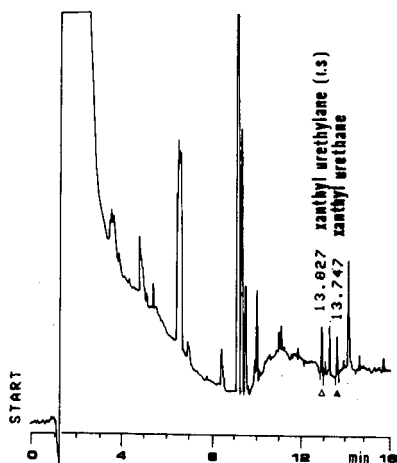


Fig. 6. GC profile of an aqua vitae (grappa) sample, treated as described in the text, with nitrogen-phosphorus detection using a $30\text{ m} \times 0.24\text{ mm}$ I.D. DB 5 fused-silica capillary column (film thickness $0.25\text{ }\mu\text{m}$). The amount of urethane found is $78\text{ }\mu\text{g/l}$.

results obtained by other laboratories (range $7\text{--}360\text{ }\mu\text{g/l}$) with validated GC-MS methods.

The urethane levels found in the home-made batches were higher than those in samples from distillery companies, thus confirming the hypothesis that inadequate temperature control during the distillation process increases urethane formation.

Finally, some standards and analytes were analysed using nitrogen-phosphorus detection (Carlo Erba NPD 40 detector). The sensitivity limit reached, even though higher than that obtained with MS detection, nevertheless made it possible to determine urethane in samples and to obtain comparable results with typical chromatographic profiles such as those depicted in Fig. 6.

ACKNOWLEDGEMENT

The authors are indebted to Dr. Luigi Zerilli, Merrel Dow Research Institute, Lepetit Research Centre, Gerenzano (VA), Italy for his suggestions regarding the mass spectra.

REFERENCES

- 1 J. W. F. K. Barnick, *Chem.-Ing.-Tech.*, 28 (1973) 255.
- 2 C. S. Ough, *J. Agric. Food Chem.*, 24 (1976) 323.
- 3 C. S. Ough, *J. Agric. Food Chem.*, 24 (1976) 328.
- 4 C. S. Ough, *Chem. Eng. News*, 65 (1987) 19.
- 5 S. S. Mirvish, *Adv. Cancer Res.*, 11 (1968) 1.
- 6 F. L. Joe, D. A. Kline, E. M. Mileta, J. A. G. Roach, E. L. Roseboro and T. Fazio, *J. Assoc. Off. Anal. Chem.*, 60 (1977) 509.
- 7 M. J. Dennis and N. Howarth, R. C. Massey, I. Parker, M. Scotter and J. R. Startin, *J. Chromatogr.*, 369 (1986) 193.
- 8 H. B. S. Conacher, B. D. Page, B. P. Y. Lau, J. F. Lawrence, R. Bailey, P. Calway, J. P. Hanchay and B. Mori, *J. Assoc. Off. Anal. Chem.*, 70 (1987) 749.
- 9 T. Cairns, E. G. Siegmund, M. A. Luke and G. M. Doose, *Anal. Chem.*, 59 (1987) 2055.
- 10 B. P. Y. Lau, D. Weber and B. D. Page, *J. Chromatogr.*, 402 (1987) 233.
- 11 G. Gaetano and M. Matta, *Bull. OIV*, 60, No. 671-672 (1987) 36.
- 12 M. G. Dennis, M. C. Massey, M. Pointer and P. Willets, *J. High Resolut. Chromatogr.*, 13 (1990) 247.
- 13 R. Bailey, D. North, D. Myatt and J. F. Lawrence, *J. Chromatogr.*, 369 (1986) 199.
- 14 R. H. M. Van Ingen, L. M. Nijssen, F. Van der Berg and H. Maarse, *J. High Resolut. Chromatogr. Chromatogr. Commun.*, 10 (1987) 151.
- 15 A. I. Vogel, *Practical Organic Chemistry*, Longmans, London, 3rd ed., 1956, Ch. III, p. 405.
- 16 *Canadian Food and Drug Regulations (with Amendments to Dec. 1986)*, Department of National Health and Welfare, Ottawa, 1981, Division 16, Table XIV.

Separation of secondary alcohol enantiomers using supercritical fluid chromatography

Keiji Sakaki and Hirofumi Hirata

National Chemical Laboratory for Industry, Tsukuba, Ibaraki 305 (Japan)

(First received March 11th, 1991; revised manuscript received May 27th, 1991)

ABSTRACT

Secondary alcohol enantiomers were separated using pre-column derivatization with (*R*)-(-)-1-(1-naphthyl)ethyl isocyanate and supercritical fluid chromatography. The chromatographic properties of the derivatized alcohols on three kinds of achiral stationary phases were investigated in this study. The selectivity of the two enantiomers depended on the properties of the stationary phase more than those of the mobile phase. The resolution properties depended on the species of secondary alcohols. The enantiomers of secondary alcohols with a longer carbon chain were better resolved, and the resolution became poor as the hydroxyl group was located towards the center of the carbon chain.

INTRODUCTION

Optical resolution is an important subject in organic chemistry, biochemistry and pharmacology, and various separation methods such as crystallization and chromatography have been used for the purpose. The authors and other researchers have studied the optical resolution of secondary alcohol racemates with the use of enzymatic reactions [1–3]. It was required in those studies to determine the enantiomers quantitatively, and a chromatographic method using supercritical fluids as a mobile phase was used for the analysis.

Supercritical fluid chromatography (SFC) has recently become popular and has been applied to the analysis of various substances such as fatty acids and natural oils [4–6]. The advantages of SFC over liquid chromatography (LC) are lower fluid viscosity and higher efficiencies per unit time [7–9]. Further, SFC is more convenient than LC in operation, because solvent power, an important operational factor, is easily controlled by pressure and temperature of the supercritical fluids.

In this study, secondary alcohol enantiomers were derivatized into diastereomers before they were analyzed by SFC. This paper describes the influence

of operation pressure on the resolution behaviour as well as on the way the secondary alcohol derivatives resolved according to their molecular structures.

EXPERIMENTAL

Apparatus

For SFC, a modular supercritical fluid chromatograph (Jasco, Tokyo, Japan) was used. The operating conditions were as follows: temperature, 313 K; back-pressure, 10–25 MPa; mobile phase, carbon dioxide; flow-rate, 0.15 kg/h. A UV detector (Jasco) with a pressure-resistant cell was used at a wavelength of 275 nm. Three columns were used for SFC: Finepak OH (10 μ m, 250 \times 4.6 mm I.D., Jasco), Cosmosil NH₂ (10 μ m, 150 \times 4.6 mm I.D., Nacalai Tesque, Kyoto, Japan) and Inertsil ODS (5 μ m, 150 \times 4.6 mm I.D., GL Science, Tokyo, Japan). A liquid chromatograph was also used to demonstrate the difference in chromatographic mode. The operating conditions for LC were as follows: mobile phase, cyclohexane containing 0.2% (v/v) ethanol; flow-rate, 30 ml/h; column, Finepak SIL (5 μ m, 250 \times 4.6 mm I.D., Jasco).

Chemicals

The secondary alcohols used were 2-pentanol, 2-hexanol, 3-hexanol, 2-heptanol, 3-heptanol, 2-octanol, 3-octanol, 4-octanol, 2-nonanol, 3-nonanol, 4-nonanol, 2-decanol, 3-decanol, 4-decanol, 5-decanol, 2-undecanol, 3-undecanol, 4-undecanol, 5-undecanol, 2-dodecanol, 4-dodecanol and 5-dodecanol (Tokyo Kasei Kogyo, Tokyo, Japan). All of them were racemates. For a reagent to derivatize secondary alcohol enantiomers into diastereomers, (*R*)-(-)-1-(1-naphthyl)ethyl isocyanate (Aldrich, Milwaukee, WI, USA) was used.

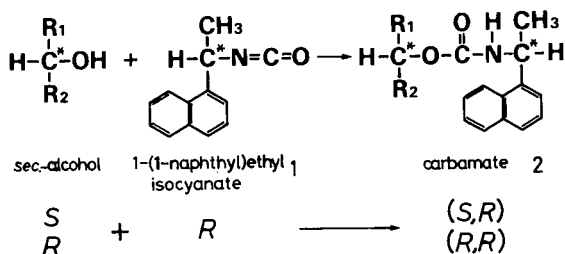


Fig. 1. Derivatization of racemic secondary alcohol with (*R*)-1-(1-naphthyl)ethyl isocyanate. The left-hand and right-hand symbols in parentheses indicate the configurations of the original alcohol and the derivatization reagent, respectively.

Derivatization procedure

The methods for chromatographic separation of optical isomers may be divided into three groups: direct separation on chiral stationary phases, separation with chiral selecting reagents in the mobile phase, and separation of diastereomers formed by pre-column derivatization with chiral reagents [10]. Secondary alcohols have a simple molecular structure, so it is difficult to resolve their enantiomers directly on chiral stationary phases. Therefore, pre-column derivatization methods are often used for their optical resolution [11]. The derivatization procedure was as follows: 30 μ l of derivatizing reagent [10% (w/v) in toluene] were added to a secondary alcohol sample (1 μ l) and the mixture was heated at 363 K for 2–3 h. The reaction scheme is shown in Fig. 1. In this report, this derivatizing reagent and the resulting carbamates are briefly represented as (*R*)-1 and (*S,R*)-2 [or (*R,R*)-2]. The resulting derivatives were injected into the super-

critical fluid chromatograph after being diluted with toluene.

RESULTS AND DISCUSSION

Influence of operation pressure

The chromatograms of 2-octanol racemates derivatized with (*R*)-1 are shown in Fig. 2. Three columns were used for the separation, and the other operating conditions are described in the legend to Fig. 2. The strength of the interaction between an alcohol derivative and the stationary phases was of the order Inertsil ODS < Finepak OH < Cosmosil NH₂. On each stationary phase, the (*S*)-2-octanol derivative [(*S,R*)-2] always eluted faster than the (*R*)-2-octanol derivative [(*R,R*)-2]. For other secondary alcohols, the elution order for the two isomers was also identical. Interestingly, the elution order was reversed when (*S*)-(+)-1-(1-naphthyl)ethyl iso-

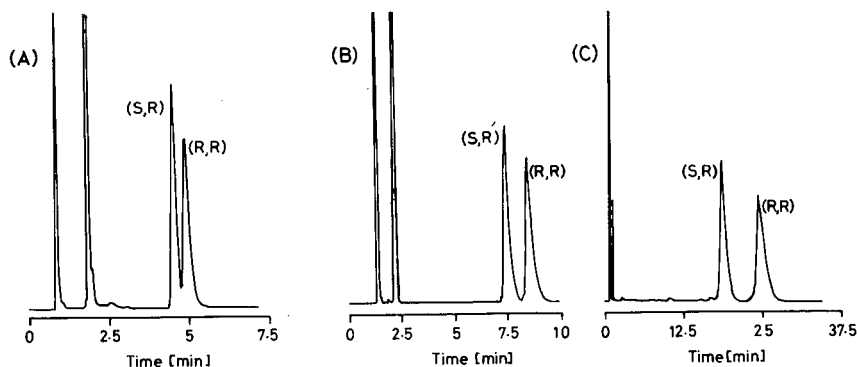


Fig. 2. Chromatographic separation of diastereomeric carbamates derived from racemic 2-octanol on (A) Inertsil ODS, (B) Finepak OH and (C) Cosmosil NH₂. Back-pressure: (A) 10 MPa, (B) 20 MPa and (C) 25 MPa. See Experimental section for other conditions.

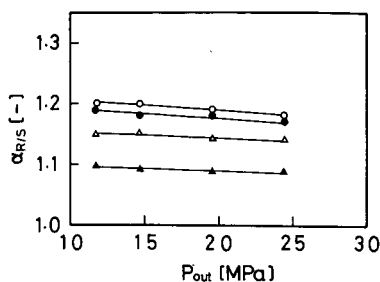


Fig. 3. Dependence of selectivity $\alpha_{R/S}$ of four pairs of diastereomers on back-pressure. A Finepak OH column was used. \circ = 2-Dodecanol; \bullet = 2-decanol; \triangle = 2-heptanol; \blacktriangle = 2-pentanol. See Experimental section for other conditions.

cyanate was used as a derivatizing reagent, although the data were omitted in this report. This is because (*S,S*)-2 and (*R,R*)-2 are enantiomers of each other and show identical retention behavior on an achiral stationary phase.

In this report, selectivity $\alpha_{R/S}$ defined according to eqn. 1 was used as an index for describing the chromatographic resolution.

$$\alpha_{R/S} = k'_R/k'_S \quad (1)$$

where k'_R and k'_S are the capacity factors of (*S,R*)-2 and (*R,R*)-2, respectively. The pressure dependence of $\alpha_{R/S}$ is shown in Fig. 3. The chromatographic conditions are described in the legend to Fig. 3. This figure shows that the selectivity slightly decreased

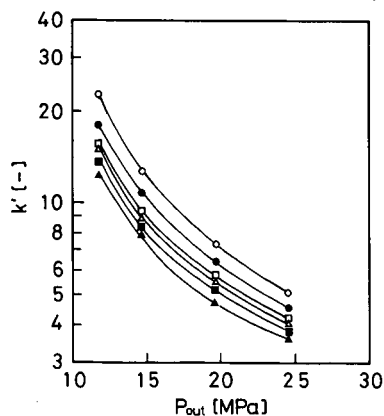


Fig. 4. Dependence of capacity factor of the carbamates derived from (*S*)-secondary alcohols on back-pressure. A Finepak OH column was used. \circ = 2-Dodecanol; \bullet = 2-decanol; \square = 2-octanol; \triangle = 2-heptanol; \blacksquare = 2-hexanol; \blacktriangle = 2-pentanol.

with increasing fluid pressure. This suggests that the stationary phase properties have a greater effect on the selectivity of the two diastereomers than mobile phase conditions. Fig. 4 shows the relation between capacity factor of (*S*)-secondary alcohol derivatives and the operation pressure. The capacity factor decreased with increasing pressure, because the solvent power of the mobile phase increased with the pressure. Figs. 3 and 4 show that the analysis time is easily controlled by regulating the fluid pressure, while the selectivity is hardly affected by the operating pressure.

In addition to selectivity, column efficiency was examined for evaluating the chromatographic separation. The separation ability of a column is often given in terms of the resolution factor R_s , defined by eqn. 2.

$$R_s = 2(t_R - t_S)/(W_R + W_S) \quad (2)$$

where t_R and t_S are retention times of (*R,R*)-2 and (*S,R*)-2, respectively, and W_R and W_S are band widths. If the bands show Gaussian distribution in shape, eqn. 2 can be rewritten as follows:

$$R_s = 1/4 \cdot N^{1/2}[(\alpha_{R/S} - 1)/\alpha_{R/S}][k'_R/(k'_R + 1)] \quad (3)$$

where N is the theoretical plate number of the column used. The resolution factor between (*R,R*)-2 and (*S,R*)-2 decreased with increasing carbon dioxide pressure, as shown in Fig. 5. The theoretical plate number showed a constant value, about 4500 for a Finepak OH column, in the range 12–25 MPa.

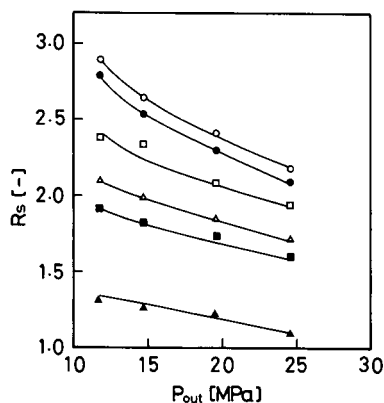


Fig. 5. Dependence of resolution factor R_s of six pairs of diastereomers on back-pressure. A Finepak OH column was used. For symbols see Fig. 4.

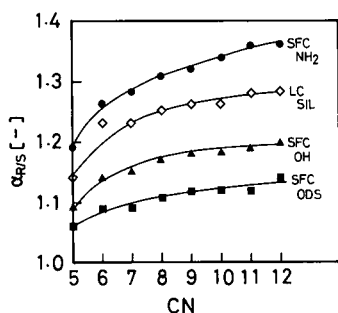


Fig. 6. Relation between selectivity $\alpha_{R/S}$ and carbon number of 2-alkanols. Back-pressures for SFC were 15 MPa for Cosmosil NH_2 and Finepak OH, and 10 MPa for Inertsil ODS. Operating conditions for SFC and LC are shown in the Experimental section.

This suggests that the decrease of R_s is due to decreases of both retention time and selectivity.

Selectivity and resolution factor of secondary alcohols enantiomers

2-Alkanol diastereomers derivatized with (*R*)-1 were separated by both SFC and LC. The relation between the selectivity $\alpha_{R/S}$ and the carbon number of the alcohols is shown in Fig. 6. On every column, the selectivity increased with the carbon number,

with the curves gradually levelling off. A similar tendency was observed for LC.

Fig. 7 shows the chromatograms of diastereomers derived from racemic 2-, 3-, 4- and 5-decanols. The bands of (*R,R*)-2 and (*S,R*)-2 came closer together as the hydroxyl group became located towards the center of the carbon chain in the original alcohol, and the bands of two diastereomers derivatized from racemic 5-decanol finally overlapped. Similar behavior was observed on other columns. Fig. 8 shows the effect of the position of the hydroxyl group on the selectivity, $\alpha_{R/S}$. On each column, the selectivity decreased as the hydroxyl group approached the center of the alcohol. This shows that the structural difference between two diastereomers becomes minor as the structures of original alcohols become symmetric. Fig. 6 also suggests that the selectivity depends on the deviation of the hydroxyl group from the center of a carbon chain.

Fig. 9 shows the relation between the capacity factor of the diastereomers and the position of hydroxyl group in the alcohols. While the capacity factor of (*S,R*)-2 scarcely varied with the position of hydroxyl group, that of (*R,R*)-2 decreased as the hydroxyl group moved toward the center of the alcohol. This means that the structural variation

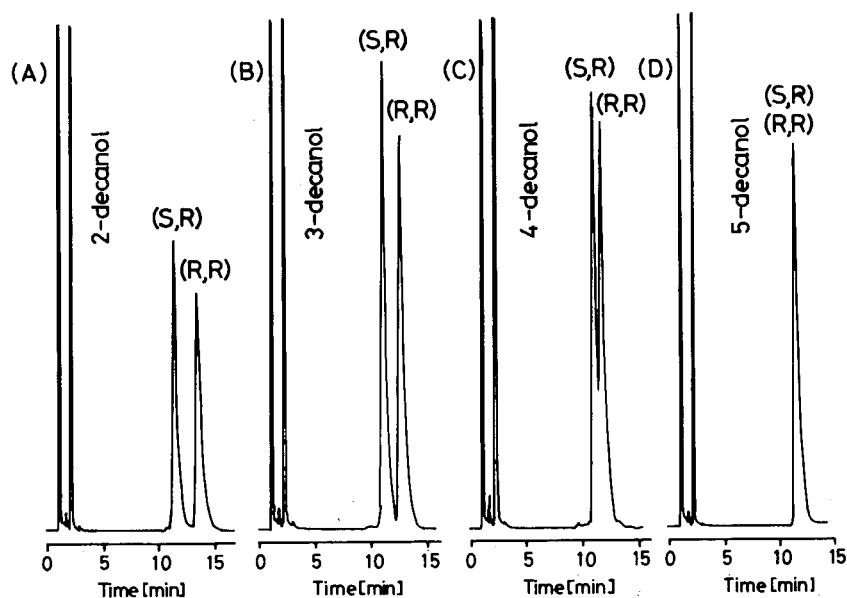


Fig. 7. Chromatographic separation of diastereomers derived from racemic (A) 2-decanol, (B) 3-decanol, (C) 4-decanol, and (D) 5-decanol. A Finepak OH column was used at 15 MPa of back-pressure.

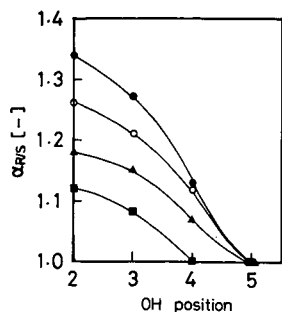


Fig. 8. Variation of selectivity, $\alpha_{R/S}$, versus the position of hydroxyl group of secondary decanols. ● = SFC NH₂; ○ = LC SIL; ▲ = SFC OH; ■ = SFC ODS. See Fig. 6 for operating conditions.

accompanying hydroxyl group position is larger in (*R,R*)-2 than in (*S,R*)-2. For reference, a stereochemical formula of the secondary alcohol derivative is shown in Fig. 10. Figs. 9 and 10 lead to the following suggestion: so long as R_1 is longer than R_2 (where $R_1 + R_2$ is constant), the interaction between a diastereomer and a stationary phase is affected by the difference in carbon chain length between R_1 and R_2 .

Selectivity relates the free energy difference as represented by eqn. 4.

$$\ln \alpha_{R/S} = -(\Delta G_R^\circ - \Delta G_S^\circ)/RT \quad (4)$$

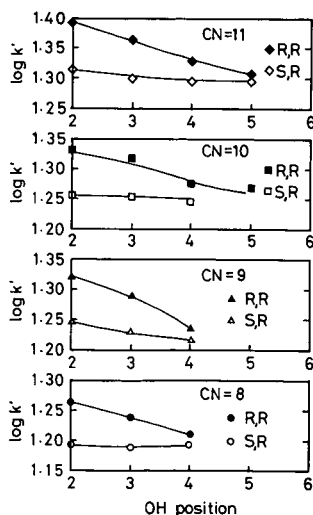


Fig. 9. Retention behavior of diastereomers, (*R,S*)-2 and (*R,R*)-2, with respect to the position of hydroxyl group in secondary alcohols. A Finepak OH column was used at 12 MPa of back-pressure. See Experimental section for operating conditions.

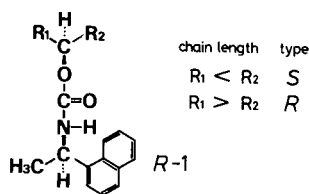


Fig. 10. Structure of the carbamate derived from secondary alcohol and (*R*)-1-(1-naphthyl)ethyl isocyanate.

where ΔG_R° and ΔG_S° are free energy changes and they are related to partition coefficients of (*R,R*)-2 and (*S,R*)-2, respectively. The free energy difference, $-(\Delta G_R^\circ - \Delta G_S^\circ)$, of each stationary phase is listed in Table I. The resolution factor between two dia-

TABLE I

$-(\Delta G_R^\circ - \Delta G_S^\circ)$ VALUES (kJ/mol) FOR 2-, 3-, 4- AND 5-DECANOL DERIVATIVES ON THREE KINDS OF COLUMNS

See Experimental section for operating conditions. Column 1 = Inertsil ODS, back-pressure 10 MPa; column 2 = Finepak OH, back-pressure 15 MPa; column 3 = Cosmosil NH₂, back-pressure 15 MPa.

Original alcohol	$-(\Delta G_R^\circ - \Delta G_S^\circ)$ (kJ/mol)		
	Column 1	Column 2	Column 3
2-Decanol	0.32	0.43	0.76
3-Decanol	0.20	0.36	0.62
4-Decanol	0	0.18	0.32
5-Decanol	0	0	0

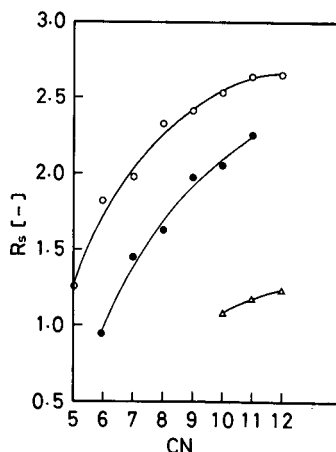


Fig. 11. Relation between resolution factor and carbon number of secondary alcohols. A Finepak OH column was used at 15 MPa of back-pressure. Position of hydroxyl group: ○ = C-2; ● = C-3; △ = C-4. See Experimental section for operating conditions.

stereomers was plotted as a function of the carbon number of the alcohols (Fig. 11), and the position of the hydroxyl group was used as another parameter. The resolution factor increased with the carbon number, because the selectivity increased with the carbon number, as already mentioned above. The resolution factor of 4-alkanol is smaller than those of 2- and 3-alkanols, since its selectivity is also smaller, as shown in Fig. 8. From the above findings, it is concluded that the separation behavior of racemic alcohols derivatized with (*R*)-1 depends on carbon number and the position of the hydroxyl group of the original alcohols.

CONCLUSION

Secondary alcohol enantiomers were derivatized with (*R*)-(-)-1-(1-naphthyl)ethyl isocyanate and the resulting diastereomers were separated by SFC on achiral stationary phases. The selectivity of the two diastereomers was more affected by the properties of the stationary phases than by those of the supercritical carbon dioxide used as a mobile phase. Both selectivity and resolution factor increased with the carbon number of the secondary alcohol enantiomers, while both decreased as the hydroxyl group of the original alcohols became situated more to-

wards the center of the molecules. The results mean that the configuration of various atomic groups in the diastereomers is significant in the interaction between a solute and a stationary phase.

ACKNOWLEDGEMENT

The authors thank Mr. Isao Iida for his technical support.

REFERENCES

- 1 H. Hirata, K. Higuchi and T. Yamashina, *J. Biotechnol.*, 14 (1990) 157.
- 2 H. Hirata, *J. Jpn. Oil Chem. Soc. (Yukagaku)*, 39 (1990) 1003.
- 3 B. Cambou and A. M. Klibanov, *J. Am. Chem. Soc.*, 106 (1984) 2687.
- 4 A. Nomura, J. Yamada, K. Tsunoda, K. Sakaki and T. Yokochi, *Anal. Chem.*, 61 (1989) 2076.
- 5 Y. Yamauchi and M. Saito, *J. Chromatogr.*, 505 (1990) 237.
- 6 M. Saito and Y. Yamauchi, *J. Chromatogr.*, 505 (1990) 257.
- 7 P. A. Peadar and M. L. Lee, *J. Liq. Chromatogr.*, 5 (1982) 179.
- 8 T. L. Chester, *J. Chromatogr. Sci.*, 24 (1986) 226.
- 9 H. Engelhardt, A. Gross, R. Mertens and M. Petersen, *J. Chromatogr.*, 477 (1989) 169.
- 10 P. Macaudiere, M. Caude, R. Rosset and A. Tambute, *J. Chromatogr. Sci.*, 27 (1989) 383, 583.
- 11 W. H. Pickle and M. S. Hoekstra, *J. Org. Chem.*, 39 (1974) 3904.

Determination of some drugs by micellar electrokinetic capillary chromatography

The pseudo-effective mobility as parameter for screening

M. T. Ackermans*, F. M. Everaerts and J. L. Beckers

Laboratory of Instrumental Analysis, Eindhoven University of Technology, P.O. Box 513, 5600 MB Eindhoven (Netherlands)

(First received March 13th, 1991; revised manuscript received May 24th, 1991)

ABSTRACT

In contrast to capillary zone electrophoresis, micellar electrokinetic capillary chromatography can be applied to the determination of compounds that are uncharged and almost insoluble in water. As a screening parameter, the pseudo-effective mobility is to be preferred to the capacity factor k' because it can be calculated if t_{MC} is unknown, and because it gives a better indication of whether components can be separated or not. Special attention should be paid, however, to the composition of the sample solution. The use of organic solvents to dissolve the sample can influence the separation enormously. Calibration graphs were constructed for some drugs and as an example dapsone in tablets was determined.

INTRODUCTION

Since the introduction of micellar electrokinetic capillary chromatography (MECC) by Terabe and co-workers [1,2], it has proved to be a highly efficient separation method. Amongst others, many compounds of pharmaceutical interest have been separated by MECC, such as vitamins, cephalosporins, penicillins, antipyretic and analgesic preparations, barbiturates and optical isomers of drugs [3-9]. Most papers, however, only present qualitative data and little attention has been paid to quantitative aspects or screening possibilities.

In classical capillary zone electrophoresis with aqueous electrolyte systems, components can only be separated if they are charged and soluble in water. In MECC, however, uncharged compounds and, because of the hydrophobic character of the micelles, compounds that are almost insoluble in water can also be separated.

In this work, we studied the applicability of

MECC to the qualitative and quantitative separation of some drugs that are uncharged and almost insoluble in water. Further, the advantage of the use of "pseudo-effective mobility" as a parameter for screening over the use of capacity factors (k') and the effect of methanol in the sample were examined.

THEORETICAL

MECC is a separation technique based on the partitioning of the components over two phases, just as in chromatographic techniques. However, two mobile phases are used, *viz.*, an electroosmotically pumped aqueous mobile phase and the hydrophobic interior of micelles. Often an analogue of the capacity factor, k' , is used, which can be calculated according to the equation [1,2]

$$k' = \frac{n_{MC}}{n_w} = \frac{t_S - t_{EOF}}{t_{EOF} \left(1 - \frac{t_S}{t_{MC}}\right)} \quad (1)$$

where n_{MC} and n_w are the total moles of solute in the micelles and in the aqueous phase, respectively, and t_s , t_{EOF} and t_{MC} are the migration times of the solute, an appropriate marker (insolubilized component) for the determination of the electroosmotic flow (EOF) and the micelles, respectively.

Application of this concept of k' in MECC shows that for higher values of k' very low values of the resolution, R_s [2], result. Further, a slight inaccuracy in the determination of t_s leads to a large difference in the calculated k' value, especially for t_s values near the t_{MC} . This means that the use of k' values for screening purposes is limited whereas the suggestion that a large difference between higher values of k' leads to a separation is false.

Moreover, the EOF can change with time and therefore the t_{EOF} and the t_{MC} have to be measured in each experiment in order to calculate the appropriate k' . The t_{MC} can be obtained by applying a micelle (MC) marker such as Sudan III or anthracene [2,10] or by methods such as extrapolation with iteration or frontal analysis [11]. However, especially when organic co-solvents are used, it is still a subject of discussion how to obtain the "true t_{MC} ". If the velocity of the micelles is small or even negative, t_{MC} cannot be measured and, according to eqn. 1, k' can not be calculated, even when the components show normal migration behaviour. For all these reasons k' is often not suitable for use in MECC.

Another way to describe the migration behaviour of components in MECC is in terms of mobilities [12]. The velocity of the aqueous mobile phase is determined by the mobility of the EOF, m_{EOF} , and that of the micelles by the apparent mobility of the micelles, $m_{app,MC}$, defined as

$$m_{app,MC} = m_{eff,MC} + m_{EOF} \quad (2)$$

where $m_{eff,MC}$ is the effective mobility of the micelles. The mobilities are negative for anions and positive for cations. For ionic species m_{eff} can be obtained from the mobility at infinite dilution, correcting for relaxation and retardation effects according to the Debye-Hückel-Onsager theory. For micelles, $m_{eff,MC}$ will also be strongly dependent on the composition of the micellar phase.

For a given surfactant concentration in a specific electrolyte system, a constant composition of the micellar phase can be expected, through which the effective mobility of the micelles and the k' for the

components must be constant.

In CZE the effective mobility can be used as a parameter for screening [13]. In MECC often uncharged particles with no electrophoretic mobility are analysed. As they are solubilized in the charged micelles for $k'/(k'+1)$ part of the time, they will acquire a net velocity of

$$v_s = \frac{k'}{1+k'} \cdot v_{MC} + \frac{1}{1+k'} \cdot v_{EOF} \quad (3)$$

or

$$v_s = \frac{k'}{1+k'} (m_{eff,MC} + m_{EOF}) E + \frac{1}{1+k'} \cdot m_{EOF} E \quad (4)$$

or

$$v_s = \left(\frac{k'}{1+k'} \cdot m_{eff,MC} + m_{EOF} \right) E \quad (5)$$

where v_s , v_{MC} and v_{EOF} are the velocities of the solubilized sample component, the micelle marker and the EOF marker, respectively.

From eqn. 5, it is clear that for uncharged particles pseudo-mobilities can be defined, similar to the mobilities of charged particles, satisfying the conditions

$$v_s = m_{app,S}^{ps} E \quad (6)$$

with

$$m_{app,S}^{ps} = m_{eff,S}^{ps} + m_{EOF} \quad (7)$$

and

$$m_{eff,S}^{ps} = \frac{k'}{1+k'} \cdot m_{eff,MC} \quad (8)$$

A great advantage of working with pseudo-effective mobilities compared with k' is that for the calculation of the pseudo-effective mobilities t_{MC} or $m_{eff,MC}$ is not required, as can be seen from the equation

$$m_{eff,S}^{ps} = m_{app,S}^{ps} - m_{EOF} = \frac{l_c l_d}{V t_s} - \frac{l_c l_d}{V t_{EOF}} \quad (9)$$

where l_c and l_d are the total length of the capillary and the length of the capillary from injection to detection, respectively, and V is the applied voltage.

To demonstrate the effect of a small inaccuracy in the determination of migration times on k' and pseudo-effective mobilities, we calculated the values of k' and $m_{eff,S}^{ps}$ for several values of t_{EOF} , t_s and t_{MC}

with an accuracy in the determination of the t_s of 0.5%. In Table I all calculated values are given.

From Table I, it can be concluded that especially for t_s values near the t_{MC} values a dramatic change in k' results, whereas the pseudo-effective mobilities are nearly constant for small differences in t_s .

EXPERIMENTAL

Instrumentation

For all experiments the P/ACE System 2000 HPCE instrument (Beckman, Palo Alto, CA, USA) was used. All experiments were carried out in a fused-silica capillary from Polymicro Technologies (Phoenix, AZ, USA), 50 μm I.D., total length 27.65 cm, distance between injection and detection 20.85 cm. The capillary was treated with 10 M hydrochloric acid for 5 h at 160°C in order to obtain a high m_{EOF} . The wavelength of the UV detector was 214 nm. All experiments were carried out applying a constant voltage of 10 kV with the anode at the inlet and the cathode at the outlet side. Data analysis was performed using the laboratory-written data analysis program CAESAR.

Separation conditions

For all analyses an electrolyte system of 0.02 M tris(hydroxymethyl)aminomethane (Tris) with 100 mM sodium dodecyl sulphate (SDS) at pH 8.5 adjusted by adding boric acid was used. It must be noted however, that owing to difficulties in preparing reproducible electrolyte compositions, differences can occur in k' or $m_{\text{eff},s}^{\text{ps}}$ using different batches. In all experiments the sample was introduced by pressure injection for 5 s.

If the capillary tube is filled with a solution of SDS, the UV signal of a solution of 0.001 M mesityl oxide in SDS introduced by pressure injection can be observed after 192 s. This means that with a separation volume of about 410 nl, the volume injected with a 5-s pressure injection is about 11 nl. Although the minimum injection time with our apparatus is 1 s, we chose a pressure injection time of 5 s for the sake of reproducibility.

Chemicals

All drugs were kindly donated by the State Institute for Quality Control for Agricultural Products (RIKILT, Wageningen, Netherlands). Dapsone

tablets (OPGFarma 89c08-90067) were obtained at a local pharmacy.

RESULTS AND DISCUSSION

In order to study the applicability of MECC to the analysis of water-insoluble components we selected eight drugs, the structural formulae of which are given in Fig. 1.

For the preparation of a sample mixture, water cannot be used as solvent and therefore we first studied the effect of the presence of methanol in a sample on the separation.

Effect of the presence of methanol in the sample

In order to study the effect of methanol in the sample on t_{EOF} and t_{MC} , we prepared three sample solutions of creatinine (which proved to be uncharged and an insolubilized component in this electrolyte system) and Sudan III in 100 mM SDS solution and added methanol to concentrations of 0, 10 and 20%. Three separations were carried out, injecting twice in each separation. The first injection was the sample (a) without, (b) with 10% and (c) with 20% methanol. After a separation for 3 min at 10 kV we injected the sample mixture without methanol in all three instances, whereafter the separation was completed. The three electropherograms are shown in Fig. 2.

As can be seen in Fig. 2a, the time differences between t_{EOF} and t_{MC} of the first injection (t_1) and that of the second injection (t_2) are equal. By the addition of only 10% methanol to the sample in the first injection (case b), t_1 decreases whereas t_2 is nearly constant, and in case c a strong decreasing effect on t_1 can be seen at constant t_2 .

The fact that the time intervals between the two t_{EOF} values are nearly constant in all instances means that by the addition of methanol to a sample the velocity of the EOF is not influenced. The sample components, however, show a different migration behaviour. They tend to remain in the methanol plug (EOF) for a longer time, resulting in shorter migration times, owing to a strong solubility effect and a local breakdown of the micelles. The results of this effect on the efficiency of the separations are demonstrated in Fig. 3, where the electropherograms are given for the separation of a mixture of phenol, *p*-cresol and 2,6-xyleneol (all at 10^{-4} M , in all

TABLE I

CALCULATED CAPACITY FACTORS, k' , AND PSEUDO-EFFECTIVE MOBILITIES, $10^5 m_{\text{eff},S}^{\text{ps}}$ ($\text{cm}^2/\text{V}\cdot\text{s}$) FOR SEVERAL VALUES OF THE MIGRATION TIMES (min) FOR THE EOF MARKER, t_{EOF} , A SAMPLE COMPONENT, t_s , AND THE MC MARKER, t_{MC}

The accuracy in the determination of t_s is taken as 0.5% ($l_c = 27$ cm, $l_d = 20$ cm, applied voltage 10 kV).

Fixed values	t_s	k'			$m_{\text{eff},S}^{\text{ps}}$		
		$t_s - 0.5\%$	t_s	$t_s + 0.5\%$	$t_s - 0.5\%$	t_s	$t_s + 0.5\%$
$t_{\text{EOF}} = 2$ min; $t_{\text{MC}} = 10$ min	8.00	14.61	15.00	15.41	-33.69	-33.75	-33.81
	8.50	20.93	21.67	22.44	-34.36	-34.41	-34.46
	9.00	33.28	35.00	36.88	-34.95	-35.00	-35.05
	9.30	48.58	52.14	56.21	-35.27	-35.32	-35.37
	9.50	68.06	75.00	83.40	-35.48	-35.53	-35.67
	9.80	155.64	195.00	259.00	-35.77	-35.82	-35.86
	9.90	262.56	395.00	787.08	-35.86	-35.91	-35.95
$t_{\text{EOF}} = 10$ min; $t_{\text{MC}} = 20$ min	11.0	0.21	0.22	0.24	-0.78	-0.82	-0.86
	12.0	0.48	0.50	0.52	-1.46	-1.50	-1.54
	13.0	0.83	0.86	0.88	-2.04	-2.08	-2.11
	14.0	1.29	1.33	1.37	-2.54	-2.57	-2.60
	15.0	1.94	2.00	2.06	-2.97	-3.00	-3.03
	16.0	2.90	3.00	3.10	-3.35	-3.38	-3.40
	17.0	4.48	4.67	4.86	-3.68	-3.71	-3.73
	18.0	7.57	8.00	8.47	-3.97	-4.00	-4.02
	19.0	16.26	18.00	20.10	-4.24	-4.26	-4.29
19.5	31.47	38.00	47.69	-4.36	-4.38	-4.41	
$t_{\text{EOF}} = 10$ min; $t_{\text{MC}} = 50$ min	20.0	1.64	1.67	1.69	-4.48	-4.50	-4.52
	25.0	2.96	3.00	3.04	-5.38	-5.40	-5.42
	30.0	4.93	5.00	5.08	-5.98	-6.00	-6.01
	35.0	8.18	8.33	8.49	-6.42	-6.43	-6.44
	40.0	14.61	15.00	15.41	-6.74	-6.75	-6.76
	45.0	33.28	35.00	36.88	-6.99	-7.00	-7.01
	46.0	42.28	45.00	48.05	-7.03	-7.04	-7.05
	47.0	56.82	61.67	67.33	-7.08	-7.09	-7.09
	48.0	84.29	95.00	108.64	-7.12	-7.13	-7.13
	49.0	155.64	195.00	259.90	-7.15	-7.16	-7.17

sample solutions) with the MC marker Sudan III, with an increasing percentage of methanol in the sample.

It can be clearly seen that, although t_{EOF} (methanol) is nearly constant in all electropherograms, the migration times of all components strongly decrease and the separation efficiency declines dramatically. The addition of methanol to sample solutions for solvation effects or as an EOF marker generally must be avoided, as it can greatly affect the separation, as shown before. A better way to dissolve water-insoluble components is to use an SDS solution.

In Table II, the calculated values for k' according to eqn. 1 are given for the components of the sample used for the electropherograms in Fig. 3 (up to 70% methanol). It is clear that the k' values depend strongly on the presence of methanol in the sample. In Table III the average k' values (standard deviation) from ten experiments are given for a sample of eight drugs dissolved in SDS without methanol and containing 20% methanol. Although the k' values are affected by the presence of methanol in the sample, the repeatability is fairly good at a given methanol concentration, hence the k' values can be monitored for screening purposes by this means.

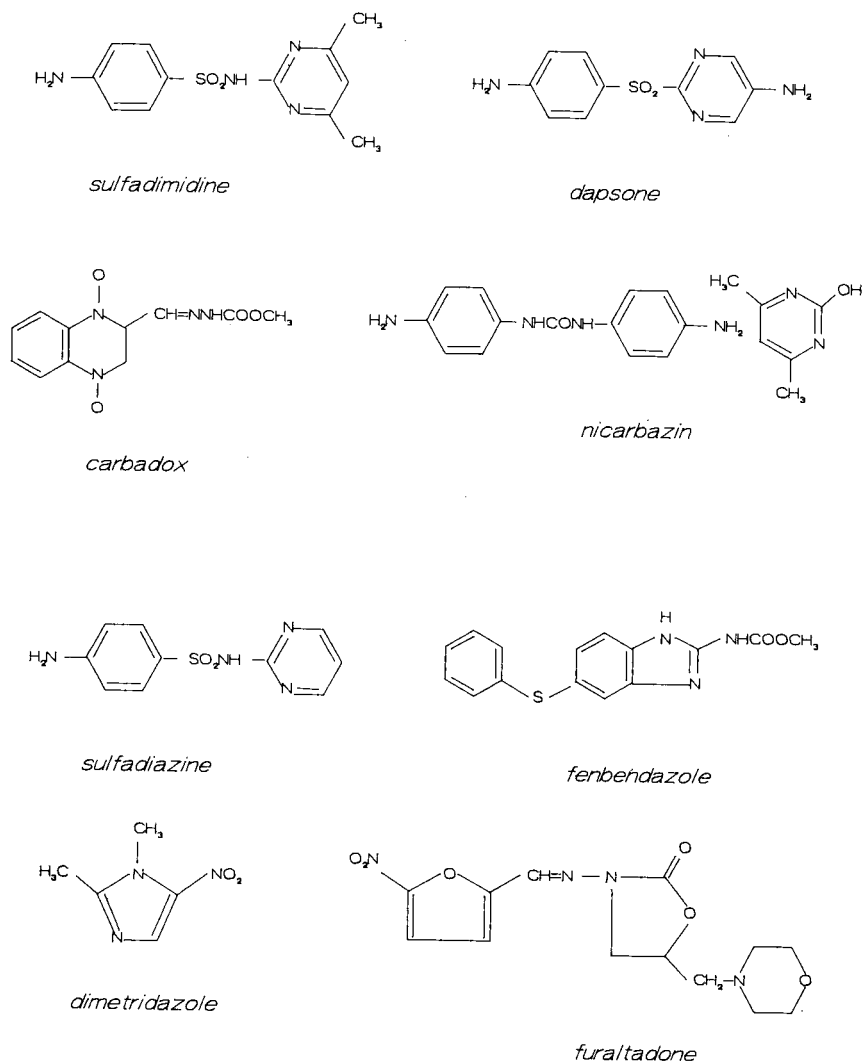


Fig. 1. Structural formulae of drugs insoluble in water (nicarbazin is a 1:1 mixture of the two given components).

k' values versus pseudo-effective mobilities

In the theoretical part we discussed some advantages in the use of the $m_{\text{eff},S}^{\text{ps}}$ over k' . The most important advantage was that $m_{\text{eff},S}^{\text{ps}}$ can also be calculated if t_{MC} values are unknown. To demonstrate this advantage we carried out eight experiments with a sample mixture of the eight drugs for different m_{EOF} varying between $50 \cdot 10^{-5}$ and $40 \cdot 10^{-5} \text{ cm}^2/\text{V} \cdot \text{s}$. In order to change the m_{EOF} , the capillary was rinsed extensively with 1 M HCl

and/or KOH, followed by a rinsing step with distilled water. Fenbendazole was used as an MC marker. In Table IV the average calculated values with standard deviations of k' and $m_{\text{eff},S}^{\text{ps}}$ are given for the five experiments in which t_{MC} could be measured (high EOF) and three experiments (low EOF) without a t_{MC} . The $m_{\text{eff},S}^{\text{ps}}$ values obtained from both series of experiments agree, whereas in the latter instance no k' values could be calculated.

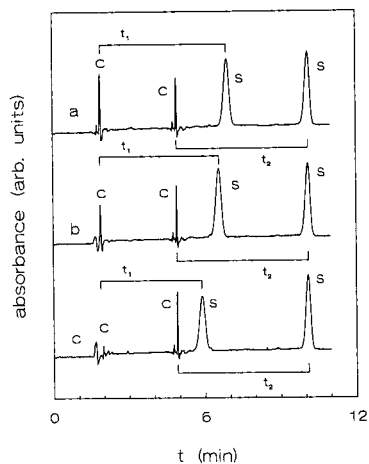


Fig. 2. Electropherograms for the determination of creatinine (C) and Sudan III (S) with and without methanol in the sample. In each experiment two injections were made, the first injection (a) without, (b) with 10% and (c) with 20% methanol in the sample and the second injection without methanol in the sample in all instances. A separation step for 3 min at 10 kV was performed between the two injections. In all instances the sample contained 0.15 mg/ml of creatinine and 0.035 mg/ml of Sudan III and the injection volume was about 11 nl. For further explanation, see text.

Quantitative analysis

To study the quantitative possibilities of MECC, experiments were carried out with a sample mixture consisting of 0.30 mg/ml of nicarbazin, dimetridazole, carbadox and furaltadone, 0.15 mg/ml of

TABLE II

CALCULATED CAPACITY FACTORS, k' , FOR PHENOL, *p*-CRESOL AND 2,6-XYLENOL FOR SAMPLES WITH INCREASING AMOUNTS OF METHANOL IN THE SAMPLE

$$k'_{\text{CH}_3\text{OH}} = 0; k'_{\text{Sudan III}} = \infty.$$

Methanol (%)	k'		
	Phenol	<i>p</i> -Cresol	2,6-Xylenol
10	0.98	2.59	4.72
20	0.92	2.43	4.38
30	0.85	2.20	4.06
40	0.81	2.05	3.76
50	0.77	1.85	3.46
60	0.78	1.72	3.14
70	0.79	1.60	2.98

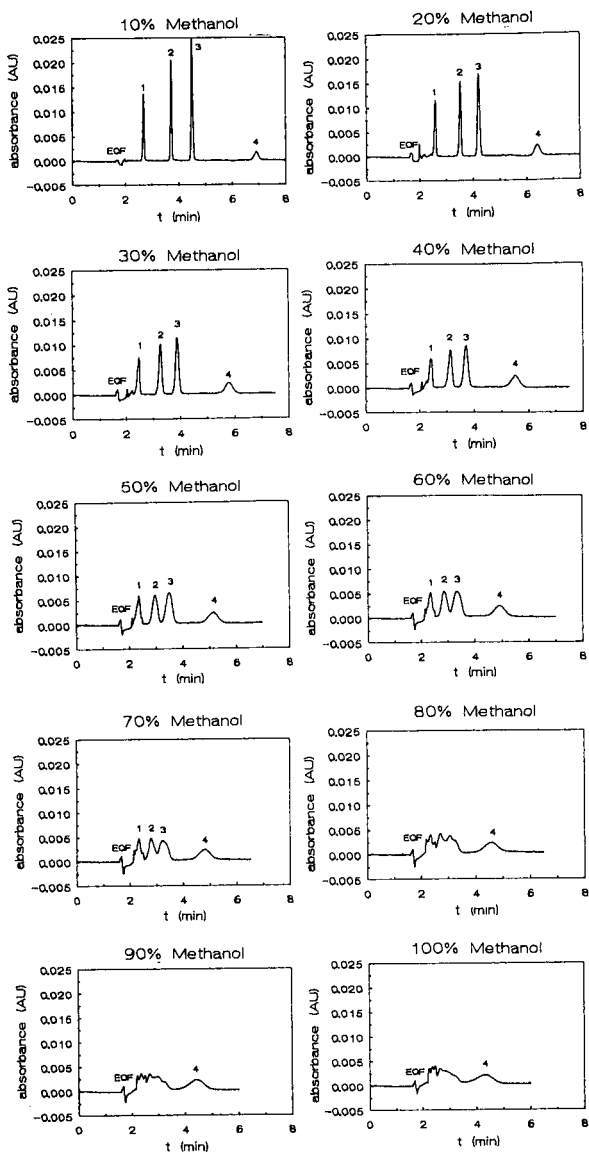


Fig. 3. Electropherograms for the separation of (1) phenol, (2) *p*-cresol, (3) 2,6-xylenol and (4) Sudan III with increasing amounts of methanol in the sample. The concentration of all sample components was 0.0001 M and the injection volume was about 11 nl.

sulphadimidine, sulphadiazine and dapsone and 0.030 mg/ml of fenbendazole dissolved in a 100 mM SDS solution. This sample was diluted 1.2-, 1.5-, 2-, 3-, 6- and 10-fold. All these dilutions were measured

TABLE III

AVERAGE VALUES OF THE CAPACITY FACTORS, k' , FOR THE SAMPLE COMPONENTS WITH STANDARD DEVIATIONS (IN PARENTHESES) FOR TEN EXPERIMENTS

Component	k'	
	Without methanol	With 20% methanol
Nicarbazin	0.375 (0.002)	0.398 (0.037)
Dimetridazole	0.565 (0.004)	0.563 (0.007)
Sulphadimidine	0.852 (0.005)	0.797 (0.009)
Sulphadiazine	1.833 (0.025)	1.570 (0.026)
Carbadox	2.137 (0.012)	1.905 (0.023)
Furaltadone	3.061 (0.012)	2.787 (0.023)
Dapsone	5.378 (0.018)	4.754 (0.038)
Fenbendazole	∞ -	∞ -

TABLE IV

AVERAGE CALCULATED VALUES WITH STANDARD DEVIATIONS (IN PARENTHESES) FOR k' AND $10^5 m_{\text{eff},S}^{\text{ps}}$ ($\text{cm}^2/\text{V} \cdot \text{s}$) FOR EIGHT DRUGS IN EXPERIMENTS WITH VARYING m_{EOF}

Compound	k' ($n = 5$)	$m_{\text{eff},S}^{\text{ps}}$ ($n = 5$)	$m_{\text{eff},S}^{\text{ps}}$ ($n = 3$)
EOF	0	45.71 (2.87)	41.13 (0.47)
Nicarbazin	0.271 (0.005)	- 8.06 (0.20)	- 8.25 (0.04)
Dimetridazole	0.447 (0.006)	-11.68 (0.24)	-11.94 (0.07)
Sulphadimidine	0.714 (0.004)	-15.75 (0.22)	-16.09 (0.03)
Sulphadiazine	1.615 (0.052)	-23.35 (0.56)	-22.72 (1.11)
Carbadox	1.890 (0.031)	-24.73 (0.42)	-24.60 (0.70)
Furaltadone	2.756 (0.021)	-27.75 (0.36)	-28.10 (0.03)
Dapsone	4.875 (0.070)	-31.38 (0.43)	-31.81 (0.04)
Fenbendazole	∞	-37.81 (0.44)	

TABLE V

AVERAGE MIGRATION TIME, t (min), $10^5 m_{\text{eff},S}^{\text{ps}}$ ($\text{cm}^2/\text{V} \cdot \text{s}$), SLOPE AND INTERCEPT (ARBITRARY UNITS) AND CORRELATION COEFFICIENT OF CALIBRATION GRAPHS FOR THE DIFFERENT SAMPLE COMPONENTS WITH STANDARD DEVIATIONS IN PARENTHESES

Compound	t	$m_{\text{eff},S}^{\text{ps}}$	Slope	Intercept	Correlation coefficient
Nicarbazin	2.57 (0.020)	-11.73 (0.096)	78.96	-0.40	0.999
Dimetridazole	2.86 (0.026)	-15.48 (0.078)	123.70	-0.63	0.999
Sulphadimidine	3.17 (0.043)	-18.71 (0.194)	133.85	-1.43	0.998
Sulphadiazine	4.37 (0.058)	-27.03 (0.196)	195.33	-0.24	0.999
Carbadox	4.64 (0.065)	-28.33 (0.130)	92.43	-1.36	0.997
Furaltadone	5.36 (0.081)	-31.10 (0.125)	119.19	-1.50	0.999
Dapsone	6.66 (0.127)	-34.69 (0.141)	429.19	-2.54	0.999
Fenbendazole	11.30 (0.342)	-40.60 (0.137)	258.87	-2.62	0.997

three times and using the measured peak areas calibration graphs were constructed. In Table V all measured migration times and calculated $m_{\text{eff},s}^{\text{ps}}$ values for the components, the slopes, intercepts and the correlation coefficients of the calibration graphs are given, with standard deviations. From Table V it can be concluded that linear calibration graphs (nearly passing through the origin) are obtained. In Fig. 4 the calibration graphs obtained by applying the average values of the three experiments for all dilutions are shown.

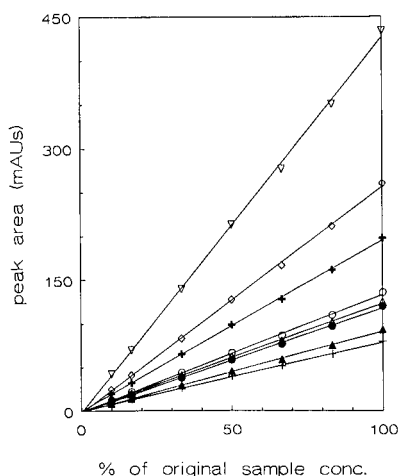


Fig. 4. Calibration graphs for (+) nicarbazine, (Δ) dimetridazole, (\circ) sulphadimidine, (+) sulphadiazine, (\blacktriangle) carbadox, (\bullet) furaltadone, (∇) dapson and (\diamond) fenbendazole. For further explanation, see text.

ably, owing to a small difference in t_{EOF} , the calculated $m_{\text{eff},s}^{\text{ps}}$ values are nearly identical.

CONCLUSIONS

In MECC the capacity factor, k' , provides fundamental information concerning the distribution coefficient over the aqueous and the micellar phase,

Determination of dapson in tablets by MECC

As an application we determined the amount of dapson in a tablet of mass 202.8 mg stated to contain 100 mg of dapson per tablet. The tablet was pulverized and 15.4 mg were dissolved in 50 ml of 100 mM SDS solution containing about 0.1 mg fenbendazole as t_{MC} marker. As duplicate, a 2-fold diluted solution was used. From the calibration graph, we found 104.5 mg (S.D. = 1.2 mg) and 105.8 mg (S.D. = 1.4 mg) of dapson, respectively, in the tablet, showing that MECC is suitable for the determination of dapson in tablets. In Fig. 5 the electropherogram of the standard sample mixture with the eight drugs and the electropherogram of the sample mixture from the tablet are given. Although the migration times for peaks 7 and 8 differ consider-

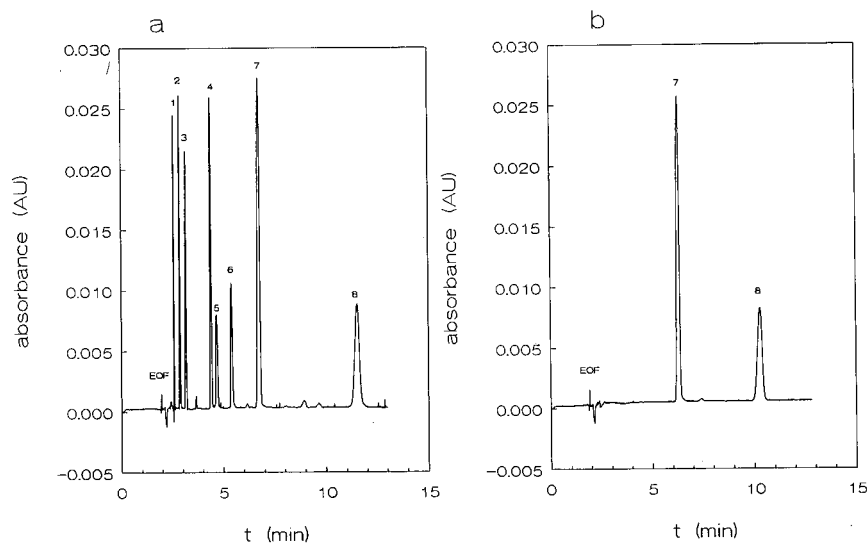


Fig. 5. Electropherogram of (a) a standard sample of (1) nicarbazine, (2) dimetridazole, (3) sulphadimidine, (4) sulphadiazine, (5) carbadox, (6) furaltadone, (7) dapson and (8) fenbendazole, and (b) a sample of a dapson tablet with fenbendazole added as t_{MC} marker. The injection volume was about 11 nl (see text for composition of the sample).

which can give a guide to improving the resolution according to the resolution equation of micellar electrokinetic capillary chromatography. For screening purposes, pseudo-effective mobilities are to be preferred to capacity factors because they can be calculated even if t_{MC} is unknown and because they are less sensitive to inaccuracies in the determination of the migration times. Moreover, pseudo-effective mobilities give a better indication of whether components can be separated or not. The addition of an organic solvent to the sample affects the values of k' and pseudo-effective mobilities and the resolution of the separation. Although in our experiments a large injection volume was applied in order to examine in detail the effect of methanol in the sample, a better way is to dissolve in water-insoluble components in an SDS solution. Linear calibration graphs were obtained for the different drugs and the results for the determination of dapsona in tablets without any sample pretreatment were satisfactory.

ACKNOWLEDGEMENT

The authors express their gratitude to the State Institute for Quality Control for Agricultural Prod-

ucts (RIKILT) for supplying the pharmaceutical compounds and for financial support of this investigation.

REFERENCES

- 1 S. Terabe, K. Otsuka, K. Ichikawa, A. Tsuchiya and T. Ando, *Anal. Chem.*, 56 (1984) 113.
- 2 S. Terabe, K. Otsuka and T. Ando, *Anal. Chem.*, 57 (1985) 834.
- 3 S. Fujiwara, S. Iwase and S. Honda, *J. Chromatogr.*, 447 (1988) 133.
- 4 D. E. Burton, M. J. Sepaniak and M. P. Maskarinek, *J. Chromatogr. Sci.*, 26 (1988) 406.
- 5 H. Nishi, N. Tsumagara and S. Terabe, *Anal. Chem.*, 61 (1989) 2434.
- 6 Y. Miyashita, S. Terabe and H. Nishi, *Chromatogram*, 11 (1990) 7.
- 7 S. Fujiwara and S. Honda, *Anal. Chem.*, 59 (1987) 2773.
- 8 H. Nishi, T. Fukuyama, M. Matsuo and S. Terabe, *J. Microcolumn Sep.*, 1 (1989) 234.
- 9 A. Wainright, *J. Microcolumn Sep.*, 2 (1990) 166.
- 10 J. Gorse, A. T. Balchunas, D. F. Swaile and M. J. Sepaniak, *J. High Resolut. Chromatogr. Chromatogr. Commun.*, 11 (1988) 554.
- 11 M. M. Bushey and J. W. Jorgenson, *J. Microcolumn Sep.*, 1 (1989) 125.
- 12 K. Ghowsi, J. P. Foley and R. J. Gale, *Anal. Chem.*, 62 (1990) 2714.
- 13 J. L. Beckers, F. M. Everaerts and M. T. Ackermans, *J. Chromatogr.*, 537 (1991) 407.

Separation of antibiotics by high-performance capillary electrophoresis with photodiode-array detection

S. K. Yeo, H. K. Lee and S. F. Y. Li*

Department of Chemistry, National University of Singapore, Kent Ridge, Singapore 0511 (Singapore)

(First received February 13th, 1991; revised manuscript received May 21st, 1991)

ABSTRACT

The separation of six antibiotics by high-performance capillary electrophoresis (HPCE) with UV photodiode-array detection is reported. The effect of pH on the separation was studied. Simultaneous detection at different wavelengths and characterization of separated components by spectral analysis were performed.

INTRODUCTION

Capillary zone electrophoresis (CZE) has developed into a high-efficiency separation technique for small samples of ionic species [1–6]. In CZE, ionic species separate under the influence of a high-voltage (15–40 kV) potential field based on their electrophoretic mobilities. Although high-performance liquid chromatography (HPLC) has been the conventional method used for the analysis of antibiotics, in recent years the use of capillary electrophoresis (CE) has assumed considerable importance [7,8]. However, the use of photodiode-array detection for the CE analysis of antibiotics has not been studied. Further, the study of antibiotics has usually involved only one family of the antibiotics, *e.g.*, the study of β -lactam antibiotics by Nishi *et al.* [7] and the separation and determination of aminoglycoside antibiotics by Gambardella *et al.* [8]. In this work, the separation of selected antibiotics of different types was investigated. The separation of these antibiotics has not previously been performed using either HPLC or HPCE. A photodiode-array detector was employed for detection at different wavelengths simultaneously.

EXPERIMENTAL

The experiments were performed on a laboratory-built HPCE system. A 15-kV laboratory-built power supply was used to deliver the necessary potential across the column. A fused-silica capillary tube (50 μm I.D. \times 50 cm effective length) (Polymicro Technologies, Phoenix, AZ, USA) was used as the separation column. The peaks were detected with an SPD-M6A UV-VIS photodiode-array detector (Shimadzu, Kyoto, Japan) with accompanying software. The detector cell was modified as described by Kobayashi *et al.* [9].

Six antibiotics (Fig. 1) were purchased from Sigma (St. Louis, MO, USA) and sodium dihydrogenphosphate dihydrate and sodium tetraborate from Fluka (Buchs, Switzerland). Buffer solution was prepared by dissolving sodium dihydrogenphosphate and sodium tetraborate in water purified with a Milli-Q system (Millipore, Bedford, MA, USA). The pH conditions studied were 6.07, 6.57, 7.07, 7.50, 8.09 and 8.50.

Samples were introduced by the gravity feed method. This was carried out by placing the tip of the separation column at the high-potential end in the sample solution at a level 8 cm higher than the buffer reservoir. The time for each injection was 8 s. The capillary end was then rinsed by dipping into

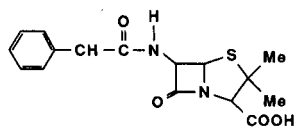
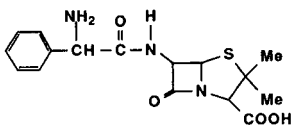
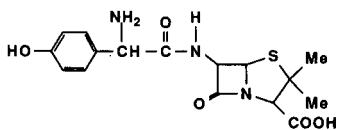
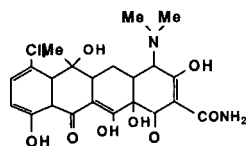
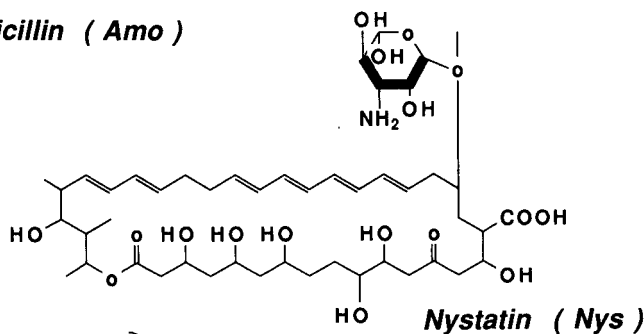
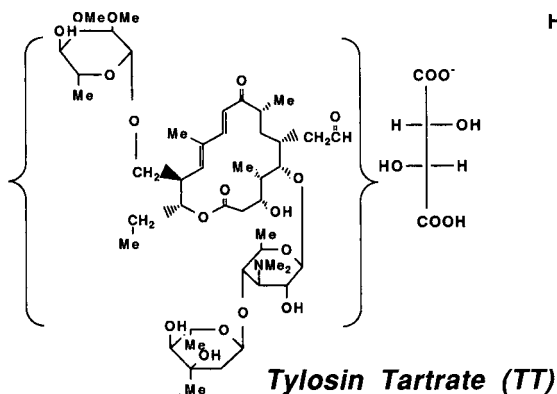
**Penicillin-G (Pen-G)****Ampicillin (Amp)****Amoxicillin (Amo)****Chlortetracycline (CT)****Nystatin (Nys)****Tylosin Tartrate (TT)**

Fig. 1. Structures of the six antibiotics. Me = Methyl.

a rinsing solution of similar composition to the electrophoretic medium. The capillary end was then transferred back to the reservoir before the power supply was switched on. The amount injected by this method is estimated to be 3 nl per injection. The capillary column was flushed periodically with water. The relative standard deviation for the migration times was found to be 0.78% ($n = 8$). In all

electrophoretic runs, methanol was used as the electroosmotic marker.

Solutions of the six antibiotics were prepared in methanol at the following concentrations: tylosin tartrate 2.5 mM, chlortetracycline 4.3 mM, amoxicillin 4.6 mM, penicillin G sodium 3.4 mM, ampicillin (sodium salt) 4.6 mM and nystatin 2.1 mM. As antibiotics degrade rapidly, all samples were kept in

a refrigerator when not in use and new solutions were prepared every few days.

A tablet obtained commercially, which was stated to contain 250 mg of ampicillin trihydrate, was analysed for the presence of the antibiotic. The tablet was pulverized and then 200 ml of methanol were added to extract the ampicillin present. After shaking the mixture for about 5 min, the suspension was filtered through a Whatman No. 1 filter-paper and the filtrate was evaporated by a rotatory evaporator (Eyela; Tokyo Rikakikai, Tokyo, Japan) at room temperature until white residue was observed. The white residue was dissolved in 100 ml of methanol, the solution obtained was filtered and 10 ml of methanol were used for rinsing. The resulting solution was analysed for ampicillin using the standard addition method.

RESULTS AND DISCUSSION

Results of the capillary electrophoretic experiments are shown in Fig. 2. The antibiotics migrated in the following order of increasing migration times: TT < NYS < AMO < AMP < CT < PEN-G. TT has the shortest migration time. The reason could be that it contains a tertiary amino group, which could be protonated under the pH conditions studied, resulting in it having a positive charge. As a result, both electrophoretic and electroosmotic flows would be in the same direction. Consequently, it migrated faster than methanol, which is neutral. The other five antibiotics migrated more slowly than methanol.

The above trend was observed at pH 7.07, 7.50 and 8.09. At pH 6.07, it was observed that CT migrated faster than AMO and AMP. This could be due to the fact that at lower pH, deprotonation of the OH groups is suppressed, resulting in CT being less negatively charged than AMO and AMP. At pH 8.50, CT migrated faster than AMP because the charge on CT can be delocalized over the four rings whereas the charge on AMP is not delocalized.

UV photodiode-array detection was found to be very useful in the identification of the antibiotic peaks. All six antibiotics absorb in the region 198–200 nm. Nystatin and tylosin tartrate were also found to absorb in the region 306–308 nm (peaks 1' and 3' in Fig. 3), whereas chlortetracycline absorbs in the region 388–390 nm (peak 6' in Fig. 4). With the

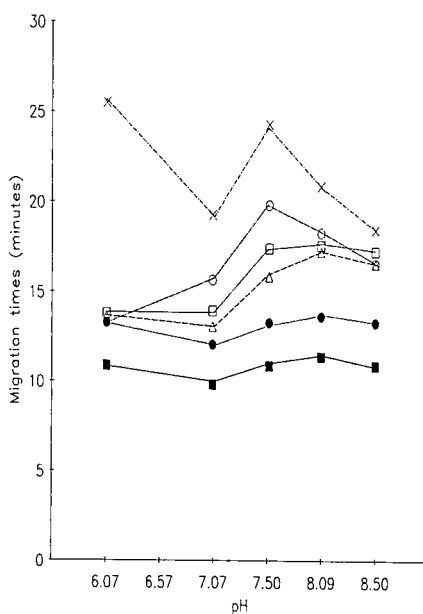


Fig. 2. Plot of migration time against pH conditions studied. ■ = TT; □ = AMP; △ = AMO; ○ = CT; ● = NYS; × = PEN-G.

use of two different channels at the same time, the identification of these peaks would be unambiguous as they would appear in both electropherograms.

To demonstrate the usefulness of the procedure,

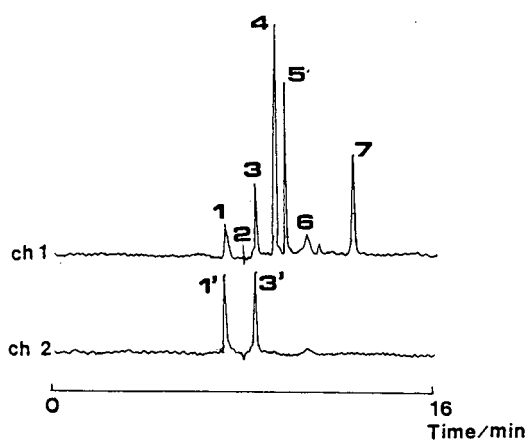


Fig. 3. Electropherogram of the six antibiotics. 1 = TT; 1' = TT; 2 = methanol; 3 = NYS; 3' = NYS; 4 = AMO; 5 = AMP; 6 = CT; 7 = PEN-G. Electrophoretic solution, 0.05 M phosphate-0.1 M borate buffer (pH 7.06); separations tube, 50 cm × 50 μm I.D. fused-silica capillary; voltage, 15 kV, 36 μA; detection wavelengths, channel 1 198–200 nm and channel 2 306–308 nm.

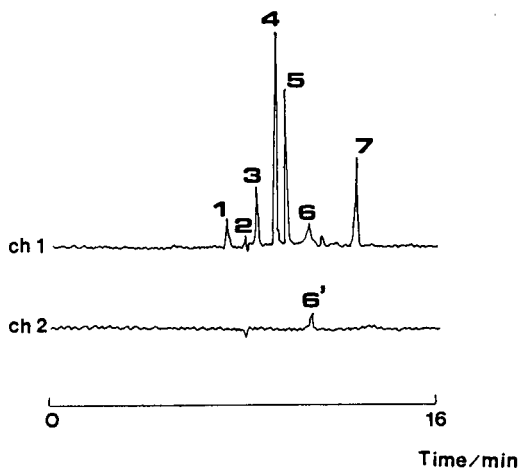


Fig. 4. Electropherogram of the six antibiotics. 1 = TT; 2 = methanol; 3 = NYS; 4 = AMO; 5 = AMP; 6 = CT; 6' = CT; 7 = PEN-G. Electrophoretic solution, 0.05 *M* phosphate-0.1 *M* borate buffer (pH 7.06); separation tube, 50 cm × 50 μm I.D. fused-silica capillary; voltage, 15 kV, 36 μA; detection wavelengths, channel 1 198–200 nm and channel 2 380–390 nm.

a commercially available tablet was analysed for the presence of ampicillin. Fig. 5 is an electropherogram of the extracted sample of an ampicillin tablet together with the UV spectrum obtained on-line for ampicillin. A peak purity check (purity index = 0.9951) and the contour plot (Fig. 6) confirmed that ampicillin was the only antibiotic present in the tablet. It was found that the amount of ampicillin present was 220 mg [relative standard deviation =

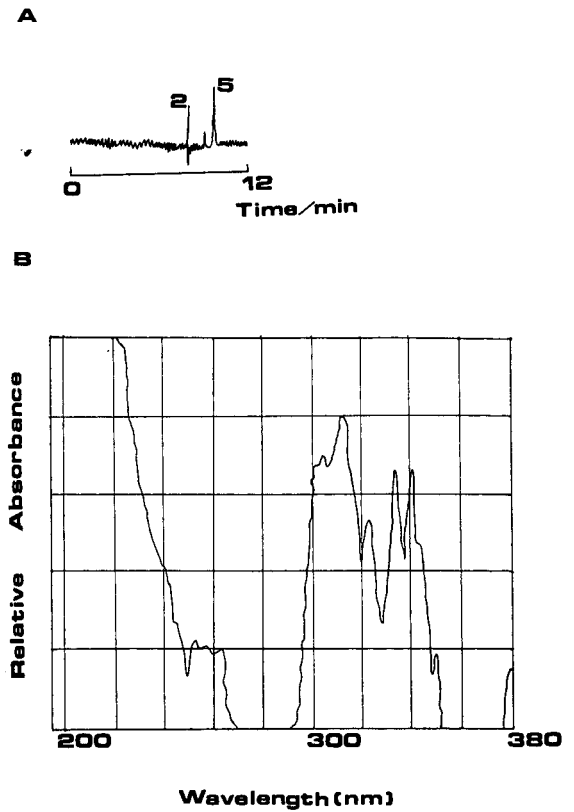


Fig. 5. (A) Electropherogram of ampicillin extract. (2) Methanol; (5) AMP. (B) Spectrum of ampicillin. Electrophoretic solution, 0.05 *M* phosphate-0.1 *M* borate buffer (pH 7.06); separation tube, 50 cm × 50 μm I.D. fused-silica capillary; voltage, 15 kV, 36 μA; detection wavelength, channel 1 198–200 nm.

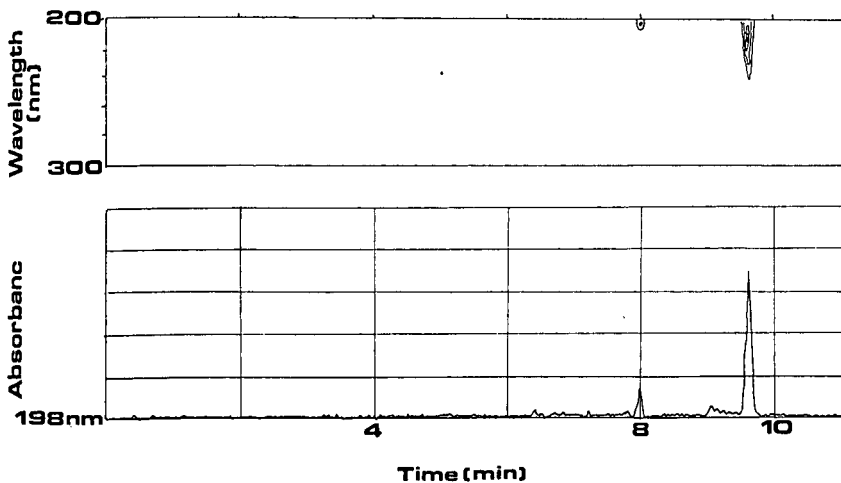


Fig. 6. Contour plot of ampicillin extract and its electropherogram at 198 nm.

9.6% ($n = 3$)]. Considering that for every 1.15 mg of trihydrate only 1 mg of ampicillin is present [10], the amount of ampicillin trihydrate present in the tablet was calculated to be 253 mg. This value agrees very well with the stated amount of 250 mg.

ACKNOWLEDGEMENT

The authors thank the National University of Singapore for financial support.

REFERENCES

- 1 K. Otsuka, S. Terabe and T. Ando, *J. Chromatogr.*, 396 (1987) 350.
- 2 S. Fujiwara and S. Honda, *Anal. Chem.*, 59 (1987) 2773.
- 3 H. Nishi, T. Fukuyama, M. Matsuo and S. Terabe, *J. Pharm. Sci.*, 79 (1990) 519.
- 4 H. Nishi, T. Fukuyama, M. Matsuo and S. Terabe, *J. Chromatogr.*, 513 (1990) 279.
- 5 T. Nakagawa, Y. Oda, A. Shibukawa and H. Tanaka, *Chem. Pharm. Bull.*, 36 (1988) 1622.
- 6 T. Nakagawa, Y. Oda, A. Shibukawa, H. Fukuda and H. Tanaka, *Chem. Pharm. Bull.*, 37 (1989) 707.
- 7 H. Nishi, N. Tsumagari, T. Kakimoto and S. Terabe, *J. Chromatogr.*, 477 (1989) 259.
- 8 P. Gambardella, R. Puniziano, M. Gionti, C. Guadalupi and G. Mancini, *J. Chromatogr.*, 348 (1985) 229.
- 9 S. Kobayashi, T. Ueda and M. Kikumoto, *J. Chromatogr.*, 480 (1989) 179.
- 10 G. Lancini and F. Parenti, in M. P. Starr (Editor), *Antibiotics—An Integrated View*, Springer, New York, 1982, Ch. 1, pp. 1–12.

Micellar electrokinetic capillary chromatography of vitamin B₆ with electrochemical detection

Y. F. Yik, H. K. Lee, S. F. Y. Li and S. B. Khoo*

Department of Chemistry, National University of Singapore, Kent Ridge, Singapore 0511 (Singapore)

(First received February 13th, 1991; revised manuscript received May 14th, 1991)

ABSTRACT

A system for interfacing electrochemical detection with micellar electrokinetic capillary chromatography is demonstrated. This system couples the separation column to a short length of the same column material together with a section of porous graphite tubing which forms an electrically conductive joint. The joint is immersed in a buffer reservoir together with the ground electrode of the high-power source (15 kV). The reservoir is electrically insulated from the electrochemical cell containing the carbon fibre detector. This configuration effectively separates the detector from the high separation potential applied. Amperometric detection with micellar solutions is demonstrated for a mixture of B₆ vitamers on a 50 μ m I.D. column. A detection limit of *ca.* 4 fmol is obtained. The linear dynamic range of the calibration plot is slightly over two orders of magnitude (from *ca.* 1 to 200 ppm).

INTRODUCTION

Zone electrophoresis in capillaries [capillary zone electrophoresis (CZE)] [1,2] is a rapidly developing field of research. CZE employs extremely high potential fields resulting in highly efficient separations of ionic solutes. In order to extend the advantages of CZE to neutral compounds, micellar electrokinetic capillary chromatography (MECC), first introduced by Terabe and co-workers [3,4], was developed. MECC employs buffers to which surfactants have been added at concentrations above their critical micelle concentrations. Separation is based on micellar solubilization and electrokinetic migration [4]. The two distinct phases, an aqueous phase and a micellar phase, present within the column, migrate at different velocities towards the electrode. As the electroosmotic flow of the aqueous phase is predominant, the micelles are transported towards the cathode, but exhibit a slower net velocity than the bulk aqueous phase. Thus non-ionic solutes appear to partition between the aqueous and micellar phases, which results in solute zone velocities between those of the two phases.

Although CZE has advanced rapidly, some limi-

tations in detection still exist. Owing to the small column dimensions and the extremely small zone widths, there is a need for on-column detection or detectors with very small effective volumes (less than a few nanolitres) in order to preserve the high efficiency of CZE. In addition, the detection technique must not disturb the potential field across the column. Based on these limitations, spectroscopic detectors capable of on-column detection before the cathodic reservoir have been used almost exclusively. Amongst these, laser-induced fluorescence [5,6] is the most sensitive on-column detection mode available for CZE and MECC, providing detection limits as low as sub-femtomoles [5]. However, a drawback of this detection mode is the need to derivatize most samples of interest. UV absorption, although more versatile, has poorer detection limits, generally in the picomole range or higher.

Electrochemical detection (ED) has been shown to be among the most sensitive methods available for capillary chromatography, with detection limits as low as 20 amol being reported [7]. In addition, ED allows the use of smaller diameter columns without losses in sensitivity [8].

Wallingford and Ewing [9,10] were the first to re-

port amperometric detection with CZE and MECC. Owing to the necessity to keep the detection end of the column in a buffer reservoir, electrochemistry, if performed in this reservoir, suffers from high noise levels due to the presence of a high-voltage electric field. To prevent this, the electrochemical detector was decoupled from the separation capillary by a small break in the capillary surrounded by a porous glass capillary. This ensures that the applied potential drops across the joint, while electroosmotic flow forces the buffer and analyte past the joint to the carbon fibre working electrode positioned inside the end of the capillary. Recently, a new design of CZE-ED was reported by Huang *et al.* [11], in which the use of the aforementioned joint is no longer necessary. This is because the inside diameter of the separation capillary is so small ($5\ \mu\text{m}$) that very little current is passed. With these systems, electrochemical detection of catecholamines, catechols and fluorescamine-labelled amino acids has been demonstrated with MECC [9–11].

Notwithstanding the work described, in general, MECC with ED has been largely unexplored. Our laboratory has recently demonstrated an alternative CZE-ED system that is based on the use of a porous graphite joint created in the column near the cathodic end. Ease of insertion of a carbon fibre electrode into the capillary is due mainly to the design of the electrochemical cell.

In this work, the sensitivity of the CZE-ED system was tested with norepinephrine. Application of the system to the separation and determination of vitamin B₆ and its vitamers was also investigated. Limits of detection, linearity and reproducibility data are presented for the vitamers.

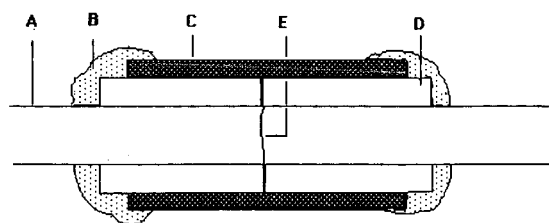


Fig. 1. Schematic diagram of porous graphite joint. A = Fused silica capillary; B = epoxy; C = graphite tube; D = PTFE tube; E = joint.

EXPERIMENTAL

Electrokinetic apparatus

Untreated fused-silica capillaries of $50\ \mu\text{m}$ I.D. were obtained from J&W Scientific. The capillaries were filled with buffer and sodium dodecyl sulphate (SDS) solutions via a syringe. A high-voltage d.c. power supply was used to apply the potential field of 15 kV for separations. Injections were made at the anodic end of the capillary by siphoning from the sample solution at a higher level than the electrophoretic solution in which the other end of the tube was immersed.

Construction of the porous joint

A detailed diagram of the porous graphite joint is shown in Fig. 1. The surface of the polyimide-coated silica capillary, *ca.* 2.5 cm from one end, was lightly nicked with a sharp pen-knife. Gentle pressure applied to this region caused the column to break cleanly. A clean cut was also made at the centre of a 1.5-cm length of PTFE capillary (GL Sciences; O.D. 1.5 mm, I.D. 0.25 mm). Under a microscope, the PTFE capillaries were placed carefully over each end of the cut capillaries such that the joint could be re-formed easily. These two sections of the column were then positioned to form a clean joint in a 1-cm long porous graphite tube of 1.6 mm O.D. Slow-setting epoxy glue (Araldite; Ciba-Geigy) was applied to each end of the graphite segment and also along the region of capillary which was in contact with the PTFE capillary. After being allowed to cure at room temperature, the assembly was placed in a T-shaped glass container (Shown in Fig. 2). The two ends of the T-shaped glass container, containing the protruding capillaries, were sealed with epoxy so that the porous graphite joint and a region of the column were positioned inside the container filled with buffer.

After filling the coupled capillary with buffer, the anodic end was placed in a buffer reservoir. Platinum wires were placed in each reservoir so that a potential of 15 kV could be applied across the longer segment of the capillary (47.5 cm in length), which is termed the separation capillary.

Electrochemical detection

Electrochemical detection was performed with $7\text{-}\mu\text{m}$ diameter carbon fibres (Goodfellow) pro-

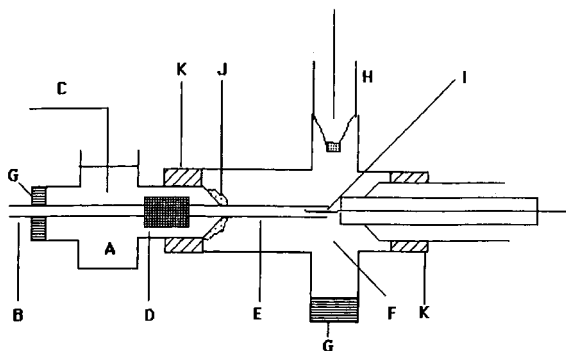


Fig. 2. Schematic diagram of the electrochemical cell. A = Buffer reservoir; B = separation capillary; C = platinum wire; D = graphite joint; E = detection capillary; F = electrolyte; G = stopper; H = reference electrode; I = carbon fibre working electrode; J = epoxy; K = ground-glass joint.

truding 1.0–1.5 mm from drawn glass capillaries as the working electrodes. The procedure for the construction of these electrodes is as follows. The carbon fibre (1.5–2.0 cm) was cemented onto the copper wire with silver-loaded epoxy (Epoxy Technology). This was then pulled through a drawn glass capillary such that *ca.* 0.5–1.0 cm of the fibre was extended from the tip of the capillary which was sealed with epoxy. The epoxy was allowed to cure at 70°C for 1 day. The carbon fibre was then cut so that *ca.* 1.0–1.5 mm was left exposed.

The electrochemical cell is shown in Fig. 2. The end of the detection capillary was positioned in the centre of the cell. The microelectrode was manipulated through the opposite end and into the detection capillary while viewing under a microscope. In operation, the detector was employed in a two-electrode mode. A sodium-saturated silver/silver chloride (Ag/AgCl) electrode was used as the second electrode. The cell was filled with electrolyte solution of 0.01 M phosphate buffer containing 10 mM SDS. The whole assembly was placed in an aluminium box which functions as a Faraday cage. Potential was applied between the reference and working electrodes using a waveform generator (Model PRR1; Hi-Tek Instruments). Oxidation currents were amplified and recorded with a Keithley Model 617 programmable electrometer and a Linear Instruments 1200 chart recorder, respectively.

Cyclic voltammetry

A conventional three-electrode voltammetric cell was used. An aqueous Ag/AgCl electrode, joined with a salt bridge, and platinum wire served as the reference and counter electrodes, respectively. Glassy carbon (3 mm diameter) was used as the working electrode. Cyclic voltammetry was performed with an EG & G Princeton Applied Research Model 264A polarographic analyser and voltammograms were recorded using a Graphtec W × 1100 recorder.

Chemicals

Sodium dihydrogenphosphate and sodium dodecyl sulphate were obtained from Fluka. The buffer solutions were prepared with water obtained from an Alpha Q water purification system (Millipore). Norepinephrine was purchased from Aldrich and pyridoxal, pyridoxol and pyridoxamine hydrochloride from Merck. Vitamin B₆ tablets containing 100 mg of pyridoxol hydrochloride per tablet as stated on the label were obtained from Blackmones.

Procedure for determination of volume injected

The anodic end of the capillary was immersed in the sample solution and lifted to an injection height of 8 cm and injection was performed for 5 s. The capillary was then immersed in the buffer reservoir at the same injection height. The solute plug was allowed to migrate in the tube by gravity and the migration time was measured.

Determination of vitamin B₆

All calibration standards of B₆ vitamers were prepared in the electrophoretic medium used. Solutions of these standards were stored at pH 4.60 in the dark and used for only 1–3 days.

The sample solution was prepared by dissolving one pulverized tablet in 20 ml of buffer followed by filtration through 0.7- μ m Millipore filters. This stock sample was further diluted (1:250) with the electrophoretic medium before injection.

RESULTS AND DISCUSSION

Electrochemical detection interface

The heart of the MECC–ED system is the porous graphite joint created at the junction of the separation and detection capillaries. This porous conductive joint facilitates the isolation of the detector from

the high separation potential. The current arising from this separation potential is about $8\ \mu\text{A}$ whereas the signal from the amperometric detector typically ranges from pico- to nanoamps. Therefore, if the detector is not isolated from the high electric field, small fluctuations in the separation current can amount to very high noise levels (maybe several orders of magnitude greater than the detector signal). For low-level current measurements as in this instance, the use of a two-electrode mode with the cell shielded from external electrical noise has been recommended [12].

The porous conductive joint was constructed easily by pushing the two capillaries through the graphite tube. With the gauge of the PTFE capillary, which forms a tight fit between the graphite tube and silica capillary, the separation and detection capillaries can be aligned easily within the porous graphite tube. When this coupler assembly is immersed in the buffer with the cathode, the separation potential can be applied selectively to the separation capillary. The strong electroosmotic flow generated in this column serves to force the solvent and analyte zones past the joint and through the second section to the detector.

In this work, a major concern with coupling the off-column detector to the capillary column is band broadening due to the graphite interface and the dead volume in the detection capillary. The band broadening aspect of the porous glass coupling system has been discussed in detail previously [9]. It was realized that the major sources of added band broadening stem from dispersion along the length of the detection capillary and the difficulty in attaining precision in the alignment of the two sections [10]. To overcome these problems, the detection capillary was kept as short as possible (not longer than 2.5 cm) in order to minimize band broadening. Further, good alignment was achieved by using tight-fitting tubings. The success of the coupling system was demonstrated by injecting norepinephrine (NE). The peak observed (Fig. 3) showed no indication of severe band broadening. The peak width for a similar length of column and migration time is comparable to those in previous work [10]. A detection limit (signal-to-noise ratio = 3) of the order of 0.4 fmol has been extrapolated for NE.

The currents (*ca.* $8\ \mu\text{A}$) flowing through the column due to the application of a 15-kV high

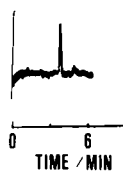


Fig. 3. Electropherogram of 0.2 ppm of norepinephrine on a 50 μm I.D. column. 0.01 M phosphate buffer (pH 4.60) containing 10 mM SDS; separation potential, 15 kV ($7.4\ \mu\text{A}$); electrode potential, 0.82 V vs. Ag/AgCl.

voltage were found to be in the same range as those observed with an MECC system without ED that had a similar length and diameter of column filled with buffer solution of similar concentration. This implies that the porous graphite joint in no way impedes the flow of current between the two ends of the high separation potential. Further, the graphite coupler is mechanically strong, which leads to ease of handling and manipulation in the T-shaped buffer reservoir. The use of ground-glass connections in the electrochemical cell (see the assembly in Fig. 2) also allows for simple dismantling of the set-up for cleaning and changing of solutions and ease of insertion of the carbon fibre working electrode.

One of the problems observed with this assembly is the deterioration of epoxy in buffer solutions. This deterioration was manifested in unacceptable noise levels due to leakage of current from the separation potential field. This problem can be alleviated by winding sealing film tightly over the epoxy. Finally, it is important to keep the graphite joint immersed in buffer to prevent it from drying out. It was noticed that if the joint was allowed to dry (for *e.g.*, in the oven), then on re-immersion in the buffer the detector could not be used for several hours owing to displacement of tiny air bubbles from the pores of the graphite tube which escaped through the detection capillary. However, once the air bubbles had been completely removed, this problem vanished.

Determination of vitamin B₆

Vitamin B₆ is not a single chemical entity but consists of pyridoxine (pyridoxol, PN), pyridoxamine (PM) and pyridoxal (PL), all of which are biologically equivalent. In the human body, pyridoxal and pyridoxamine, which are metabolites of pyridoxine, are precursors of important coenzymes.

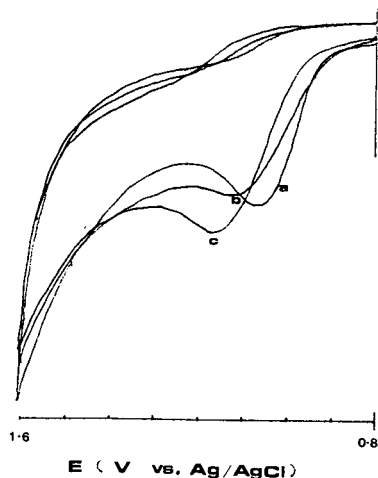


Fig. 4. Oxidation of $1 \cdot 10^{-3} M$ (a) PM, (b) PN and (c) PL in $0.01 M$ phosphate buffer containing $10 mM$ SDS at a carbon-fibre electrode. Reference electrode, Ag/AgCl; scan rate, $50 mV s^{-1}$.

MECC has been employed to separate and determine B₆ vitamers in biological fluids [13] using laser-excited fluorescence detection. In this work, we report the use of ED, which allows better sensitivity.

The cyclic voltammograms of the three B₆ vitamers are shown in Fig. 4. They were obtained at the glassy carbon electrode in phosphate buffer solution containing $10 mM$ SDS and $0.1 M$ sodium perchlorate as supporting electrolyte. From Fig. 4, it was observed that the oxidation reactions were irreversible, with peak potentials at 1.06, 1.14 and 1.16 V for PM, PN and PL, respectively.

For the separation of the B₆ vitamers, a separation potential of 15 kV was applied, resulting in a current of $7.3 \mu A$. Detection was effected by applying a potential of 1.20 V with respect to the Ag/AgCl (saturated NaCl) electrode. This potential is at least 40 mV past the peak potential for all the three compounds. From Fig. 5, it can be observed that this technique exhibits the selectivity and efficiency needed to separate the B₆ vitamers.

The limits of detection obtained in this work are given in Table I. They were determined by injecting 1 ppm solutions prepared from serial dilutions of the concentrated standards. The limits of detection were extrapolated to a signal-to-noise ratio of 3 and the results obtained were two orders of magnitude lower than those reported for a laser-excited fluorescence detector [13].

The quantities listed in Table I are injected

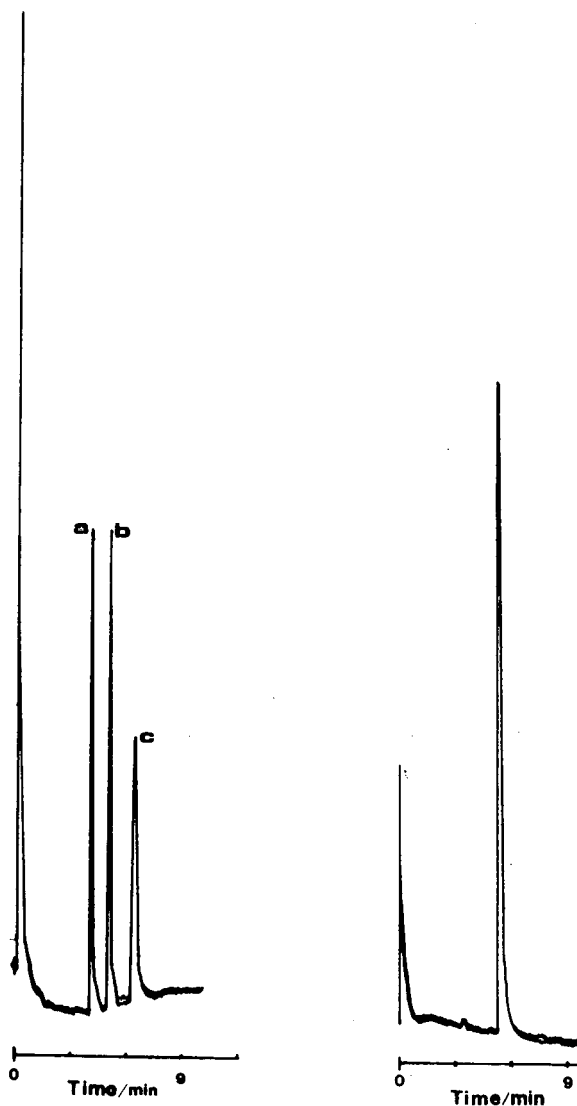


Fig. 5. Electropherogram of (a) PL, (b) PN and (c) PM. Electrode potential, 1.2 V vs. Ag/AgCl; other conditions as in Fig. 3.

Fig. 6. Electropherogram of a 250-fold dilution of extracted vitamin B₆. Electrode potential, 1.2 V vs. Ag/AgCl; other conditions as in Fig. 3.

amounts determined by the procedure given under Experimental. With the diameter of the capillary and the velocity of solute plug being known, the volume injected by gravity feed at this injection height can be calculated and subsequently the amount injected can be determined. The calculated volume of the sample plug injected in this manner

TABLE I
CALIBRATION DATA

Vitamer	DL ^a (pg)	R.S.D. ^b (%)	ρ^c
PN	1.0	3.9	0.999
PL	2.0	2.6	0.992
PM	1.0	4.1	0.996

^a Detection limit (based on a signal-to-noise ratio of 3; concentration of injected solution = 1 ppm).

^b Relative standard deviation ($n = 3$).

^c Correlation coefficient.

was *ca.* 2.4 nl, which is sufficiently small to preclude any overloading effects that can be detrimental to efficiency [14,15].

Table I also shows the reproducibility of the injections. These range from 2.6 to 4.1% relative standard deviation (R.S.D.), which is satisfactory. Calibration graphs for the three vitamers were obtained with good linearity (correlation coefficients from 0.992 to 0.999) over two orders of magnitude (from *ca.* 1 to 200 ppm). All experiments were performed in triplicate.

A chromatogram of the vitamin B₆ sample is shown in Fig. 6. The peak is that of pyridoxol hydrochloride (PN). This sample is a 1:250 dilution of the solution prepared by dissolving one tablet in 20 ml of micellar solution. The concentration of PN is *ca.* 19.7 ppm, as determined by standard addition. This corresponds to 98.3 mg (R.S.D. 0.98%) of PN in one tablet, which is close to that stated on the label (100 mg).

CONCLUSION

A simple, rugged, yet sensitive electrochemical detection system was developed for capillary electro-

phoresis. Satisfactory performance of the system was demonstrated with the determination of vitamin B₆. Preliminary results indicate that the MECC-ED system has the potential to achieve high sensitivity as a microanalytical method. Currently, our efforts are directed towards the optimization of the operating conditions of the system.

ACKNOWLEDGEMENT

Thanks are due to the National University of Singapore for financial support.

REFERENCES

- 1 J. W. Jorgenson and K. D. Lukacs, *Anal. Chem.*, 53 (1981) 1298.
- 2 Y. Walbroaehl and J. W. Jorgenson, *Anal. Chem.*, 58 (1986) 479.
- 3 S. Terabe, K. Otsuka, K. Ichikawa, A. Tsuchiya and T. Ando, *Anal. Chem.*, 56 (1984) 111.
- 4 S. Terabe, K. Otsuka and T. Ando, *Anal. Chem.*, 57 (1985) 834.
- 5 P. Gozel, E. Gassmann, H. Michelson and R. N. Zare, *Anal. Chem.*, 59 (1987) 44.
- 6 M. J. Sepaniak and R. D. Cole, *Anal. Chem.*, 59 (1987) 472.
- 7 R. L. St. Claire, III, and J. W. Jorgenson, *J. Chromatogr. Sci.*, 23 (1985) 186.
- 8 L. A. Knecht, E. J. Guthrie and J. W. Jorgenson, *Anal. Chem.*, 56 (1984) 479.
- 9 R. A. Wallingford and A. G. Ewing, *Anal. Chem.*, 59 (1987) 1762.
- 10 R. A. Wallingford and A. G. Ewing, *Anal. Chem.*, 60 (1988) 258.
- 11 X. Huang, R. N. Zare, S. Sloss and A. G. Ewing, *Anal. Chem.*, 63 (1991) 189.
- 12 A. M. Bond, M. Fleischmann and J. Robinson, *J. Electroanal. Chem.*, 180 (1984) 257.
- 13 D. E. Burton, M. J. Sepaniak and M. P. Maskarinec, *J. Chromatogr. Sci.*, 24 (1986) 347.
- 14 H. H. Lauer and D. McManigill, *Trends Anal. Chem.*, 5 (1986) 11.
- 15 D. Stigter, *J. Phys. Chem.*, 68 (1964) 3603.

Purification of ovalbumin and lysozyme from a commercial product by recycling isotachopheresis

Jitka Caslavská, Petr Gebauer[☆] and Wolfgang Thormann*

Department of Clinical Pharmacology, University of Berne, Murtenstrasse 35, CH-3010 Berne (Switzerland)

(First received April 4th, 1991; revised manuscript received June 4th, 1991)

ABSTRACT

The aim of this work was to test the suitability of using recycling isotachopheresis (RITP) for the purification of ovalbumin (OVA) and/or lysozyme (LYSO) from a commercial OVA product containing LYSO and conalbumin (CAL) as major proteinaceous impurities. The search for suitable electrolyte systems and spacers was carried out by capillary isotachopheresis. RITP was performed in a recycling free-flow focusing apparatus in the batch mode with immobilization of the advancing zone structure via a controlled counterflow. Typically 700 mg of the commercial product were processed within 2 h. Enhancement of the sample load was achieved by a feed of sample under counterflow control. The collected fractions were analysed separately for conductivity, pH and ultraviolet absorption, and selected fractions were characterized by analytical capillary electrophoretic methods. All three proteins could be separated and fractionated using suitable spacers. Depending on the chosen conditions either OVA or LYSO could be purified in amounts larger than milligrams per hour (OVA 300 mg/h; LYSO 10 mg/h). The instability of CAL in solution prevented its isolation in the investigated configurations.

INTRODUCTION

Most investigations involving preparative isotachopheresis (ITP) use solid support media (for overviews, see Holloway and Battersby [1] and Sloan *et al.* [2]). Several other papers indicate a renaissance of using free-fluid preparative ITP as a purification method for proteins. Continuous-flow ITP [3-5], recycling ITP (RITP) [2,5,6] and segmented column ITP [6] are currently being investigated; these methods provide high resolution coupled with high protein concentration, large throughput and control over fractionation pH, as well as the potential for automation. The purification of monoclonal antibodies from mouse ascites fluid and tissue culture media [7] and the fractionation of apolipoprotein B-containing lipoproteins from fasting and postprandial sera derived from normolipidaemic individuals [8] are two recent ap-

plications using continuous-flow ITP. This laboratory is in the process of exploring RITP as a free-fluid approach for the ITP determination of proteins on the gram scale [2,5,6]. In this method the fluid flows rapidly through a narrow channel and the effluent from each channel is reinjected into the electrophoresis chamber through the corresponding input port. The residence time in the cell is of the order of 1 s per single pass, which does not allow complete separation, thus recycling is essential to attain a steady state. Immobilization of the advancing zone structure is obtained via a controlled counterflow.

Egg proteins are important constituents of the human diet and have been the subject of many investigations. The isolation of egg proteins, such as ovalbumin (OVA), is typically performed through repetitive crystallization, salt removal and lyophilization [9]. One paper reports the fractionation of egg white proteins by recycling isoelectric focusing [10]. A commercial OVA was found to contain major proteinaceous impurities which, in a cationic ITP configuration around a leader pH of 4.75, migrate

* Permanent address: Institute of Analytical Chemistry, Czechoslovak Academy of Sciences, CS-611 42 Brno, Czechoslovakia.

in front of OVA [6]. It was demonstrated that using γ -amino-*n*-butyric acid (GABA) as a spacer, OVA could be purified by RITP and determination by capillary ITP revealed that the major OVA fractions were essentially free of these impurities. This example constitutes an interesting model system for an in-depth evaluation of RITP. This sample was therefore further investigated and this paper reports the removal, separation and identification of the two major proteinaceous impurities, lysozyme (LYSO) and conalbumin (CAL), as well as the purification of LYSO compared to that of OVA.

EXPERIMENTAL

Chemicals

All chemicals used were of research-grade purity.

Tris(hydroxymethyl)aminomethane (TRIS), GABA and hydroxypropylmethylcellulose (HPMC, No. 7509) were from Sigma (St. Louis, MO, USA). OVA from chicken egg ($5 \times$ crystallized, Lot No. 11840/D8), LYSO from chicken egg white, CAL and tetrapropylammonium bromide (TPAB) were from Serva (Heidelberg, Germany). Tetrabutylammonium bromide (TBAB) was purchased from Fluka (Buchs, Switzerland) and creatinine (CREAT), potassium acetate and acetic acid were from Merck (Darmstadt, Germany).

RITP

The RITP instrument used in this work is the same as described previously [6]. Briefly, it consists of a recycling free-flow focusing apparatus (Model RF3, Protein Technologies, Tucson, AZ, USA; distributor, Rainin Instrument, Woburn, MA, USA) with modification for RITP. Throughout this work, a separation cell of 20 cm length and 4 cm width with a fluid layer thickness of 0.75 mm and providing 30 fractions was used. The total processing volume was about 130 ml. The outlet temperature was monitored to be about 13°C (cooling bath 2–5°C) with a recycling pump rate of 30% and a constant current of 50 mA.

For operation in the ITP mode, the electrolyte chambers were separated from the separation channel by dialysis membranes which, for better stability, were backed up by two layers of chromatographic paper (3MM CHR, Whatman, Maidstone, UK). Electrode buffer reservoirs of 250 ml (RF3

standard 60 ml) were used and filled with buffers of ten-fold higher concentration than those used within the separation cell. Unless otherwise stated, the sample was injected in channel 2, which is near the terminator electrolyte chamber, and the vent was moved to channel 14. The advancing protein boundary was detected by a 2138 Uvicord S spectrometer (Pharmacia LKB Biotechnology, Uppsala, Sweden) with a 277-nm filter. The detector was inserted into the recycling loop of channel 26 (near the leading electrolyte chamber). The counterflow inlet and outlet were placed into channels 30 and 1, respectively. The counterflow was generated using a low-pulse peristaltic pump (Minipuls 3, Gilson Medical Electronics, Middleton, WI, USA) together with a laboratory-made pulse damper and bubble trap, and was either regulated manually with registration of the output signal from the boundary detector on a strip-chart recorder or automatically using a REX-G9 high-performance digital controller (RKC Instrument, Tokyo, Japan).

All experiments were performed in the batch mode. The separation cell was filled with the leading electrolyte. The multichannel peristaltic pump was set to a pumping rate of 30% and the recycling of the electrolytes was started. The sample, dissolved in a maximum of 10 ml of the leading electrolyte and filtered through a 0.45- μ m membrane syringe filter, was slowly and carefully injected into the electrolyte stream inside the separation cell. After sample injection the power was applied at a constant current of 50 mA. When the absorbance changed in the monitoring loop, the counterflow was activated to maintain a constant absorbance level. The ITP zone structure was thereby immobilized. Typically the counterflow pumping rate did not exceed 3.0 ml/min.

Analysis of collected fractions

For pH measurements a Model 720 pH meter and a ROSS Model 8103 SC pH electrode, (both from Orion Research, Cambridge, MA, USA) were used. The conductivity was measured with a Model 101 conductivity meter (Orion Research) equipped with a Model PW 9510/65 cell (Philips, Eindhoven, Netherlands). The absorbance was measured at 280 nm in a UV-visible Lambda 15 spectrophotometer (Perkin-Elmer, Überlingen, Germany). In some instances the fractions containing the protein zones

had to be diluted ten times and for presentation of the data the absorbance values were multiplied by ten. Some CAL-containing fractions with high turbidity had to be filtered prior to analysis.

Selected fractions and model mixtures were analysed by capillary ITP using a Tachophor 2127 analyser (LKB, Bromma, Sweden). This instrument was equipped with a 28 cm \times 0.5 mm I.D. PTFE capillary and a conductivity and UV detector (filter 277 nm) at the column end. The measurements were performed at a constant current of 150 μ A. The data were registered with a two-channel strip-chart recorder and/or with a data acquisition system comprising a PC integration pack (version 2.50, Kontron Instruments, Zürich, Switzerland), together with a Mandax AT 286 computer system. This integration pack features two channels for data acquisition, automatic range switching and a dynamic sampling rate, allowing sampling every 10 ms for quickly changing signals. The leader employed was composed of 0.01 *M* potassium acetate and acetic acid ($\text{pH}_L = 4.75$). The terminator was 0.01 *M* acetic acid.

Similar analyses were performed in a laboratory-made capillary electrophoretic analyser described in detail previously [11]. Briefly it features a 90 cm \times 75 μ m I.D. fused-silica capillary (Product TSP/075/375, Polymicro Technologies, Phoenix, AZ, USA), together with a fast-scanning multiwavelength Model UVIS 206 PHD detector and an on-column capillary detector 9550-0155 cell (both of Linear Instruments, Reno, NV, USA) placed towards the capillary end. The effective separation distance was 70 cm. Sample application occurred manually via gravity through lifting the anodic capillary end, dipped into the sample vial, by 34 cm for a specified time interval. Multiwavelength data were read, evaluated and stored using a Mandax AT 286 computer system and running the 206 detector software package version 2.0 (Linear Instruments) with Windows 286 version 2.1 (Microsoft, Redmont, WA, USA). Throughout this work the 206 detector was used in the high-speed polychrome mode by scanning from 195 to 320 nm at 5-nm intervals (26 wavelengths). The same electrolytes as with the Tachophor were used, except the leader contained 0.3% HPMC. All runs were performed with a constant voltage of 20 kV. During an experiment, the current decreased from 12 μ A (initial) to about 4 μ A (time

of detection). The details of protein analyses with this instrument are described elsewhere [12].

RESULTS AND DISCUSSION

For all RITP experiments, a cationic ITP system with 0.01 *M* potassium acetate and acetic acid ($\text{pH}_L = 4.75$) as leader was used. The cathodic electrode compartment contained a ten-fold higher concentration of the same electrolyte, whereas 0.1 *M* acetic acid (terminator) was in the anodic electrode compartment. A commercial OVA product containing LYSO and CAL, as well as separate commercial LYSO and CAL samples, were used. Previous investigations by analytical ITP and RITP showed that GABA can successfully be used as a spacer between OVA and its two major proteinaceous impurities [6]. RITP fractionation data of a commercial sample of OVA (710 mg of OVA from Serva 11840/D8 with 15 mg GABA) into pure OVA and CAL-LYSO is presented in Fig. 1A. In this experiment, immobilization of the advancing zone pattern was obtained via automated regulation of the counterflow employing a digital controller. The OVA plateau concentration (fraction 16) was 22 mg/ml and the typical processing throughput was calculated as 300 mg/h. Comparing these results with previously reported data [6] reveals that the automated regulation provides broader zone boundaries than with a manually controlled counterflow. The protein distribution in the collected fractions was analysed by capillary ITP in the Tachophor after spiking the sample with GABA and TRIS. The areas of the UV absorption peaks, determined by manual integration, are shown in Fig. 1B. These data show that the separation of OVA and its major proteinaceous impurities was successful and that LYSO migrates ahead of CAL. The goals of the following experiments were the separation of LYSO and CAL and the purification of LYSO.

Investigations using capillary ITP revealed that CAL and LYSO separate well in the given electrolyte system using different spacers. Typical pherograms obtained on the Tachophor are presented in Fig. 2. The ITP zone formation of the two proteins without spacer is shown in Fig. 2A. LYSO migrates ahead of CAL, their separation being indicated by a sharp UV signal spike which marks the location of the common interface. TRIS (Fig. 2B) was found to

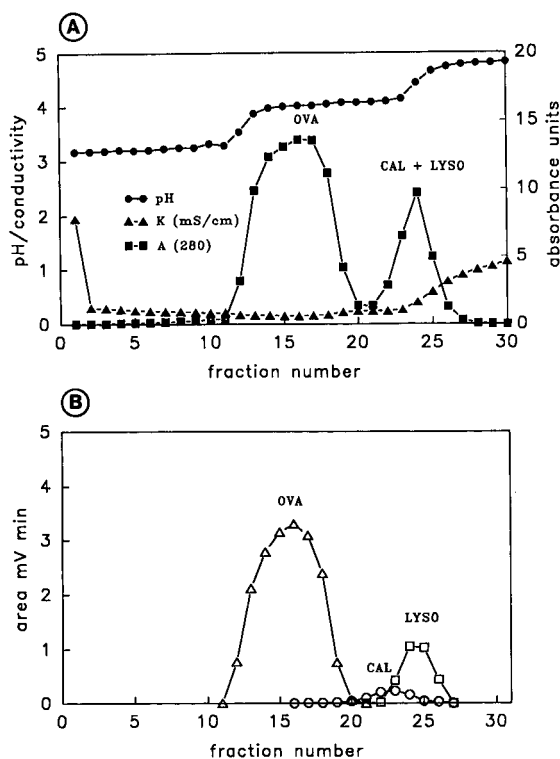


Fig. 1. RITP data after processing 710 mg of OVA and 15 mg of GABA. The voltages across the cell assembly at the beginning of counterflow (60 min) and at collection time (133 min) were 518 and 558 V, respectively. The total charge applied was 399 C. (A) Absorbance, pH and conductivity distributions measured on the collected fractions; (B) processed data of analytical capillary ITP runs on the Tachophor. Volumes of 1 μ l of the undiluted fractions and 1 μ l of a spacer mixture of GABA and TRIS were injected and analysed. For each fraction and protein the peak area of the UV signal (277 nm) was plotted.

separate the two proteins. Its net mobility, however, is too fast for proper separation with LYSO. Therefore no resolution was obtained using this spacer in RITP (data not shown). According to the analytical data (Fig. 2C), CREAT should be a suitable spacer for the separation of LYSO and CAL. However, the RITP data depicted in Fig. 3 show that this was not the case. In the first experiment (Fig. 3A) 7.54 mg of LYSO, 3.00 mg of CAL and 31.33 mg of CREAT were processed for 47 min and fractionated without counter flow. Significant mixing of the two proteins within the spacer zone was observed and no steady state was reached. The data from a similar experiment but with the application of

counter flow for 194 min are shown in Fig. 3B. Although the operation of counter flow improved the separation, some mixing between LYSO and CREAT was still present. Therefore, CREAT in that system cannot be used for an efficient RITP purification of LYSO. Furthermore, tetrabutylammonium (TBA, Fig. 2E) was too slow for the proper separation of the two proteins of interest. In RITP experiments, LYSO was strongly enriched at the front boundary of the spacer, but CAL was distributed across the entire TBA zone.

The best RITP results were obtained with tetrapropylammonium (TPA) as spacer, a configuration which also provided good analytical data (Fig. 2D). RITP data showing the removal of OVA and the separation of LYSO and CAL with TPA are presented in Fig. 4. The sample was composed of 740 mg OVA and 64 mg TPAB, processed for 60 min without counterflow followed by 206 min of manually controlled counterflow. GABA (0.05 M) was added to the anodic electrode solution and therefore acted as a terminator in the separation cell. This resulted in the accumulation of OVA at the membrane which separates the anodic electrode compartment from the cell (recycling channel 1) and its complete removal from the system during counterflow operation. Neither protein shows a plateau concentration at the given sample load. The peak concentration of LYSO (fraction 23) was 2.25 mg/ml. A similar example but with TPAB (0.05 M) instead of GABA as the additive to the anodic electrode solution is presented in Fig. 5. Here 710 mg of the OVA product was processed and counterflow was activated for 213 min. This configuration allowed the isolation and purification of LYSO alone. During that experiment, both OVA and CAL were first pushed by electromigration towards the membrane near the sample inlet and then swept out during counterflow operation. The total amount of LYSO in fractions 18–26 was determined to be 21 mg and its processing rate 4.6 mg/h. For that run analytical data obtained in both capillary instruments are shown in Figs. 6 and 7. Panels B of the two figures depict data obtained after injection of the commercial OVA product, which was spiked with GABA and TPAB. It was interesting that the small amount of CAL in the OVA sample could not be detected with a fused-silica capillary (Fig. 6B), but could be readily monitored in the PTFE capil-

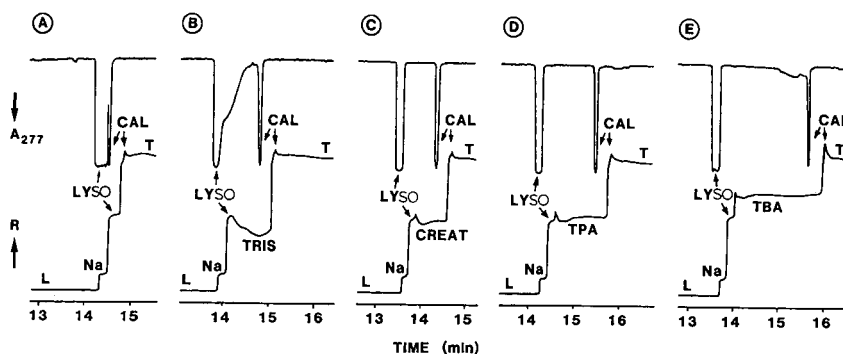


Fig. 2. Capillary ITP data obtained with model mixtures of commercial LYSO and CAL on the Tachophor. (A) Data without a low-molecular-mass spacer; (B-E) corresponding data with TRIS, CREAT, TPA and TBA as spacers, respectively. The lower and upper graphs represent the conductivity (expressed as a increase in resistance R) and UV absorbance at 277 nm, respectively. L = leader; T = terminator; Na = sodium impurity from electrolyte system.

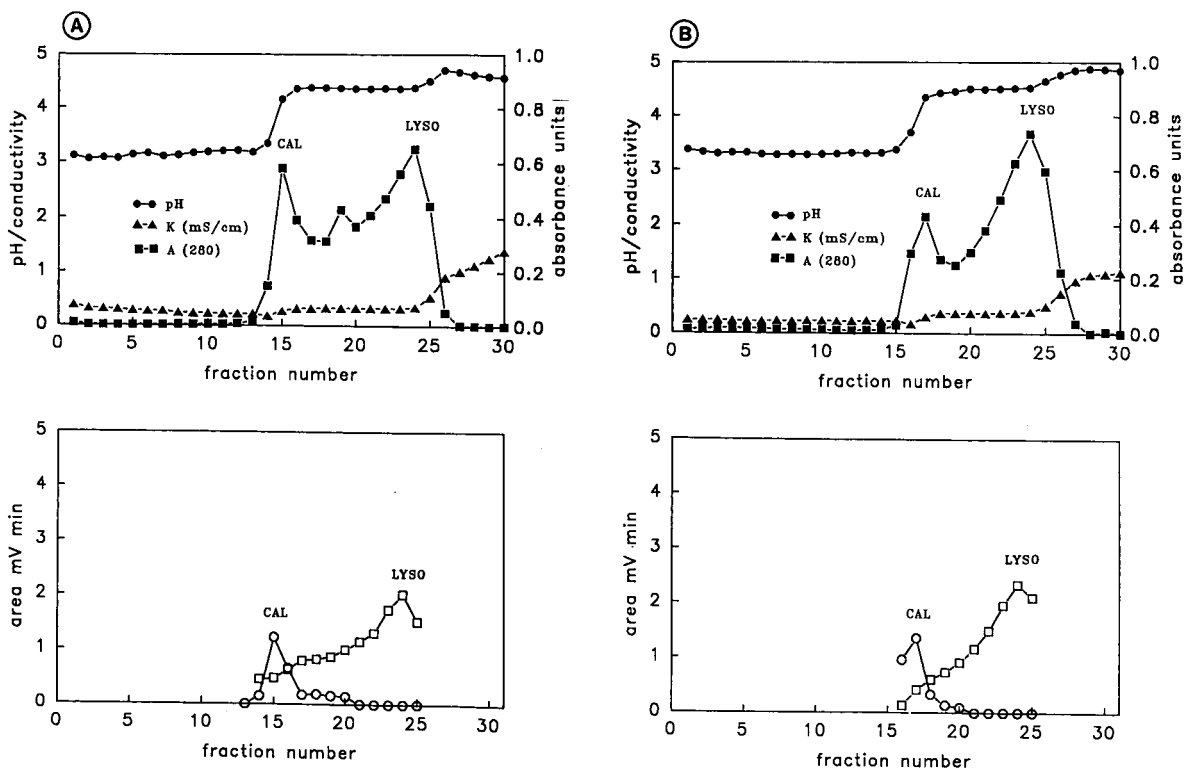


Fig. 3. (A) RITP data of LYSO (7.54 mg), CREAT (31.33 mg) and CAL (3.00 mg) after processing for 47 min (total charge 144 C) without counterflow; (B) Similar data with 7.00 mg LYSO, 31.87 mg CREAT and 3.00 mg CAL after running for 47 min without and 194 min with a manually controlled counterflow (total processing charge 737 C). The upper graphs depict absorbance, pH and conductivity distributions measured on the collected fractions. The lower graphs show processed data of analytical capillary ITP runs on the Tachophor. A 7- μ l volume of undiluted fractions spiked with additional CREAT was injected and analysed. Peak areas were determined with the PC pack.

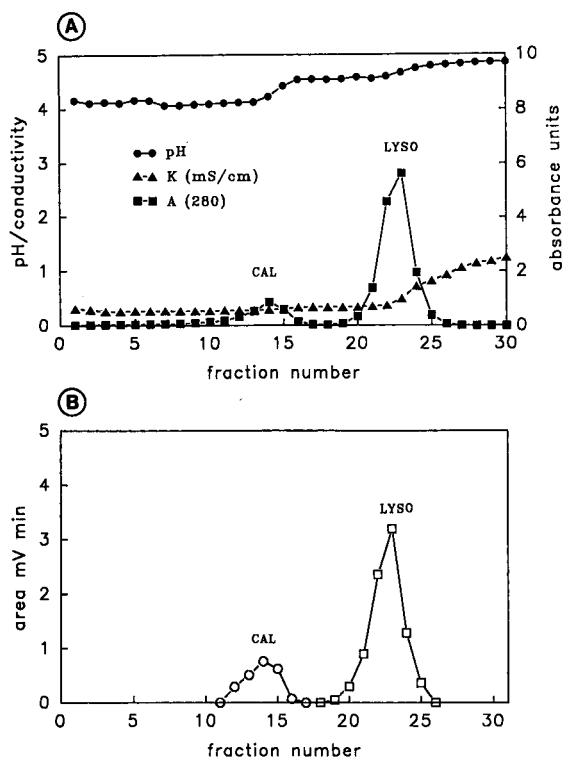


Fig. 4. RITP data after processing of 740 mg of OVA and 64 mg of TPAB with 0.05 M GABA in the terminating electrolyte. The total voltages at the beginning of counterflow and collection time were 354 and 404 V, respectively, and the total processing charge was 801 C. (A) Absorbance, pH and conductivity distributions measured on the collected fractions. The CAL-containing fractions were filtered prior to analysis. (B) Processed data of analytical capillary ITP runs on the Tachophor. A 1- μ l volume of undiluted fractions and 1 μ l of a spacer mixture of GABA and TPA were injected and analysed. Peak areas were determined with the PC pack.

lary (Fig. 7B) (see Gebauer and Thormann [12] for further explanations). The analysis of fraction 22 (with the addition of the same two spacers) is shown in panels C of the two figures. The isolated LYSO is fairly pure as determined by spectral analysis of the protein peak (Fig. 6).

Owing to a solubility restriction of the crude OVA product and a limitation of the applicable sample volume to about 10 ml at the beginning of a RITP run, not much more than 700 mg of the crude OVA product could be loaded onto the apparatus in one step. For this reason, other possibilities of sample introduction were investigated. Fig. 8 shows

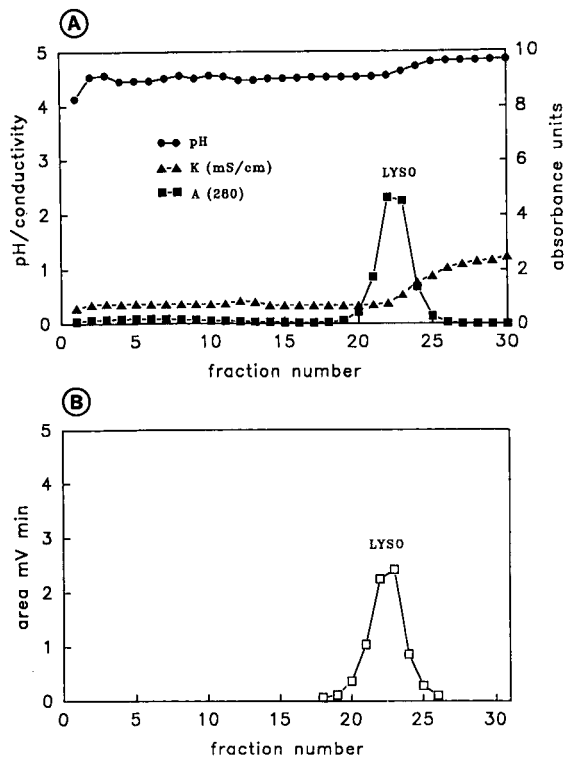


Fig. 5. RITP data after processing of 710 mg of OVA with a mixture of 0.05 M TPAB and 0.1 M acetic acid as terminator. The total voltages at the beginning of counterflow and collection time were 304 and 324 V, respectively, and the total charge was 819 C. The peak concentration of LYSO (fraction 22) was 1.86 mg/ml. Other conditions are the same as in Fig. 4.

a possible solution to increasing the sample load, *i.e.* using a continuous sample feed mode of operation during part of the experiment. In other respects, the run was similar to that shown in Fig. 5. First RITP was performed with 710 mg of crude OVA as described earlier and with applied counterflow for 60 min. Thereafter additional sample (710 mg of OVA dissolved in 110 ml of leader) was infused (1.91 ml/min) through counterflow action. This was followed by counterflow of pure leader for 78 min prior to sample collection. Analysis of fractions 16–27 revealed a yield of 46 mg of LYSO and the processing rate was 10.6 mg/h. Compared with the run depicted in Fig. 5 substantially more LYSO could be purified with the same amount of charge passed, but, at collection time, some residual OVA

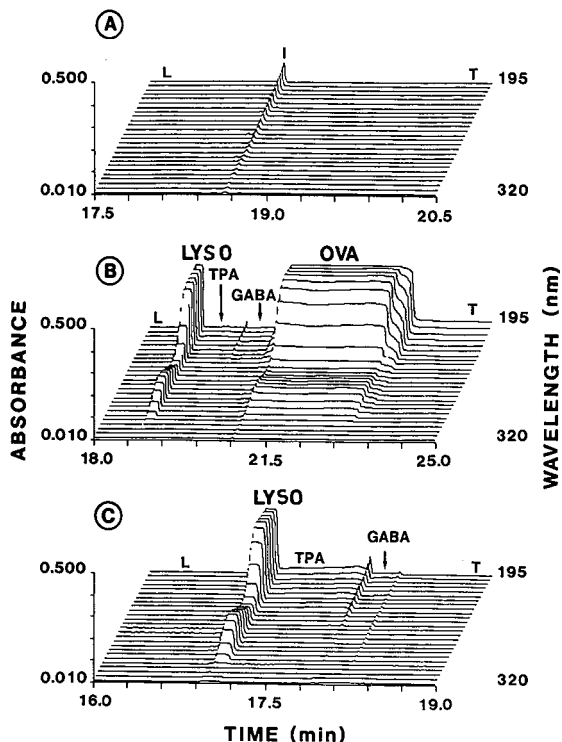


Fig. 6. Capillary ITP data of the purification depicted in Fig. 5 using a 75 μ m I.D. fused-silica capillary and a scanning UV absorbance detector towards the capillary end. (A) Blank; (B) analysis of commercial OVA spiked with GABA and TPAB; (C) analysis of fraction 22 together with the two spacers. L = leader; I = impurity; T = terminator.

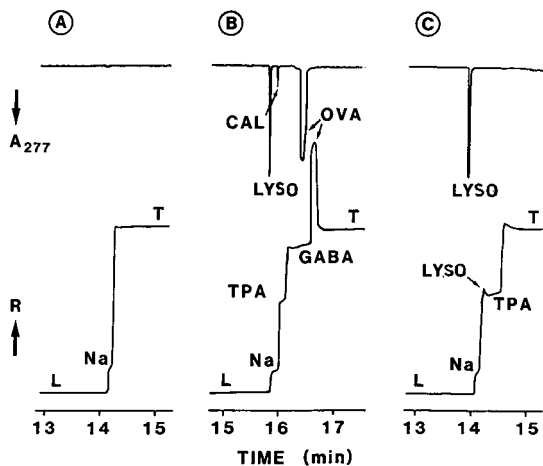


Fig. 7. Capillary ITP data of the purification depicted in Fig. 5 using the Tachophor analyser. Other conditions are the same as in Fig. 6.

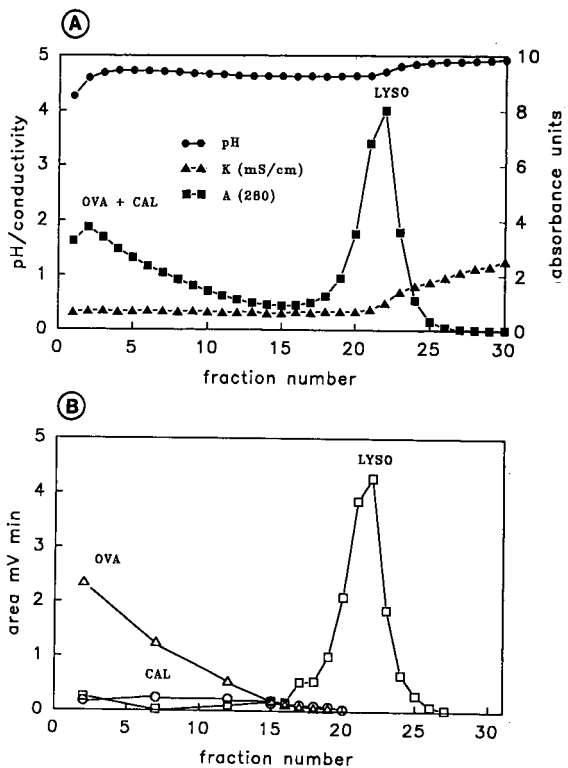


Fig. 8. RITP data of a run with first 710 mg of OVA (60 min until activation of a 60 min counterflow), then counterflow infusion of another 710 mg of OVA dissolved in the leader for 63 min, followed by a final counterflow operation for 78 min. The voltages across the cell at the beginning of counterflow, the beginning and end of counterflow sample infusion, and at collection time were 317, 327, 296 and 302 V, respectively. The total processing charge was 783 C. The peak concentration of LYSO (fraction 22) was 3.2 mg/ml. Other conditions are the same as in Fig. 5.

and CAL were still present in the processing solution.

CONCLUSIONS

RITP is an attractive free-fluid electrophoretic approach for the fractionation of proteins. Depending on selected spacers and working conditions both minor and major proteins can be separated and purified from the same crude sample. The data on the purification of LYSO (up to 10 mg/h) from a commercial OVA sample demonstrate the capability of using RITP to isolate a minor component (here approximately 3% of the protein content),

whereas the RITP purification of OVA itself (300 mg/h) represents an attractive polishing step for that protein. Scale-up to higher throughputs and a continuous mode of operation are the subjects of forthcoming investigations.

ACKNOWLEDGEMENTS

The generous loan of the Tachophor 2127 by LKB (Bromma, Sweden) is gratefully acknowledged. The authors thank Kontron (Zürich, Switzerland) for the loan of a PC integration pack. P.G. acknowledges his employer for granting study leave. This work was supported by the Swiss National Science Foundation.

REFERENCES

- 1 C. J. Holloway and R. V. Battersby, *Methods Enzymol.*, 104 (1984) 281, and references cited therein.
- 2 J. E. Sloan, W. Thormann, G. E. Twitty and M. Bier, *J. Chromatogr.*, 457 (1988) 137.
- 3 R. Kuhn and H. Wagner, *Electrophoresis*, 10 (1989) 165.
- 4 S. Hoffstetter-Kuhn, R. Kuhn and H. Wagner, *Electrophoresis*, 11 (1990) 304.
- 5 W. Thormann, M. A. Firestone, J. E. Sloan, T. D. Long and R. A. Mosher, *Electrophoresis*, 11 (1990) 298.
- 6 J. Caslavka, P. Gebauer, A. Odermatt and W. Thormann, *J. Chromatogr.*, 545 (1991) 315.
- 7 G. Schmitz, A. Boettcher, H. G. Kahl and T. Brüning, *J. Chromatogr.*, 431 (1988) 327.
- 8 G. Nowicka, T. Bruening, B. Grothaus, G. Kahl and G. Schmitz, *J. Lipid Res.*, 31 (1990) 1173.
- 9 H. L. Fevold, *Adv. Protein Chem.*, 6 (1951) 187.
- 10 M. Bier and N. B. Egen, in H. Haglund, J. W. Westerfield and J. T. Ball (Editors), *Electrofocuss '78*, Elsevier North Holland, Amsterdam, 1979, pp. 35-48.
- 11 P. Gebauer and W. Thormann, *J. Chromatogr.*, 545 (1991) 299.
- 12 P. Gebauer and W. Thormann, *J. Chromatogr.*, 558 (1991) 423.

Preparative high-yield electroelution of proteins after separation by sodium dodecyl sulphate–polyacrylamide gel electrophoresis and its application to analysis of amino acid sequences and to raise antibodies

Toshitaka Ohhashi, Chie Moritani, Hiromi Andoh, Sachiko Satoh and Shinji Ohmori
Faculty of Pharmaceutical Sciences, Okayama University, Tsushima-Naka-1, Okayama 700 (Japan)

Friedrich Lottspeich

Gene Center of the Max-Planck-Institute for Biochemistry, Am Klopferspitz 18a, 8033 Martinsried (Germany)

Mikiko Ikeda*

Faculty of Pharmaceutical Sciences, Okayama University, Tsushima-Naka-1, Okayama 700 (Japan)

(First received February 27th, 1991; revised manuscript received May 24th, 1991)

ABSTRACT

A method for the preparative high-yield electroelution of proteins from sodium dodecyl sulphate (SDS) polyacrylamide gel strips was established. The method consisted of SDS–polyacrylamide gel electrophoresis, detection of proteins with sodium acetate and electrophoretic elution at 200 V for 3 h by utilizing a horizontal flat-bed gel electrophoresis apparatus. Standard proteins with molecular masses of 14–66 kilodalton (cytochrome *c*, aldolase, ovalbumin and bovine serum albumin) were recovered with an average yield of 73.6 ± 2.3%. A membrane-bound protein, rat skeletal muscle Ca²⁺-ATPase (100 kilodalton) was also well recovered (over 60%). This method was applicable to the purification of proteins required for N-terminal amino acid sequencing and to raise antibodies.

INTRODUCTION

Sodium dodecyl sulphate–polyacrylamide gel electrophoresis (SDS-PAGE) is a powerful technique for the separation of complex protein mixtures not only on an analytical scale but also on a preparative scale. Several methods for the extraction of proteins from gels have been reported: diffusion of protein from crushed gel slices [1], electroelution [2], electrophoretic transfer onto surface-modified glass fibre (SGF) [3–5] and extraction with solvents [6,7].

During our studies on a Cl⁻-translocating ATPase isolated from *Acetabularia acetabulum* [8,9], protein chemical characterization was carried out to obtain information on the primary structure. The

N-terminal sequences of the subunits, a (54 kilodalton) and b (50 kilodalton), were obtained by the direct sequencing of the electroblotted proteins onto SGF sheets [3]. Both subunits separated by SDS-PAGE were subjected to chemical cleavage using CNBr, NCS and NH₂OH on gel slices, and fragments were also separated by SDS-PAGE and subjected to electroblotting and sequencing from the N-terminus. Several sequences were successfully obtained, but CNBr-cleaved fragments gave mixed sequences in most instances [10].

Preparative separation of the respective subunits was thus required. For this purpose, we applied chromatofocusing on Mono P and reversed-phase high-performance liquid chromatography (RP-HPLC) on C₄, C₈ and C₁₈ columns, which were,

however, unsuccessful. SDS-PAGE was the only means of separating the respective subunits. Sakakibara *et al.* [11] reported the electrophoretic separation of proteins on SDS-agarose gel and also described the extraction of proteins from agarose gels. We have applied this method to our proteins, but the recoveries were very low (<5%). As reported by Tsugita *et al.* [7], extraction of proteins with 70% formic acid was also tried using bovine serum albumin (*ca.* 100 μg) and the recovery was less than 5%. Several types of apparatus for electroelution are commercially available, but a larger gel piece, *i.e.* a relatively large amount of protein, cannot be processed at one time. The aim of this study was to separate the a and b subunits on a preparative scale (> 100 μg), to digest the respective subunits by proteases, to purify the fragments by RP-HPLC and to subject them to automatic N-terminal sequencing. In this paper, a simple and preparative method for the electroelution of proteins from gel strips is described, which is applicable to the purification of proteins required for amino acid sequence analysis and to raise antibodies.

EXPERIMENTAL

Chemicals and instruments

Bovine serum albumin (BSA), ovalbumin (OVA), cytochrome *c*, *Staphylococcus aureus* V₈ protease (type XVIII) and trypsin (type III) were purchased from Sigma (St. Louis, MO, USA). Aldolase from rabbit muscle was obtained from US Biochemical (Cleveland, OH, USA) and Extracti-Gel D from Pierce (Rockford, IL, USA). Dialysis tubes were obtained from Sanko Junyaku (Tokyo, Japan) and closers of dialysis tubes from Spectrum (Los Angeles, CA, USA). Centricon YM-10 and YM-30 and YM-30 membranes from Amicon (Grace, Danvers, MA, USA) were used for the concentration of proteins, and a Konica Immunostain HRP kit (Konica, Tokyo, Japan) for detection of reactions with antibodies. Acetonitrile of HPLC grade was purchased from Kanto Chemical (Tokyo, Japan). Other reagents of analytical-reagent grade were purchased from Wako (Osaka, Japan).

A fast protein liquid chromatographic (FPLC) system and a Mono Q HR5 column from Pharmacia (Uppsala, Sweden) were used for the purification of proteins, and a Waters Assoc. Model 600E

HPLC system for the separation of protease-digested fragments. A Wakosil 5C18 reversed-phase HPLC column (150 mm \times 4 mm I.D.) was obtained from Wako.

Purification of proteins

Ca²⁺-ATPase was isolated from rat skeletal muscle according to the method described by MacLennan [12]. However, Ca²⁺-ATPase was not completely purified and the final preparation showed a major band around 100 kilodalton and several minor bands with molecular masses <100 kilodalton on SDS-gel. The 100-kilodalton polypeptide was therefore purified by electroelution as described here.

CF₁-ATPase was purified from spinach leaves as described by Binder *et al.* [13].

Ribulose-1,5-bisphosphate carboxylase (RubisCo) was isolated from crude chloroplast-rich fraction of *A. acetabulum* prepared as follows. Axenic cells of *A. Acetabulum* (3–5 cm long, 58 g wet weight) were cut into small pieces with scissors, suspended in a homogenization buffer consisting of 50 mM piperazine-N,N'-bis-2-ethanesulphonic acid (PIPES)-Tris buffer (pH 7.6), 0.55 M sorbitol, 0.5 M sorbitol, 0.5 mM MgSO₄ and 2 mM dithiothreitol (DTT) (100 ml) and stirred for 2–3 min. The cell extracts were passed through four layers of gauze. Cell debris was treated twice in the same manner. All the cell extracts (*ca.* 300 ml) were centrifuged at 5000 *g* for 2 min. The precipitates were resuspended in the homogenization buffer (100 ml) and centrifuged as described above. The washed pellets were suspended in 10 mM NaCl (30 ml) and centrifuged at 12 000 *g* for 10 min. The pellets were washed twice with 10 mM NaCl. All the supernatants (*ca.* 30 ml) were combined and concentrated by ultrafiltration in an Amicon cell with a YM-30 membrane filter. The concentrated fraction was applied to a Mono Q HR 5 column, which had previously been equilibrated with a buffer containing 25 mM PIPES-Tris buffer (pH 7.0), 0.25 M sorbitol, 6 mM MgSO₄ 1 mM ethylene glycol 1-bis(β -aminoethyl ether) N,N,N',N'-tetraacetic acid, 2 mM DTT and 0.125 mM phenylmethanesulphonyl fluoride (PMSF). Proteins were eluted by a linear increase in Na₂SO₄ from 0 to 0.2 M [8]. RubisCo was eluted at about 150 mM Na₂SO₄, concentrated and desalted by ultrafiltration and stored at –70°C.

SDS-PAGE

In most experiments 10% acrylamide gels were prepared according to the method of Laemmli [14] either on mini gels or preparative gels. For separation of cytochrome *c* 12.5% gels were used.

Electrophoretic elution of proteins from gel strips

After SDS-PAGE, proteins were revealed as transparent bands with 4 M sodium acetate solution [15] and excised using a razor blade. Proteins in gel strips were fixed in 50% (v/v) methanol solution for 15 min. They were then equilibrated twice in 0.125 M Tris-HCl buffer (pH 6.8) and 2% 2-mercaptoethanol for 15 min each. Equilibration of gel strips in the above buffer with 1% (w/v) SDS were performed as described above. The equilibrated gel strips were inserted in a dialysis tube with a minimum amount of the buffer with SDS (25 mM Tris, 190 mM glycine and 0.1% SDS, see below). The dialysis tubes were treated and electroelution was carried out in similar manners to those described by Findlay [16]. In this work, a horizontal flat-bed mini-gel electrophoresis apparatus (Renner, Darmstadt, Germany) was used for electroelution at 200 V for 3 h at 4°C. The buffer consisted of 25 mM Tris, 190 mM glycine and 0.1% SDS (pH 8.3). At the end of electrophoresis, the polarity of electrodes was changed for 30 s in order to avoid the adsorption of proteins on the dialysis tubes. The buffer inside the dialysis tubes was collected and the tubes were washed three times with a minimum volume of the buffer and concentrated by using Centricon YM-30 or YM-10.

Removal of SDS from the sample solution

The concentrated sample solution (100–200 μ l, 1–2 mg protein/ml) was applied to an Extracti-gel D detergent-removing gel, which had previously been equilibrated with 50 mM Tris-HCl buffer (pH 8.0). The effluent was collected and concentrated by ultrafiltration as described above.

Digestion with proteases

The sample solution was added to 0.1% (w/v) SDS and proteases in a weight ratio of 50:1 (protein to protease) and digested at 37°C overnight. After digestion, the sample solution was stored at –20°C.

Purification of the digested fragments by RP-HPLC

The digested solution was added to formic acid at a final concentration of *ca.* 10% (v/v) and centrifuged at 15 000 g for 5 min, then the supernatant was applied to an RP-HPLC column. The solvents used for HPLC were 0.1% (v/v) trifluoroacetic acid (TFA) in water (solvent A), and 0.1% TFA and 60% (v/v) acetonitrile (solvent B), with a linear gradient from 0 to 100% solvent B in 60 min. The flow-rate was 1 ml/min. Chromatography was performed at 40°C. The peaks were collected and rechromatographed by RP-HPLC with a minute change in the linear gradient of acetonitrile. The collected sample solutions were evaporated under reduced pressure by using a Speed-Vac concentrator (Savant). The residues were dissolved in doubly distilled, deionized water and subjected to N-terminal sequencing.

N-Terminal sequencing based on Edman degradation

Amino acid sequence analysis based on Edman degradation was performed on a Model 470A gas-phase protein/peptide sequencer and a Model 120A-01 on-line PTH analyser (Applied Biosystems, Foster City, CA, USA).

Protein determination

Proteins were determined by the method described by Heil and Zillig [17]. BSA was used as a standard protein. When the recoveries of standard proteins (BSA, OVA, aldolase and cytochrome *c*) were determined, the respective protein solution was used as standard.

Antibodies

The CF₁ complex (α , β , γ , δ and ϵ subunits) was prepared as described above, and the respective subunits were separated by electroelution as described here. Ca²⁺-ATPase from rat skeletal muscle was also purified by electroelution.

The respective protein solution (200–500 μ g of protein in 0.5 ml) was added to 0.5 ml of Freund's Complete Adjuvant (Difco) and an emulsion was prepared. Male albino rabbits (*ca.* 2.5 kg body weight) were immunized intramuscularly and subcutaneously. After 2 weeks, rabbits were again immunized with 125–250 μ g protein in the same manner. After 1 week, whole blood was collected and the serum was separated and stored frozen at

–20°C. The reactions of the proteins with the antibodies were tested by Western blotting as described by Ikeda *et al.* [8], except that a Konica Immunos-tain HRP kit was used for detection of the reactions.

RESULTS

Recoveries of standard proteins from gel slices by electroelution

Recoveries of standard proteins from gel slices by the present method are summarized in Table I, and ranged from 70 to 75.2% for 14–66-kilodalton proteins. The 100-kilodalton protein Ca²⁺-ATPase was eluted at 200 V for 6 h, after SDS-PAGE on 10% acrylamide gel, and the recovery was above 60%. Recoveries of proteins from the Extracti-gel D column were about 90%, when removal of SDS is required.

Application to raise antibodies

The results are shown in Fig. 1. The respective antiserum against the α , β , γ , δ and ϵ subunits of the the CF₁ complex from spinach and the antiserum against Ca²⁺-ATPase showed high specificity as in Fig. 1. The antisera against the respective CF₁ component did not show any cross-reactivity with Ca²⁺-ATPase and *vice versa* (data not shown).

Application to N-terminal sequencing

RubisCo was isolated from *A. Acetabulum* and the large subunit (53 kilodalton) was separated by electroelution as described. The recovery was 77% when RubisCo (272 μ g of protein) was separated by

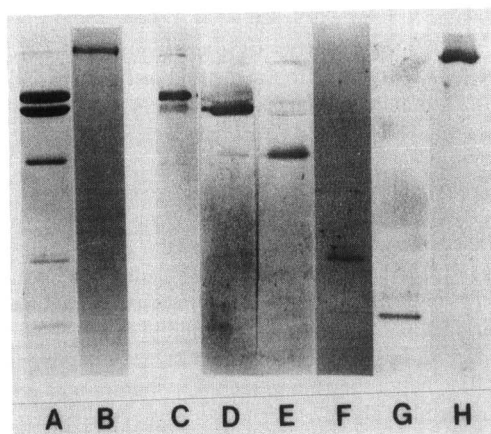


Fig. 1. Immunoblot of spinach CF₁ components (α , β , γ , δ and ϵ subunits) and rat skeletal muscle Ca²⁺-ATPase. Purified CF₁ complex (ca. 4 μ g) and Ca²⁺-ATPase (ca. 2 μ g) were subjected to SDS-PAGE and to immunoblotting. The reactions with the respective antiserum (diluted 1:250 to 1:500) were performed at room temperature for 1 h, and were revealed by using a Konica Immunos-tain HRP kit. Lanes: A and B = Coomassie Blue stain of the isolated CF₁ complex and Ca²⁺-ATPase, respectively; C = reaction of the CF₁ complex with the antiserum against the α subunit (diluted 1:500); D = reaction of the CF₁ complex with the anti- β serum (1:500); E = reaction of the CF₁ complex with the anti- γ serum (1:500); F = reaction of the CF₁ complex with the anti- δ serum (1:250); G = reaction of the CF₁ complex with the anti- ϵ serum (1:500); H = reaction of Ca²⁺-ATPase with the antiserum against Ca²⁺-ATPase (1:500).

preparative SDS-PAGE (3 cm wide \times 11 cm long \times 1.5 mm thick) (10%) and electroeluted.

The elution patterns of RubisCo large subunit from *A. Acetabulum* are shown in Fig. 2a and b

TABLE I
RECOVERIES OF STANDARD PROTEINS FROM GEL STRIPS

BSA, OVA and aldolase were subjected to SDS-PAGE using 10% gel and cytochrome *c* using 12.5% gel.

Standard protein	Amount of protein applied (μ g)	Amount of protein recovered (μ g)	Recovery (%)
BSA (66 kilodalton)	110	81.1 \pm 4.4 (<i>n</i> = 4)	73.7
OVA (45 kilodalton)	110	82.5 \pm 2.8 (<i>n</i> = 4)	75.0
Aldolase (40 kilodalton)	75	52.7 \pm 7.1 (<i>n</i> = 3)	70.3
Cytochrome <i>c</i> (14.3 kilodalton)	150	113 \pm 6.3 (<i>n</i> = 3)	75.2

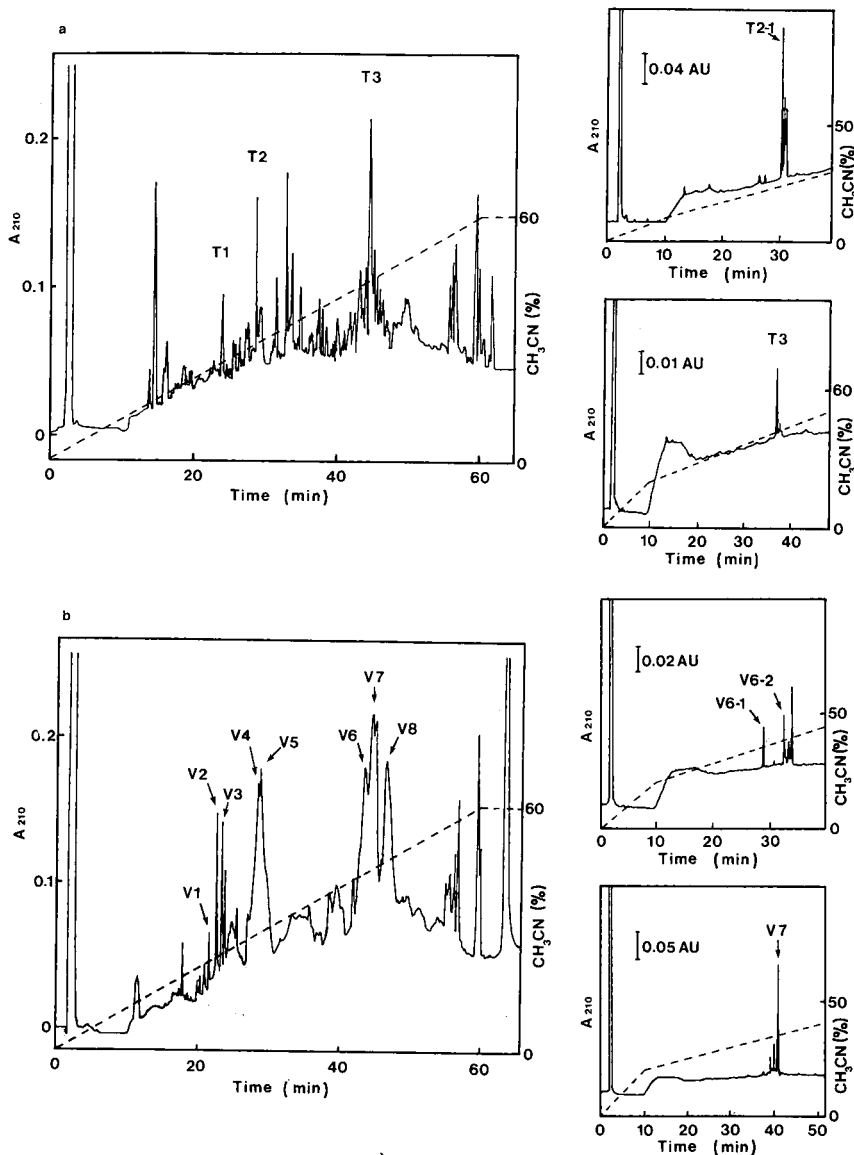


Fig. 2. High-performance liquid chromatograms of Rubisco large subunit after (a) Trypsin and (b) V_8 protease digestions. (a) Rubisco large subunit (ca. 180 μg) was digested with trypsin at 37°C overnight and chromatographed as described under Experimental. In the two chromatograms on the right, examples of rechromatography of peaks T_2 and T_3 are shown. (b) Rubisco large subunit (ca. 300 μg) was digested with V_8 protease at 37°C overnight. In the two chromatograms on the right examples of rechromatography of peaks V_6 and V_7 are shown.

after trypsin and V_8 protease digestion, respectively. The amino acid sequences obtained from the purified fragments are summarized in Table II. The data support the close similarity (56–100%) of Rubisco from *A. acetabulum* to those of alfalfa Rubisco large subunit.

DISCUSSION

The electroelution method presented here is a combination of SDS-PAGE, detection with sodium acetate (but not with Coomassie Blue dyes), which facilitate evaluation of the protein concentrations

TABLE II

AMINO ACID SEQUENCES OBTAINED FROM *A. ACETABULUM* RUBISCO LARGE SUBUNIT

Single-letter coding for amino acids used.

Digestion		Amino acid sequence ^a	Alignment ^b
Trypsin	T1	<i>AGAGF</i>	ATVGF
	T2-1	<i>LNATAPT(S)ETMLQR</i>	LNATAGTCEEMMKR
	T3	<i>LTYYPDPYQVLGTXVL</i>	LTYYPDPYETKDTDIL
V ₈ protease	V1-1	<i>AXVQARNE</i>	ACVQARNE
	V1-2	<i>AIYK</i>	AIYK
	V2	<i>YAAAVAAE</i>	AGAAVAAE
	V3-1	<i>LAAAXE</i>	LAAACE
	V4-2	<i>G/NGDIIR</i>	GGDHIH
	V6-2	<i>IF(T/G)DDAXLQFGGGTLG</i>	IFGDDSVLQFGGGTLG
	V7	<i>SSTGT(W)TTV(W)T(D)GXT</i>	SSTGTWTTVWTDGLT
	V8-1	<i>TKAGAGFXAGVXXYRL</i>	TKATVGFKAGVKDYRL
	V8-2	<i>(D/N)LRIPQ(S)FVTTFLGVV</i>	DLRIPAAVYVKTFQGGP

^a Identical amino acids are italicized.^b Alfalfa chloroplast RubisCo large subunit.

and electrophoretic elution of proteins from gel strips with high recoveries, which is similar to electroelution of DNA from agarose gel strips. The most important point was the fixation of proteins in gel strips by 50% methanol, as without fixation diffusion of proteins occurred, which led to lower recoveries of proteins.

The technique presented here has following advantages: it does not require special expensive apparatus and reagents, preparative-scale amounts of proteins can be processed, it is not time consuming and takes about 8 h to obtain pure proteins or subunits, proteins are eluted under mild conditions and therefore little degradation of proteins occurs, it is applicable not only to soluble proteins but also to membrane-bound proteins and it is applicable to raise antibodies and to the N-terminal sequencing.

Of course, as mentioned in the Introduction, numerous methods for the isolation of proteins or subunits have been reported. We have also tried several of those methods for our purposes, but were unsuccessful. For example, an electroendosmotic preparative electrophoresis unit (Genefit) purchased from Funakoshi Pharmaceutical (Tokyo, Japan) did not allow the separation of OVA (45 kilodalton) and BSA (66 kilodalton), the procedure is troublesome and the apparatus is expensive. The extraction of proteins from gel slices with 70% for-

mic acid was not suitable on a preparative scale (> 100 µg of protein). Feick and Shiozawa [6] reported extraction of proteins with formic acid-acetonitrile-isopropanol-water, and this method gave high recoveries for several hydrophobic proteins. This method, however, has the disadvantage that acid-labile proteins cannot be processed by the method. SDS-agarose gel electrophoresis as described by Sakakibara *et al.* [11] gave poor resolution of proteins such as α (56 kilodalton) and β (50 kilodalton) subunits of CF₁-ATPase from spinach. In addition, 3–4% agarose gels are difficult to prepare and the use of, for example, NuSieve or low-melting agarose is too expensive for the separation of proteins on a preparative scales. A similar method to that reported in this paper has already been presented by Findlay [16]. However, no details of recoveries and no application data were reported.

With the present method, one could readily obtain milligram amounts of proteins or polypeptides, which is applicable to raise antibodies and N-terminal sequencing after protease digestion.

REFERENCES

- 1 D. A. Hager and R. R. Burgess, *Anal. Biochem.*, 109 (1980) 76.
- 2 R. M. Hewick and M. W. Hundkapiller, in A. Darbre and M.

- D. Waterfield (Editors), *Practical Protein Chemistry — A Handbook*, Wiley, Chichester, 1986, pp. 473–490.
- 3 R. H. Aebersold, D. B. Teplow, L. E. Hood and S. B. H. Kent, *J. Biol. Chem.*, 261 (1986) 4229.
 - 4 C. Vandekerckhove, G. Bauw, M. Puype, J. Van Damme and M. Van Montagu, *Eur. J. Biochem.*, 125 (1985) 9.
 - 5 C. Eckerskorn, W. Mewes, H. Goretzki and F. Lottspeich, *Eur. J. Biochem.*, 176 (1988) 509.
 - 6 R. G. Feick, and J. A. Shiozawa, *Anal. Biochem.*, 187 (1990) 205.
 - 7 A. Tsugita, T. Ataka and T. Uchida, *J. Protein Chem.*, 6 (1987) 121.
 - 8 M. Ikeda, R. Schmid and D. Oesterhelt, *Biochemistry*, 29 (1990) 2057.
 - 9 M. Ikeda and D. Oesterhelt, *Biochemistry*, 29 (1990) 2065.
 - 10 T. Ohhashi, C. Moritani, F. Lottspeich, D. Oesterhelt and M. Ikeda, unpublished results.
 - 11 R. Sakakibara, N. Tominaga, A. Sakai and M. Ishiguro, *Anal. Biochem.*, 162 (1987) 150.
 - 12 D. H. MacLennan, *Methods Enzymol.*, 32 (1974) 291.
 - 13 A. Binder, A. Jagendorf and E. Ngo, *J. Biol. Chem.*, 253 (1978) 3094.
 - 14 U. K. Laemmli, *Nature (London)*, 227 (1970) 680.
 - 15 R. C. Higgins and M. E. Dahmus, *Anal. Biochem.*, 93 (1979) 257.
 - 16 J. B. C. Findlay, in B. D. Hames and D. Rickwood (Editors), *Gel Electrophoresis of Proteins — A Practical Approach*, Academic Press, New York, 2nd ed., 1990, pp. 83–89.
 - 17 A. Heil and W. Zillig, *FEBS Lett.*, 11 (1970) 165.

Short Communication

Data compression in computerized signal processing for isocratic chromatography

J. C. Reijenga

Laboratory of Instrumental Analysis, University of Technology, 5600 MB Eindhoven (Netherlands)

(First received February 22nd, 1991; revised manuscript received June 17th, 1991)

ABSTRACT

A data compression technique for isocratic liquid or isothermal gas chromatography is introduced that effectively stores the information contained in the chromatogram in a reduced-size array. The resulting compressed peaks have an approximately uniform width, which is an obvious advantage for the peak detection and integration algorithm. For identification, the apparent retention times in the compressed array are used, the reproducibility of which does not deteriorate with respect to the original signal. Some improvement of the signal-to-noise ratio is seen.

INTRODUCTION

The computerized signal acquisition of Gaussian-shaped signals originating from chromatographic detection generally requires choosing an optimum sampling rate (number of data points per second). The number of data points per σ of the Gaussian peak shows such an optimum rate of approximately 5, assuring an adequate description of the Gaussian profile. For non-Gaussian or tailing peaks, an adequate description of the peak requires a larger number of data points [1,2].

When too large a sampling frequency is chosen, over-sampling occurs. The disadvantages of over-sampling are: the inefficient use of computer memory, increased sensitivity to high-frequency disturbances (resulting in spikes) and possibly a loss of speed in the integration algorithm. Under-sampling leads to the loss of information with respect to identification (retention time) and quantitation (peak area). Most data acquisition hardware uses a constant sampling rate, matched by the rule of thumb

outlined above. In isocratic liquid or isothermal gas chromatography, however, where the peaks become broader as retention increases, this rapidly leads to an over-sampling of the signal at increasing retention times.

This paper describes a method of data compression for sampled chromatographic signals that adapts the apparent sampling rate to minimize the amount of memory needed to store the information contained in the chromatogram.

DATA COMPRESSION

Consider a sampled isocratic chromatogram contained in an array of n points. The initial sampling rate is adjusted so that the standard deviation of the earliest peak, σ_1 , is sampled by at least p points. The σ values of subsequent peaks are larger than σ_1 and can be calculated from the plate number, N , of those peaks.

The plate number is first assumed constant over the k' range considered and is equal to:

$$N = (i/\sigma_i)^2 \quad (1)$$

in which σ_i is the standard deviation at retention time i , both in dimensionless units of data points. Data compression now compresses each data point by a reduction factor k_i . This reduction factor k_i is unity at the beginning of the chromatogram and gradually increases with increasing retention time. The standard deviation σ should be sampled p times after data compression, so that:

$$k_i = \sigma_i/p \quad (2)$$

with the restriction that k is not less than unity. With this restriction, the combination of eqns. 1 and 2 yields:

$$k_i = 1 + i/pN^{1/2} \quad (3)$$

In the compressed array, several data points are combined, with $1/k_i$ as a weighing factor, into one new point. If n is the number of points in the original array, then the number of points in the reduced array, m , can be calculated by summation of $1/k_i$ over all i values:

$$m = \sum_{i=1}^n 1/k_i = \sum_{i=1}^n pN^{1/2}/(pN^{1/2} + i) \quad (4)$$

The implications of eqn. 4 are that much is to be gained from data compression at low plate numbers, where peaks become broader at relatively short retention times. Not much is to be gained at very high plate numbers. The break-even value of n/m is unity.

An important factor is the number of data points per σ required. A number of rules of thumb are in use, ranging from 1 to 10 [3-5], depending on the aim of data acquisition (*e.g.* determination of retention, peak area, peak moments, exact reconstruction). For normal integration purposes $p = 5$ is acceptable.

In Fig. 1, m is plotted *versus* n on log scales for different plate number N and $p = 5$ points per σ . The values were calculated by summation of eqn. 4. From this figure it can be concluded that, for a given value of p , the net gain depends on the plate number (N) and on the size of the original data array (n). Peak-to-peak differences in plate numbers, especially in high-performance liquid chromatography, are due to a number of effects which are beyond the scope of this paper [1,6]. The effect of these fluctuations is limited by the square-root term in eqns. 3 and 4.

When compressing such a chromatogram, there are two options: (1) to be safe, a larger value of p can be used; and (2) a better strategy is to take a plate number slightly higher than the highest value

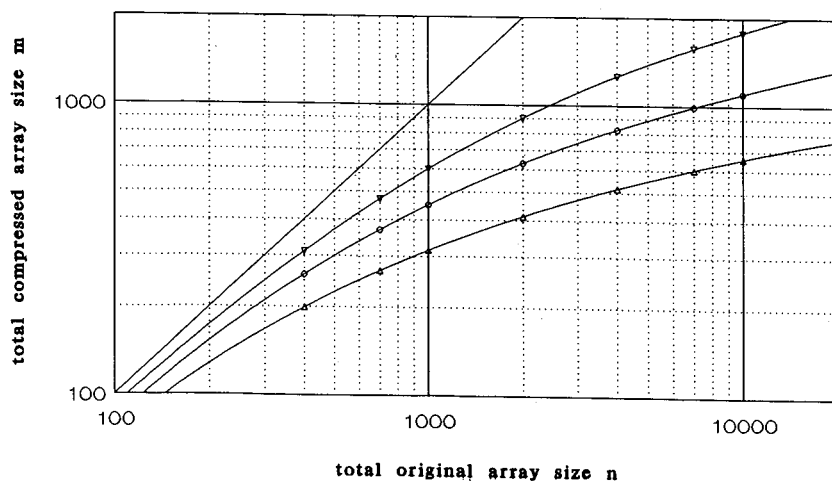


Fig. 1. Size of the reduced data array (m) plotted *versus* the size of the original data array (n) at different plate numbers, using eqn. 4. Peaks are compressed to $p = 5$ data points per σ . The straight line represents the break-even point in terms of array size, the other curves are fourth-order polynomial fits to the points indicated: (Δ) $N = 1000$; (\circ) $N = 4000$; (∇) $N = 16000$.

expected from different peaks. In this instance the signal can never be over-compressed.

Real-time or post-run compression

The compression algorithm is executed fairly fast compared with the corresponding analysis time. Consequently, a choice can be made between real-time and post-run compression. If the data acquisition rate is sufficiently low not to be limited by the conversion rate of the hardware used, real-time compression can be considered. The advantage of this is that full use can be made of the reduction of the memory required.

Retention data after compression

When comparing the chromatograms, compressed in an identical manner, the reproducibility of the apparent retention times is not deteriorated with respect to the original retention times. This can be explained by the non-linear relationship between the original and compressed time axes (Fig. 1).

If, in addition, values for k' or real retention times are required, the additional information on the compression factor, stored in a separate array, is necessary. To obtain a real retention time, values in this array are accumulated up to the corresponding apparent retention time (in units of data points). However, exact reconstruction of the original raw data is not possible because of the averaging performed by the compression algorithm.

Signal amplitude after compression

An additional advantage of this data compression technique is that the signal-to-noise ratio is improved when $k_i > 1$.

Compression decreases the amplitude of the random white noise. A net gain of $k_i^{1/2}$ for the signal-to-noise results [2,7], which is especially of importance at longer retention times.

Temperature-programmed or gradient elution chromatography

In temperature-programmed gas chromatography or gradient elution liquid chromatography, a dynamic change in retention behaviour generally results in chromatograms in which the peak width is less dependent on the retention time [1]. Most often, the highest plate numbers are calculated from peaks with long retention times.

If the sampling rate of the initial data acquisition is adjusted so that the first peak is sampled by, for instance, 5 points per σ (and N is calculated from the last peak), compression offers few advantages, but the application of the compression algorithm does not lead to a loss of information.

RESULTS AND DISCUSSION

Computer simulations were carried out using an ordinary XT-type personal computer with an 8087 co-processor. Any high-level programming language, supporting the use of a co-processor and the available graphics display, can be applied. Quickbasic 4.5 (Microsoft) was used in this work; the source of the algorithm is available from the author on request.

Fig. 2a shows a simulated chromatogram of 5000 data points with 2500 plates. Because of the limitation of the resolution of the graphics screen (EGA or CGA), the representation is limited to each 16th point. After compression with $p = 5$ points per σ ,

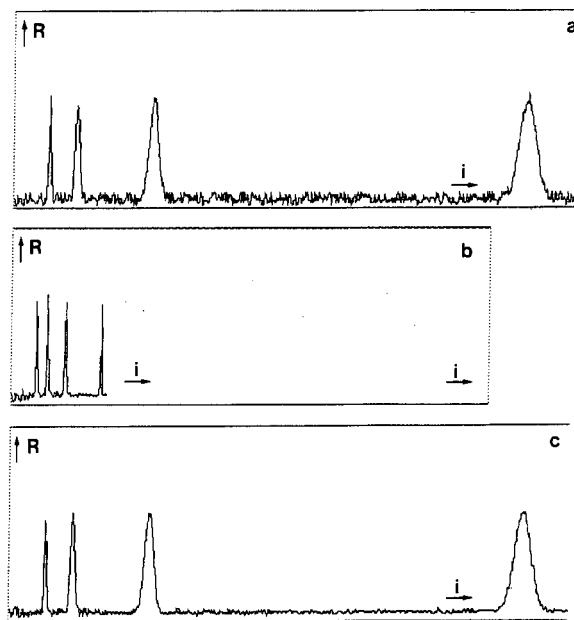


Fig. 2. Simulated chromatogram of 5000 data points (a) reduced to 782 points when compressed to $p = 5$ data points per σ with a plate number of 2500 (b). After decompression, some data reduction remains (c). See text for further details. The axes in this figure represent arbitrary response (R) and time (t).

782 data points are sufficient (Fig. 2b). This number is reduced with the same factor 16 to illustrate the factor 6.4 gain.

The plate number, needed for compression, is not critical. Column deterioration, leading to the loss of plate numbers, will therefore not be a problem. Column deterioration will usually also lead to change of retention time. The sensitivity of the compression algorithm for slight changes in retention times was checked by a series of chromatograms, produced by a gas chromatography simulator [8]. The standard deviation of the apparent retention times in the compressed chromatogram was always smaller than that in the original signal.

CONCLUSIONS

The data compression algorithm effectively stores the information contained in the chromatogram. The resulting chromatogram with peaks of uniform width is treated as a normal chromatogram. The standard deviation of retention does not deteriorate with respect to the original signal. Some noise reduction has taken place, while at the same time the effect of baseline drift is apparently amplified. The area of the peaks is decreased by a factor k but the

signal-to-noise ratio is increased. When the plate number is not the same for all peaks, compression with the highest plate number expected is advised. This will not lead to a loss of information, only to a slight variation of the peak widths in the compressed signal.

When restoring the original chromatogram using the array with the compressions factors, some reduction of data is inevitable, as seen by the lower noise level due to averaging. The original retention data is now obtained (Fig. 2c).

REFERENCES

- 1 E. Heftmann (Editor) *Chromatography, Part A (J. Chromatogr. Library, Vol. 22A)*, Elsevier, Amsterdam, 1983.
- 2 P. A. Leclercq, in J. Novak, *Quantitative Analysis by Gas Chromatography (Chromatographic Science Series, Vol. 41)*, Marcel Dekker, New York, 1988, p. 163.
- 3 K. L. Rowlen, K. A. Duell, J. P. Avery and J. W. Birks, *Anal. Chem.*, 61 (1989) 2624.
- 4 G. Guiochon and M. J. Sepaniak, *Anal. Chem.*, 63 (1991) 73.
- 5 K. A. Duell, J. P. Avery, K. L. Rowlen and J. W. Birks, *Anal. Chem.*, 63 (1991) 73.
- 6 P. A. Bristow, *LC in Practice*, HETP, Handforth, 1976.
- 7 D. L. Massart, B. G. M. Vandeginste, S. N. Deming, Y. Michotte and L. Kaufman, *Chemometrics, A Textbook*, Elsevier, Amsterdam, 1988.
- 8 J. C. Reijenga, *J. Chromatogr.*, in press.

Short Communication

High-performance liquid chromatographic determination of dinitroaniline herbicides in soil and water

Paolo Cabras* and Marinella Melis

Istituto di Farmacologia e Tossicologia Sperimentali, Viale Diaz 182, 09126 Cagliari (Italy)

Lorenzo Spanedda and Carlo Tuberoso

Istituto di Merceologia, Viale Fra' Ignazio 74, 09123 Cagliari (Italy)

(First received March 13th, 1991; revised manuscript received June 11th, 1991)

ABSTRACT

A high-performance liquid chromatographic method for the simultaneous determination of the dinitroaniline herbicides dinitramine, ethalfluralin, trifluralin, pendimethalin and isopropalin in soil and surface water is reported. The soil was extracted with diethyl ether and analysed without any clean-up. The water was analysed after purification and concentration on a C₁₈ cartridge. The average recoveries were in the range 89–104%. The detection limits for the five herbicides were 0.02 mg/kg in dry soil and 0.5 µg/l in surface water.

INTRODUCTION

Dinitramine (**I**), ethalfluralin (**II**), trifluralin (**III**), pendimethalin (**IV**) and isopropalin (**V**) (Fig. 1) are dinitroaniline herbicides used to control most of the annual grasses and broad-leaved weeds in a wide variety of agronomic crops [1]. The behaviour and fate of dinitroaniline herbicides in soil are well known [2]. These compounds are among the least mobile herbicides and therefore the run-off is the principal route, which could lead to the contamination of surface waters.

The traditional method for determining residues of these herbicides in soil involves extraction with an organic solvent, followed by purification. The purified extract is then analysed by gas chromatography (GC) [3–6]. Only one method for the determination of pendimethalin in water has been described [7], and so far no high-performance liquid

chromatographic (HPLC) method for the separation and determination of dinitroaniline herbicides in soil and water has been reported.

In this paper, an HPLC method is described which allows the simultaneous determination of dinitramine, ethalfluralin, trifluralin, pendimethalin and isopropalin in soil and surface water.

EXPERIMENTAL

Apparatus

A Model 5020 liquid chromatograph (Varian, Palo Alto, CA, USA) was used, fitted with a UV-100 variable-wavelength UV-VIS detector and a Rheodyne injection valve (50-µl loop), connected to a Model 3390 A reporting integrator (Hewlett-Packard, Avondale, PA, USA).

The extraction of the herbicides from water was performed with a Vac-Elut vacuum system

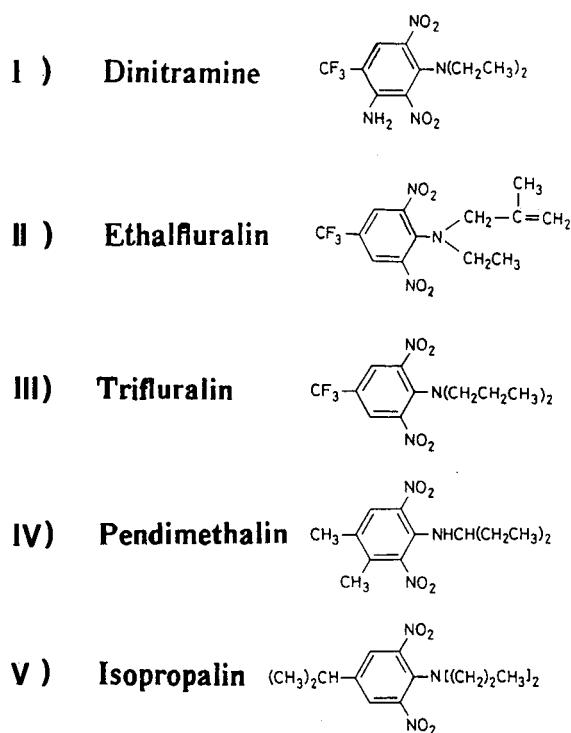


Fig. 1. Structures of dinitroaniline herbicides.

(Analytichem International, Harbor City, CA, USA).

Chromatography

Spherisorb (Waddinxveen, Netherlands) C₁, C₆, C₈, ODS-1 and ODS-2 (10 μm) columns (250 mm × 4.6 mm I.D.) were used; the mobile phase was water-acetonitrile in various ratios at a flow-rate of 1.0 ml/min. The analyses were performed at 220 nm for the simultaneous determination of I-V or, for low concentrations, at different wavelengths depending on the previously determined absorbance maxima for dinitramine (220 nm), ethalfuralin (200 nm), trifluralin (200 nm), pendimethalin (240 nm) and isopropalin (200 nm) with a Model DMS 90 UV-VIS spectrophotometer (Varian).

Chemicals and materials

Acetonitrile, methanol and diethyl ether were of HPLC grade (Carlo Erba, Milan, Italy); water was distilled twice and filtered through a Milli-Q apparatus (Millipore, Molsheim, France) before use. Di-

nitramine, ethalfuralin, pendimethalin, trifluralin and isopropalin were analytical standards purchased from Erhenstorfer (Augsburg, Germany).

Stock standard solutions (*ca.* 100 ppm each) were prepared in acetonitrile; working standard solutions were obtained by dilution with the mobile phase.

Three soils of different physical and chemical characteristics and one surface water (Table I) were used to set up the extraction procedure.

Soil extraction procedure

A 25-g amount of air-dried soil was weighed in a 250-ml screw-capped flask, 50 ml of diethyl ether were added and the mixture was agitated in a flask shaker (Stuart Scientific) for 30 min. The soil was left to settle and the clear organic layer was transferred into a 20-ml screw-capped tube containing 2 g of anhydrous sodium sulphate. A 2-ml aliquot of the extract was transferred into a 10-ml beaker and evaporated nearly to dryness in a thermo-ventilated stove. The extract was then allowed to evaporate completely in the air; the residue was recovered with 1 ml of mobile phase and injected for HPLC analysis.

Surface water extraction procedure

For sample clean-up, the Vac-Elut system was employed with Bond-Elut C₁₈ (500 mg per 2.8 ml)

TABLE I
PHYSICAL AND CHEMICAL CHARACTERISTICS OF THE SOILS

Characteristic	Soil		
	A	B	C
Sand (%)	71	43	71
Silt (%)	20	32	14
Clay (%)	9	25	16
pH (in water)	6.7	8.0	5.5
Organic matter (%)	1.9	3.9	0.6
	Water		
pH	7.9		
Conductance (μS cm ⁻¹)	745		
Hardness (mg/l CaCO ₃)	240		
Oxygen (dissolved) (mg/l O ₂)	1.9		

cartridges (Analytichem International). The extraction procedure was carried out as follows. The cartridge was treated with 10 ml of methanol, followed by 10 ml of water. The sample (100 ml of surface water) was then added (using a reservoir) and allowed to percolate slowly (1 ml/min). The reservoir was removed and the cartridge washed with 5 ml of methanol-water (50:50, v/v), followed by 5 ml of water. The cartridge was air-dried under vacuum for 2 min and then the pesticides were eluted with 2 ml of diethyl ether and collected in a 2-ml conical tube. The diethyl ether layer was transferred into a 10-ml beaker with a Pasteur pipette and the procedure was carried out as for the soil ethereal extract.

Recovery assays

Untreated soils were air-dried to <10% (w/w) water content and sieved through a soil sieve (2-mm mesh). The samples were then fortified by adding 250- μ l portions of solutions of the five herbicides in acetonitrile at 0.05 and 1.00 ppm. The solvent was evaporated in a fume-hood (*ca.* 1 h).

Untreated water was fortified with 100- μ l portions of a solution of the five herbicides at 0.002 ppm.

The soil and water fortified samples were processed according to the above-described extraction procedure.

RESULTS AND DISCUSSION

In order to achieve the separation of dinitroaniline herbicides, different reversed-phase (C₁, C₆, C₈, ODS-1 and ODS-2) columns were employed (Table II). Each column allowed the separation of the five herbicides with different water-acetonitrile mixtures. The elution order was the same (first and last, respectively) for dinitramine and isopropalin on all the columns tested, whereas ethalfuralin, trifluralin and pendimethalin were eluted with different orders on the different columns.

Calibration graphs for each compound were constructed by plotting concentration vs. peak height. Good linearities were achieved in the range 0–1.5 ppm with correlation coefficients between 0.9990 and 0.9998.

For recovery assays of the herbicides, three different soils that had never been treated with any pesticide and one surface water were used. The blanks of the soil extraction solvents did not give any interfering peaks at the retention times of the compounds studied, so making any further clean-up unnecessary. With water samples, different solvents (*n*-hexane, dichloromethane, benzene, acetonitrile and diethyl ether) were tested for the elution of the herbicides, but only diethyl ether allowed satisfactory recoveries without any presence of interfering

TABLE II
RETENTION TIMES OF DINITROANILINE HERBICIDES WITH DIFFERENT COLUMNS AND ELUENTS

Flow-rate, 1.0 ml/min.

Column	Water-acetonitrile ratio	Retention time (min)				
		I	II	III	IV	V
ODS-1	25:75	6.63	8.70	9.82	10.45	13.24
	35:65	10.08	15.41	18.34	18.34	25.68
ODS-2	25:75	6.08	8.92	10.60	11.15	15.87
	35:65	10.18	19.14	23.86	22.81	37.78
C ₈	35:65	8.71	13.86	16.26	14.12	21.95
	40:60	11.76	20.68	24.79	20.48	34.56
C ₆	25:75	5.44	7.47	8.39	7.95	10.80
	35:65	8.68	14.47	16.96	14.47	23.12
C ₁	40:60	7.17	10.12	11.03	9.67	12.70
	45:55	9.52	14.79	16.46	13.60	19.38

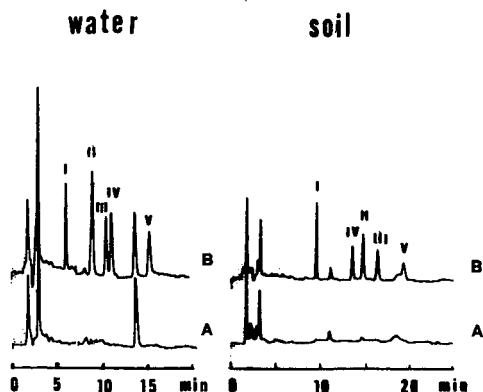


Fig. 2. Left: chromatography of dinitroaniline herbicides in surface water on an ODS-2 column. Mobile phase, water-acetonitrile (25:75, v/v); flow-rate, 1 ml/min; detection, UV at 220 nm. (A) Control; (B) sample fortified with 2 $\mu\text{g/l}$ of each herbicide. Right: chromatography of dinitroaniline herbicides in soil on a C_1 column. Mobile phase, water-acetonitrile (45:55, v/v); flow-rate, 1 ml/min; detection, UV at 220 nm. (A) Control; (B) sample fortified with 50 $\mu\text{g/l}$ of each herbicide.

compounds. The recoveries from soil and water with diethyl ether ranged between 89% and 104% for all the herbicides studied.

Representative chromatograms for the simulta-

neous determination of dinitroaniline herbicides are shown in Fig. 2. Under the optimum conditions, the detection limit was 0.02 mg/kg in soil and 0.5 $\mu\text{g/l}$ in water for all compounds.

The method described allows the rapid determination of dinitroaniline herbicides in soil and water, and could be employed for routine monitoring of environmental pollution. Further, the possibility of achieving the separation of dinitroaniline herbicides by means of different columns could be useful as a confirmatory assay or to overcome the problem of interfering compounds.

REFERENCES

- 1 *The Agrochemicals Handbook*, Royal Society of Chemistry, Nottingham, 2nd ed., 1988.
- 2 C. S. Helling, *J. Environ. Qual.*, 5 (1976) 1.
- 3 A. E. Smith, *J. Chromatogr.*, 97 (1974) 103.
- 4 J. H. Miller, P. E. Keeley, C. H. Carter and R. J. Thullen, *Weed Sci.*, 23 (1975) 211.
- 5 R. L. Zimdahl and S. M. Gwynn, *Weed Sci.*, 25 (1977) 247.
- 6 E. W. Day, in G. Zweig and J. Sherma (Editors), *Analytical Methods for Pesticides and Plant Growth Regulators*, Vol. X, Academic Press, New York, 1978, p. 341.
- 7 A. Copin and R. Delen, *Anal. Chim. Acta*, 208 (1988) 331.

Short Communication

Determination of carotenoid pigments in several tree leaves by reversed-phase high-performance liquid chromatography

Javier De Las Rivas*, Jose Carlos G. Milicua and Ramon Gomez

Department of Biochemistry, Science Faculty, University of the Basque Country, P.O. Box 644, 48080 Bilbao (Spain)

(First received August 22nd, 1990; revised manuscript received June 11th, 1991)

ABSTRACT

A rapid and simple reversed-phase high-performance liquid chromatographic method has been used to analyse all carotenoid pigments from leaves of five different trees. The pigments were separated on an octadecylsilane radial compression column, using a mobile phase mixtures of acetonitrile, methanol–water and ethyl acetate in three isocratic steps. This method resolves all higher plant photosynthetic pigments, carotenoids and also chlorophylls in less than 15 min, while achieving a relatively good separation of *trans*-lutein—the major carotenoid—from its isomers zeaxanthin and *cis*-lutein.

INTRODUCTION

Carotenoids are essential for the survival of photosynthetic organisms. No green plants which occur in nature lack carotenoid pigments since they have several significant functions in photosynthesis [1,2]. Thus, these coloured octaprenoids act as photoprotective agents, protecting against light-induced destruction by molecular oxygen (photo-oxidative damage). They also function in plants as accessory light-harvesting pigments, allowing autotrophic organisms to utilize light energy over a wider spectral range. A third function—specific of xanthophylls—is to act as carriers of light-induced reductive deoxygenations [3]. The first of these functions is essential for living organisms, and it must be quite clearly stated that without carotenoids there would be no photosynthesis in the presence of oxygen [4].

Specific separation and quantitative determination of each photosynthetic pigment (chlorophylls

and carotenoids) of plants are essential to determine the function and role of each of these pigments in envelope and thylakoid chloroplastic membranes. In most plant physiology laboratories the analysis of photosynthetic pigments is still mainly concentrated on chlorophyll analysis (chlorophyll *a* and *b*) and it is carried out spectrophotometrically [5]. This method of determination is also usually used to determine the total carotenoid content; however, a differentiated estimation of the quantitative molecular pattern of each carotenoid pigment is needed in order to study in depth the role of carotenoids in photosynthetic organisms and the changes in their stoichiometry under ecological, physiological or biochemical influences.

The carotenoids of all functional chloroplasts in higher plants and green algae include β -carotene, lutein, violaxanthin and neoxanthin as major and regular components of the photochemically active thylakoids. The xanthophylls antheraxanthin, ta-

raxanthin and zeaxanthin are regular but minor carotenoid components [5]. Therefore, it can be seen that a good analytical chromatographic system for these pigments must allow separated elution of compounds of widely divergent polarity: from more polar xanthophylls (like neoxanthin, 5',6'-epoxi-3,5,3'-triol) to non-polar carotenoids (β -carotene, which has no oxygenated group).

This paper describes the use of a rapid, simple and sensitive reversed-phase high performance liquid chromatographic (RP-HPLC) method for the analytical separation and quantitative determination of all major carotenoids contained in the green leaves of five different deciduous trees. An accurate quantitative determination of each carotenoid present in these leaves was obtained from HPLC analyses, which also provided interesting data about the specific carotenoid composition of different leaves. The pigments were separated on an octadecylsilane radial compression column, using as mobile phase mixtures of acetonitrile, methanol-water and ethyl acetate in three isocratic steps. Detection of the pigments, after chromatographic separation, was carried out using a photodiode array detector.

EXPERIMENTAL

Leaf collection and pigment extraction

Pigments were extracted from sunlit leaves of five common deciduous trees: *Populus alba*, *Populus nigra*, *Acer pseudoplatanus*, *Quercus robur* and *Tilia tomentosa*. All species were grown in local gardens at Lejona (Vizcaya, Spain) (latitude 43°20' north, < 100 m altitude), under well watered conditions. The leaves used for experiments were collected in spring—late May or early June—and were sunlit leaves with a photon flux density (PFD) incident from 1600 to 2000 $\mu\text{mol photon m}^{-2} \text{s}^{-1}$, and with a daylength range from 14 to 15 h.

Several clean leaves (4–8) stripped of main stems and veins were cut into small pieces for pigment extraction, and 1 g fresh weight was placed in a mortar and ground to a fine powder with acetone in the presence of sodium ascorbate as an antioxidant. The grinding and extracting were repeated with several volumes of acetone until no more colour could be eluted (the total volume of acetone used was about 50 ml/g of leaf tissue).

All the extractions were conducted in the cold (at 4°C) and in subdued artificial light (dim light). Reagents and solvents were of analytical grade. Before use, acetone was treated with sodium bicarbonate to neutralize any remaining acidity.

The acetonic extracts were filtered twice through a 0.45- μm HVLP Millipore filter to remove any insoluble particles, and were kept in darkness at -30°C until they were analysed. Pigments in the acetonic solution were analysed by injecting 20- μl aliquots onto the HPLC column.

Liquid chromatography

The HPLC system used for the pigment analyses consisted of a high-pressure pump (Waters M-45), a Rheodyne injector (7010-7011) fitted with a 20- μl loop, and a Shimadzu UV-visible detector (SPD-6AV) set at 450 nm and connected to a Shimadzu C-R3A integrator. A radial compression column, NovaPak C₁₈ (Waters Rad-PakA, 100 \times 8.0 mm I.D., with 4- μm spherical particles of octadecylsilane), was used with this chromatograph. The column was contained in a radial compression module (Waters RCM 8 \times 10) and protected by an RCSS Guard-Pak (Waters, 10 \times 8.0 mm I.D., 10 μm particle size) and a pre-column filter. A Waters 990 UV-visible photodiode array detector, covering the range 300–600 nm and connected to a NEC APC III computer, was used in some analyses for determination of the spectra of each peak separated by HPLC (Fig. 2).

The mobile phase composition was: (A) acetonitrile-methanol (7:1) (2 min); (B) acetonitrile-methanol-water (7:0.96:0.04) with 20% ethyl acetate (1.5 min); and (C) acetonitrile-methanol-water (7:0.96:0.04) with 50% ethyl acetate (8 min) if there was only β -carotene or (C') acetonitrile-methanol-water (7:0.96:0.04) with 40% ethyl acetate (10 min) for separation of α - and β -carotene.

Reagents

HPLC-grade solvents, methanol, isopropanol, acetonitrile, ethyl acetate, tetrahydrofuran, dichloromethane and chloroform (Scharlau, France), were used. They were filtered through a 0.45- μm membrane filter (Fluoropore, Millipore, USA, for ethyl acetate and Ultipor NX, Millipore, for the other solvents) and degassed with a stream of helium before use.

Reference samples of carotenoids for calibration were purified from leaves according to published procedures. Purified standards of all-*trans*- β -carotene and zeaxanthin were provided by Hoffman-La Roche (Basle, Switzerland) and by Dr. G. Britton (University of Liverpool, UK).

Identification and quantitative evaluation

Peak identification was based on the comparison of retention times in HPLC with those of known standards, and on the isolation of each peak and the comparison of its absorbance maxima in the visible spectrum in different solvents (ethanol, acetone, chloroform and hexane) with standards values [6–9].

In order to carry out quantitative analysis of the data, peaks were monitored at 450 nm. The method was calibrated as by De Las Rivas *et al.* [10]. Most of the coefficients used for quantification of the pigments were the same as those previously reported [10]. However, some of them were modified after more accurate calibration. For these the new normalized coefficients were: taraxanthin, 1.03; antheraxanthin, 1.04; zeaxanthin, 1.01; α -carotene, 0.96; β -carotene, 0.93.

RESULTS AND DISCUSSION

The present work shows the quantitative determination of carotenoid composition in green spring leaves of five different trees, obtained by using the RP-HPLC method [10] modified as described in ref. 11. The analysis with this simple and reproducible RP-HPLC method allowed the resolution and quantification of all major photosynthetic pigments, with separation and detection of low levels of carotenoid isomers: zeaxanthin and α -carotene. The HPLC separation of the leaf pigments obtained with this method is shown in Fig. 1. This figure presents two chromatograms of the total green leaf pigment extract from two trees (*Tilia tomentosa* and *Quercus robur*), showing the separation of ten carotenoids (neoxanthin, *cis*-neoxanthin, violaxanthin, taraxanthin, antheraxanthin, lutein, zeaxanthin, *cis*-lutein, α -carotene and β -carotene) and two chlorophylls (chlorophyll *a* and *b*).

The short test-time (11.5–13.5 min) permitted analysis of a large number of samples, and the data shown in Table I are average values of eight differ-

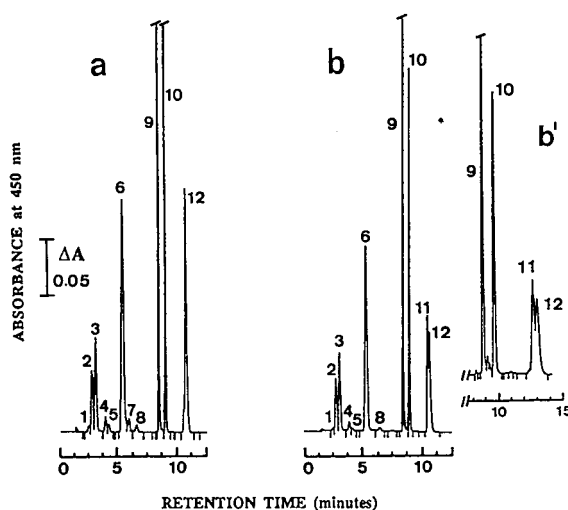


Fig. 1. Reversed-phase HPLC absorbance (450 nm) profiles of the pigment extracts from green leaves of the trees *Quercus robur* (a) and *Tilia tomentosa* (b), using the solvent system constituted by three isocratic phases: (A) acetonitrile–methanol (7:1) (2 min); (B) acetonitrile–methanol–water (7:0.96:0.04) with 20% ethyl acetate (1.5 min); and (C) acetonitrile–methanol–water (7:0.96:0.04) with 50% ethyl acetate (8 min). (b') Separation of the same sample of *Tilia tomentosa* using C' as the third solvent [C': acetonitrile–methanol–water (7:0.96:0.04) with 40% ethyl acetate (10 min) for better separation of α - and β -carotene]. Flow-rate, 2.00 ml/min; column, NovaPak C₁₈, 4 μ m (100 \times 8.0 mm I.D.); detection, 450 nm; volume injected, 20 μ l; injection solvent, acetone. Peaks: 1 = neoxanthin; 2 = *cis*-neoxanthin; 3 = violaxanthin; 4 = taraxanthin; 5 = antheraxanthin; 6 = lutein; 7 = zeaxanthin; 8 = *cis*-lutein; 9 = chlorophyll *b*; 10 = chlorophyll *a*; 11 = α -carotene; 12 = β -carotene.

ent leaf samples for each species assayed. The analysed species were all deciduous-leaf trees, and trees very common in gardens and heaths. Proper coefficients for quantitative analysis of each carotenoid were calculated as in ref. 10, in order to provide an accurate quantitative evaluation of these pigments. The carotenoid composition (% w/w) of the green leaves of the five deciduous trees analysed is shown in Table I.

This accurate pigment determination has provided interesting figures about the normal carotenoid composition of the leaves of the trees studied, and about the specific difference that appears for each plant when precise quantitation is obtained. Moreover, the use of a photodiode array detector allows a quick identification of the peaks eluted from the

TABLE I

CAROTENOID COMPOSITION OF THE GREEN LEAVES FROM FIVE DECIDUOUS TREES AND RETENTION TIMES FOR EACH PIGMENT RESOLVED

Pigment	Retention time ^a (mean ± S.D.) (min)	Carotenoid composition of leaves (% w/w)				
		<i>Populus alba</i>	<i>Populus nigra</i>	<i>Tilia tomentosa</i>	<i>Acer pseudoplatanus</i>	<i>Quercus robur</i>
Neoxanthin	2.60 ± 0.11					
<i>cis</i> -Neoxanthin	2.87 ± 0.11	10.1	9.4	13.7	10.4	12.6 ^b
Violaxanthin	3.19 ± 0.11	19.7	17.2	15.4	26.6	14.7
Taraxanthin	3.97 ± 0.18	—	—	1.9	—	2.3
Antheraxanthin	4.29 ± 0.22	1.1	0.8	0.6	2.4	1.3
Lutein	5.68 ± 0.29	40.8	41.6	40.9	34.4	39.8
Zeaxanthin	6.19 ± 0.22	—	—	—	1.2	1.7
<i>cis</i> -Lutein	6.60 ± 0.26	0.8	1.1	1.1	0.8	1.4
Chlorophyll <i>b</i>	8.57 ± 0.18					
Chlorophyll <i>a</i>	9.12 ± 0.18					
α -Carotene	10.39 ± 0.26	—	—	13.8	—	1.3
β -Carotene	10.70 ± 0.22	27.5	29.9	12.5	25.0	26.1

^a Retention time of each pigment using solvent systems A, B and C (see Experimental section). S.D. = Standard deviation of the retention times (mean of fifteen samples).

^b Percentage of neoxanthin and *cis*-neoxanthin.

HPLC column, since it provides the visible absorption spectra of each pigment eluted in the mobile phase. The spectra of the main pigments present in a green extract obtained with this detector (shown in Fig. 2) were consistent with the spectra of the standards dissolved in similar solvents.

Lutein is the major component in all the leaves analysed, showing a percentage composition which is very constant, within the range of 39.4–41.6% (w/w). Leaves from *Acer pseudoplatanus* show slightly less lutein because of an increase in other xanthophylls, but the absolute amount is very similar to the other trees. Neoxanthin, the most polar carotenoid and the only one which presents *cis* configuration [12], represents around 12% (10.4–13.7%) of total carotenoid content. The xanthophyll cycle pool (violaxanthin, antheraxanthin and zeaxanthin) presents more variations: from 16.0% in *Tilia tomentosa* to 32.0% in *Acer pseudoplatanus*. This difference could mean a difference in the capacity of each plant to adapt to high-intensity light, in accordance with the recently proposed function for the xanthophyll cycle of dissipation of excess excitation energy, by formation and accumulation of zeaxanthin [13]. The data obtained show that the normal green leaves have very low levels of zeaxan-

thin (Table I), usually less than 3%, indicating that no particular situation of stress had affected the fresh mature green leaves from the trees studied.

The quantitation of carotenoids from leaves of *Tilia tomentosa* and *Quercus robur* show significant differences in the content of carotenenes, since the former contains appreciable amounts of α -carotene (13.8%) and the latter has only 1.3% α - and 26.1% β -carotene. Not many quantitative data have been previously reported concerning these specific differences in the carotenoid content of extracts from chloroplasts. Recently, Thayer and Björkman [14] also reported the significant presence of α -carotene in leaves of some species: *Monstera deliciosa*, *Calycanthus occidentalis* and *Asarum caudatum*. These authors demonstrated that α -carotene is an important carotenoid constituent of shade plants [14]. This carotene is also present in significant quantities in gymnosperms [15].

The focus of this work, using an RP-HPLC method for analytic determination of carotenoids from leaves, is a first step to elucidating the role of each carotenoid in the photosynthetic apparatus of plants, which is not yet well known. The carotenoid content data given in this paper (Table I) reveal characteristic differences in the leaves of each spe-

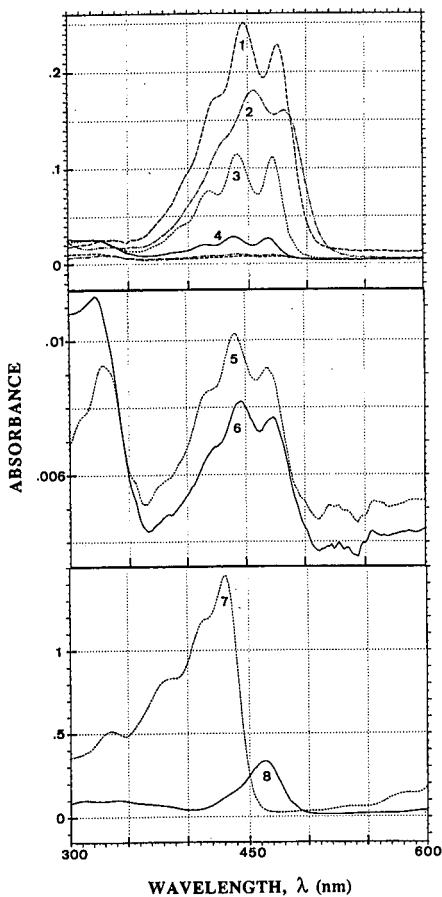


Fig. 2. Photodiode array absorption spectra between $\lambda = 300$ and 600 nm of the major pigments (carotenoids and chlorophylls) of green leaves separated by RP-HPLC. Sample: extract from *Populus alba* green leaves. The spectra correspond to the pigments in the eluent obtained at the outlet of the HPLC column with the photodiode array detector; therefore the pigments are in the mixture of acetonitrile, methanol and ethyl acetate that corresponds to the mobile phase where each one elutes. The concentration of the green extract injected was approximately $40 \mu\text{g}$ of chlorophyll per ml. Peaks: 1 = lutein; 2 = β -carotene; 3 = violaxanthin; 4 = *cis*-neoxanthin; 5 = *cis*-lutein; 6 = antheraxanthin; 7 = chlorophyll *a*; 8 = chlorophyll *b*.

cies. Further studies involving more species and different growing conditions will be needed to establish the presence and function of each xanthophyll and carotene in leaves, chloroplasts, thylakoids and protein complexes of photosynthetic membranes.

REFERENCES

- 1 D. Siefermann-Harms, *Biochim. Biophys. Acta*, 881 (1985) 325–355.
- 2 D. Siefermann-Harms, *Physiol. Plant.*, 69 (1987) 561–568.
- 3 H. Thommen, *Pure Appl. Chem.*, 51 (1979) 867–869.
- 4 R. Cogdell, in T. W. Goodwin (Editor), *Plant Pigments*, Academic Press, London, 1988, pp. 183–230.
- 5 H. K. Lichtenthaler, *Methods Enzymol.*, 148 (1987) 350–382.
- 6 B. H. Davies, in T. W. Goodwin (Editor), *Chemistry and Biochemistry of Plant Pigments*, Vol. 2, Academic Press, New York, 2nd ed., 1976, pp. 38–165.
- 7 J. C. Bauernfeind (Editor), *Carotenoids as Colorants and Vitamin A Precursors*, Academic Press, New York, 1981, pp. 838–938.
- 8 S. W. Wright and J. D. Shearer, *J. Chromatogr.*, 294 (1984) 281–295.
- 9 G. Britton, *Methods Enzymol.*, 111 (1985) 113–149.
- 10 J. De Las Rivas, A. Abadia and J. Abadia, *Plant Physiol.*, 91 (1989) 190–192.
- 11 J. De Las Rivas, *Dissertation*, University of the Basque Country, Bilbao, 1990.
- 12 T. W. Goodwin and G. Britton, in T. W. Goodwin (Editor), *Plant Pigments*, Academic Press, London, 1988, pp. 61–132.
- 13 B. Demmig-Adams and W. W. Adams III, *Photosynth. Res.*, 25 (1990) 187–197.
- 14 S. S. Thayer and O. Björkman, *Photosynth. Res.*, 23 (1990) 331–343.
- 15 D. Grill and H. W. Pfeifhofer, *Phyton (Horn)*, 25 (1985) 1–15.

Short Communication

Determination of calcium ions tightly bound to proteins

Katsutoshi Nitta* and Akihiro Watanabe

Department of Polymer Science, Faculty of Science, Hokkaido University, N10 W8 Kita-ku, Sapporo, Hokkaido 060 (Japan)

(First received April 9th, 1991; revised manuscript received May 27th, 1991)

ABSTRACT

A rapid and sensitive procedure is described for the determination of calcium ions tightly bound to proteins using high-performance gel filtration chromatography, followed by the destabilization of the protein conformation and fluorimetric analysis with Quin-2. With this method, contaminating, unbound calcium can be eliminated simultaneously and one can determine the content of a calcium ion in a protein utilizing less than 200 pmol of the protein.

INTRODUCTION

In order to investigate a calcium-binding protein, one must first determine the number of calcium ions bound to that protein by means of, for example, atomic absorption spectrometry. However, using this method contamination by calcium ions from labware is frequently a source of trouble; one must eliminate contaminating non-bound calcium ions carefully, and additionally with this method, samples once burned are not recoverable. Thompson *et al.* [1] reported a suitable method for comparing the migration rates of a protein in polyacrylamide gel electrophoresis with and without ethylene glycol tetraacetate for the purpose of detecting calcium-binding proteins. However, the specificity of their method is considered to be insufficient. Metalloproteins binding metals other than calcium ions would be equally detected.

To overcome such disadvantages, a microanalytical method has been developed in this study, using high-performance gel-filtration chromatography together with the use of a calcium-specific fluorescent reagent. With this method, one can determine the number of bound calcium ions with less than

200 pmol of the protein. The analysis and elimination of the contaminating calcium ions are performed simultaneously and one can recover the protein because the sample need not be burned.

EXPERIMENTAL

Materials

Quin-2 was purchased from Wako (Osaka, Japan). Special-grade urea for biochemical use was obtained from Nacalai Tesque (Kyoto, Japan). Other reagents were all of guaranteed grade from Nacalai Tesque.

Bovine α -lactalbumin [2] and equine lysozyme [3] were prepared previously. Carp parvalbumin III was prepared from carp white muscle according to the literature [4]. Absorptivities, $A^{1\%}$, of these proteins are known to be 20.1 at 280 nm for bovine α -lactalbumin [5], 23.5 at 280 nm for equine lysozyme [44] and 1.76 at 259 nm for carp parvalbumin III [6].

Methods

A schematic diagram of the apparatus is shown in Fig. 1. A Biofine PO-4K gel filtration column (Ja-

pan Spectroscopic) (300 mm × 7.5 mm I.D., exclusion limit 4000 dalton) was equilibrated with 0.01 M 4-(2-hydroxyethyl)-1-piperazineethanesulphonic acid (HEPES) buffer (pH 7.5, 0.1 M KCl), which had been decalcified with a Chelex A-100 ion-exchange column. The same buffer was introduced to the column at a flow-rate of 1 ml/min by a high-performance liquid chromatographic pump (1) (Model 885 PU; Japan Spectroscopic). A volume of 10 μ l of sample or standard solution was applied from a sample injector with a microsyringe (Hamilton, Reno, NV, USA). With this column, macromolecular proteins and low-molecular-weight ions were separated. From reservoir 2, 8 M aqueous urea containing 20 μ M Quin-2 [6], which had also been decalcified, was transmitted with another pump (2) (Model 880 PU; Japan Spectroscopic) at a flow-rate of 1 ml/min and combined with the eluate from the column. After passing through a 150-cm mixing coil, the solution was introduced to the flow cell of a spectrofluorimeter (Model FP 210; Japan Spectroscopic), with excitation at 335 nm and emission at 492 nm. The resulting fluorescence intensity was recorded with a Chromatocoder 12 (System Instruments, Tokyo, Japan) and integrated with time coordinates by an internal computer. Bound and

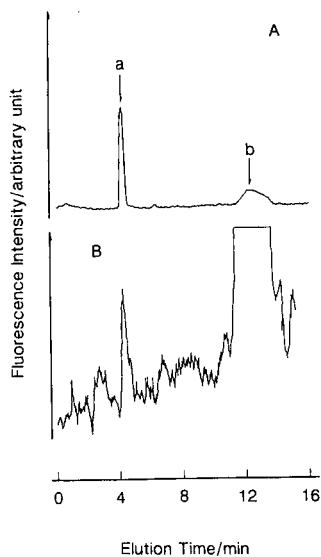


Fig. 2. Elution profiles of calcium bound to α -lactalbumin. amount of α -lactalbumin loaded: (A) 10 μ l of 100 μ M; (B) 10 μ l of 1 μ M. Peak 1, elution peak of calcium bound to α -lactalbumin; peak 2, non-bound, contaminating calcium.

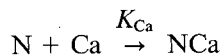
contaminating calcium ions were detected at *ca.* 5 and 13 min after injection, respectively (Fig. 2).

RESULTS AND DISCUSSION

The binding strengths of calcium-binding proteins are high and in many instances exceed those of typical chelating reagents. For example, the first binding constant of carp parvalbumin III has been reported to be $6.3 \cdot 10^8$ l mol⁻¹ [7]. On the other hand, among many reported fluorescent calcium indicators [8–10], Quin-2 binds calcium ions the most tightly, but the binding constant is $10^{7.1}$ l mol⁻¹, one order of magnitude less than that of carp parvalbumin III.

Calcium-binding protein binds a calcium ion only when it is in the native conformation. Unfolded protein binds the ion with a far lower binding strength, if it binds at all.

Accordingly, binding equilibrium may be expressed as follows:



(1)

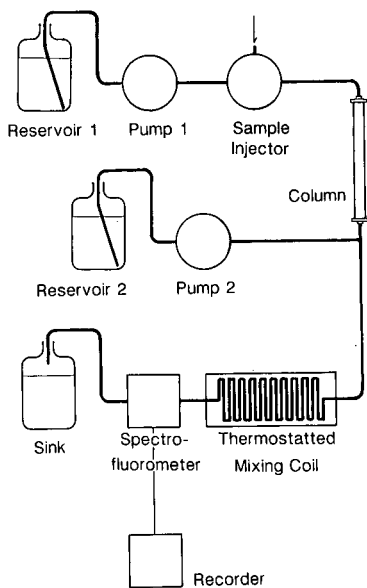


Fig. 1. Schematic diagram of the apparatus.



where N, NCa and U represent apoprotein in the native conformation holoprotein and unfolded apoprotein, respectively, K_{Ca} is the binding constant of native apoprotein and K_U is the equilibrium constant of the unfolding of the apoprotein. From eqns. 1 and 2, one can deduce an apparent binding constant (K_{app}) of the protein as follows:

$$K_{app} = \frac{[NCa]}{([N] + [U])[Ca]} = \frac{K_{Ca}}{1 + K_U} \quad (3)$$

One can decrease the binding strength by increasing the value of the denominator on the right-hand side of eqn. 3. The reduction in the conformational stability of apoprotein results in the reduction of the binding strength of the protein. In this study, aqueous urea, used for destabilization, and Quin-2, which binds calcium ions the most tightly among the fluorescent calcium ion indicators [8–10], were used. It should be noted that the sample protein need not be denatured. It is sufficient if the apparent binding constant is decreased to be sufficiently lower than that of Quin-2 for this study.

Calcium chloride solution (100 μM) was used as a standard, and the concentration of bound calcium was determined by the comparison of the areas under the peaks of the chromatograms. The results are shown in Fig. 3. Without the urea solution, calcium was not detected quantitatively (data not shown). With bovine α -lactalbumin and equine lysozyme, heating of the mixing coil was unnecessary. Bound calcium was analysed quantitatively at room temperature. However, with carp parvalbumin III, bound calcium was quantified only to 90% at room temperature. For more accurate quantification, the mixing coil had to be heated to 40°C. The results for carp parvalbumin III in Fig. 3 were obtained by heating to 40°C.

The linear least-squares method was applied to the data in Fig. 3 with the equation

$$C_{Ca} = n C_p + c \quad (4)$$

where C_{Ca} is the observed concentration of bound calcium, n is the number of bound calcium ions per

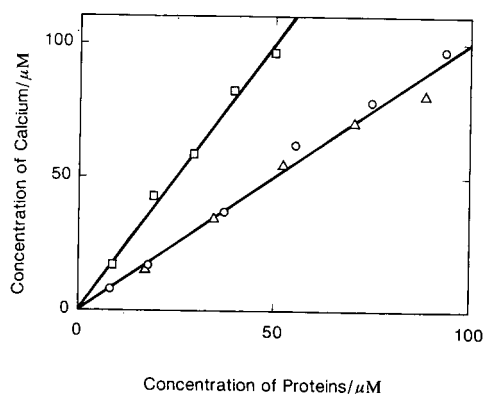


Fig. 3. Relationships between the concentrations of applied calcium-binding proteins and the observed calcium concentrations. ○ = Bovine α -lactalbumin; △ = equine milk lysozyme; □ = carp parvalbumin III. The upper and lower straight lines show the relationships for proteins containing two and one calcium ions, respectively.

protein molecule, C_p is the concentration of the protein of the injected solution and c is a constant. The values of n obtained (\pm standard deviations) were 1.07 ± 0.03 , 0.94 ± 0.07 and 1.93 ± 0.15 for bovine α -lactalbumin, equine lysozyme and carp parvalbumin III, respectively. The results were quite satisfactory, as these proteins bind one [11], one [3], and two calcium ions [7], respectively. The values of c were obtained as -1.2 ± 1.4 , 1.6 ± 4.3 , and $2.1 \pm 5.3 \mu M$, respectively, which were equal to 0 μM within standard errors.

To examine the limit of detection of calcium proteins, dilute solutions of α -lactalbumin were applied. The result utilizing 1 μM α -lactalbumin is shown in Fig. 2B. A peak for bound calcium ions can be seen above the noise level and is well separated from a very large contaminating, non-bound calcium ion.

After decreasing the binding strength with urea, bound calcium ions react quantitatively with Quin-2. One can employ other denaturants such as guanidinium hydrochloride or sodium dodecyl sulphate equally for the same purpose. Quin-2 was employed in this study because it binds calcium ions the most tightly, and it is the cheapest among the commercially available fluorescent calcium indicators. Other indicators, such as Fura-2 and Indo-1, are 30 times more fluorescent than Quin-2 [9]. Their use may improve the sensitivity, but they are 100

times more expensive than Quin-2. Such indicators may be used for very precious proteins.

A gel filtration column with a low exclusion limit was employed in this study. Another gel filtration column with a higher exclusion limit or another column with a different separation mechanism could be employed, assuming that the contamination by calcium could be sufficiently suppressed and calcium-binding proteins and non-bound calcium can be separated. With this method, one can determine bound calcium with sufficient accuracy by using less than 200 pmol of a protein. Moreover, this method is doubly specific for calcium; not only does Quin-2 show a high stability constant for calcium against magnesium, but also the emission spectrum of the calcium complex of Quin-2 is totally different from that of the magnesium complex [8].

REFERENCES

- 1 M. P. Thompson, M. L. Groves, D. P. Brower, H. N. Farrell, Jr., R. Jenness and C. E. Kotts, *Biochem. Biophys. Res. Commun.*, 157 (1988) 944.
- 2 M. Hamano, K. Nitta, K. Kuwajima and S. Sugai, *J. Biochem.*, 100 (1986) 1617.
- 3 K. Nitta, H. Tsuge, S. Sugai and K. Shimazaki, *FEBS Lett.*, 223 (1987) 405.
- 4 J.-F. Pecheure, J. Demaille and J.-P. Capony, *Biochim. Biophys. Acta*, 236 (1971) 391.
- 5 M. J. Kronman and R. E. Andreotti, *Biochemistry*, 3 (1964) 1145.
- 6 E. A. Permyakov, *Parvalbumin and Related Calcium-Binding Proteins*, Akademiya Nauk SSSR, Moscow, 1985, p. 12 (in Russian).
- 7 E. A. Permyakov, *Parvalbumin and Related Calcium-Binding Proteins*, Akademiya Nauk SSSR, Moscow, 1985, p. 37 (in Russian).
- 8 R. Y. Tsien, *Biochemistry*, 19 (1980) 2396.
- 9 G. Grynkiewicz, M. Poenie and R. Y. Tien, *J. Biol. Chem.*, 260 (1985) 3440.
- 10 A. Minta, J. P. Y. Kao and R. Y. Tsien, *J. Biol. Chem.*, 264 (1989) 8171.
- 11 H. Hiraoka, T. Segawa, K. Kuwajima, S. Sugai and N. Murai, *Biochem. Biophys. Res. Commun.*, 95 (1980) 1098.

Short Communication

Enhanced resolution of organic compounds from sediments by isotopic gas chromatography-combustion-mass spectrometry

Eric Lichtfouse*[☆], Katherine H. Freeman, James W. Collister and Dawn A. Merritt

Biogeochemical Laboratories, Geology Building, Indiana University, Bloomington, IN 47405 (USA)

(First received April 24th, 1991; revised manuscript received June 20th, 1991)

ABSTRACT

The resolution of organic compounds from sediments is increased by $^{13}\text{C}/^{12}\text{C}$ isotopic gas chromatography-combustion-mass spectrometry relative to gas chromatography with flame ionization detection. Impurities which elute close together with *n*-alkanes, phytane and a C_{32} hopanoid acid methyl ester are resolved with a valley increase of up to 100%. This phenomenon is probably due to fractionation during gas chromatographic elution and enhanced detection monitoring of the isotopic composition of the carbon dioxide produced by the combustion of the eluting substances.

INTRODUCTION

The development of gas chromatography-combustion-mass spectrometry (GC-C-MS) allows the direct measurement of the $^{13}\text{C}/^{12}\text{C}$ isotopic composition of individual organic substances eluting in GC [1]. This method has found interesting applications in molecular organic biogeochemistry such as the linking of sedimentary organic compounds with their biological sources [2] or with the atmospheric partial pressure of carbon dioxide at the time of deposition [3].

During the GC-C-MS analysis of complex organic mixtures from sediments including petroleum, it was observed that compounds assumed to be "pure" (one peak) by routine GC almost co-elute with unidentified compounds. We report here se-

lected examples of this phenomenon and discuss its origin and consequences.

EXPERIMENTAL

Alkane fractions were obtained from methylene chloride extracts of Paris Basin sediments or petroleum by silver nitrate-silica gel thin-layer chromatography (TLC) with *n*-hexane as the eluent (R_F 0.8-1). Acid fractions were obtained from extracts by potassium hydroxide-silica gel column chromatography, then derivatized with 15% boron trifluoride-methanol and purified by TLC using ethyl acetate-hexane (5%, v/v) as the eluent; monocarboxylic acid methyl ester fractions were obtained [4-6].

The GC-C-MS conditions (Delta S, Finnigan, Hewlett-Packard GC) were as follows: on-column injection; 50 m \times 0.25 mm column; Ultra 1 phase (100% polymethylsiloxane, 0.5 μm); column head pressure, 20 p.s.i.; helium flow-rate, 1.5 ml/min; GC

* Present address: Institut für Chemie, ICH-5, Postfach 1913, D-5170 Jülich, Germany.

temperature programme, 60–100°C (30°C/min), 100–320°C (4°C/min), hold 60 min at 320°C; combustion furnace temperature, 850°C; MS, electron ionization (3 kV), simultaneous Faraday cup detection at m/z 44, 45 and 46, 0.25-s integration periods.

The basis of GC–C–MS has been described by Hayes and co-workers [1,2]. Briefly, after separation by GC, the eluting compounds, e.g. hydrocarbons, are burnt on copper(II)oxide at 850°C. The water is removed and the helium carrier stream en-

ters the ion source through a restrictor capillary (1 m \times 0.11 mm I.D.). The isotopic compositions are calculated by comparison with co-injected standards (n -C₁₆²H₃₄, n -C₂₀²H₄₂, n -C₂₄²H₅₀ and n -C₃₆²H₇₄) which elute before n -alkanes of the same carbon number (Fig. 1d).

The C₃₂ hopanoid acid methyl ester from an extract of the Green River Formation (CO, USA) was identified by GC–MS (m/z 191, 263, 369, 484) and compared with previously reported values [6,7]; the

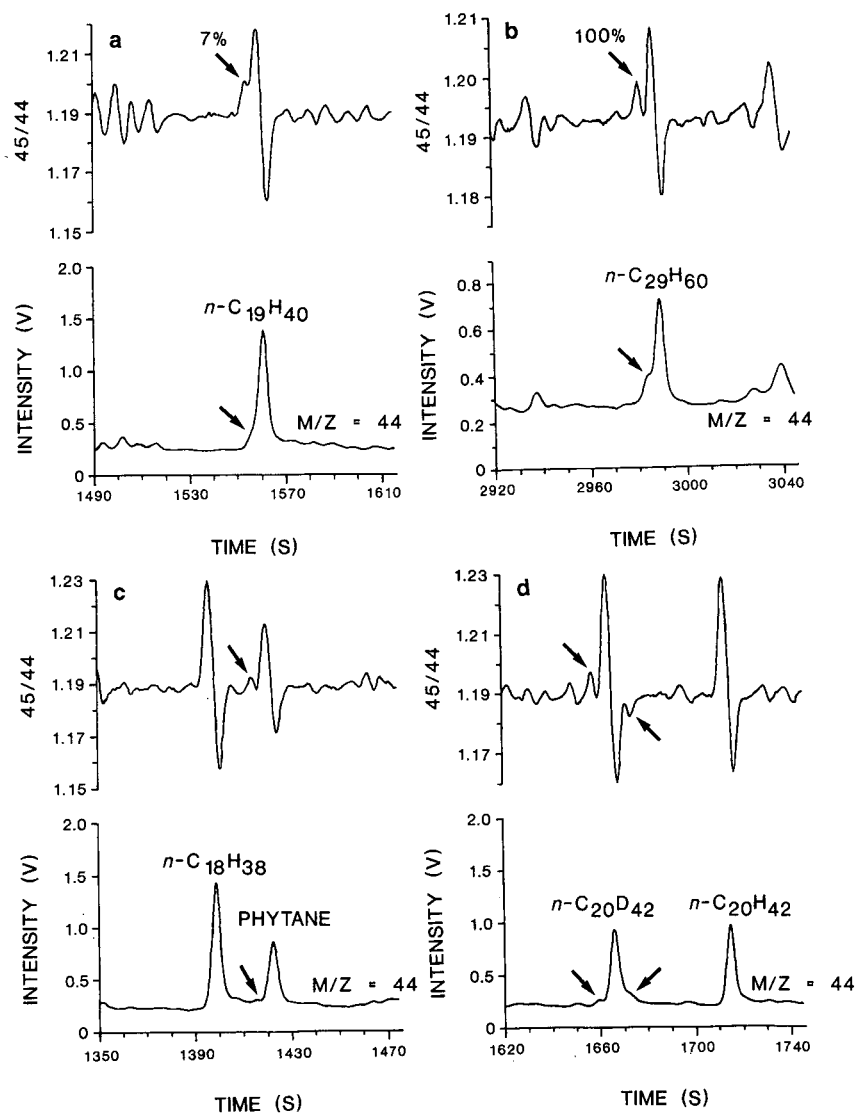


Fig. 1. m/z 44 fragmentogram and 45/44 trace of sedimentary alkanes analysed by GC–C–MS. D = Deuterium.

unknown compound eluting before this ester was tentatively identified as a ring A methylated hopanoid acid methyl ester based on the presence of a 205 mass fragment and the occurrence of ring A methyl hopanoids in sediments [8] and bacteria [9–11]. These two hopanoids give one peak in GC with flame ionization detection (GC–FID) or in the total ion current trace in GC–MS, but the ring A methylated hopanoid acid methyl ester has a slightly shorter retention time, as shown by a comparison of the 191 and 205 ion currents.

RESULTS

Sedimentary alkane fractions usually contain *n*-alkanes extending from C₁₀ to C₄₀, pristane and phytane, as major compounds. Other compounds such as branched and/or cyclic alkanes are minor but numerous, especially in mature sediments, and they are often poorly resolved in GC–FID. The *m/z* 44 ion current trace (¹²C¹⁶O₂) and the 45/44 isotopic trace of selected alkanes from Paris Basin sediments are shown on Fig. 1. The *m/z* 44 ion current is similar to the signal obtained by either GC–FID or conventional GC–MS with total ion current monitoring.

A pure compound with a Gaussian isotopic distribution gives a positive or negative peak or both on the 45/44 trace, depending on its ¹³C/¹²C isotopic composition relative to the baseline [12]. For example, *n*-C₂₀H₄₂ gives a positive peak followed by a negative peak corresponding to the ¹³C-enriched and ¹³C-depleted isotopic compositions of the carbon dioxide produced, respectively, relative to the baseline (Fig. 1). The inflections of the 45/44 trace allow the improved resolution of closely eluting components. For example, the peak representing *n*-C₁₉H₄₀ in the *m/z* 44 trace is regular in shape, except for its slightly enlarged base. A second component is clearly distinguished in the 45/44 trace with a valley of 7%. Similarly, an increase of about 100% valley is observed for *n*-C₂₉H₆₀. Such close elutions have been detected for *n*-alkanes, phytane and polydeuterated standards in petroleum and shale of various maturities, ages and locations. Two negative peaks were observed on the 45/44 trace of a C₃₂ hopanoid acid methyl ester (Fig. 2).

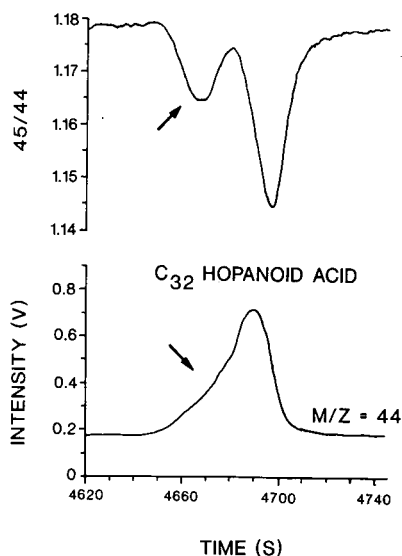


Fig. 2. *m/z* 44 fragmentogram and 45/44 trace of a sedimentary C₃₂ hopanoid acid methyl ester analysed by GC–C–MS.

DISCUSSION

Strong ¹³C/¹²C isotopic fractionation has been observed previously in eluting methane or carbon dioxide in GC on various phases; the front portion of the effluent was enriched in ¹³C [13]. This is due to an inverse isotope effect associated with the interaction of the eluent with the stationary phase [14]. The same behaviour is apparent on 45/44 traces, which show that the ¹³C enriched carbon dioxide elutes first (Fig. 1). Therefore the resolution increase for various compounds (compared with GC–FID or GC–MS with total ion current monitoring) probably results from the chromatographic fractionation and enhanced sensitivity of GC–C–MS to the variations of the ¹³CO₂/¹²CO₂ ratio with increasing time. The 45/44 trace of a C₃₂ hopanoid acid methyl ester shows that even peaks which are only negative can be better resolved (Fig. 2), excluding a possible artificial effect of the baseline level.

Alkanes fractions from sediments usually contain *n*-alkanes as major compounds and minor but numerous branched and/or cyclic alkanes. Unresolved GC areas are therefore common and the compounds which elute close together could be struc-

turally different compounds, isomers, or compounds with the same configuration but a different isotopic composition.

Enhanced resolution by isotopic GC-C-MS will be useful when dealing with complex mixtures. The isotopic ratios of compounds eluting close together cannot be measured accurately if the isotopic compositions of the co-eluting substances are unknown. Accordingly, in organic geochemistry, simpler fractions are needed for isotopic studies, provided that there is no isotopic fractionation during previous separations. These observations also strengthen the conclusion that one GC-FID peak is not a definitive proof of purity.

CONCLUSIONS

A significant increase in resolution has been observed by isotopic GC-C-MS relative to GC-FID or GC-MS with total ion current monitoring. This phenomenon is probably due to the fractionation of eluents during GC and the enhanced sensitivity of GC-C-MS to $^{13}\text{CO}_2/^{12}\text{CO}_2$ variations. Such enhanced resolution will be useful in studies of complex mixtures.

ACKNOWLEDGEMENTS

This work was supported by DOE Grant DE-FG02-88ER13978 to Professor J. M. Hayes, to

whom we are grateful for helpful discussions. We also thank the French Petroleum Institute and the Colorado Geological Survey for the supply of sediments.

REFERENCES

- 1 D. E. Matthews and J. M. Hayes, *Anal. Chem.*, 50 (1978) 1465-1473.
- 2 K. H. Freeman, J. M. Hayes, J.-M. Trendel and P. Albrecht, *Nature (London)*, 343 (1990) 254-256.
- 3 J. P. Jasper and J. M. Hayes, *Nature (London)*, 347 (1990) 462-464.
- 4 R. D. McCarthy and A. H. Duthie, *J. Lipid Res.*, 3 (1962) 117-119.
- 5 Z. Ramljak, A. Solc, P. Arpino, J. M. Schmitter and G. Guiochon, *Anal. Chem.*, 49 (1977) 1222-1225.
- 6 J. M. Schmitter, P. Arpino and G. Guiochon, *J. Chromatogr.*, 167 (1978) 149-158.
- 7 A. Van Dorsselaer, *Thesis*, Louis Pasteur University, Strasbourg, 1975.
- 8 R. E. Summons and L. L. Jahnke, *Geochim. Cosmochim. Acta*, 54 (1990) 247-251.
- 9 M. Rohmer and G. Ourisson, *Tetrahedron Lett.*, 40 (1976) 3641-3644.
- 10 M. Zundel and M. Rohmer, *Eur. J. Biochem.*, 150 (1985) 23-27.
- 11 P. Bisseret, M. Zundel and M. Rohmer, *Eur. J. Biochem.*, 150 (1985) 29-34.
- 12 K. H. Freeman, *Ph. D. Dissertation*, Indiana University, Bloomington, IN, 1991.
- 13 B. D. Gunter and J. D. Gleason, *J. Chrom. Sci.*, 9 (1971) 191-192.
- 14 W. A. Van Hook, *Isotope Effects in Chemical Processes (Advances in Chemistry Series)*, American Chemical Society Publications, Washington, DC, 1969, p. 99.

Short Communication

Simultaneous effect of geometrical isomerism and chelate ring size of tris(aminocarboxylato)cobalt(III) complexes on their behaviour in thin-layer chromatography on silica gel and alumina

G. Vučković*, N. Juranić, D. Miljević and M. B. Čelap

Chemical Faculty, Faculty of Science, University of Beograd, P.O. Box 550, 11001 Beograd (Yugoslavia)

(First received March 28th, 1991; revised manuscript received June 11th, 1991)

ABSTRACT

The simultaneous effects of geometrical isomerism and chelate ring enlargement of octahedral complexes on their R_F values obtained by chromatographing twelve isomers of complexes of the general formula $[\text{Co}(\text{gly})_{3-x}(\beta\text{-ala})_x]$ ($n = 0-3$; glyH = glycine; $\beta\text{-alaH} = \beta\text{-alanine}$) on thin layers of silica gel and alumina by using five monocomponent solvent systems was investigated. It was found that in most instances the effect of the ring size was predominant. Within the series of facial or meridional isomers it was established that with the enlargement of the chelate ring the R_F values of the complexes decreased on silica gel but increased on alumina, which was ascribed to the formation of hydrogen bonds of different strengths between the complexes and the adsorbent.

INTRODUCTION

In earlier work we investigated the effects of geometrical isomerism [1,2] and the chelate ring size [3,4] of transition metal complexes on their behaviour in thin-layer chromatography on silica gel. It was found that when monocomponent solvent systems were applied, lower R_F values were obtained for the *cis* isomers than for the corresponding *trans* isomers. Also, there is a linear dependence between the number of five-membered rings substituted by six-membered rings and the R_M values of the corresponding complexes. Finally, an analogous dependence was established between the chelate diamine ring size and the R_F values of complexes containing five-, six- and seven-membered rings.

Continuing these investigations, in this work we

studied the simultaneous effect of both of these factors on the behaviour of tris(aminocarboxylato)cobalt(III) complexes in thin-layer chromatographic (TLC) separations on silica gel and alumina. The complete series of twelve tris(aminocarboxylato)cobalt(III) complexes, which are formed by glycinate and β -alaninato chelate ligands, were considered (Fig. 1). This study is of interest for cases in which both of these factors are operating, as then it is uncertain which regularity (or whether any) will be manifested.

EXPERIMENTAL

Syntheses of the investigated complexes were carried out according to the procedure described previously [5].

Chromatographic separations were performed by the ascending chromatographic method on thin-layers of silica gel (H and G Type 60) and neutral alumina (Type 60/E) from Merck (Darmstadt, Germany) by using five monocomponent solvent systems (Table I). The working technique was described previously [3]. The reproducibility of R_F values was ± 0.03 .

The solubilities of complexes were determined as described previously [2].

RESULTS AND DISCUSSION

As can be seen from Table II, it was established that in all instances the facial (*fac*) isomers exhibit lower R_F values (or the same R_F values within the

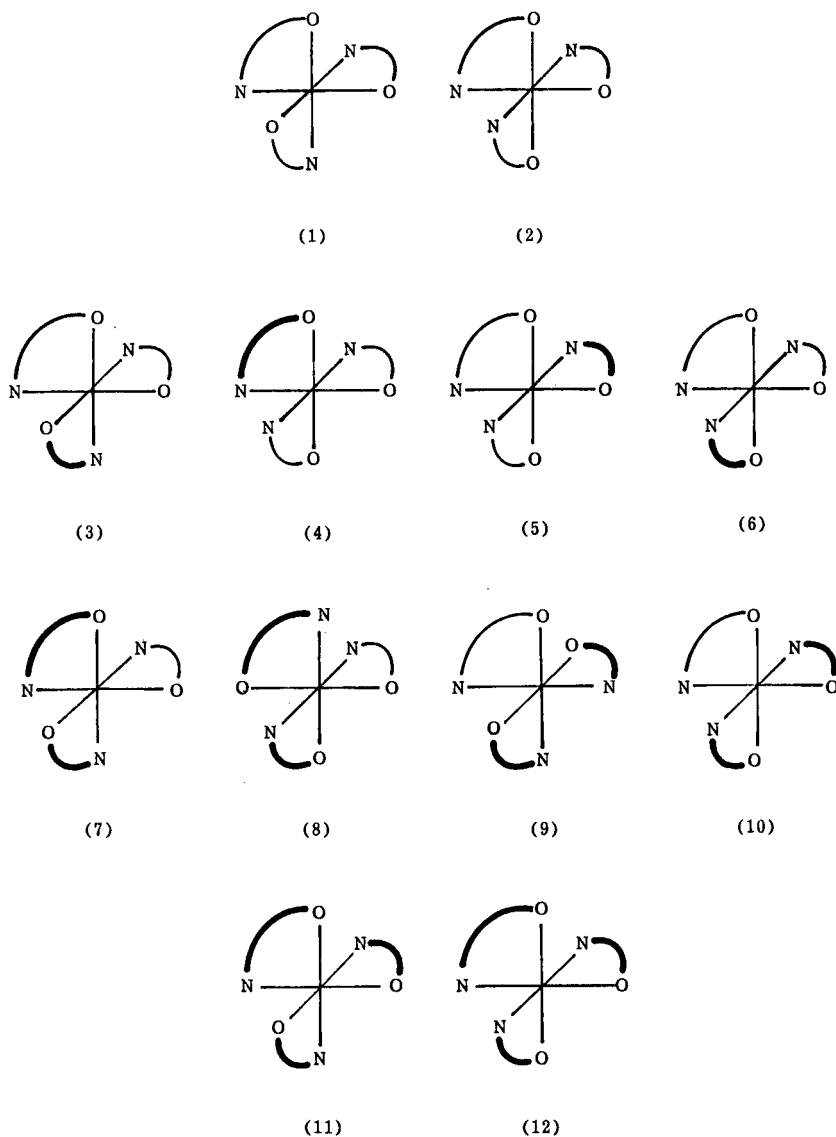


Fig. 1. Tris(aminocarboxylato)cobalt(III) complexes which are formed by glycinate and β -alaninato chelate ligands. β -Alaninato chelate is marked by thick lines; numbers of complexes as in Table II.

TABLE I
SOLVENTS USED

No.	Composition	Development time	
		Silica gel	Alumina
1	Distilled water	35 min	15 min
2	Methanol	50 min	30 min
3	1,2-Propanediol	16 h	15 h
4	1,3-Propanediol	24 h	22 h
5	Ethylene glycol	11 h	17 h

limits of the experimental error) in comparison with the meridional (*mer*) isomers of the same composition. These findings represent an extension of the earlier proposed rule [1,6] which related only to pairs of facial-meridional isomers.

Successive replacement of the glycinato ligand (which forms a five-membered ring with cobalt atom) by a β -alaninato ligand (which forms a six-

membered ring) within a series of facial or meridional isomers resulted in decreasing R_F values on thin layers of silica gel (Table II), which is also in accordance with our previously proposed rule [3]. In contrast, on thin layers of alumina a reverse order was observed (Table II), which had not previously been described in the literature. In order to explain this difference, we assumed that in the course of separation of complexes on silica gel hydrogen bonds are formed between hydrogens of silanol groups of the adsorbent and highly electronegative oxygens from the carboxylato groups of the ligand; on thin layers of alumina, however, hydrogen bonds are formed between hydrogens of the amino group of the aminocarboxylato ligands and oxygens of the adsorbent [7]. In connection with the latter it should be pointed out that the glycinato and β -alaninato chelates exhibit differences in the ability for coordinate bond formation, whereby the β -alaninato chelate is a considerably weaker ligand than the glycinato chelate, although it is a stronger

TABLE II
 R_F VALUES OF THE INVESTIGATED COMPLEXES

No.	Complex composition ^a	Complex isomers	$R_F \times 100^b$																		
			Silica gel ^c				Alumina														
			1		2		3		4		5		1		2		3		4		5
H	G	G	H	G	G	G															
1	[Co(gly) ₃]	<i>fac</i> -	95	89	—	—	39	38	94	93	2	23	2	83							
2		<i>mer</i> -	96	97	40	72	72	66	98	94	5	54	14	90							
3	[Co(gly) ₂ β -ala]	<i>fac</i> -	87	86	—	43	34	35	90	95	4	44	7	82							
4		<i>trans</i> -(N ₅)	88	93	28	58	66	54	92	97	5	55	15	86							
5		<i>trans</i> -(O ₅)	92	96	36	68	74	65	89	97	7	67	18	88							
6		<i>trans</i> -(N ₅ O ₅)	89	92	27	63	70	52	96	95	12	76	26	93							
7	[Co gly (β -ala) ₂]	<i>fac</i> -	79	75	—	36	18	34	—	94	5	46	9	86							
8		<i>trans</i> -(N ₆ O ₆)	84	88	25	56	63	47	81	99	10	88	23	88							
9		<i>trans</i> -(O ₆)	82	85	21	47	53	45	76	98	14	93	41	93							
10		<i>trans</i> -(N ₆)	76	86	19	41	48	44	90	98	21	94	45	94							
11	[Co (β -ala) ₃]	<i>fac</i> -	64	79	—	18	2	32	77	95	13	73	33	91							
12		<i>mer</i> -	76	79	19	40	46	33	74	98	33	95	64	95							

^a glyH = glycine; β -alaH = β -alanine.

^b The compositions of solvent systems 1-5 used are given in Table I.

^c H = Silica gel H; G = silica gel G.

base [8], *i.e.*, a potentially better bidentate ligand. In case of cobalt(III) complexes, a weaker ligand field of the β -alaninato chelate relative to that of glycinate chelate is clearly observed in electronic absorption [9] and ^{59}Co NMR spectra [10].

Also, a considerably smaller coordination shift is observed in the ^{15}N NMR spectrum of the amino group nitrogen of the β -alaninato than the glycinate ligands, and they may be correlated with a weaker link between the metal and the ligand [11]. Such behaviour is due to the steric hindrance appearing in the course of incorporating the six-membered ring whereby overlapping of metal and ligand orbitals is reduced [12,13]. Therefore, the coordinated β -alaninato ligand which gives off its electrons to the metal to a markedly smaller extent possesses a greater electron density than the coordinated glycinate ligand, which renders it more capable of hydrogen bonding through the oxygen of the carboxylic group (in the case of silica gel), but less capable of hydrogen bond formation through the hydrogen of the amino group (in the case of alumina).

The geometrical isomers of mixed complexes of the same composition exhibit the same order (within the limits of the experimental error) with all the solvent systems used in TLC separations on alumina, which is not the case on silica gel (Table II), which could be attributed to the solvent effects [14]. Thus in the investigated systems solute-solvent interaction cannot be neglected because of the possible hydrogen bond formation between the solvent and solute molecules.

When considering the R_F values of all twelve isomers of the investigated complexes on both adsorbents (Table II), it is seen that as a rule (within the limits of experimental error and except in 12% of cases on silica gel and 9% of cases on alumina), with increasing number of glycinate ligands substituted by the β -alaninato ligands the R_F values of the complexes decrease on silica gel but increase on alumina, regardless of the geometrical isomerism of the complex. In connection with this, it is worth mentioning that the aforesaid deviations appear mostly with facial isomers, which probably may be ascribed to their relatively low solubility. On the basis of these results, it may be concluded that with the investigated complexes the predominant effect on the R_F values is the chelate ring size relative to the effect of geometrical isomerism.

We also attempted to correlate the R_F values of isomers by using methanol as the solvent system with their solubilities in methanol. On the basis of the results obtained (Table III), it is evident that the solubilities of the facial-meridional pairs are in accordance with the R_F values obtained on both adsorbents. Thus the facial isomers are less soluble and exhibit lower R_F values than the meridional isomers of the same composition. These findings are also in agreement with the fact that the facial isomers are more polar than the meridional isomers and are therefore more strongly adsorbed.

However data on the solubilities (Table III) do not correspond to R_F values of complexes containing chelate rings of different size, or to R_F values of geometrical isomers of mixed complexes of the same composition obtained by TLC separations on both adsorbents, which means that the solubility is not the major factor affecting the R_F values.

Finally, we compared the R_F values of the investigated complexes obtained by TLC on silica gel H using water with the order of their elution from a column of a cationic exchanger in the hydrogen form [5]. In both instances an adsorption separation mechanism is expected, as neutral complexes are separated with water, which represents monocomponent solvent system. From Table II it can be concluded that in most instances a similar order of R_F values was found with other monocomponent organic solvent systems, suggesting the same separa-

TABLE III
SOLUBILITY (mmol/dm^3) AND R_F VALUES OF SOME OF THE INVESTIGATED COMPLEXES IN METHANOL

Complex ^a	Solubility	$R_F \times 100$	
		Silica gel G	Alumina
<i>fac</i> -[Co(gly) ₃]	2.1	0	2
<i>fac</i> -[Co(gly) ₂ β -ala]	4.7	0	4
<i>fac</i> -[Co(β -ala) ₃]	4.3	0	13
<i>mer</i> -[Co(gly) ₃]	5.7	40	5
<i>trans</i> -(O ₅)-[Co(gly) ₂ β -ala]	6.4	36	7
<i>trans</i> -(N ₆ ,O ₆)-[Co(gly)(β -ala) ₂]	5.8	25	10
<i>trans</i> -(N ₆)-[Co(gly)(β -ala) ₂]	3.2	19	21
<i>mer</i> -[Co(β -ala) ₃]	13.0	19	33

^a Abbreviations as in Table II.

TABLE IV

COMPARISON OF THE ORDER OF ELUTION OF THE INVESTIGATED COMPLEXES FROM A CATION-EXCHANGE COLUMN IN H⁺ FORM WITH THE R_F VALUES OBTAINED BY THEIR CHROMATOGRAPHY ON THIN LAYER OF SILICA GEL H WITH DISTILLED WATER

Cation-exchange column in hydrogen form [5] ^a	R _F × 100
<i>mer</i> -[Co(gly) ₃]	96
<i>fac</i> -[Co(gly) ₃]	95
<i>trans</i> -(N ₅ ,O ₃)-[Co(gly) ₂ β-ala]	89
<i>trans</i> -(N ₂)-[Co(gly) ₂ β-ala]	88
<i>trans</i> -(O ₅)-[Co(gly) ₂ β-ala]	92
<i>trans</i> -(O ₆)-[Cogly(β-ala) ₂]	82
<i>fac</i> -[Co(gly) ₂ β-ala]	87
<i>trans</i> -(N ₆)-[Cogly(β-ala) ₂]	76
<i>trans</i> -(N ₆ ,O ₆)-[Cogly(β-ala) ₂]	84
<i>mer</i> -[Co(β-ala) ₃]	76
<i>fac</i> -[Co(β-ala) ₃]	64

^a Abbreviations as in Table II.

tion mechanism. As can be seen from Table IV, the order of separation on the column is also dependent mainly on the chelate ring size and not on the effect of the geometrical isomerism of complexes, although the order of elution from the column is not identical with the order obtained on thin layers of silica gel. It seems that these differences are due to the fact that silica gel has several active centres [15], which is not the case with the ion exchanger used. Consequently, these results support our hypothesis that the investigated isomers are separated on thin layers of silica gel by the mechanism of hydrogen bond formation, in view of the fact that they behave similarly on a cation exchanger in the hydrogen form.

ACKNOWLEDGEMENT

The authors are grateful to the Serbian Republic Research Fund for financial support.

REFERENCES

- 1 T. J. Janjić, Ž. Lj. Tešić, G. N. Vučković and M. B. Čelap, *J. Chromatogr.*, 404 (1987) 307, and references cited therein.
- 2 G. Vučković, N. Juranić and M. B. Čelap, *J. Chromatogr.*, 361 (1986) 217.
- 3 M. B. Čelap, G. Vučković, M. J. Malinar, T. J. Janjić and P. N. Radivojša, *J. Chromatogr.*, 196 (1980) 59, and references cited therein.
- 4 G. Vučković, M. J. Malinar and M. B. Čelap, *J. Chromatogr.*, 454 (1988) 362.
- 5 N. Juranić, B. Prelesnik, Lj. Manojlović-Muir, K. Anđelković, S. R. Niketić and M. B. Čelap, *Inorg. Chem.*, 29 (1990) 1491.
- 6 F. Jursik, F. Petru and B. Hajek, *J. Chromatogr.*, 45 (1969) 319.
- 7 B. Fried and J. Sherma, *Thin-layer Chromatography (Chromatographic Science, Vol. 35)*, Marcel Dekker, New York, 2nd ed., 1986, p. 22.
- 8 L. G. Sillen and A. E. Martell, *Stability Constants*, Chemical Society, London, 1971, pp. 264 and 299.
- 9 M. B. Čelap, M. J. Malinar and T. J. Janjić, *Rev. Chim. Min.*, 13 (1976) 278.
- 10 N. Juranić, M. B. Čelap, D. Vučelić, M. J. Malinar and P. N. Radivojša, *J. Coord. Chem.*, 9 (1979) 117.
- 11 N. Juranić and R. L. Lichter, *Inorg. Chim. Acta*, 62 (1982) 131.
- 12 N. Juranić and R. L. Lichter, *J. Am. Chem. Soc.*, 105 (1983) 406.
- 13 N. Juranić, M. J. Malinar, P. N. Radivojša, I. Juranić and M. B. Čelap, *J. Serb. Chem. Soc.*, 51 (1986) 417.
- 14 L. R. Snyder, in Cs. Horvath (Editor), *High-Performance Liquid Chromatography, Advances and Perspectives*, Vol. 3, Academic Press, New York, 1983, p. 157.
- 15 S. G. Perry, R. Amos and P. I. Brewer, *Practical Liquid Chromatography*, Plenum Press, New York, 1972; Russian translation, Mir, Moscow, 1974, p. 74.

Journal of Chromatography

Request for manuscripts

Zdenek Deyl will edit a special, thematic issue of the *Journal of Chromatography* entitled "Applications of Chromatography and Electrophoresis in Food Science". Both reviews and research articles will be included.

Topics such as the following will be covered:

- General strategies for food analysis by chromatographic methods
- Chromatography of volatiles and odours
- Assessing food quality by chromatographic and electrophoretic methods
- Sample preparation for food analysis by chromatography and electrophoresis
- Analysis of toxic substances in food
- Analysis of food colours and dyes
- Analysis of individual food components
- Analysis of agrochemicals and drugs in food
- Analysis of compounds arising during food preparation and storage

Potential authors of reviews should contact Zdenek Deyl (Institute of Physiology, Czechoslovak Academy of Sciences, Vídeňská 1083, CS-14220 Prague, Czechoslovakia; tel.: +42-2-531267; fax: +42-2-4712253) prior to any submission. Research papers should be submitted to the above address as well.

The deadline for receipt of submissions is **January 31, 1992**. Manuscripts submitted after this deadline can still be published in the *Journal*, but then there is no guarantee that an accepted article will appear in the special, thematic issue. **Three** copies of the manuscript should be submitted to Zdenek Deyl. All manuscripts will be reviewed and acceptance will be based on the usual criteria for publishing in the *Journal of Chromatography*.

PUBLICATION SCHEDULE FOR 1992

Journal of Chromatography and Journal of Chromatography, Biomedical Applications

MONTH	O 1991	N 1991	D 1991	
Journal of Chromatography	585/1	585/2 586/1 586/2 587/1	587/2 588/1 + 2	The publication schedule for further issues will be published later
Cumulative Indexes, Vols. 551-600				
Bibliography Section				
Biomedical Applications				

INFORMATION FOR AUTHORS

(Detailed *Instructions to Authors* were published in Vol. 558, pp. 469-472. A free reprint can be obtained by application to the publisher, Elsevier Science Publishers B.V., P.O. Box 330, 1000 AH Amsterdam, The Netherlands.)

Types of Contributions. The following types of papers are published in the *Journal of Chromatography* and the section on *Biomedical Applications*: Regular research papers (Full-length papers), Review articles and Short Communications. Short Communications are usually descriptions of short investigations, or they can report minor technical improvements of previously published procedures; they reflect the same quality of research as Full-length papers, but should preferably not exceed five printed pages. For Review articles, see inside front cover under Submission of Papers.

Submission. Every paper must be accompanied by a letter from the senior author, stating that he/she is submitting the paper for publication in the *Journal of Chromatography*.

Manuscripts. Manuscripts should be typed in double spacing on consecutively numbered pages of uniform size. The manuscript should be preceded by a sheet of manuscript paper carrying the title of the paper and the name and full postal address of the person to whom the proofs are to be sent. As a rule, papers should be divided into sections, headed by a caption (*e.g.*, Abstract, Introduction, Experimental, Results, Discussion, etc.). All illustrations, photographs, tables, etc., should be on separate sheets.

Introduction. Every paper must have a concise introduction mentioning what has been done before on the topic described, and stating clearly what is new in the paper now submitted.

Abstract. All articles should have an abstract of 50-100 words which clearly and briefly indicates what is new, different and significant.

Illustrations. The figures should be submitted in a form suitable for reproduction, drawn in Indian ink on drawing or tracing paper. Each illustration should have a legend, all the *legends* being typed (with double spacing) together on a *separate sheet*. If structures are given in the text, the original drawings should be supplied. Coloured illustrations are reproduced at the author's expense, the cost being determined by the number of pages and by the number of colours needed. The written permission of the author and publisher must be obtained for the use of any figure already published. Its source must be indicated in the legend.

References. References should be numbered in the order in which they are cited in the text, and listed in numerical sequence on a separate sheet at the end of the article. Please check a recent issue for the layout of the reference list. Abbreviations for the titles of journals should follow the system used by *Chemical Abstracts*. Articles not yet published should be given as "in press" (journal should be specified), "submitted for publication" (journal should be specified), "in preparation" or "personal communication".

Dispatch. Before sending the manuscript to the Editor please check that the envelope contains four copies of the paper complete with references, legends and figures. One of the sets of figures must be the originals suitable for direct reproduction. Please also ensure that permission to publish has been obtained from your institute.

Proofs. One set of proofs will be sent to the author to be carefully checked for printer's errors. Corrections must be restricted to instances in which the proof is at variance with the manuscript. "Extra corrections" will be inserted at the author's expense.

Reprints. Fifty reprints of Full-length papers and Short Communications will be supplied free of charge. Additional reprints can be ordered by the authors. An order form containing price quotations will be sent to the authors together with the proofs of their article.

Advertisements. The Editors of the journal accept no responsibility for the contents of the advertisements. Advertisement rates are available on request. Advertising orders and enquiries can be sent to the Advertising Manager, Elsevier Science Publishers B.V., Advertising Department, P.O. Box 211, 1000 AE Amsterdam, Netherlands; courier shipments to: Van de Sande Bakhuysenstraat 4, 1061 AG Amsterdam, Netherlands; Tel. (+31-20) 515 3220/515 3222, Telefax (+31-20) 6833 041, Telex 16479 els vi nl. *UK:* T. G. Scott & Son Ltd., Tim Blake, Portland House, 21 Narborough Road, Cosby, Leics. LE9 5TA, UK; Tel. (+44-533) 753 333, Telefax (+44-533) 750 522. *USA and Canada:* Weston Media Associates, Daniel S. Lipner, P.O. Box 1110, Greens Farms, CT 06436-1110, USA; Tel. (+1-203) 261 2500, Telefax (+1-203) 261 0101.

Gas Chromatography in Air Pollution Analysis

by V.G. Berezkin, A.V. Topchiev Institute of Petrochemical Synthesis, Moscow, USSR and Y.S. Drugov, I.M. Gubkin Institute of Oil and Gas, Moscow, USSR

Journal of Chromatography Library Volume 49

Air pollution determination is one of the most important fields of gas chromatography application in practice. This book provides a systematic description of the main stages of air pollution determination, ranging from sampling problems to the quantitative estimation of the acquired data.

Special attention is paid to the problem of gas, vapor, spray and solid particles extraction from air. The main methods of sampling procedure, namely, container utilization, cryogenic concentration, absorption, adsorption, chemisorption and filter usage, and successive impurities extraction are also handled. Sorption theory and the problems of sorption and desorption efficiency for hazardous impurities being extracted from traps with sorbents are discussed in detail. The practical utilization of different sorbents (silica, activated carbon, polymers etc.) to carry out sampling procedures for 200 main pollutants with known TLV (USSR and USA) is also considered.

This highly informative book, reflecting several insufficiently known techniques as well as the experience of

both western and Soviet researchers, should be of interest to both beginners and skilled researchers.

Contents:

Chapter 1. Introduction. Chapter 2. Air as an Object of Analysis. Chapter 3. Gas Chromatography in the Analysis of Air Pollutants. Chapter 4. Detectors for the Gas Chromatographic Determination of Impurities. Chapter 5. Collection and Pretreatment of Samples for Chromatographic Analysis. Chapter 6. The Reactive-Sorption Method and its Application for Concentrating Pollutants. Chapter 7. Quantitative Methods for the Determination of Impurities. Chapter 8. Practical Application of Gas Chromatography to the Determination of Air Pollutants. *Each chapter contains References.*

1991 xii + 212 pages

Price: US \$ 125.50 / Dfl. 245.00

ISBN 0-444-98732-0

Distributed in the East European Countries, China, Cuba, Mongolia, North Korea and Vietnam by Akademische Verlagsgesellschaft Geest & Portig K.-G., Leipzig, Germany



Elsevier Science Publishers

P.O. Box 211, 1000 AE Amsterdam, The Netherlands

P.O. Box 882, Madison Square Station, New York, NY 10159, USA